The University Of Sheffield.

The abundance, persistence and mineralisation of phytate (*myo*-inositol hexakisphosphate) in monogastric faecal waste and soil.

Niall Bradshaw

A thesis submitted in partial fulfilment of the requirements for the degree of Doctor of Philosophy

The University of Sheffield
Faculty of Engineering
Department of Chemical & Biological Engineering

September 2019

Contents

List of Figures ..... *vi*
List of Tables ..... *viii*
Acknowledgements ..... *ix*
Thesis Summary ..... *x*
Abbreviations ..... *xi*
1: General Introduction **1**
1.1 Human use of Phosphorus 1
1.2 Phosphorus Sustainability 4
1.3 Phytate (*myo*-inositol hexakisphosphate) and its quantification 8
1.3.1 Sample Extraction 9
1.3.2 Enzymatic Quantification 10
1.3.3 Chromatographic Techniques 11
1.3.4 Solution ^{31}P NMR 12
1.4 The behaviour of phytate in environmental samples 15
1.4.1 Phytate in livestock manure 15
1.4.2 Phytate in human excreta 16
1.4.3 Phytate in soil 18
1.5 Phytate mobilisation 20
1.5.1 Phytase enzymes 20
1.5.2 Mobilisation of soil phytate by phytases 20
1.5.3 Applications of phytase enzymes 23
1.6 Aims and Objectives of this Thesis 24
1.6.1 Phytate analysis by ESI-ToF-MS 25
1.6.2 Phytate in sewage sludge 25
1.6.3 Phytate in soil 26
1.6.4 Enzymatic biofertilization of phytate-treated plants 26
2: Analysis of phytate and the lower inositol phosphates by ESI-ToF-Mass Spectrometry **27**
2.1 Summary 27

2.2 Introduction 28
2.2.1 Detection of Inositol Phosphates in ^{31}P NMR 28
2.2.2 Electrospray Ionisation Time-of-Flight Mass Spectrometry (ESI-ToF-MS) 29
2.2.3 Inositol phosphate analysis by ESI-ToF-MS 31
2.2.4 Aims & Objectives 32
2.3 Methods 33
2.3.1 Solution ^{31}P NMR 33
2.3.2 ESI-ToF-MS of phytate 33
2.3.3 ESI-ToF-MS of the phytate-phytase reaction 34
2.4 Results & Discussion 35
2.4.1 Phytate in ^{31}P NMR 35
2.4.2 ESI-ToF-MS of Phytate 37
2.4.3 The effect of concentration and source voltage of fragmentation patterns 43
2.4.4 Cone Voltage 45
2.4.5 Application of ESI-ToF-MS to the analysis of the enzymatic dephosphorylation of phytate 49
2.5 Conclusions 53
3: Analysis of phytate through an advanced anaerobic sludge treatment process 55
3.1 Summary 55
3.2 Introduction 56
3.2.1 Wastewater treatment in the UK 56
3.2.2 Anaerobic digestion (AD) of sludge 58
3.2.3 Sludge pre-treatment 60
3.2.4 Sludge phosphorus recovery and reuse 60
3.2.5 Aims and Objectives 62
3.3 Methods 64
3.3.1 Wastewater treatment plant (WWTP) & Sampling 64
3.3.2 Sample Processing 64
3.3.3 Colorimetric analysis 67
3.3.3.1 Sludge and sludge extract total phosphorus 67
3.3.3.2 Colorimetric determination of extract MRP and phytase-labile P 67
3.3.4 Solution ^{31}P NMR 68

3.3.4.1 Sample Preparation 68
3.3.4.2 ^{31}P NMR Parameters 68
3.3.4.3 ^{31}P NMR Optimisation 69
3.3.5 Statistical Analysis 69
3.4 Results 71
3.4.1 Total phosphorus of sludge 71
3.4.2 Total extractable phosphorus 71
3.4.3 Colorimetric determination of sludge MRP and phytase-labile P 71
3.4.4 ^{31}P NMR Optimisation 74
3.4.5 ^{31}P NMR determination of sludge orthophosphate and phytate 77
3.5 Discussion 82
3.5.1 Sludge total phosphorus and extraction efficiency 82
3.5.2 ^{31}P NMR Optimisation 83
3.5.3 Orthophosphate-P in sludge treatment 84
3.5.4 Phytate-P in sludge treatment 85
3.5.4.1 Phytase-labile P 86
3.5.4.2 ^{31}P NMR 87
3.5.4.3 Methodological Comparison 87
3.5.5 Implications for soils amended with AD sludge 90
3.5 Conclusions 93
4: Measurement of phytate in soils with varied land-use history 95
4.1 Summary 95
4.2 Introduction 96
4.2.1 Phytate accumulation in soil 96
4.2.2 Land-use history 96
4.2.3 Aims and Objectives 98
4.3 Methods 100
4.3.1 Soil sampling 100
4.3.2 Sample processing 103
4.3.3 Colorimetric analysis 104
4.3.3.1 Soil and soil extract total phosphorus 104
4.3.3.2 Colorimetric determination of extract MRP and phytase-labile P 104

4.3.4 Solution ^{31}P NMR 104
4.3.5 Statistical Analysis 106
4.4 Results 107
4.4.1 Soil properties (pH and organic matter) 107
4.4.2 Total phosphorus of soil 107
4.4.3 Total extractable phosphorus 107
4.4.4 Colorimetric measurement of MRP and phytase-labile P 109
4.4.5 ^{31}P NMR Optimisation 112
4.4.6 ^{31}P NMR determination of soil orthophosphate and phytate 113
4.4.6.1 Orthophosphate-P 113
4.4.6.2 Phytate-P 116
4.4.6.3 Residual-P 118
4.5 Discussion 119
4.5.1 Soil pH and organic matter 119
4.5.2 Soil total phosphorus and extraction efficiency 122
4.5.3 Soil ^{31}P NMR Optimisation 123
4.5.4 Colorimetric analysis of soil P 124
4.5.5 Solution ^{31}P NMR analysis of soil P 126
4.5.5.1 Major features of soil ^{31}P NMR spectra 126
4.5.5.2 Spen farm soils 127
4.5.5.3 Wardlow soils 130
4.5.6 Accumulation in phytate in pig pen soil 131
4.6 Conclusions 133
5: Use of a phytase enzyme to liberate phosphate from phytate in a model soil substrate 135
5.1 Summary 135
5.2 Introduction 136
5.2.1 Phytate dephosphorylation by phytases in environmental samples 136
5.2.2 Aims and Objectives 138
5.3 Methods 140
5.3.1 Experimental set-up 140
5.3.2 Sample processing 143

5.3.3 Sample analysis 143
5.3.4 Statistical analysis 144
5.4 Results 145
5.4.1 Plant Biomass 145
5.4.2 Total plant P uptake 145
5.4.3 Plant P concentration 147
5.4.4 Substrate phytoavailable P 151
5.4.5 Substrate total P 151
5.5 Discussion 154
5.5.1 Overall effects of clay, phosphorus and enzyme treatments 154
5.5.2 Effect of clay and enzyme in phytate-treated plants 157
5.5.3 Phytate adsorption 159
5.5.4 Phytase enzymes in soil and substrate matrices 161
5.6 Conclusions 165
6: General Discussion **167**
6.1 Phosphorus Sustainability 167
6.2 Evaluating and optimising the available analytical methods for quantifying different chemical species of P 170
6.3 Phytate survives anaerobic sludge treatment 172
6.4 Land-use has a major effect on soil P and phytate concentrations 175
6.5 Phytase catalytic activity is lost when applied directly to substrate 177
6.6 Conclusions and Future Recommendations 179
References **182**
Appendices **199**
Appendix A: Solution ^{31}P NMR spectra of sludge extracts 199
Appendix B: Solution ^{31}P NMR spectra of soil extracts 204
Appendix C: Soil P availability as affected by soil pH 209

List of Figures

1.1: Overview of Natural & Anthropogenic P Fluxes 2

1.2: Common soil phosphorus forms 7

1.3: Energy states of nuclei in NMR 12

1.4: Typical solution ^{31}P NMR spectrum of a soil extract 14

1.5: Molecular structures of phytate and the lower inositol phosphates 21

2.1: Schematic diagram of Electrospray Ionisation (ESI) 30

2.2: Solution ^{31}P NMR spectra of three concentrations of sodium phytate 35

2.3: Mass spectrum of 0.5mM sodium phytate 38

2.4: Mass spectrum of 0.5mM potassium phytate 40

2.5: Mechanism for the fragmentation of phytate 42

2.6: The effect of source voltage and analyte concentration on absolute and relative ion intensity 44

2.7: The effect of source voltage on fragmentation of 0.5mM sodium phytate after cone voltage optimisation 47

2.8: Mass spectrum of 0.5mM sodium phytate after cone voltage optimisation 48

2.9: ESI-ToF-MS analysis of the phytase-mediated dephosphorylation of phytate 50

2.10: Mean ± SEM for each inositol phosphate during the phytase-mediated dephosphorylation of phytate 52

3.1: Schematic diagram of a typical wastewater treatment process 57

3.2: Schematic diagram of a typical wastewater treatment process with sampling points 65

3.3: Schematic diagram of the methods used in Chapter 3 66

3.4: Sludge total phosphorus concentration 72

3.5: Sludge extract total phosphorus and mean extraction efficiency 72

3.6: Absolute and proportional concentrations of P fractions in sludges measured colorimetrically 73

3.7: The effect of relaxation delay time on peak integrals of MDP, Orthophosphate and Phytate in sludge samples 75

3.8: Solution ^{31}P NMR spectra of sludge cake (CK), spiked with phosphate and phytate 76

3.9: Selected ^{31}P NMR spectra of sludge extracts 77

3.10: Concentration of orthophosphate-P in sludge extracts analysed by ^{31}P NMR 78

3.11: Concentration of phytate-P in sludge extracts analysed by ^{31}P NMR 78

3.12: Absolute and proportional concentrations of P fractions in sludges measured by ^{31}P NMR 79

3.13: Linear regressions of sludge phosphate-P and phytate-P measured by colorimetry and ^{31}P NMR 80

4.1: Aerial views of soil sampling sites 102

4.2: Soil total phosphorus concentration 108

4.3: Soil extract total phosphorus concentration and mean extraction efficiency 108

4.4: Absolute and proportional concentrations of P fractions in soils measured colorimetrically 110

4.5: The effect of relaxation delay time on peak integrals of MDP, Orthophosphate and Phytate in soil samples 111

4.6: Solution ^{31}P NMR spectra of Arable (SAra) soil, spiked with phosphate and phytate 112

4.7: Selected ^{31}P NMR spectra of soil extracts 114

4.8: Linear regressions of soil phosphate-P and phytate-P measured by colorimetry and ^{31}P NMR 115

4.9: Concentration of orthophosphate-P in soil extracts analysed by ^{31}P NMR 116

4.10: Absolute and proportional concentrations of P fractions in soils measured by ^{31}P NMR 117

4.11: Concentration of phytate-P in soil extracts analysed by ^{31}P NMR 118

5.1: Schematic diagram of plant experimental set-up 140

5.2: The effect of clay, P and phytase enzyme on plant biomass 146

5.3: The effect of clay, P and phytase enzyme on total plant P uptake 148

5.4: The effect of clay, P and phytase enzyme on plant P concentration 149

5.5: The effect of clay, P and phytase enzyme on substrate phytoavailable P 150

5.6: The effect of clay, P and phytase enzyme on substrate total P 152

6.1: Current and future anthropogenic P cycles 168

A.1: ^{31}P NMR Spectra of Primary Sludge (PS) 199

A.2: ^{31}P NMR Spectra of Secondary Sludge (SS) 200

A.3: ^{31}P NMR Spectra of Digester Feed (DF) 201

A.4: ^{31}P NMR Spectra of Digested Sludge (DS) 202

A.5: ^{31}P NMR Spectra of Cake (CK) 203

B.1: ^{31}P NMR Spectra of Spen Arable Soil (SAra) 204

B.2: ^{31}P NMR Spectra of Spen Pasture Soil (SPas) 205

B.3: ^{31}P NMR Spectra of Spen Pig Pen Soil (SPig) 206

B.4: ^{31}P NMR Spectra of Wardlow Acid Soil (WAc) 207

B.5: ^{31}P NMR Spectra of Wardlow Calcareous Soil (WCal) 208

C: Soil P availability as affected by soil pH 209

List of Tables

2.1: Published and observed chemical shifts of IP6 and IP5 36

2.2: Peak identities for mass spectra of 0.5mM sodium phytate 39

2.3: Peak identities for mass spectrum of 0.5mM potassium phytate 41

3.1: UK sewage sludge disposal 1992-2010 58

4.1: Spen Farm crop history of sampled fields from 2001-2018 103

4.2: pH and Organic Matter content of Spen and Wardlow Soils 107

5.1: Modified Hoagland's nutrient solutions 142

5.2: Results of three-way ANOVA for final plant biomass 146

5.3: Results of two-way ANOVAs for measured parameters in phytate-treated plants 147

5.4: Results of three-way ANOVA for total plant P uptake 148

5.5: Results of three-way ANOVA for plant P concentration 149

5.6: Results of three-way ANOVA for substrate phytoavailable P 150

5.7: Results of three-way ANOVA for final substrate total P 152

Acknowledgements

Firstly, my thanks go to my supervisors, Rob Falconer and Duncan Cameron for their continuous guidance over the past four years. Their doors were always open when I had a question, a problem or a breakthrough, and I couldn't have asked for better support. Special thanks go to Duncan, who has been a mentor not just throughout this PhD, but my undergraduate studies and masters too. Without him I certainly would not be where I am today.

I'd like to thank Irene Johnson for the countless hours of technical advice and training she's provided, along with her support in designing my experiments. Huge thanks must also go to Heather Walker for her help setting up and troubleshooting the Mass Spec, and also to Andrea Hounslow for getting me started with NMR. I'd like to express my gratitude to the Grantham Centre for Sustainable Futures for their generous funding, and to its staff and my fellow scholars for providing me with numerous opportunities to engage with people and organisations that I would otherwise not have met.

I'm privileged to have met so many amazing people throughout my PhD. Major thanks go to all the C57 lab members, and especially to Emanga, Lizzy, Ingrid, Kirsty, Chris, Dave, Hayden, Emma and Hannah for making CMezz a great office to work in. A special mention is reserved for Nichola, who has been a constant source of encouragement, friendship and ridiculous memes. I'm really going to miss our trips to the pub and putting the world to rights on our strolls. Thanks also go to the brilliant undergraduate students May Appleby and Lewis Rowney, for all their hard work.

To my friends outside of Uni, thanks for the downtime, the numerous BBQs, nights out, nights in, and for being a great bunch of people overall. Whilst I'm leaving Sheffield, I definitely won't be a stranger.

Dad, Dawn, Ryan and Ciaran, Nan and my dearly missed Mum, thank you for all you've given to get me here. I'm so lucky to have such a great and supportive family. Finally, to my incredible boyfriend, Fin. I don't think I'd have made it through this PhD without you by my side. Thanks for your unwavering patience, your love and your big smile. I'm so excited for what the future holds.

Thesis Summary

Phosphorus is essential for global food production but is a finite resource that is used inefficiently. There is therefore an urgent need for increased recycling of phosphorus from organic wastes and reduced chemical fertiliser application. Recycling will involve mobilising phytoavailable phosphate from sources including phytate, an organic phosphate which is prevalent in manures and soils.

Phytate is present in human excreta, but its fate through sludge treatment processes is unclear. This thesis set out to investigate whether phytate is mineralised during anaerobic digestion or persists to comprise a fraction of phosphorus in land-spread sludge. A further aim was to measure phytate and orthophosphate concentrations in a range of soils to assess how land-use affects P speciation. Where phytate is abundant, phytase enzymes may play a key role in crop biofertilisation. A final aim was to assess the performance of a commercial phytase when used for the liberation of phytate-P for plants.

Evaluation of the available methods for quantifying phosphorus species showed that solution ^{31}P Nuclear Magnetic Resonance (NMR) spectroscopy remains the most powerful technique available, due to the occurrence of in-source fragmentation in mass spectrometry. Subsequently, ^{31}P NMR analysis showed that phytate does persist through sludge treatment, comprising 4.5% of phosphorus in the digested product. Land-use had a major impact on soil phosphorus speciation as agricultural soils were dominated by orthophosphate, reflecting their intensive management compared to grassland soil. Phytate was scarce in arable soil, but abundant in pig-pen soil due to inputs of monogastric manure.

Finally, phytase activity was lost in substrates via the immobilisation of both the enzyme and phytate on the solid phase. A greater understanding of rhizosphere biochemistry, such as the role of organic acids in desorption and maintenance of phytase activity, will improve the recycling of soil phytate-P and reduce our reliance on unsustainable fertilisers.

Abbreviations

0% Clay	Substrate comprising 50% peat moss & 50% sand (Chapter 5)
10% Clay	Substrate comprising 50% peat, 40% sand and 10% bentonite clay
^{31}P NMR	^{31}P Nuclear Magnetic Resonance
AD	Anaerobic Digestion
CK	Cake – Samples taken from the final stage of the wastewater treatment process
Cphy	Cysteine phytase
DF	Digester Feed - Samples taken from the third stage of the wastewater treatment process
DS	Digested Sludge – Samples taken from the fourth stage of the wastewater treatment process
ESI	Electrospray Ionisation
ESI-ToF-MS	Electrospray Ionisation Time-of-Flight Mass Spectrometry
FID	Free Induction Decay – the observable signal generated by the spin of nuclei in ^{31}P NMR
HAP	Histidine Acid Phosphatase (phytase)
HPIC	High-performance ion chromatography
HPLC	High-performance liquid chromatography
IP0	*myo*-inositol (with no phosphate groups)
IP1	*myo*-inositol monophosphate
IP2	*myo*-inositol bisphosphate
IP3	*myo*-inositol trisphosphate
IP4	*myo*-inositol tetrakisphosphate
IP5	*myo*-inositol pentakisphosphate
IP6	*myo*-inositol hexakisphosphate, phytate, or phytic acid

m/z	Mass to charge ratio
MDP	Methylene diphosphonate – used as an internal standard in ^{31}P NMR
MRP	Molybdate-reactive P. The fraction of P that reacts to cause the blue colour change in molybdate colorimetry
MUP	Molybdate-unreactive P. The fraction of P that does not react and causes no colour change in molybdate colorimetry
P	Phosphorus
PAP	Purple acid phosphatase (phytase)
P_I	Inorganic phosphorus
P_O	Organic phosphorus
PS	Primary Sludge – Samples taken from the first stage of the wastewater treatment process
P_T	Total Phosphorus (Inorganic + Organic P)
RF pulse	Radiofrequency pulse – applied during ^{31}P NMR to provide energy to, or 'excite' nuclei
SAra	Spen Arable – soil samples from the arable field of Spen Farm
SPas	Spen Pasture – soil samples from the pasture field of Spen Farm
SPig	Spen Pig – soil samples from the pig pen field of Spen Farm
SS	Secondary Sludge – Samples taken from the second stage of the wastewater treatment process
T1	Relaxation time constant. A measure of the time taken for a molecule to relax to its equilibrium state following excitation in ^{31}P NMR
THP	Thermal hydrolysis plant – A step used in modern WWTP in which sludge is hydrolysed at high temperature and pressure
WAc	Wardlow Acidic – soil samples from the acidic grassland of Wardlow Hay Cop (Chapter 4)
WCal	Wardlow Calcareous – soil samples from the calcareous grassland of Wardlow Hay Cop (Chapter 4)
WWTP	Wastewater treatment plant
βPP	Beta-propeller phytase

1: General Introduction

1.1 Human use of Phosphorus

Phosphorus (P) is an essential element for life, and is used by organisms in numerous capacities, including the production of nucleic acids and phospholipids, and for the transport of energy in adenosine triphosphate (ATP; Vaccari, 2009). Plants obtain their entire P requirement from the soil, but are only able to absorb inorganic phosphate that is freely dissolved in the soil solution. The slow biogeochemical cycling of P and its resulting scarcity in natural soils means that it is often the main nutrient limiting plant growth (Cordell et al., 2009). Traditionally, this limitation was addressed by the input of locally sourced organic material, such as animal manure and 'night soil' (human excreta) to the soil. However, soil degradation and recurring famines in the 17th and 18th centuries led to the pursuit of alternative P sources (Cordell et al., 2009). The first synthetic phosphate-rich fertiliser, ordinary superphosphate ($Ca(H_2PO_4)_2$), was patented by Sir John Bennett Lawes of Rothamstead Research and Sir James Murray in 1842 (Ivell, 2012; Blackwell et al., 2019). Superphosphate, highly soluble and more phosphate-concentrated than traditional manures, was initially produced via the dissolution of animal bones and coprolites in sulphuric acid (Ivell, 2012). When demand for bones outstripped supply, new sources of phosphate such as guano (deposits of phosphate- and nitrate- rich bird and bat manure) and phosphate-rich rock were developed, giving rise to the modern phosphate fertiliser industry (Blackwell et al., 2019). Since the 'green revolution' of the mid-20th century, humans have mined vast amounts of phosphate rock as a source of fertiliser to sustain an increasing human population. However, bypassing the slow, natural biogeochemical P cycle in this way has caused an imbalance, distributing unnaturally vast amounts of P over a huge geographical area of the planet, causing environmental issues such as eutrophication, and generating concern for the future supplies of this finite resource (Cordell et al., 2009).

Phosphate rock refers to natural resources of phosphate-rich sedimentary and igneous rock, typically containing between 5-13% P (Cordell & White, 2011). Sedimentary phosphate rock often originates from marine sediments on the slopes of continental

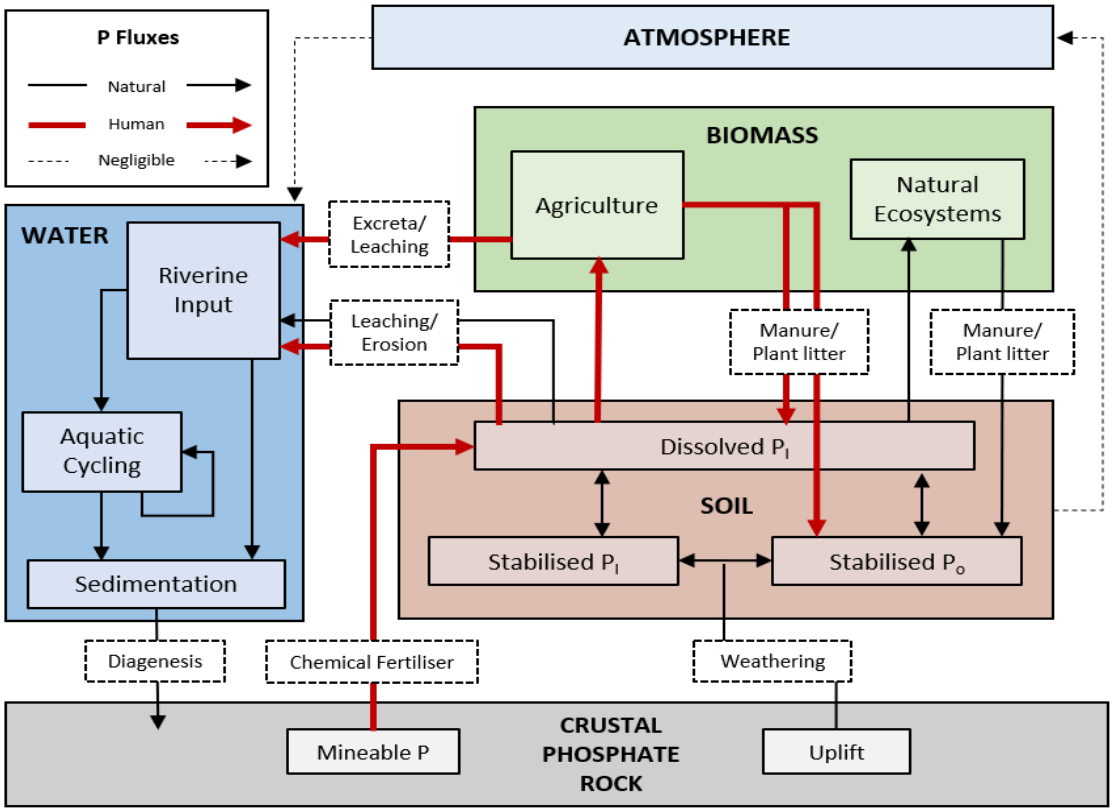

Figure 1.1: A simplified overview of natural and anthropogenic fluxes in the phosphorus cycle. Black arrows indicate natural flues, black dashed arrows indicate negligible flux, and red arrows indicate anthropogenic flows. Figure adapted from Peñuelas et al., (2013).

shelves, such as the major deposits in Morocco, China, the Middle East and the US, and predominates known resources (Reijnders, 2014), comprising approximately 80% of the total world phosphate rock production (Ptáček, 2016). Igneous resources such as those found in Brazil, Canada, Finland, Russia and South Africa (Jasinski, 2019), are much less abundant by comparison, and are often of lower grade, containing less than 5% P_2O_5. However, they can often produce higher quality beneficiation products, containing fewer impurities (Ptáček, 2016). In the natural biogeochemical P cycle (Figure 1.1), P in soil is derived from the natural weathering of these P-rich minerals such as apatite ($Ca_{10}(PO_4)_6(OH,F,Cl)_2$) from uplifted and exposed sedimentary rock, and to a lesser extent minerals from igneous sources. Once present in soil, labile and soluble inorganic phosphate (P_I) is available for plant uptake, but much of the P in soil exists in forms unavailable for absorption by biota, being adsorbed to the soil solid phase, precipitated by metal cations, or immobilised in organic phosphate compounds (Shen et al., 2011; Turner et al., 2005a). The P_I that is absorbed by plant biomass is eventually returned to

the soil in manure or plant litter, where it is cycled between labile and non-labile forms by microorganisms (Ruttenberg, 2003). As soil P is largely immobile, its movement into waterways is predominantly caused by the gradual erosion of soils, and by leaching of the small soluble fraction with precipitation (Ruttenberg, 2003; Shen et al., 2011). From riverine inputs, P makes its way to the sea, where the residence time of dissolved P can range between 16,000-30,000 years (Ruttenberg, 1993), within which time P is cycled extensively before undergoing passive burial and diagenesis, eventually becoming incorporated in sedimentary rock (Ruttenberg, 2003). The application of vast amounts of mined phosphate to agricultural land has caused an imbalance in this cycle. The 'green revolution' dramatically increased worldwide food production by popularising the use of new high-yielding agricultural crops and the application of concentrated chemical fertilisers to soils (Cordell et al., 2009). These fertilisers, such as ordinary superphosphate, contain roughly ten times the concentration of P that is typically found in manures, and all but rectified the issue of P-deficiency in the agricultural soils of developed countries.

We are now reliant on chemical P fertilisers for worldwide food production, with projected demand for P fertiliser increasing by an average of 2.19% annually between 2015-2020 (FAO, 2017). However, mined phosphate rock is a finite resource, and a temporary 700% spike in the price of phosphate in 2008 when demand outstripped supply led to global fears of an imminent 'peak phosphorus' scenario, the point at which global phosphate rock supplies are largely depleted and the quality and supply of phosphate fertilisers begins to fall, which by early calculations was predicted to occur by as soon as 2033 (Jasinski, 2008; Cordell et al., 2009; Cordell & White, 2011). Estimated global phosphate rock reserves have increased from an estimate of 18 Billion metric tonnes in 2008 (Jasinski, 2008), to 70 Billion metric tonnes in 2019 (Jasinski, 2019), owing predominantly to the discovery of vast reserves in Morocco, easing fears of an imminent crisis. However, according to the latest US Geological Survey data, Morocco now controls 71% of the entire global phosphate rock reserve (Jasinski, 2019), which is a major geopolitical cause for concern owing to Morocco's continued occupation of Western Sahara and control over its phosphate rock resources (Cordell et al., 2009). A further issue is that unlike igneous resources, sedimentary phosphate rock resources,

including those from Morocco, often contain high concentrations of contaminants such as the heavy metal, cadmium. When applied to soil in contaminated phosphate fertilisers, cadmium is absorbed and accumulated by plants. When consumed by humans, cadmium can accumulate in the liver and kidneys, sometimes leading to organ failure, decreased bone density and cancer (Walan, 2013). As the purest phosphate rock is mined first, it is likely that the concentration of cadmium in fertilisers will increase over time. For this reason, the EU, which imports the majority of their phosphate rock ore from Morocco, has recently introduced regulations to limit the concentration of cadmium in fertilisers to a maximum of 60mg cadmium per kilogram of phosphorus pentoxide (Ulrich, 2019). These levels can be achieved via the mixing of high cadmium rock with low cadmium igneous supplies, but due to the relative scarcity of these, decadmination of phosphate rock and phosphoric acid, along with increased substitution of phosphate rock with alternative recycled P sources will be the likely outcome of these regulations (Ulrich, 2019).

1.2 Phosphorus Sustainability

Despite an easing over the concerns for future P security, the global interest generated by the 2008 price spike served to draw attention to the fragile and finite nature of global P supplies, and called into question the sustainability of food production in a P-scarce future (Cordell & White, 2014). A recent paper estimates that at current rates of extraction, there is 259 years remaining of future supply (Blackwell et al., 2019). Whilst this suggests that there are no immediate concerns, this estimate was revised down from 300 years supply estimated in 2016, reflecting the effect of increasing demand. The FAO (2009) predicted that food global production must increase by 70% by 2050 to feed the projected population of 9 billion. Phosphorus usage is expected to increase year on year to meet this requirement, but demand may rise substantially owing to increased wealth in developing countries, increased meat consumption, and increased competition for fertilisers from biofuel crops (Cordell & White, 2011). Furthermore, the quality of phosphate rock ore is already in decline (Smil, 2000), and remaining reserves are increasingly difficult to access, contain more impurities, and require more energy-intensive processing (Neset et al., 2016).

As well as issues of scarcity, the mobilisation of vast amounts of P to agricultural soils has led to environmental pollution of inland and coastal waters in the form of eutrophication (Peñuelas et al., 2013). Overapplication of phosphate can lead to its movement into waterbodies via soil erosion or leaching in the solution phase, and can result in hypoxia and the creation of dead zones, where waterbodies are stripped of oxygen by phytoplankton blooms (Cordell & White, 2014). Phosphorus absorbed by plants and consumed by humans is often lost by the disposal of sewage to waterbodies, further exacerbating the eutrophication issue, and highlighting the linear nature of anthropogenic P use, in which P is applied to soil, absorbed by plants, consumed, then lost permanently to waterbodies (Figure 1.1).

For these reasons, over the past decade, a substantial amount of research has sought to explore opportunities for increasing efficiency of fertiliser application and reducing our reliance on mined phosphate rock. Depending on soil types, quality and chemistry, no more than 8% of fertiliser P added to soils is absorbed by crops, with the remainder becoming stabilised in soils or lost to waterbodies (Blackwell et al., 2019). However, the lack of a significant gaseous phase in the P cycle, and the low mobility and tendency of P to accumulate in soil and other matrices means that there is great potential for its recycling and recovery from the largely linearised anthropogenic P cycle. A calculation based on global P flows estimated by Cordell et al., (2009), approximates that almost 54% of P in livestock manure and human excreta is lost to landfill, non-arable soils or water bodies annually. Much work is being done to stem this leakage, but challenges lie in the uneven local and global distributions of both manure and human excreta, impeding its use on arable land. Bennett et al., (2010) noted that global manure production was concentrated in specific 'hotspot' regions. Within these regions, it is also often concentrated near urban areas and ports (European Commission, 2013), and likewise, human excreta is most concentrated in large towns and cities, far from the arable land in which it is most necessary.

Major innovations in recent years have included the recovery of P from wastewater streams generated by the dewatering of digester effluent, which can have P concentrations of 200-500 mg P L^{-1}, via the precipitation of struvite (Magnesium ammonium phosphate, $NH_4MgPO_4 \cdot 6H_2O$; Batstone et al., (2015)). The retention time for

this process can be very short, as demonstrated in struvite nucleation experiments by Mehta & Batstone, (2013), where the P concentration of 1L batches of digester effluent were reduced from ~120 mg P L^{-1} to <10 mg P L^{-1} in under 60 minutes. Struvite is a mineral high in phytoavailable phosphate, which can be applied to soil much like a regular fertiliser, but is lower in solubility than conventional chemical fertilisers, so reduces the risk of runoff and eutrophication (Talboys et al., 2016). Phosphorus recovery from wastewater is also often achieved indirectly via the application of manure and sludges, along with their incinerated ashes, to soils. In the UK, since the introduction of the EU Urban Waste Water Treatment Directive in 1999, disposal of sludge to sea has been eliminated, and disposal to landfill has declined significantly, with the majority of treated sludge produced instead spread on arable land (DEFRA, 2012).

Soil application of manures, sludges, food waste and plant litter facilitates the recycling of both inorganic P and organic P forms to the soil (Figure 1.2). Whilst inorganic P present as soluble phosphate is available for uptake by plants and other organisms, organic P (P_O) is not immediately phytoavailable, and can accumulate in soils as a significant untapped P source (George et al., 2018). P_O comprises a wide group of compounds that contain both organic groups and phosphate groups, and include orthophosphate monoesters such as inositol hexakisphosphate (phytate), orthophosphate diesters (DNA, RNA), organic polyphosphates (ATP) and phosphonates (Figure 1.2; George et al., 2017). Each of these compounds varies in lability dependent on soil conditions, with some forming strong interactions within the soil. For example, phytate can become strongly bound within the soil solid phase or form insoluble precipitates with metal cations due to the high charge density of the molecule owing to the presence of six phosphate moieties (Turner et al., 2002). Mobilisation and conversion of P_O to phytoavailable forms is predominantly mediated by the actions of a range of phosphatase enzymes, which are often specific to particular compounds (George et al., 2018). Alternative approaches to increasing P sustainability aim to reduce exogenous P requirements by increasing the bioavailability of these immobilised or organic P forms that have accumulated within soils from many decades of P fertilisation. Some work has focussed on improving P uptake from organic sources by introducing genes for the expression of phosphatase enzymes into the roots of plants. George et al., (2005b)

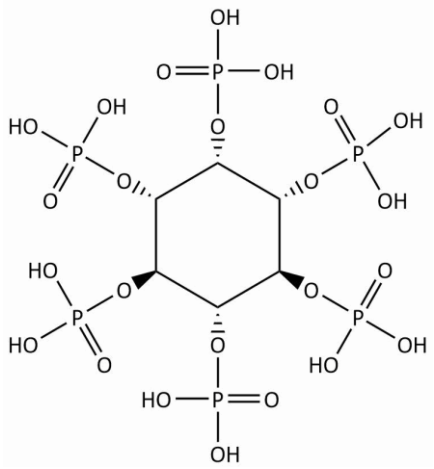

Myo-inositol hexakisphosphate (Phytate)
Orthophosphate monoester (P-O-C bond)

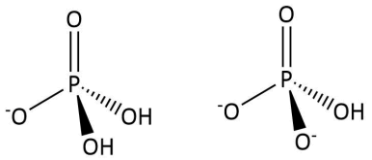

Orthophosphate ($H_2PO_4^-$ or HPO_4^{2-})
(Phytoavailable inorganic P)

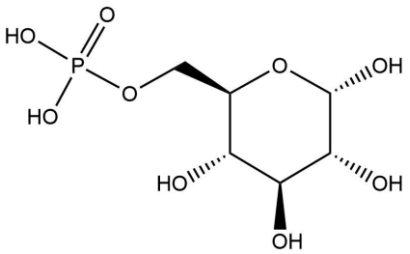

Glucose-6-phosphate
Orthophosphate monoester (P-O-C bond)

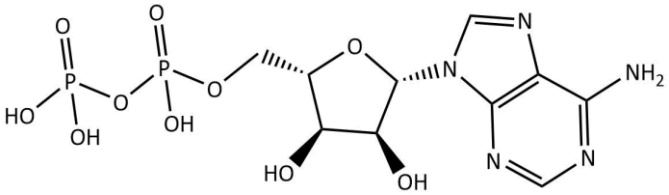

Adenosine diphosphate (ADP)
Organic polyphosphate (P-O-P bond)

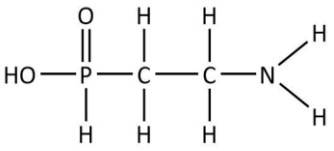

2-aminoethylphosphoric acid
Phosphonate (C-P bond)

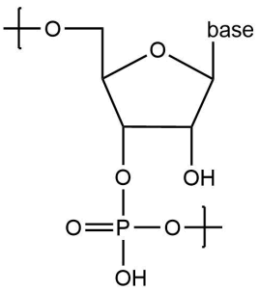

Ribonucleic acid (RNA) monomer
Orthophosphate diester (P-O-C bond)

Figure 1.2: Example forms of common soil phosphorus groups. Orthophosphate is inorganic and is phytoavailable when dissolved in the soil solution. All other compounds shown are organic phosphate compounds, and orthophosphate must be liberated from these compounds to be available for plant uptake. Figure adapted from George et al. (2017).

generated tobacco plants that expressed an *Aspergillus niger* phytase gene, finding that transgenic plants were able to accumulate 3.7-fold more P from phytate-supplemented sterile agar than control plants. However, this effect was not replicated when plants were grown in P-limited soil, possibly due to phytate being bound and unavailable for enzymatic dephosphorylation (George et al., 2005a, 2005b). Many plants respond to P deficiency by upregulating the exudation of low molecular weight organic acids such as citrate from roots into the rhizosphere, which can modify the rhizosphere chemistry to mobilise various P compounds (Richardson et al., 2009). Increasing organic acid exudation, along with increasing the abundance of phosphatase enzymes may therefore be a promising research avenue for the mobilisation of this accumulated 'legacy P'.

1.3 Phytate (*myo*-inositol hexakisphosphate) and its quantification

The inositol phosphates are a family of organic orthophosphate monoesters comprising a central six-carbon inositol ring, with one to six phosphate groups linked via an ester bond (Figure 1.2). Four stereoisomers occur naturally, three of which: *scyllo*-; *neo*-; and *D-chiro*- inositol phosphate are relatively poorly understood (Turner et al., 2002, 2012). *Myo*-inositol hexakisphosphate, also known as phytate, is the most abundant of the inositol phosphates found in nature and is the most important in terms of P sustainability, as it presents a huge reservoir of P which is often highly recalcitrant in soils. For this reason, much work over the past decade has focussed on the quantification, behaviour and manipulation of phytate within environmental matrices.

Phytate is synthesized in plants, forming the main P storage compound in seeds and grains (Gerke, 2015). Lott et al., (2000) estimated that 51 million tonnes of phytate is produced annually in commercial crops, which is equivalent to 67% of annual worldwide phosphate application in chemical fertilizers (Gerke, 2015). Monogastric animals (swine, poultry, fish and humans) are not capable of the efficient digestion and absorption of phytate-P owing to the lack of significant levels of phytate-specific phosphatase enzymes (phytases) in the gut (Menezes-Blackburn et al., 2013). This means that much of the vast amounts of phytate ingested in high-grain diets passes through the digestive tract and is excreted in manure, which can then serve as an important phytate input to receiving soils (Lott et al., 2000; Menezes-Blackburn et al., 2013).

A major challenge faced in the analysis of organic phosphates, including phytate, in environmental samples is the lack of a direct and sensitive analytical technique for their detection and quantification. Direct techniques such as solid-state ^{31}P NMR, fourier-transform infrared spectroscopy (FT-IR) and P-K edge x-ray adsorption resonance spectroscopy (XANES) are useful for the identification and quantification of prepared metal-phytate salts (He et al., 2007a, 2007b), however their use with manure and soil samples is complicated by broad and poorly resolved phytate peaks, owing to the presence of paramagnetic ions in the sample matrix, and the wide variety of P compounds producing overlapping resonances (Giles & Cade-Menun, 2014).

1.3.1 Sample extraction

Most studies instead extract phytate and other P_O from environmental matrices prior to their analysis. Many procedures involve alkaline extractants such as sodium hydroxide (NaOH), which solubilize P_O by increasing the negative charge within matrix components creating electrostatic repulsion, and by substituting strong polyvalent bridging cations such as Al^{3+} with weaker cations such as Na^+ (Turner et al., 2005a). However, the extraction efficiency of alkaline solvents can depend on the sample pH. For example, in alkaline (calcareous) soils, calcium precipitates can form, which are relatively insoluble in alkaline extractants (Turner et al., 2005a). For this reason, some studies employed a two-step extraction procedure, first extracting in an acid, then an alkali (Mehta et al., 1954; Steward & Oades, 1976). Extractions using strong acid and alkali solvents however may pose the risk of hydrolysis of P_O to P_I (Turner et al., 2005a). In response to this, milder extraction techniques have been adopted recently, with the most popular involving a fast, single-step extraction with 0.25M NaOH in the presence of 0.05M Ethylenediaminetetraacetic acid (EDTA) (Bowman & Moir, 1993; Turner et al., 2005a; Giles & Cade-Menun, 2014). EDTA releases P from paramagnetic ion complexes (Turner et al., 2005a), improving P solubility and increasing extraction efficiency. Despite the improvements achieved in P_O extraction with the NaOH + EDTA solvent, extraction efficiency can still vary depending on the sample matrix. In relatively organic samples, a high P recovery is often achieved. For example, in manures of poultry, cattle and swine, Turner, (2004) achieved recoveries of 96%, 80% and 95% of total P by extraction in 0.25M NaOH + 0.05M EDTA. Similarly high extraction efficiency was found by He et al.,

(2009) in poultry and cattle manure, and in anaerobically digested human sludge, recovery of 92% of total P was achieved (Annaheim et al., 2015). Soils are more heterogenous in nature than these organic matrices, containing diverse minerals and clays, varying organic matter content, and exhibiting wide-ranging pH. As a result, the extraction efficiency achieved is often more variable, with greater recovery in soils with high P concentrations from organic amendments, and lowest in alkaline soils (Cade-Menun & Liu, 2014), due to the low solubility of calcium precipitates in the alkaline solvent. This heterogeneity means that it is unlikely that a universally effective extractant will be developed, but the NaOH + EDTA extractant is currently the most effective, often extracting the greatest concentration and greatest diversity of P compounds than other solvents, with less hydrolysis of compounds (Cade-Menun & Preston, 1996), and is the standard extractant in the field, enabling more straightforward comparison of results between studies (Cade-Menun & Liu, 2014).

1.3.2 Enzymatic Quantification

Numerous analytical methods exist for the identification and quantification of phytate and other P_O compounds. Enzymatic hydrolysis procedures are able to provide information on enzyme-labile P_O forms via the determination of the inorganic phosphate released during enzyme incubation by molybdate colorimetry (Giles et al., 2011). Molybdate colorimetry is based on the production of phosphomolybdate heteropoly-acid from the reaction between free dissolved inorganic phosphate with acidified ammonium molybdate. The phosphomolybdate is then reduced, producing a blue colour that can be measured by spectrophotometry (Murphy & Riley, 1962; Turner et al., 2006). In an enzyme assay, inorganic P is measured before and after an enzyme incubation, with the difference in phosphate concentration attributed to the hydrolysed phosphate from the target P_O compound. He et al., (2009) successfully measured phytate in NaOH + EDTA extracts of poultry and cattle manures by phytase incubation, but incubations of soil have had more limited success. Turner et al., (2003a) used a range of enzymes to measure P_O in water extracts of Australian pasture soils. They found that preparations of phosphomonoesterase and phosphodiesterase enzymes were specific to their target compounds, but their crude phytase preparation had a wide substrate specificity, hydrolysing other compounds in addition to phytate. Furthermore, they

found that activity of phytase appeared to be reduced in extracts of moist soils, possibly due to inhibition by humic and mineral substances (Turner et al., 2003a). The substrate specificity of many phytases also extends to the stereoisomers *scyllo-, D-chiro-,* and *neo*-inositol phosphates, which are often present in soils, albeit at lower concentrations, meaning that the specific quantification of phytate is unlikely and results should instead be interpreted as 'phytase-labile P' (He et al., 2011).

1.3.3 Chromatographic Techniques

Whilst enzyme hydrolysis methods are often less time-consuming, less complex and less expensive than more specific analytical techniques, the information that they can provide is often limited to broad groups of P_O compounds. Chromatographic procedures such as high-performance liquid chromatography (HPLC), and high-performance ion chromatography (HPIC) can provide more detailed information by separating specific compounds in a sample based on their structure and interaction with the stationary phase of a separation column (Giles et al., 2011). A difficulty with these methods is the general requirement for acidic extraction of samples, as alkaline solvents may damage separation columns and cause interference (Ray et al., 2012). Furthermore, the detection of phytate and other inositol phosphates is difficult as phytate lacks a chromophore, meaning that traditional detection by UV absorption is not possible (Rugova et al., 2014). Leytem et al., (2008) analysed P compounds in poultry manure by HPLC of acidic extracts, and determined phytate concentrations by post-column derivatisation with $FeCl_3$, followed by spectrophotometric detection. Their results correlated well with parallel sample analysis by alkaline extraction and solution ^{31}P NMR, likely due to the high extraction efficiency achieved by both methods. More direct detection has been achieved recently by McIntyre et al., (2019), who developed a method for the separation and quantification of phytate in alkaline extracts of soil by anion-exchange chromatography with detection by high-resolution electrospray ionisation mass spectrometry. Chromatographic separation and detection by mass spectrometry is a promising analytical technique, as it highly sensitive and able to provide both structural and quantitative information (McIntyre et al., 2017), and it will undoubtedly gain popularity in coming years for phytate and wider P_O research.

1.3.4 Solution ^{31}P NMR

Solution ^{31}P NMR analysis of NaOH-EDTA extracts is by far the most popular analytical method for the detection and quantification of organic phosphate compounds in environmental samples such as manure, sludge and soil as it provides the most detailed and accurate data available (Doolette & Smernik, 2011).

Atomic nuclei that have an odd number of protons and neutrons (^{31}P, ^{1}H, ^{13}C) have magnetic properties, acting as dipoles due to their positive charge and spin properties (Cade-Menun, 2011). When these nuclei are exposed to an external magnetic field in NMR, their orientation ceases to be random and they align either parallel or antiparallel (precisely 180° in the opposite direction) to the magnetic field. These orientations are described as low or high energy configurations respectively, with the low-energy state being the most favourable at thermal equilibrium (James, 1998). At this thermal equilibrium, nuclei may spontaneously but infrequently transition between the two energy states. However, when a radio frequency (RF) pulse with energy equal to the difference between the two energy states is applied to the nuclei, they can absorb energy and 'resonate', transitioning between the two energy states with much greater frequency (Figure 1.3). The absorption of energy by the spinning nuclei induces a voltage that can then be detected as a signal, with the signal displayed as a free induction decay (FID) (James, 1998; Cade-Menun, 2011). Different compounds within a sample have

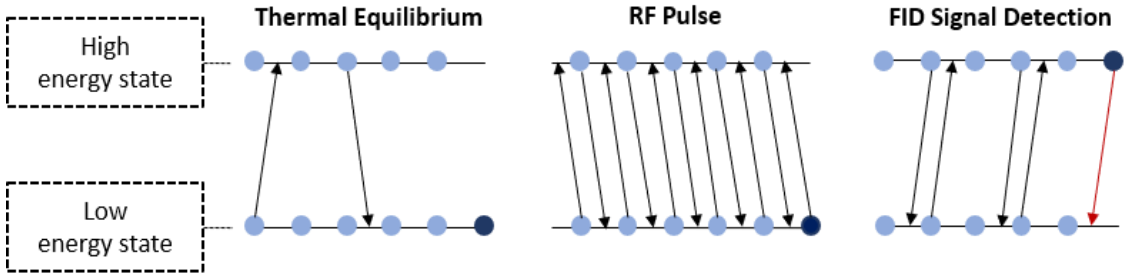

Figure 1.3: Transitions of nuclei (blue) between energy states in NMR. At thermal equilibrium, there is a small excess in the population of nuclei in the lower energy state (dark blue), and infrequent transitions between the two states (black arrows). On application of the RF pulse, resonating nuclei transition between energy states at the same rate, but with much greater frequency. Due to the excess population in the low energy state at thermal equilibrium, there are more transitions from low to high energy state, creating a non-equilibrium population of nuclei at the high energy state. Following the RF pulse, the FID is produced only from nuclei in this excess population as they transition back to the low energy state (red arrow), because the other nuclei effectively cancel each other out. Figure adapted from James, (1998).

varying electron configurations which can shield the nuclei, meaning the amount of energy required for their resonance is different depending on the chemical environment of the nuclei. Therefore, nuclei in different environments absorb and emit energy in different ways, producing different resonance signals in the FID. The FID is then Fourier-transformed to produce an NMR spectrum with peaks for nuclei in each chemical environment plotted as 'chemical shift' (Cade-Menun, 2011).

As ^{31}P is the only naturally occurring stable isotope of P, ^{31}P NMR is theoretically able to detect all P species in a sample in a single analysis, and under the appropriate experimental parameters is robustly quantitative, as the area under each spectral peak is proportional to the number of P nuclei in a particular molecular configuration (Cade-Menun, 2005). However, ^{31}P NMR suffers from limitations of both low sensitivity and low resolution.

Sensitivity in NMR is inherently low because the FID signal can only be detected in the small excess population of nuclei that exists in the low energy state relative to the high energy state at thermal equilibrium (James, 1998). For example, in a population of nuclei at thermal equilibrium, the ratio between the nuclei in the low and high energy states might be 0.999872. This means that in a population of 2,000,000 nuclei, there would be 1,000,000 nuclei in the high energy state, and 1,000,128 in the low energy state. When the RF pulse is applied, nuclei resonate between the low and high energy states at the same rate, but as the population of nuclei is greater in the low energy state, there will be more transitions from low to high, resulting in nonequilibrium populations (Figure 1.3). The resonance of only the 128 excess nuclei is detected when the RF pulse is applied because the other nuclei effectively cancel each other out (Figure 1.3; James, 1998). Sensitivity can be improved by increasing the sample concentration, thereby increasing the population of nuclei in a sample, and this is commonly achieved in analyses of soil extracts by freeze-drying and resuspending extracts.

Resolution in ^{31}P NMR can also be an issue. Figure 1.4 shows a typical ^{31}P NMR spectrum of a soil extract. Many peaks are clearly separated and well resolved. However, some signals, particularly those generated by orthophosphate monoesters such as phytate, are densely packed into a small region, and often overlap, leading to difficulty in peak

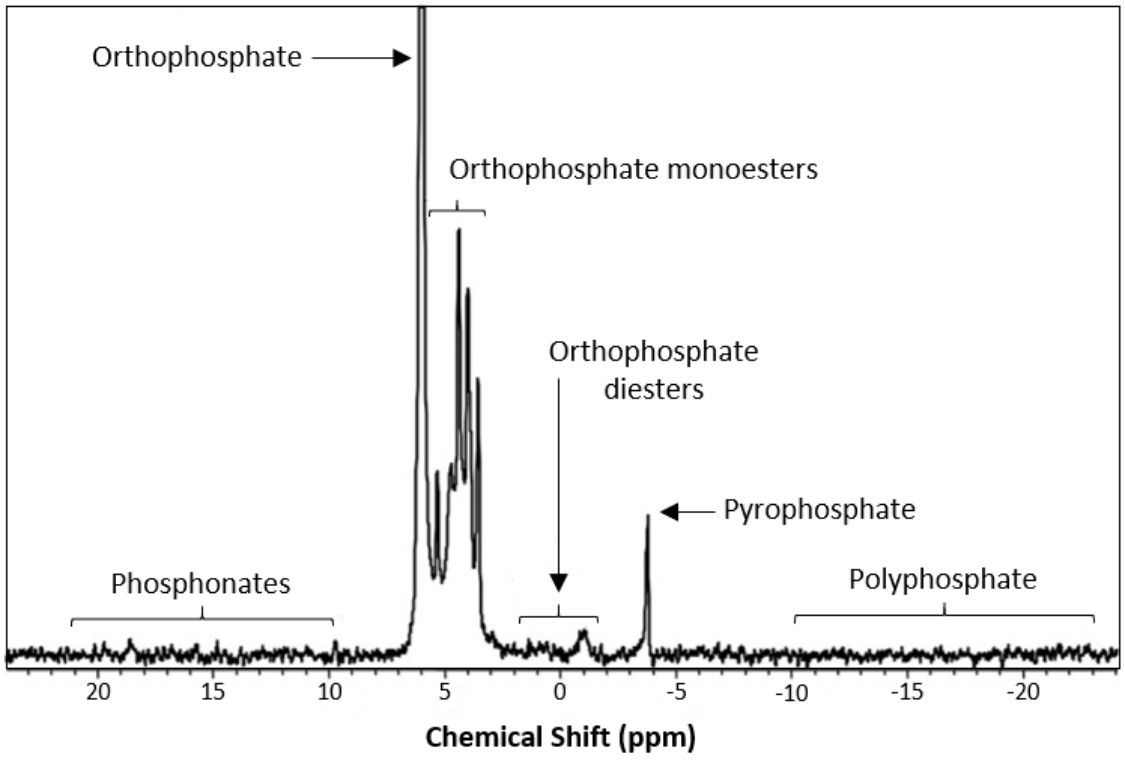

Figure 1.4: A typical solution ^{31}P spectrum of a NaOH-EDTA extract of soil. For some compound groups, peaks are sharp and well separated. However, the orthophosphate monoester region can often be crowded and poorly resolved. Figure adapted from Cade-Menun et al., (2012).

assignment and quantification (Doolette & Smernik, 2011). Compounds can be quantified by measuring the areas under peaks generated for nuclei in a particular compound and comparing them to the peak area of an internal standard of known concentration. A major consideration within this procedure is that for quantitative experiments, nuclei must be allowed to relax to thermal equilibrium between scans. Larger molecules have a shorter relaxation time constant (T1) than smaller molecules, meaning that their nuclei return to equilibrium at a faster rate after the RF pulse. This means that an experiment using inadequately short relaxation delay times between scans is likely to generate less signal for small molecules relative to larger molecules, as the small molecules are less likely to have reached equilibrium before the subsequent application of an RF signal, and means that some compounds are likely to be underestimated relative to others (Doolette & Smernik, 2011). This is often overcome by using long delay times between RF pulses (scans) to allow full relaxation, but because of the low inherent sensitivity of NMR, many thousands of scans are commonly required to generate an acceptable signal to noise ratio in the spectrum, resulting in unacceptably

long analysis times. Robertson, (2018) developed a ^{31}P NMR method that enabled the quantitative measurement of both orthophosphate and phytate using a short delay time of 1s. In this method, short experiments were run prior to soil analysis on soil extracts spiked with orthophosphate and phytate, in which spectra were produced over sets of 100 scans with increasing delay times. A correction factor could then be calculated to predict the peak area of the fully relaxed compound relative to that produced at 1s, allowing both an increase in sensitivity due to the facilitation of a greater number of scans when using a short delay time, and quantitative interpretation of the spectra produced when employing a relaxation delay time of 1 second.

1.4 The behaviour of phytate in environmental samples

1.4.1 Phytate in livestock manure

The development of standard methods for phytate analysis and their application to wide-ranging environmental samples has resulted in a much-improved understanding of the behaviour of phytate in environmental samples and the role it plays in the anthropogenic P cycle. The abundance of phytate in manures depends on the physiology of the animal, and the amount of phytate in its diet. The manure of grain-fed poultry typically has the highest phytate concentration (Ajiboye et al., 2007; Giles & Cade-Menun, 2014), due to their monogastric digestive system, which has low phytase enzyme activity compared to ruminant animals. Swine are also monogastric, and it would be assumed that their manure would be rich in phytate due to largely grain based diets in commercial farms. However Leytem & Thacker, (2008) measured only low levels (<6%) of phytate in manure from swine fed a range of high-phytate diets, suggesting that microflora present in the pigs hind gut are able to produce phytase enzymes to dephosphorylate phytate. Despite this phytase activity in the hind gut, modern swine diets are often supplemented with commercial phytase enzymes and the benefits of this are two-fold. There is little evidence that phosphate is absorbed in the hindgut (Leytem & Thacker, 2008), meaning that swine gain little benefit from phytate dephosphorylation occurring there. Supplementation with phytase releases phosphate from phytate earlier in the digestive tract, where it can be absorbed in the small intestine, reducing the need for supplementation of feed with exogenous phosphate.

Furthermore, phytate degradation reduces its tendency to complex important nutritional cations such as calcium, iron and zinc, again reducing the need for supplementation of diets with these minerals (Jorquera et al., 2008).

Due to the vast global population of cattle and their greater rate of excretion, bovine manure is responsible for a greater input of phytate to soil than monogastric animals, despite the presence of phytase in their ruminant gut (Menezes-Blackburn et al., 2014). The gut microflora of cattle is able to produce phytase enzymes that dephosphorylate ingested phytate (Menezes-Blackburn et al., 2013), but phytate is degraded surprisingly inefficiently. Toor et al., (2005) noted a reduction in phytate from 32% of total P in feed to 18% in manure, with the persistence of phytate possibly due to its high concentration, its rapid passage through the gut, or via its precipitation to insoluble salts (Menezes-Blackburn et al., 2013).

1.4.2 Phytate in human excreta

As with livestock, the amount of phytate in human excreta depends on the amount consumed in diets. Phytate is the main P compound in grain, and so is abundant in human diets, and particularly so in those high in grain (Raboy, 2003). Phytate cannot be directly absorbed in the human gut, and being monogastric, humans lack phytase enzymes for its efficient dephosphorylation. Despite the large amount of studies that have quantified phytate in animal manures, very little work has focused on the phytate content of human excreta. Joung et al., (2007) used HPLC to measure phytate concentrations in faeces of women consuming high- and low-phytate diets. They found that like in swine, a considerable amount (74-93%) of consumed phytate is degraded in the human gut, concluding that much of this degradation takes place in the colon. Despite this level of degradation, faecal phytate-P concentrations varied between 4-11mg P g^{-1} excreta, constituting between 24-54% of total faecal P.

In many modern societies, human excreta is processed in wastewater treatment plants (WWTPs), in which solids, nutrients and pathogens are removed from waste water which can then be cleaned and returned safely to the environment (DEFRA, 2012). This process produces a large volume of solid waste known as sludge, which is then often processed via anaerobic digestion to reduce its volume, destroy pathogens, and to yield

methane gas which can be used as an energy resource. The resulting digested solids are rich in nutrients and organic matter, and in the UK 80% of these are returned to land as a soil conditioner and nutrient source (DEFRA, 2012). Industry and stakeholder agreed guidelines known as the 'Safe Sludge Matrix' provide a code of practice for land application of sludge in the UK (Water UK, 2010; BRC et al., 2001). Alongside government guidelines, this ensures that application is strictly controlled, with the requirement that soil is tested prior to sludge application to provide an indication of nutrient requirement and to ensure that heavy metal concentrations remain within limits. Untreated or low quality sludges containing unacceptable pathogen or heavy metal loads are not permitted to be spread and must undergo further processing or be subject to alternative routes of disposal (Water UK, 2010).

The increasing adoption of P recovery and direct application of sludge to land has brought elevated interest in the characterisation of P species within wastewater and sludge. Considering that plants are only able to take up dissolved inorganic orthophosphate, much of which can be rapidly immobilised within the soil environment much like phytate, it is important to understand P speciation and concentration within sludge prior to its application to soils (Peng et al., 2010). With human faecal phytate content measured at 24-54% of total P (Joung et al., 2007), it is likely that wastewater sludge is rich in phytate. In anaerobically digested sludges, inorganic orthophosphate has been found to be the predominant P form (Hinedi et al., 1989; Escudey et al., 2004; Li et al., 2018; Cade-Menun, 2005), whereas aerobically digested sludges tend to have a greater variety and concentration of organic P species (Peng et al., 2010; Hinedi et al., 1989). In anaerobically digested sludge, Annaheim et al., (2015) used ^{31}P NMR to analyse P speciation and revealed 91% to be present as inorganic orthophosphate, with the remaining 9% identified as phytate. Few studies have attempted to assess the speciation of phytate throughout the various treatment stages in a WWTP. Smith et al., (2006) characterised P compounds in undigested liquid sludge, anaerobically digested liquid sludge and dewatered cake from a single WWTP. ^{31}P NMR analysis identified orthophosphate as the dominant pool of P in all three sludge types, making up 65-77% of the total extracted P, but they also found that levels of phytate remained unaltered by anaerobic digestion, comprising close to 10% of the total P content in all sludge

extracts. In contrast, despite not measuring phytate concentration specifically, Li et al., (2019) found that orthophosphate monoesters were completely degraded by anaerobic digestion, with orthophosphate being the only P compound detected in digested sludge.

These potentially contradictory results show that it is unclear whether phytate persistence during anaerobic sludge treatment process is ubiquitous, and further work is required to measure phytate concentration through the multiple stages of the process. Recently, large, modern WWTPs have begun to employ 'advanced anaerobic digestion' processes, in which an additional sludge hydrolysis step is performed prior to digestion. This step hydrolyses cells within the sludge via thermal, chemical or mechanical processes, improving the destruction of pathogens, and releasing cell contents , resulting in an improved efficiency of AD and increased methane production (Carrère et al., 2010). There are currently no studies that have assessed the impact that the introduction of this hydrolytic step has had on P speciation in digested sludges, and it is possible that improved cell lysis, and the resulting increased microbial degradation of released compounds will have a large effect on anaerobically digested sludge P.

1.4.3 Phytate in soil

Phytate enters the soil in plant residues and animal faeces, and is often the dominant P_O species in the soil due to relatively low lability, caused by its tendency to form strong interactions with the soil solid phase (Jørgensen et al., 2015). The six phosphate groups of phytate and its resulting high anionic charge density mean that phytates can bind much more strongly to soil solids than most other P compounds. For example, on a per molecule basis, phytate sorption capacity is in the region of four times that of the orthophosphate anion (Richardson et al., 2006). Strong adsorption of phytate to soil compounds such as metal oxides is also governed by the negative charges of the phosphate moieties. Shang et al., (1990) found that fully phosphorylated phytate (containing 6 phosphate moieties) adsorbed to an aluminium oxide much more rapidly than the largely dephosphorylated phytate subsidiary *myo*-inositol monophosphate (1 phosphate moiety), due to its greater affinity for the aluminium oxide surface, which indicates that phytate may compete for adsorption sites with other P compounds. Phytate also associates with clays in soil via interaction of the multiple phosphate groups

with positively charged multivalent bridging cations such as Fe^{3+} and Al^{3+} on the clay surface (Giaveno et al., 2008).

Due to the low lability and low degradation of phytate relative to other organic P compounds, phytate undergoes preferential stabilisation, and it is often stated that it preferentially accumulates in soils (Turner et al., 2002; Menezes-Blackburn et al., 2013; Celi et al., 2001). For example, Dao, (2004) reported that seven repeated applications of dairy manure at a rate of 30 kg P ha^{-1} increased soil storage of complexed phytase-labile P to a concentration of approximately 80 mg P kg^{-1}. However, in the past decade, studies have shown that phytate applied to soils can also become rapidly hydrolysed. Doolette et al., (2010) demonstrated that when applied to calcareous soils, only 12% of initial applied sodium phytate was present after 13 weeks of incubation, and Leytem et al., (2006) similarly showed that phytate in poultry manure added to a calcareous soil also declined over time, indicating that phytate was mineralised during incubation. These findings are not limited to calcareous soils either, as when Annaheim et al., (2015) compared acidic soils that had received continuous additions of compost, manure and dried sewage amendments, they found no difference between the soil P_O content, despite differences in P_O content of the organic amendments, indicating that no significant accumulation of specific P forms had occurred.

These findings indicate that there is no common pattern to the tendency of phytate to accumulate, and that its persistence or lability in soils is governed by a range of complex factors, that may be specific to each soil studied. It is possible that phytate accumulation is exacerbated in soils in which microbial turnover is limited. Stutter et al., (2015) analysed soil P forms in a wide range of British soils, reporting that arable soils were dominated by orthophosphate, with a large fraction of monoester P. In the same soils, P compounds that are indicators of microbial turnover such as nucleic acids and phospholipids were much lower than in grassland soils. The authors concluded that the natural ability of soil, plants and microbes to cycle organic P had been depressed in areas of high fertiliser inputs. Crop monocultures can reduce the soil microbial diversity (Stutter & Richards, 2012), and this may therefore cause accumulation of organic P such as phytate that is strongly sorbed, and therefore sparingly mineralised by microbial phytase enzymes. Soil management practices may also have an effect, as Cade-Menun

et al., (2010) measured greater phytate concentration in no-till soils than traditionally tilled soils at all depths measured.

1.5 Phytate mobilisation

1.5.1 Phytase enzymes

Phytases are a broad group of phytate-specific phosphatase enzymes which are widespread in nature and are produced by plants, animals, bacteria and fungi to catalyse the step-wise dephosphorylation of phytate into its lower ester derivatives *myo*-inositol pentakis-, tetrakis-, tri-, bis-, and mono-phosphate whilst liberating inorganic phosphate (Figure 1.5; Jorquera et al., 2008). Four sub-classes of phytase enzymes are known: histidine acid phosphatases (HAPs); cysteine phytases (CPhy); purple acid phosphatases (PAPs); and β-propeller phytase (βPP; Giles et al., 2011). Each class varies in its mechanism of dephosphorylation which can depend on pH and co-factor cations (Giles & Cade-Menun, 2014). Phytase enzymes are key to the cycling of phytate-P and are responsible for liberating phytate-P in a number of key processes, including seed germination, digestion and nutrient acquisition in plants. They have also been isolated and commercialised and are now commonly used to aid phytate digestion in livestock fed grain-based diets (Jorquera et al., 2008).

1.5.2 Mobilisation of soil phytate by phytases

Phytases in soil predominantly originate from microbial sources, with smaller inputs from phytase endogenous to animal manures, and small amounts from plant roots (Menezes-Blackburn et al., 2013; Giles & Cade-Menun, 2014), and these extracellular phytases can be produced by microbes in response to limited available P concentrations (Konietzny & Greiner, 2004). The activity of these enzymes in the soil can be governed by a wide range of factors, including soil pH, temperature, water content and soil chemical and physical conditions, and if these conditions are sub-optimal, enzymes can become rapidly immobilized or denatured (George et al., 2005a; Giles & Cade-Menun, 2014). The solubility of both the phytate substrate and the phytase enzyme in soils is

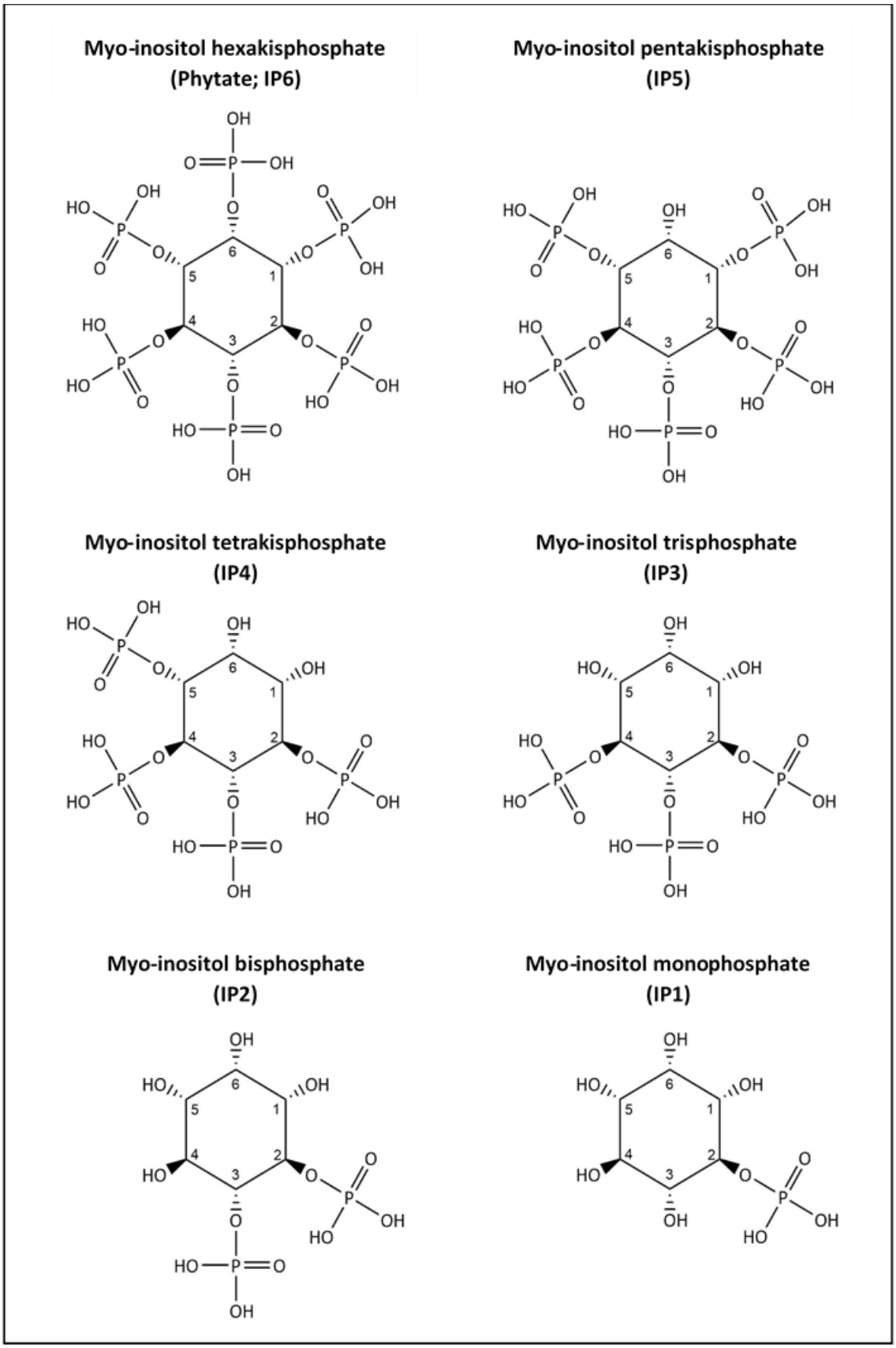

Figure 1.5: Phytate and its partially dephosphorylated subsidiaries. Phytate is sequentially dephosphorylated by enzymatic hydrolysis of the ester bond between the phosphate groups and the central 6-carbon inositol ring.

key for phytase activity in soils. Phytate that is strongly adsorbed to the soil solid phase, or precipitated with metal cations and no longer soluble is afforded a level of protection from hydrolysis (Dodd & Sharpley, 2015). Enzymes have been shown to exhibit an affinity for the interface between the soil solid and solution phases due to complex hydrophilic and hydrophobic molecular forces (Quiquampoix et al., 2002), and thus can also become immobilised in soils via adsorption to mineral surfaces and organic matter by electrostatic interaction (George et al., 2005a). Adsorption of fungal phytases seems to be dependent on both soil pH and the isoelectric point (the pH at which the enzyme carries no net electrical charge) specific to the enzyme (George et al., 2005a). These factors determine the extent of electrostatic attraction or repulsion of enzymes to the soil solid phase, and so have a significant impact on adsorptive tendencies. In their study, George et al., (2005a) found that adsorption of *Aspergillus niger* phytase was greatest at a soil pH of 4.5, below its reported isoelectric point, and decreased as pH increased, until all phytase was in solution at pH 7.5 due to greater electrostatic repulsion above the isoelectric point. Adsorption reduces the mobility of enzymes in the soil solution and can therefore reduce their interaction with substrates. It can also cause irreversible deactivation of enzymes due to conformational changes within the molecular structure (Leprince & Quiquampoix, 1996). Alternatively, adsorption may also maintain phytase activity in some circumstances by providing protection against protease activity and microbial degradation (Naidja et al., 2000), and may be a mechanism that enables the persistence of enzyme activity in soils in the long term (Giles & Cade-Menun, 2014). For example George et al., (2005a) found that the activity of an *Aspergillus* phytase adsorbed to soil declined 2-4 times slower than in the absence of soil.

Soil phytase activity is supported in the rhizosphere by the exudation of organic acids from plants and microbes (Giles & Cade-Menun, 2014; Giles et al., 2017). These organic acids such as ascorbate, citrate and oxalate enhance the solubility of phytate by chelation or dissolution of phytate complexes with metals and minerals (Giles et al., 2012), making phytate available in the soil solution for enzymatic degradation. In addition, organic acids may enhance the solubility of phytase enzymes. George et al., (2005a) found that in low-sorption capacity soil, *A. niger* phytase adsorption was reduced in rhizosphere soil compared to bulk soil, which may be due to increased

organic acid abundance in this soil which has been shown to improve the solubility of other phosphatase enzymes (Huang et al., 2003). The complementary nature of phytase and organic acid exudation was recently demonstrated by Giles et al., (2017), who showed that transgenic plants that exhibited combined phytase and citrate exudation accumulated more P, and depleted a greater proportion of soil phytase-labile P than plants that exuded either phytase or citrate individually. Work such as this shows that as our understanding of these complex soil molecular interactions increases, they could yield promising mechanisms for increasing the uptake of P from accumulated organic P sources, potentially reducing our reliance on chemical fertiliser inputs in the future.

1.5.3 Applications of phytase enzymes

Due to the ubiquity of phytate in environmental and agricultural samples such as grain, manure, excreta and soil, there has been a great deal of interest during the past two decades in the application of phytase enzymes to samples. Phytase enzymes are now commonly applied as a supplement to the grain-based feed of livestock, particularly monogastrics, where they serve to aid phytate dephosphorylation in the gut, providing otherwise unavailable P to the animal (Jorquera et al., 2008). The dephosphorylation of phytate in this application has further benefits, as it decreases the anti-nutritional chelation of valuable divalent cations (eg. Zn^{2+}, $Fe^{2+/3+}$, Ca^{2+}) by phytate in the diet, decreases the need for supplementation of diets with extra bioavailable phosphate, and thereby can decrease the concentration of P in manures by 50% (Jorquera et al., 2008).

As well as animal feeds, there is great potential for the manipulation of phytase enzymes in soil plant systems to increase P uptake from accumulated phytate. However, as discussed in section 1.5.2, the heterogeneity of soils, and the tendency of both phytate and phytase enzymes to become bound to the soil solid phase poses a challenge. George et al., (2005b) generated *Nicotiana tabacum* plants that expressed a chimeric phytase gene from the soil fungus *A. niger* and found that plants grown in a phytate-supplemented sterile agar accumulated 3.7 fold more P than non-transgenic plants. When grown in phytate amended soil, this translated to a more modest 50% increase compared to control plants, but when grown in unamended P-deficient soils, no benefit was demonstrated in transgenic plants, indicating that phytate availability is a limiting

factor. As discussed in the previous section, a greater understanding of the complex chemistry of the rhizosphere is yielding improved results, as a transgenic plant simultaneously exuding both organic acids and phytase enzymes can absorb more P than plants exuding either individually (Giles et al., 2017). This shows that there is great promise for the manipulation of soil phytase enzymes for the provision of phytoavailable P from organic P compounds. An alternative approach involves the direct application of phytase enzymes to soils in order to increase phytase activity artificially. Menezes-Blackburn et al., (2011) demonstrated that high enzyme activity could be maintained when *E. coli* and *A. niger* commercial feed-additive phytases were immobilised on allophanic nanoclays. They proposed that these phytase-nanoclay complexes could provide a novel biofertilisation strategy by maintaining and supporting the exogenous phytase activity in complex manure and soil environments. In a subsequent paper, they evaluated the ability of these complexes to dephosphorylate phytate in dairy manures. They found that the stabilised phytases were not able to hydrolyse a significant amount of P_O in unbuffered manure due to the alkaline pH, but when the phytase-treated manure was added to soil under greenhouse conditions, phytase hydrolysis proceeded to influence both P nutrition and plant growth, providing an increase in available P equivalent to 151 kg P ha^{-1} (Menezes-Blackburn et al., 2014). Work such as this highlights the potential benefits that could be gained by the use of phytase in biofertilisation strategies, and further work under field conditions will be of great interest.

1.6 Aims and objectives of this thesis

This thesis aims to use a range of analytical methods to investigate the behaviour and concentration of phytate through the wastewater treatment process, to assess whether it constitutes a substantial proportion of P in the digested sludge that is commonly spread on agricultural land in the UK. Whether phytate accumulates upon its application to soils is disputed, and this accumulation may be affected by a range of factors. Therefore, this thesis aims to assess phytate levels in agricultural and natural grassland soils, including a soil recently converted from arable land to a field housing monogastric swine, to understand whether the continuous application of phytate in monogastric manure has resulted in accumulation. Finally, phytase enzymes are a promising tool for improving P sustainability, and are now commercially available for use in animal feeds.

There is potential for their use to mobilise accumulated phytate in soils, but the use of enzymes in soils is challenging due to the low solubility of both enzyme and substrate. This thesis aims to investigate whether a commercially available phytase enzyme is able to provide phytoavailable P from phytate when applied to a simple soil-like substrate, and investigate the effect of clay content on this ability. The following sections provide an overview of the subsequent chapters in this thesis, and the research questions addressed in each.

1.6.1 Phytate analysis by ESI-ToF-MS

Solution ^{31}P NMR spectroscopy is well established as the standard method for the analysis of phytate and other organic phosphates in environmental samples, but suffers from inherent issues of low sensitivity and low resolution (McIntyre et al., 2019). In Chapter 2, the alternative analysis of phytate by electrospray ionisation time-of-flight mass spectrometry (ESI-ToF-MS) is investigated to assess whether it can provide a more sensitive method for the detection of phytate and its dephosphorylated subsidiaries than ^{31}P NMR. Solutions of sodium phytate and potassium phytate are analysed, along with lower inositol phosphates generated during the reaction of phytate with a phytase enzyme. Despite optimisation of the procedure, the occurrence of in-source fragmentation precludes the application of this method in subsequent chapters.

1.6.2 Phytate in sewage sludge

Relatively little work has been carried out to assess phytate content in sludges. As discussed in section 1.4.2, some evidence suggests that phytate is able to persist through anaerobic sludge treatment processes (Smith et al., 2006), although some work also suggests that all organic P is hydrolysed during digestion to leave only inorganic orthophosphate in the sludge (Li et al., 2019). As 80% of processed sludge in the UK is applied to agricultural land (DEFRA, 2012), it is important to understand the fate of phytate through modern advanced anaerobic treatment processes. In Chapter 3, sewage sludge sampled from 5 stages of an advanced anaerobic treatment process is analysed by both solution ^{31}P NMR, and enzymatic hydrolysis with colorimetry to address the first major research question:

1. *Is phytate present in sewage sludge, does it persist through a modern advanced anaerobic digestion sludge treatment process, and does it constitute a substantial fraction of total P in the final sludge 'cake' that is spread on land?*

1.6.3 Phytate in soil

The common assumption that phytate accumulates in soils has recently been questioned, with some research indicating that freshly applied phytate is rapidly hydrolysed in soils (Leytem et al., 2006; Doolette et al., 2010). If phytate applied in organic amendments does accumulate in soils, then this phytate could present a reservoir of P which could be mobilised for plant uptake, thereby reducing reliance on inorganic P fertilisers. In Chapter 4, phytate concentrations are measured in agricultural and grassland soils with varying land-use histories by solution ^{31}P NMR and enzymatic hydrolysis with colorimetry to address the second major research question:

2. *How does the land-use history of agricultural and grassland soils affect the concentrations of phytate in soil? Does phytate accumulate in a previously arable soil that has been converted to a pen housing monogastric swine?*

1.6.4 Enzymatic biofertilisation of phytate-treated plants

Phytase enzymes are commercially produced for use as a supplement for the improved digestion of grain-based livestock feeds, and have had a marked effect on both productivity and P sustainability by combatting the antinutritional effects of dietary phytate, reducing the need for exogenous P inputs, and reducing manure P concentrations (Jorquera et al., 2008). Their use in biofertilisation strategies to mobilise accumulated phytate-P shows great promise but is less advanced. In Chapter 5, a greenhouse-based experiment is developed to test the efficacy of a commercially available phytase enzyme in the provision of phytate-P to plants, with or without the presence of clay in a simple substrate. A number of plant and substrate variables are measured in order to address the third major research question:

3. *Can a commercially available feed-supplement phytase enzyme be used to release phytoavailable phosphate from phytate in a simple soil substrate, and how does clay content affect this ability?*

2: Analysis of phytate and the lower inositol phosphates by ESI-TOF-Mass Spectrometry

2.1 Summary

Solution ^{31}P NMR is by far the most established and successful method for the analysis of organic P in environmental matrices, and has enabled a greater understanding of the types and quantities of the major P compounds in these samples. However, ^{31}P NMR suffers from both issues of inherent low sensitivity, and low resolution, particularly in the orthophosphate monoester region of spectra. This makes the identification and quantification of P compounds that are present at low concentrations, such as the partially dephosphorylated esters of phytate, either difficult or impossible. Electrospray-ionisation time-of-flight Mass Spectrometry (ESI-ToF-MS) holds potential as a highly sensitive alternative analytical method that may enable further advances in our knowledge of the dynamics of these compounds.

Very few studies have used ESI-ToF-MS for the analysis of phytate, but in those that have, the occurrence of in-source fragmentation during phytate ionisation has been reported. This fragmentation involves the removal of phosphate groups from the phytate to produce fragment ions with coincidental mass charge ratios with true dephosphorylated phytate esters, therefore precluding the accurate quantification of these lower esters in mixed samples. Electrostatic conditions within the ionisation process have been shown to affect the severity of phytate fragmentation. The aim of this chapter was to optimise the conditions within ESI-ToF-MS to reduce or eliminate the occurrence of in-source phytate fragmentation in order to develop a highly sensitive method for the analysis of phytate and its dephosphorylated esters. Despite the optimisation of the source voltage and cone voltage within ionisation, the occurrence of fragmentation could not be eliminated, and thus seems to be dependent on numerous emergent factors. As demonstrated via the analysis of phytase-mediated dephosphorylation of phytate, the direct analysis of mixed samples by ESI-ToF-MS can provide valuable qualitative information, but interpretation of quantitative information must be approached with caution.

2.2 Introduction

2.2.1 Detection of Inositol Phosphates in ^{31}P NMR

Solution ^{31}P NMR has become established as the standard method for organic P analysis in environmental samples (Cade-Menun & Liu, 2014), and is a powerful analytical tool because ^{31}P is the only naturally occurring non-radioactive (stable) P isotope. The short half-lives of radioactive P isotopes (maximum 25.34 days; Robinson, 1969) effectively means that P is monoisotopic and thus all P species in a sample can be detected in a single analysis. Great success has been achieved in the detection and quantification of phytate in extracts of environmental matrices, due to its relatively high concentrations within these samples, and its relatively straightforward identification in ^{31}P NMR spectra by the presence of its 1:2:2:1 peak ratio. However, less success has been achieved in the detection of lower order inositol phosphates by ^{31}P NMR. These compounds, the products of hydrolysis of phosphate groups from the phytate molecule (Figure 1.5), are highly likely to be present in soil and manure samples, albeit at much lower concentrations than phytate, due to the activity of phytase enzymes in the rhizosphere or in the gut. However, their detection in these samples by ^{31}P NMR is underrepresented, with a handful of papers describing their presence, or putative presence in extracts of feed and ileal digesta in monogastric livestock (Kemme et al., 1999; Leytem et al., 2008), and an apparent absence of their detection and identification in ^{31}P NMR in extracts of soil.

As discussed in Chapter 1, Section 1.3.4, NMR suffers from the inherent issues of both low sensitivity and low spectral resolution within the orthophosphate monoester region. Sensitivity issues can be somewhat eased by pre-concentrating samples prior to the analysis, but compounds that are present at low concentrations may still not reach the limit of detection. Resolution of the orthophosphate monoester region is also a significant issue, particularly in complex soil samples where there are likely to be a wide array of organic P compounds present, leading to significant overlapping of peaks (see Figure 1.4). Resolution and sensitivity can both be improved by signal averaging, where a sample is run over many, sometimes thousands, of pulse cycles to increase signal to noise ratios, but this then leads to very long analysis time, particularly when long relaxation delay times are employed between pulses. A further complication in soil

analysis is the common observation of a broad 'humic P' peak in the orthophosphate monoester region, which is particularly prevalent in high organic matter soils, and is believed to be produced via the association of orthophosphate monoesters with high molecular weight organic compounds (Doolette et al., 2010; McLaren et al., 2019). This peak would obscure the small monoester peaks that would be generated for lower IPs, making their detection and quantification complex or impossible if they were present at detectable concentrations. An alternative technique would therefore be beneficial for the detection of lower inositol phosphates when they are present at low concentrations.

2.2.2 Electrospray ionisation time-of-flight Mass Spectrometry (ESI-ToF-MS)

Mass Spectrometry (MS) is one of the most sensitive analytical techniques for the characterisation and quantification of molecules and would appear to be a promising approach for the detection of inositol phosphates in low concentrations. In mass spectrometry, an analyte in solution is transferred to a gaseous state and is ionised via the addition ('positive mode') or loss ('negative mode') of one or more protons to give molecular ions with a positive or negative charge. For clarity, this section will discuss the production of negatively charged molecular ions in ESI. Ions are then transferred to a detector, which can record their intensity by their mass:charge ratio (m/z) to produce a mass spectrum. A number of ionisation techniques exist, but electrospray ionisation (ESI) has become the most popular, particularly in studies of large macromolecules, as it is a 'soft' ionisation technique, which reduces or eliminates the propensity for these molecules to fragment during ionisation (Banerjee & Mazumdar, 2012).

Figure 2.1 is a simplified schematic diagram illustrating the ionisation process in ESI. The analyte of interest is dissolved in a polar solvent (e.g. water, methanol) and is pumped into the ionisation chamber via a capillary. The orifice of the capillary is highly charged, with this charge known as the source voltage, and in negative mode, the solvent undergoes reduction reactions supplying negative OH^- ions to the solution (Banerjee & Mazumdar, 2012). Electrostatic repulsion between the negatively charged capillary and the solution causes the formation of a meniscus at the orifice which is then drawn into a cone due to competing electrostatic forces and solvent surface tension. From this cone, a fine jet of solvent droplets carrying the negative charge is ejected as an aerosol

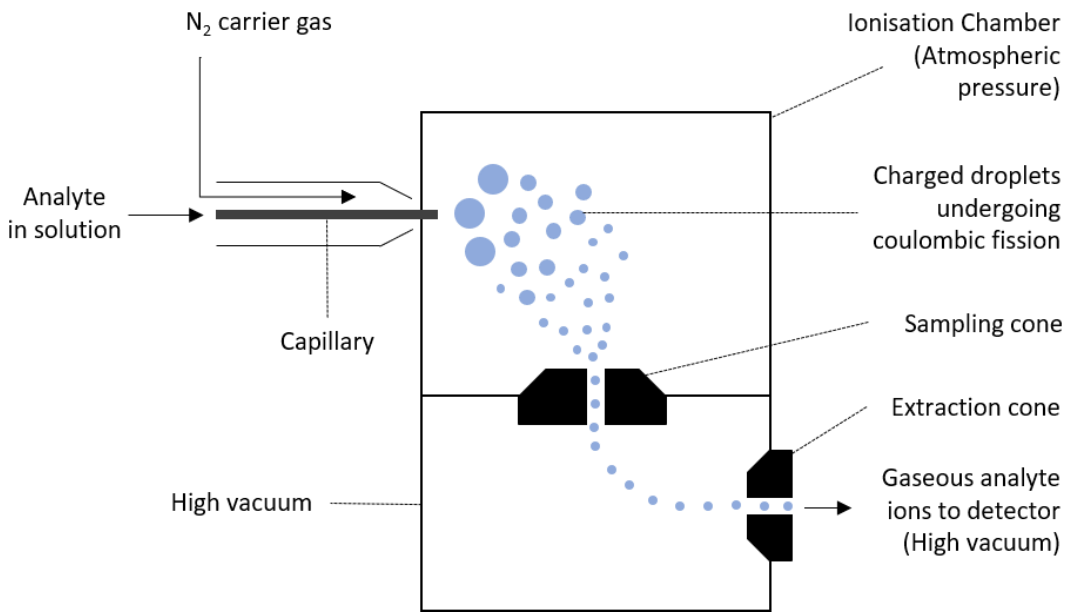

Figure 2.1: Schematic diagram of Electrospray Ionisation (ESI). Analyte in solution is introduced through a thin capillary. The tip of the capillary is highly charged and creates highly charged spray droplets. Solvent evaporates from these droplets which disintegrate into smaller and smaller droplets by coulombic fission, until fully evaporated. The analyte atoms take on the charge of the droplets, becoming naked molecular ions, which then pass down an electrical potential gradient and pressure gradient through the orifice of the sampling cone. From here they are directed through the extraction cone into the mass analyser. Figure adapted from Banerjee et al., (2012).

towards the sampling cone, which acts as a counter electrode. During the passage of droplets between the capillary and the sampling cone, the negative charges are equally distributed on the droplet surface. This means that two forces; droplet surface tension, which acts to maintain the spherical shape of the droplet; and Coulomb forces of repulsion, which act to distort the shape of the droplet; are in direct competition with each other. The nitrogen carrier gas facilitates solvent evaporation from the droplets, reducing their volume and increasing the Coulomb repulsive forces until they are no longer sustained by the surface tension (Banerjee & Mazumdar, 2012). At this point, known as the Rayleigh limit, Coulomb fission occurs, in which droplets spontaneously collapse into many smaller charged droplets (Figure 2.1). This process is repeated many times as the aerosol moves towards the sampling cone, until droplets have disintegrated to highly charged nanodroplets. With the final evaporation of solvent from these nanodroplets, the negative charges are passed from the solvent to the analyte molecules via proton loss (Banerjee & Mazumdar, 2012).

The ions are propelled through the orifice of the sampling cone and into the mass detector via the extraction cone, moving along both an electrical potential gradient and a pressure gradient as the mass detector is held at high vacuum relative to the atmospheric pressure of the ionisation chamber. Time-of-flight (ToF) mass spectrometers detect different ions based on their velocity in the electrostatic field. As all ions are moving through the same field, they have the same kinetic energy, so become separated only by their mass and charge. Detection is therefore achieved by monitoring the arrival of ions at the detector, which will depend on their m/z ratio as a function of time (Cooper et al., 2006).

2.2.3 Inositol phosphate analysis by ESI-ToF-MS

Despite the high sensitivity offered by ESI-ToF-MS analysis, there are few studies that have employed it in the analysis of inositol phosphates. The first direct analysis of a mixture of inositol phosphates by ESI-ToF-MS was carried out by Cooper et al., (2006). A mixture of phytate (IP6) and myo-inositol monophosphate (IP1; Figure 1.5) were introduced to the ion source, but upon detection, the authors were surprised to record the abundant appearance of peaks at m/z ratios that are coincidental with the m/z ratios that would be generated by inositol bis-, tris- tetrakis- and pentakis-phosphates (IP2-IP5; Figure 1.5). Although the authors could not exclude the occurrence of significant contamination of their standards with these other IPs, they concluded that phytate fragmented during the ionisation process, via the breaking of the phosphoester bond (O-P), releasing PO_3^- from the molecule (Cooper et al., 2006). The consequence of this is the production of fragment ions that have the same m/z charge ratio as would be expected for true ions of lower IPs, which therefore complicates the quantification of IPs in mixed samples. Of the few studies that have aimed to identify and quantify IPs using ESI-ToF-MS, most employ a chromatographic separation step prior to analysis in order to exclude potential contaminant IPs from samples (Paraskova et al., 2015; McIntyre et al., 2019).

The cone voltage, which is the voltage of the counter-electrode in ESI, is important in the ESI process as it guides gas-phase ions into the mass spectrometer, but it has been shown to be a critical parameter affecting the fragmentation of ions (Yan et al., 2003).

The voltage at the cone should be sufficient to guide enough ions into the detector and maintain ion intensity, but should be low enough to prevent fragmentation that might occur when the voltage is too high, resulting in increased ion velocity and collisions with other gas phase molecules. Indeed, cone voltage has been found to have a clear effect on the fragmentation of the inositol phosphates in ESI, with Cooper et al., (2006) describing significant fragmentation of all IPs at high cone voltages, and reduced but varying degrees of fragmentation at low cone voltage with a pattern of increasing fragmentation in more phosphorylated IPs.

The source voltage, the high charge at the orifice of the capillary from which the charged droplets are produced, has also recently been shown to affect phytate fragmentation in ESI. McIntyre et al., (2017) identified a pattern of increasing fragmentation with increasingly negative source voltage between -1.6kV and -3.6kV, with the relative proportion of IP6 ions decreasing, accompanied by increasing proportions of IP5 and IP4 ions.

2.2.4 Aims and Objectives

It therefore would seem that there are potentially numerous factors in ESI that affect phytate fragmentation, but of the very little work carried out on inositol phosphates in ESI-ToF-MS, none has sought to optimise more than one of these factors. The aim of this chapter was to develop a method for the direct identification and quantification of phytate and its lower inositol phosphate subsidiaries by ESI-ToF-MS. The adjustment of various ionisation conditions including source voltage, cone voltage and analyte concentration was carried out in order to optimise the system and minimise or eliminate the occurrence of in-source fragmentation. To assess the effectiveness of the optimised analytical procedure on a range of inositol phosphates, the system was used to analyse the production and dephosphorylation of the various inositol phosphates over the course of a reaction between phytate and a phytase enzyme in a continuous flow, real-time analysis. From the results obtained, a discussion follows as to whether this method would be effective for the analysis of inositol phosphates in environmental samples.

2.3 Methods

2.3.1 Solution ^{31}P NMR

For ^{31}P NMR analysis, solutions of 0.5, 0.05 and 0.005mM phytic acid sodium salt hydrate ($Na_{12}C_6H_{12}O_6(HPO_3)_6$; Sigma) were prepared by dissolution of the appropriate mass into a solution containing 9 parts 0.5M NaOH + 0.1M EDTA and 1 part deuterium oxide. 0.5mL of the sodium phytate solution was transferred to a 5mm NMR tube. ^{31}P NMR spectroscopy was performed on a Bruker Advance 500 Spectrometer with a mag1 console (Bruker, Germany). Spectra were recorded at a frequency of 202.456 MHz with a 5mm broadband probe at a temperature of 298 K (24.85°C). During each sample analysis, the following parameters were unchanged: acquisition time = 0.845s; pulse width of 22µs; pulse angle 90°; delay time = 1s; total number of scans = 16,384; pulse program = zgig. ^{31}P NMR data was processed in Bruker Topspin 4.0.3.

2.3.2 ESI-ToF-MS of phytate

Electrospray ionisation time-of-flight mass spectrometry (ESI-ToF-MS) was performed on a Waters Synapt G2-S (Waters Corp., USA). MS analysis was performed in negative ion mode over a mass range of 50-800 Da, and the apparatus was tuned to the singly charged phytate ion (m/z 658.8; $[M-H]^-$). For all analyses, source temperature was set to 350°C, cone gas (nitrogen) flow rate was 10 L H^{-1}, and desolvation gas flow rate was 700 L H^{-1}. Source voltage was varied between -1.5kV and -3.3kV. Cone voltage was initially set to 30V, and was reduced to 20V for cone voltage optimisation.

For phytate analysis, solutions of sodium phytate were prepared in a solution of 5% methanol in UHP water to concentrations of 0.5, 0.05, and 0.005mM. Phytic acid dipotassium salt ($K_2C_6H_{12}O_6(HPO_3)_6$; Santa Cruz Biotechnology) was prepared to 0.5mM in 5% MeOH in UHP. For the generation of phytate spectra, phytate solutions were added to a 25mL PTFE vessel and drawn into the 250 µL internal syringe of the mass spectrometer, then injected into the ESI source at a flow rate of 10 µL min^{-1}. Spectra were acquired as an average of 100 individual scans with a scan time of 1 second. To assess the effect of varying source voltage on phytate spectra, an experiment was programmed into the MassLynx software (Waters, USA) to automatically increase the source voltage between -1.5kV and -3.3kv at increments of 0.2kV after each 100-scan

analysis. To assess the effect of changing the cone voltage, this process was repeated after adjusting the cone voltage from 30V to 20V.

Data was processed in MassLynx (Waters Corp., USA) software to provide an average spectrum. Total intensity of separate inositol phosphate esters (IPs) was calculated in Microsoft Excel by summing the total counts for peaks identified at m/z values representing ions and their respective sodium or potassium adducts.

2.3.3 ESI-ToF-MS of the phytate-phytase reaction

For analysis of the phytase-enzyme mediated dephosphorylation of phytate, an analytical process was designed in which the reaction could be analysed in real-time via ESI-ToF-MS. A 2 FTU mL^{-1} enzyme solution was prepared by dilution of a 20,000 FTU mL^{-1} stock solution of RONOZYME HiPhos (DSM Nutritional Products, Switzerland) in UHP water. 20mM sodium phytate was prepared in UHP water. Prior to the reaction analysis, the ESI-ToF-MS system was first purged with the enzyme solution. 250 µL of enzyme solution was drawn into the internal syringe from a 25mL PTFE vessel, and pumped to the ESI source at a flow rate of 10 µL min^{-1} over a period of 25 minutes. The internal syringe was then emptied and the PTFE vessel was replaced. The reaction vessel contained 9.75mL 2 FTU mL^{-1} phytase, to which was added 0.25mL of 20mM sodium phytate, giving a final concentration of 0.5mM phytate. The reaction solution was manually agitated for 2 seconds then was connected to the mass spectrometer. 250 µL of the reaction was drawn into the internal syringe and was introduced to the ESI source at a flow rate of 10 µL min^{-1}. The reaction was then analysed over a 22-minute period comprising a total of 1288 scans with a scan time of 1 second, with ionisation achieved at a source voltage of -3.1kV, and cone voltage of 20V. Peaks were identified for each IP and their respective sodium adducts, and the total ion counts data for each identified m/z value per scan was transferred into Microsoft Excel. Total ion counts for each IP (IP6-IP1) was then calculated for each scan by summing the total counts for each ion and its respective adducts. Data was then smoothed by calculating a mean ion count for each set of 10 consecutive scans. A total of three replicate reactions were analysed in an identical manner, and a mean reaction was presented over time. Error was calculated as SEM and is presented for each IP separately in individual figures. Figures were produced in GraphPad Prism v7.04 (GraphPad Software Inc, San Diego USA).

2.4 Results & Discussion

2.4.1 Phytate in ^{31}P NMR

The low sensitivity of ^{31}P NMR analysis is demonstrated in Figure 2.2. Three concentrations of sodium phytate at 0.5, 0.05, and 0.005mM were analysed over a total of 16384 scans with a scan time of 1s in order to maximise the signal to noise ratio. Phytate (IP6) can be clearly identified in the 0.5mM solution by the presence of four distinct peaks in a 1:2:2:1 intensity ratio at chemical shifts of 5.63, 4,73, 4.37 and 4.24ppm (Cade-Menun, 2015; Watson et al., 2019). While the four phytate peaks are clearly visible at the 0.5mM concentration, these peaks are much smaller at 0.05mM and are barely visible above the baseline noise in 0.005mM solutions.

What is notable about the 0.5mM concentration is the presence of smaller contaminating peaks within the ^{31}P NMR spectrum of the pure phytate standard. These peaks have been tentatively identified as orthophosphate (5.78ppm) and *myo*-inositol

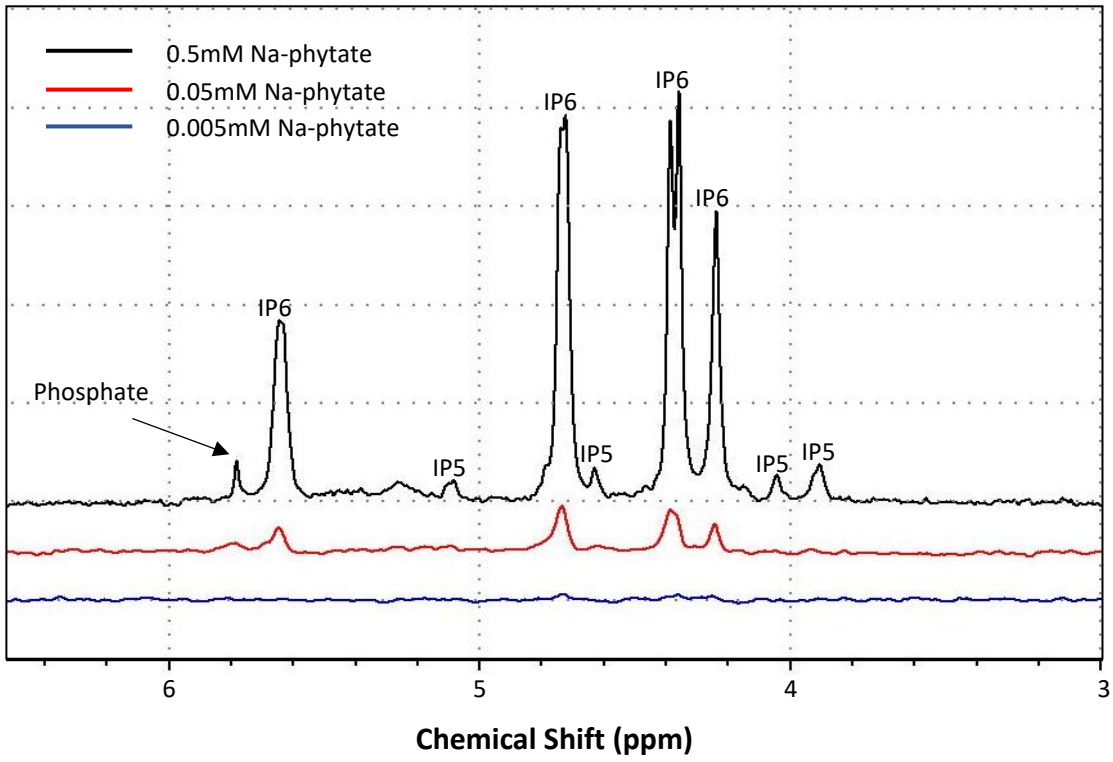

Figure 2.2: Solution ^{31}P NMR spectra of three concentrations of sodium phytate. Spectra are presented on the same intensity scale, highlighting the low resolution of ^{31}P NMR at low analyte concentrations. At 0.5mM, the phytate appears to have a small amount of inositol pentakisphosphate (IP5) impurity (10% of total peak area), which is not visible in lower concentrations. Identification of IP5 peaks was based on peak identification of Watson et al. (2019).

pentakisphosphate (IP5; peaks at 5.08, 4.63, 4.04 & 3.90ppm) by comparison of the relative chemical shifts of IP5 measured by Watson et al., (2019) (Table 2.1). In their study, the major IP5 isomer generated by thermal degradation of IP6 was unsymmetrical, and so generated a separate peak of equal intensity for each P nucleus of IP5 in the NMR spectrum. The chemical shift of these five peaks show the same approximate spectral distribution as those found in this work, although the third potential IP5 peak is obscured by the IP6 peak at 4.37ppm (Table 2.1). Whilst the sum integral of these IP5 peaks is approximately equal to 10% of the sum of IP6 peaks in the 0.5mM phytate spectrum, these IP5 peaks are not detected in the 0.05mM and 0.005mM dilutions (Figure 2.2). This IP5 contamination may be present in the original standard, as the phytate originates from rice, but could also originate due to degradation of the IP6 in the alkaline sample necessary for ^{31}P NMR analysis (Cade-Menun & Liu, 2014).

This result highlights an inherent issue with the detection of IPs by ^{31}P NMR, which is the low sensitivity of NMR as an analytical technique. The main reason for this low sensitivity is that the ratio of nuclei in the sample at the grounded energy level is almost equal to those in the higher energy state (see Section 1.3.4). In NMR, only the difference between these two nuclei populations is detected, meaning that to gain a greater signal, a greater number of nuclei (or higher analyte concentration) is required (James, 1998; Doolette & Smernik, 2011).

The poor sensitivity of NMR is overcome in the study of environmental samples by pre-concentrating samples, via lyophilisation and resuspension of soil extracts in ^{31}P NMR analysis of soil P (Cade-Menun & Liu, 2014). In soils with appreciable concentrations of phytate, this method is usually sufficient for quantitative analysis. However, for the analysis of soils with low concentrations of phytate, or quantification of partially

Table 2.1: Chemical shift (ppm) of IP6 and IP5 peaks measured by Watson et al., (2019), and measured in this study

	IP6				IP5				
Watson *et al*, 2019	5.55	4.64	4.28	4.15	5.01	4.54	4.28	3.94	3.83
This study	5.63	4.73	4.37	4.24	5.08	4.63	-	4.04	3.90
Difference	+0.08	+0.09	+0.09	+0.09	+0.07	+0.09	-	+0.1	+0.07

dephosphorylated phytate such as *myo*-inositol pentakisphosphate (IP5), which may be present in low concentrations, ^{31}P NMR lacks sufficient sensitivity for quantification.

2.4.2 ESI-ToF-MS of Phytate (Sodium phytate and Potassium phytate)

0.5mM sodium phytate was then analysed by ESI-ToF-MS (Figure 2.3). Compiled as a mean spectrum of 100 individual scans, the spectrum revealed a complex mixture of ions, with peaks present for both singly $[M-H]^-$ and doubly $[M-2H]^{2-}$ charged anions of a range of IPs with varying degrees of dephosphorylation, as well as numerous peaks for each IP that represent ion-adduct formation with one or more sodium cations. The major peaks that were identified for 0.5mM sodium phytate are presented in Table 2.2.

The spectrum generated contained substantial amounts of ions at m/z values that would be expected for the multiple dephosphorylated phytate subsidiaries (IP5-IP1), which indicates two potential issues: contamination of the phytate standard with these lower inositol phosphates; or the occurrence of 'in-source fragmentation' whereby the ionisation conditions in ESI lead to the loss of phosphate (PO_3^-) groups producing fragment ions in the mass spectrum with coincidental m/z ratios with those of true lower inositol phosphates; and these possibilities are not mutually exclusive. From the ^{31}P NMR data, it was found that there is likely to be a small but notable contamination of the sodium phytate standard with IP5. In the absence of fragmentation, this would be expected to be reflected in the mass spectrum by the presence of a small amount of IP5 alongside a dominance of IP6 ions. However, this spectrum shows a dominance of IP4 and IP5 ions, with smaller representation of IP6 ions and IP3 ions (Figure 2.3). This suggests that either the contamination of the sodium phytate standard is massively underrepresented by the ^{31}P NMR spectrum, which is unlikely due to the dominant presence of the four characteristic peaks of IP6 in the spectrum (Figure 2.2), or that during the electrospray ionisation process, the high charge state of the phytate molecule causes it's dissociation in the gas phase via the loss of one or more of its phosphate moieties $[M-x HPO_3-H]^-$ (McIntyre et al., 2017). Additionally, there are also peaks present in the mass spectrum that indicate the loss of water from the ion $[M-x HPO_3-y H_2O-H]^-$, which is a common occurrence in the ESI-MS analysis of organic compounds in negative

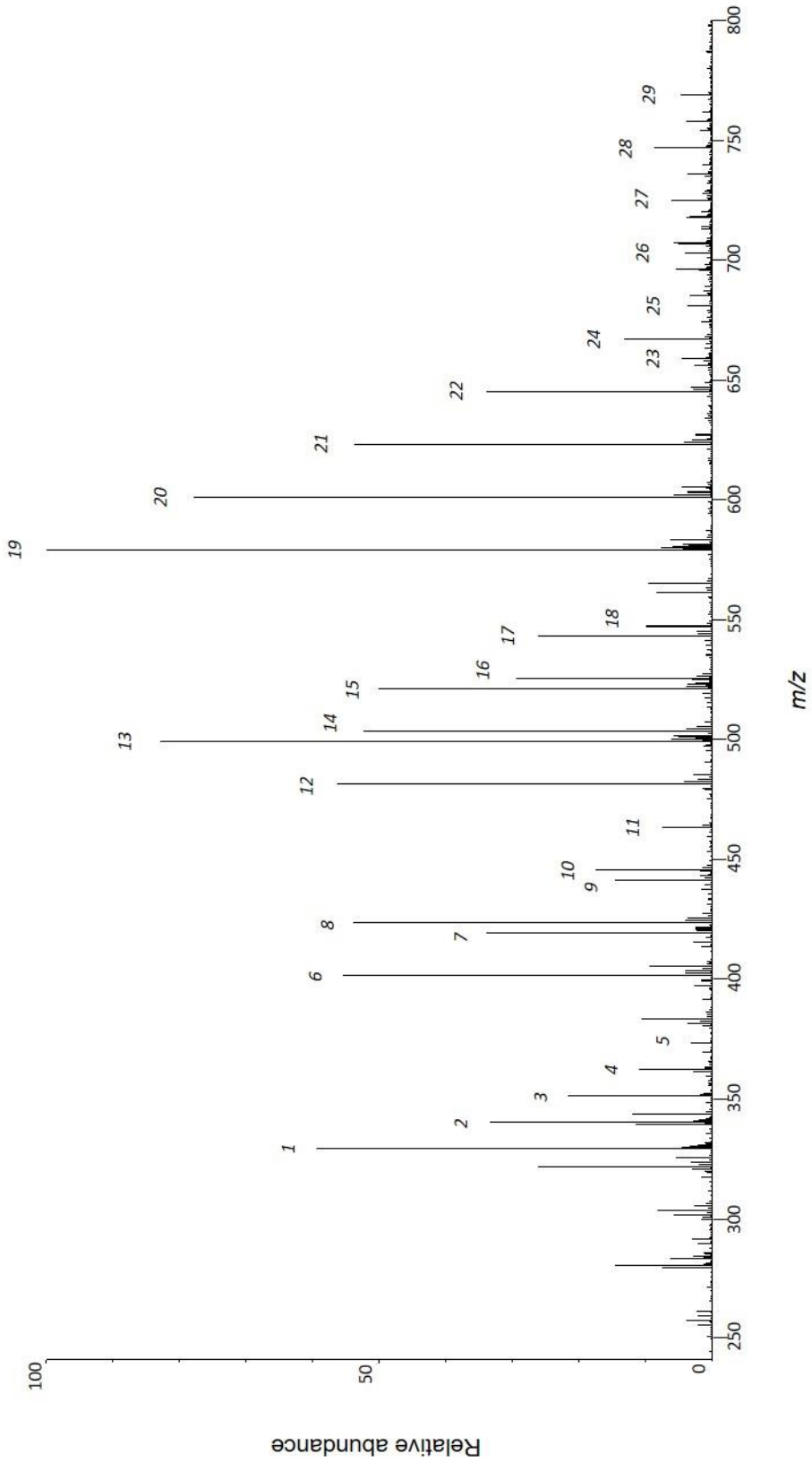

Figure 2.3: Mass spectrum of 0.5mM sodium phytate solution. Figure shows intensity of peaks relative to the most abundant. The spectrum is a mean composite of 100 scans taken at a source voltage of -3.1kV. Peak identities are presented in Table 2.2.

Table 2.2: Peak identities for the mass spectrum of 0.5mM sodium phytate (Figures 2.3 & 2.7)

Peak	m/z	Ion	Identity
1	328.9486	$[M-2H]^{2-}$	IP6
2	339.9397	$[M-3H+Na]^{2-}$	IP6 + Na
3	350.9394	$[M-4H+2Na]^{2-}$	IP6 + 2Na
4	361.9310	$[M-5H+3Na]^{2-}$	IP6 + 3Na
5	372.9232	$[M-6H+4Na]^{2-}$	IP6 + 4Na
6	400.9785	$[M-3HPO_3-H_2O-H]^-$	IP3 - H_2O
7	418.9928	$[M-3HPO_3-H]^-$	IP3
8	422.9688	$[M-3HPO_3-H_2O-2H+Na]^-$	IP3 - H_2O + Na
9	440.9780	$[M-3HPO_3-2H+Na]^-$	IP3 + Na
10	444.9460	$[M-3HPO_3-H_2O-3H+2Na]^-$	IP3 - H_2O + 2Na
11	462.9605	$[M-3HPO_3-3H+2Na]^-$	IP3 + 2Na
12	480.9583	$[M-2HPO_3-H_2O-H]^-$	IP4 - H_2O
13	498.9670	$[M-2HPO_3-H]^-$	IP4
14	502.9420	$[M-2HPO_3-H_2O-2H+Na]^-$	IP4 - H_2O + Na
15	520.9545	$[M-2HPO_3-2H+Na]^-$	IP4 + Na
16	524.9257	$[M-2HPO_3-H_2O-3H+2Na]^-$	IP4 - H_2O + 2Na
17	542.9369	$[M-2HPO_3-3H+2Na]^-$	IP4 + 2Na
18	564.9160	$[M-2HPO_3-4H+3Na]^-$	IP4 + 3Na
19	578.9441	$[M-HPO_3-H]^-$	IP5
20	600.9253	$[M-HPO_3-2H+Na]^-$	IP5 + Na
21	622.9120	$[M-HPO_3-3H+2Na]^-$	IP5 + 2Na
22	644.8939	$[M-HPO_3-4H+3Na]^-$	IP5 + 3Na
23	658.9102	$[M-H]^-$	IP6
24	666.8840	$[M-HPO_3-5H+4Na]^-$	IP5 + 4Na
25	680.8964	$[M-2H+Na]^-$	IP6 + Na
26	702.8839	$[M-3H+2Na]^-$	IP6 + 2Na
27	724.8673	$[M-4H+3Na]^-$	IP6 + 3Na
28	746.8546	$[M-5H+4Na]^-$	IP6 + 4Na
29	768.8428	$[M-6H+5Na]^-$	IP6 + 5Na

mode (Lu et al., 2013), and was also a feature of the phytate spectrum produced by McIntyre et al., (2017).

To compare the fragmentation pattern of phytate in an alternative salt form, a mean spectrum was compiled of 0.5mM potassium phytate under the same ionisation parameters (Figure 2.4). Whilst this spectrum appears 'cleaner' in terms of the density of separate peaks, the fragmentation of potassium phytate seems to be more severe than that of sodium phytate under the same conditions. The major spectral peaks are identified in Table 2.3. Neither IP6 nor IP5 were detected in the potassium phytate spectrum. Together, IP3 and its respective potassium adducts made up the dominant fraction of ions, with peaks detected for IP4, IP2 and even IP1. The difference in severity

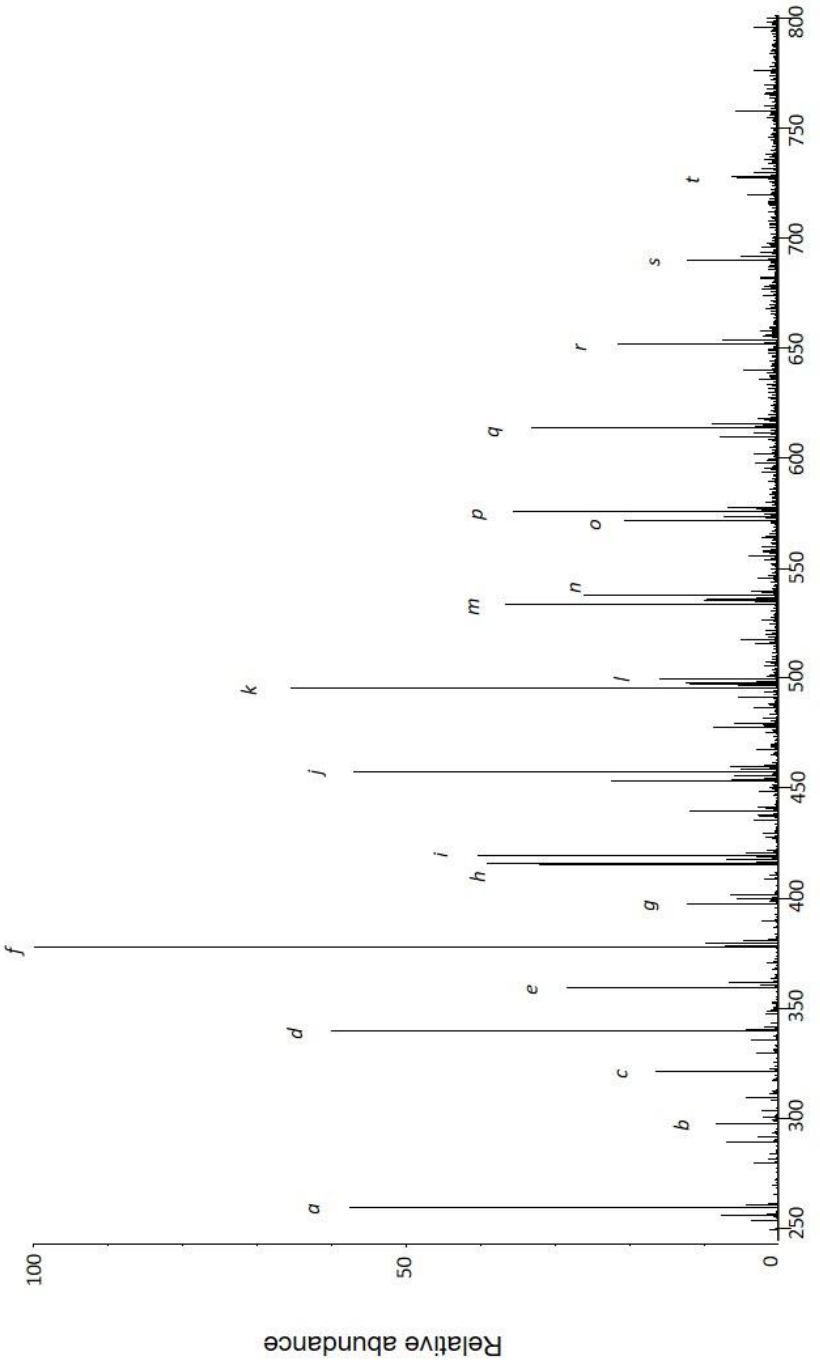

Figure 2.4: Mass spectrum of 0.5mM potassium phytate. Figure shows intensity of peaks relative to the most abundant. The spectrum is a mean composite of 100 scans taken at a source voltage of -3.1kV. Peak identities are presented in Table 2.3.

Table 2.3: Peak identities for the mass spectrum of 0.5mM potassium phytate at 3.1kV source voltage (Figure 2.4)

Peak	m/z	Ion	Identity
a	259.0424	$[M-5HPO_3-H]^-$	IP1
b	296.9986	$[M-5HPO_3-2H+K]^-$	IP1 + K
c	321.0001	$[M-4HPO_3-H_2O-H]^-$	IP2 - H_2O
d	339.0129	$[M-4HPO_3-H]^-$	IP2
e	358.9579	$[M-4HPO_3-H_2O-2H+K]^-$	IP2 - H_2O + K
f	376.9720	$[M-4HPO_3-2H+K]^-$	IP2 + K
g	396.9245	$[M-4HPO_3-H_2O-3H+2K]^-$	IP2 - H_2O + 2K
h	414.9311	$[M-4HPO_3-3H+2K]^-$	IP2 + 2K
i	418.9839	$[M-3HPO_3-H]^-$	IP3
j	456.9471	$[M-3HPO_3-2H+K]^-$	IP3 + K
k	494.9008	$[M-3HPO_3-3H+2K]^-$	IP3 + 2K
l	498.9573	$[M-2HPO_3-H]^-$	IP4
m	532.8629	$[M-3HPO_3-4H+3K]^-$	IP3 + 3K
n	536.9197	$[M-2HPO_3-2H+K]^-$	IP4 + K
o	570.8250	$[M-3HPO_3-5H+4K]^-$	IP3 + 4K
p	574.8781	$[M-2HPO_3-3H+2K]^-$	IP4 + 2K
q	612.8434	$[M-2HPO_3-4H+3K]^-$	IP4 + 3K
r	650.7947	$[M-2HPO_3-5H+4K]^-$	IP4 + 4K
s	688.7606	$[M-2HPO_3-6H+5K]^-$	IP4 + 5K
t	726.7175	$[M-2HPO_3-7H+6K]^-$	IP4 + 6K

of fragmentation indicates that the salt environment of the phytate solution influences phytate fragmentation patterns in source.

Little work has focused on the direct analysis of phytate by mass spectrometry with electrospray ionisation. The first work to note the unusual behaviour of phytate in this analysis was that of Cooper et al., (2006), who described the presence of IP2-IP5 and a number of sodium adducts in the spectrum of a solution purportedly containing a mixture of only IP6 and IP1. More recently, McIntyre et al., (2017) similarly identified numerous dephosphorylated esters of IP6 within their phytate standard when analysed by high resolution ESI mass spectrometry. To rule out contamination, they purified their standard by collecting a pure IP6 fraction from an anion exchange column separation, confirming the occurrence of in-source fragmentation in ESI with the continued appearance of these peaks at coincidental m/z ratios in the mass spectrum of the purified sample.

The dissociation of phosphate groups during ESI has been studied previously in phosphorylated peptides (Edelson-Averbukh et al., 2006; Palumbo et al., 2011; Banerjee & Mazumdar, 2012) and polyphosphates (Choi et al., 2000). Edelson-Averbukh et al., (2006) proposed a mechanism to explain the occurrence of phosphate fragmentation in negative mode electrospray ionisation. This mechanism has been adapted in Figure 2.5 to explain the dissociation of phosphate groups from phytate, to produce an ion with coincidental m/z with the IP5 product of IP6 enzymatic hydrolysis. Under the conditions of ionisation and collision in the gas phase, a phosphate group can become doubly deprotonated to produce a phosphate moiety with a double negative charge $[M\text{-}2H]^{2-}$. Electrons migrate from one oxygen to produce a double bond, with the phosphoester (C-O-P) bond breaking between O-P to yield two singly-charged fragment ions $[M\text{-}2H\text{-}(PO_3^-)]^-$ and $[PO_3]^-$. As phytate is multi-phosphorylated, this process can happen within multiple phosphate groups, to yield fragment ions that have coincidental m/z ratios with ions of the various partially hydrolysed lower inositol phosphates. The conditions that produce this double deprotonation are likely influenced by numerous factors including the charge supplied to the aerosol droplets at the source, which is dependent on the source voltage at the capillary, the concentration of the analyte (i.e the number of molecules that 'share' the charge of the droplet upon solvent evaporation), and the cone voltage, which can control the internal energy of ions, and the occurrence of collisions in the gas phase.

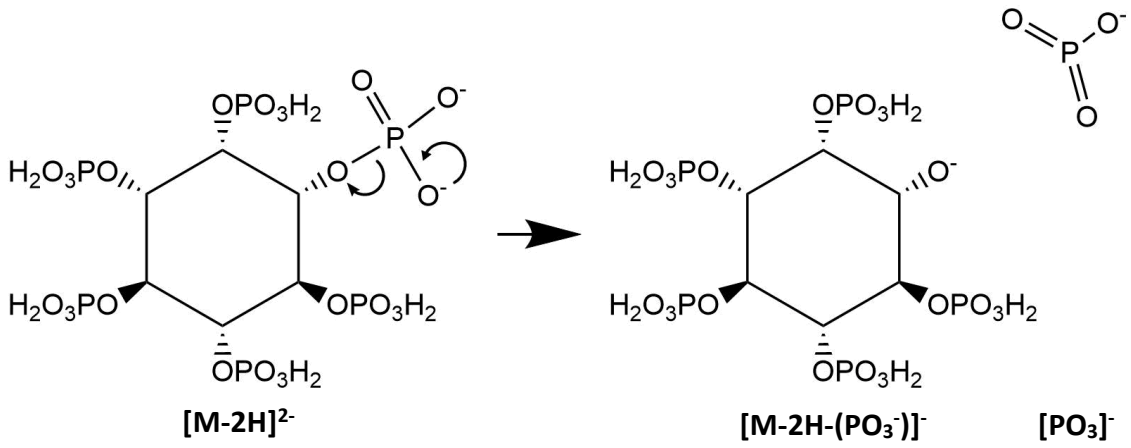

Figure 2.5: Mechanism for the fragmentation of phytate, adapted from the mechanism proposed by Edelson-Averbukh et al., (2006) for the fragmentation of phosphorylated peptides. The doubly deprotonated phosphate group of phytate produced in the ion source decomposes to form complementary fragments $[M\text{-}2H\text{-}(PO_3^-)]^-$ and $[PO_3]^-$ via the shift of an electron pair.

2.4.3 The effect of concentration and source voltage on fragmentation patterns

In order to optimise the analysis and attempt to minimise or eliminate the occurrence of fragmentation, the voltage at the orifice of the metal capillary at the inlet stage of ESI, known as the source voltage, was varied, and the mean intensity of ions over 100 scans was measured at each level (Figure 2.6 A). The data is also presented as the intensity of the molecular ion and its fragment ions relative to the most abundant (Figure 2.6 B). At the 0.5mM concentration, a clear trend can be seen for decreasing signal intensity of IP3 and IP4, whereas IP5 intensity remains stable, decreasing only slightly between -2.7kV and -3.3kV (Figure 2.6 A). IP6 became detectable at -2.1kV, increasing to a maximum at -2.3kV and remained relatively unchanged before decreasing between -2.9 and -3.3kV. In terms of relative intensities, which provides an idea of the degree of fragmentation occurring in ionised analyte, the overall trend is for decreasing proportions of IP3, accompanied by increasing proportions of IP5 and IP6 with increasingly negative source voltage. The degree of fragmentation is lowest at -3.1kV, which has the greatest proportion of both IP6 and IP5 (Figure 2.6 B).

This analysis was repeated at dilutions of 0.05mM and 0.005mM phytate to assess whether the fragmentation pattern is affected by analyte concentration. The pattern at 0.05mM phytate was much the same as the more concentrated phytate, with an overall dominance of IP3 and IP4 at less negative source voltages. Their intensities decreased with increasingly negative source voltage, whilst IP5 and IP6 increased slightly (Figure 2.6 C). In relative terms, the intensity of IP3 decreased with increasingly negative source voltage, whilst that of IP5 and IP6 increased (Figure 2.6 D). However, in the lowest concentration analysed, 0.005mM phytate, absolute intensity of all ions was stable between -1.5kV and -2.1kV, after which the intensity of all ions began to increase (Figure 2.6 E). The spectra were dominated by IP3 and IP4 up until -3.1kV, at which point there was a sharp drop in intensity of both. Despite the difference in the pattern of absolute ion intensity, the pattern of relative ion intensity is remarkably similar to those of the greater concentrations, with the dominance of IP3 at less negative voltages replaced by dominance of IP4, and accompanied by increased proportions of both IP5 and IP6 (Figure 2.6 F).

0.5mM sodium phytate

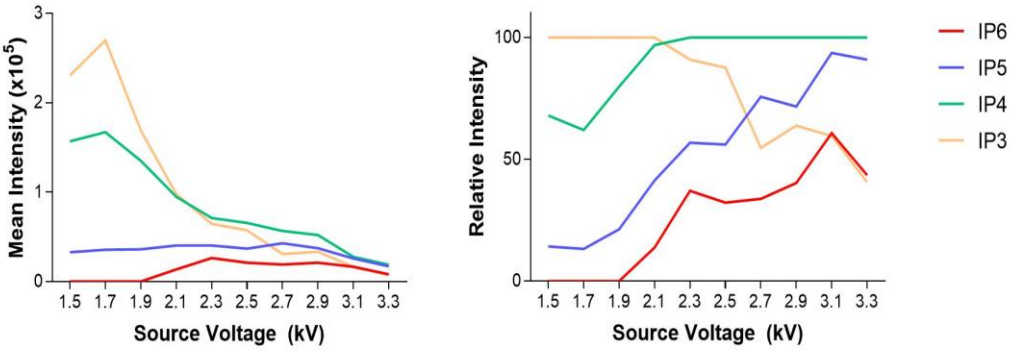

0.05mM sodium phytate

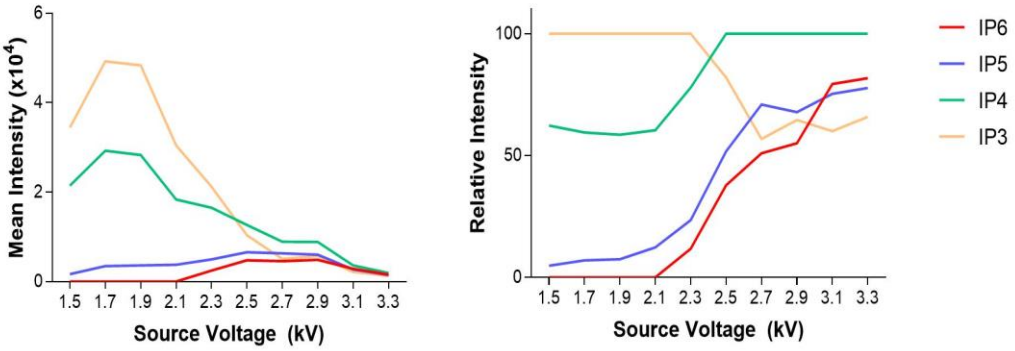

0.005mM sodium phytate

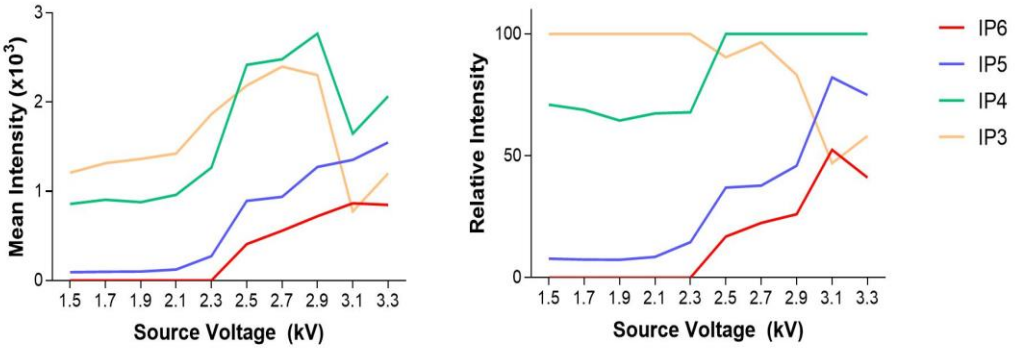

Figure 2.6: The effect of source voltage and analyte concentration on absolute ion intensity and relative ion intensity of sodium phytate solutions measured by ESI-ToF-MS. Source voltage in negative mode are negative values. At each source voltage, a mean spectrum was compiled from 100 scans. Mean intensity for each inositol phosphate was then calculated as the sum of peak intensity for each IP and its associated sodium adducts.

This analysis showed that the fragmentation pattern of phytate follows approximately the same pattern regardless of the concentration of analyte. At less negative source voltages, the degree of fragmentation is greatest, with an abundance of IP3 and IP4. The severity of fragmentation decreases when increasingly negative voltage is applied to the capillary, with IP3 levels decreasing, and levels of IP5 and IP6 increasing. However, at higher analyte concentrations, this increase in negative voltage is accompanied by an overall decrease in ionisation efficiency, with the intensity of all detected ions decreasing. This is reversed in the lower concentration, with ionisation efficiency increasing between -2.1kV and -2.9kV.

McIntyre et al., (2017) provided the first detailed study of the occurrence of in-source phytate fragmentation during electrospray ionisation. In their study, source voltage was similarly varied, and it was found that the degree of fragmentation increased at more negative source voltage between -1.6 and -3.6kV, with a fall in the relative abundance of the IP6 ion accompanied by an increase in fragment ions with coincidental m/z ratios with IP5 and IP4. Their results contrast the findings of the present study, where fragmentation was instead found to decrease with more negative source voltage. This suggests that phytate fragmentation patterns in ESI are not easily predicted with regards to the source voltage, and are affected by potentially multiple additional factors that might include the carrier solvent, salt species and concentrations, and instrumental variations.

2.4.4 Cone Voltage

The sampling cone is the orifice which a portion of the gaseous ionised analyte passes through into the mass analyser (Fenn et al., 1989). The cone voltage is the difference in electrical potential between the sampling cone and the extraction cone, and can be used to control the internal energy of the gaseous ions (Yan et al., 2003). The potential difference is necessary in order to direct ions into the detector vacuum to achieve sufficient ion transport to the detector. However, high cone voltage can induce significant in-source fragmentation as it increases the internal energy of the ions, resulting in an increase in energetic collisions with neutral molecules in the nitrogen carrier gas (Yan et al., 2003; Waters, 2015).

In the previous assessment of the effect of source voltage and analyte concentration, cone voltage was set relatively low by default to 30V in order to maintain the flow of ions from the ion source to the vacuum of the mass analyser whilst minimising the potential for energetic collisions. To assess whether the fragmentation of phytate could be improved by reducing the cone voltage, the ESI-ToF-MS analysis of 0.5mM sodium phytate was repeated over a range of source voltages, with cone voltage reduced from 30V to 20V (Figure 2.7 A). Data was not collected at a cone voltage of 10V as there was a large drop in sensitivity. Interestingly, a similar pattern of increased fragmentation at less negative source voltages was observed, but the severity of the fragmentation was greatly reduced, with IP6 present in the spectra even at the lowest applied source voltage. A sharp proportional increase in IP6 was found between -1.9kV and -2.1kV, with IP6 becoming the most abundant ion in the spectrum (Figure 2.7 B). The proportional prevalence of IP4 and IP3 simultaneously fell from -1.5kV to -2.9kV, followed by an increase. At this cone voltage, the optimal source voltage was found to be -2.9kV as the proportional abundance of both IP3 and IP4 was lowest relative to IP6. The mass spectrum for 20V cone voltage and -2.9kV source voltage is presented in Figure 2.8, with major peaks listed in Table 2.2. This was the optimal source voltage when a cone voltage of 20V was used, and in this spectrum the IP6 ion and its sodium adducts are present as predominantly doubly deprotonated ions $[M\text{-}2H]^{2-}$, whereas fragment ions are singly charged (eg. $[M\text{-}2H\text{-}(PO_3^-)]^-$). Cooper et al., (2006) originally identified cone voltage as a significant factor affecting phytate fragmentation. In their study, a mixture of each inositol phosphate (IP1-IP6) was analysed at a low cone voltage of 20V, and a high voltage of 60V. At 60V, they found that all IPs were fragmented to a significant extent, but at 20V, the overall intensity of ions was increased, with a pattern of increasing fragmentation with greater phosphorylation. Although the present optimisation was only performed on fully phosphorylated phytate rather than a mixture of IPs, the reduction of cone voltage in this analysis has reduced the occurrence of phytate fragmentation, yielding a much greater proportion of the IP6 molecular ion than at 30V. This result is logical, as a reduction in cone voltage reduces the internal energy of ions as they are propelled into the cone orifice, reducing the collision energy between ions and carrier gas molecules (Yan et al., 2003).

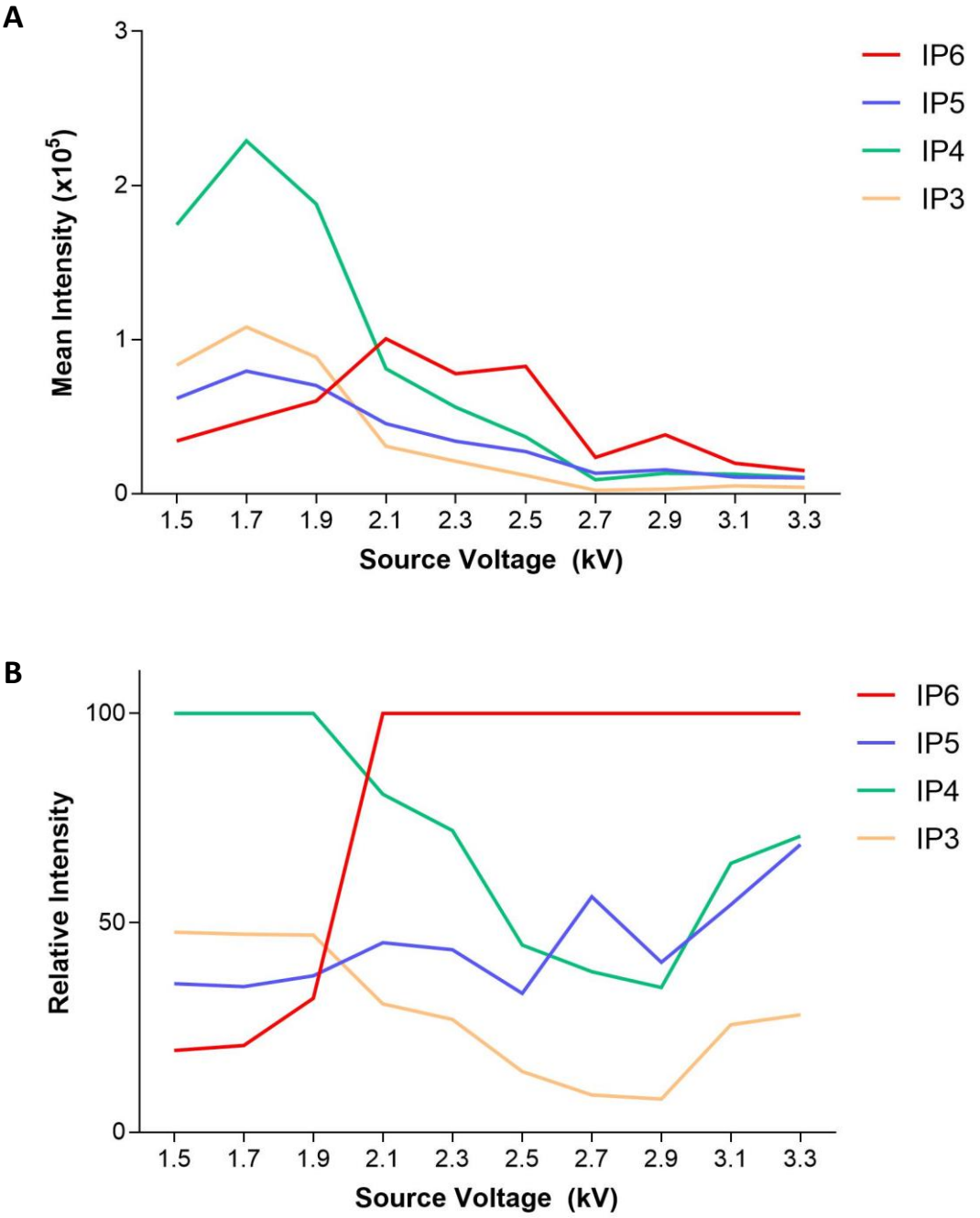

Figure 2.7: The effect of source voltage on fragmentation of 0.5mM sodium phytate solution following optimization of sampling cone voltage to 20V. **A**: Mean absolute ion intensity at each source voltage; **B**: Intensity of IP ions relative to the most abundant.

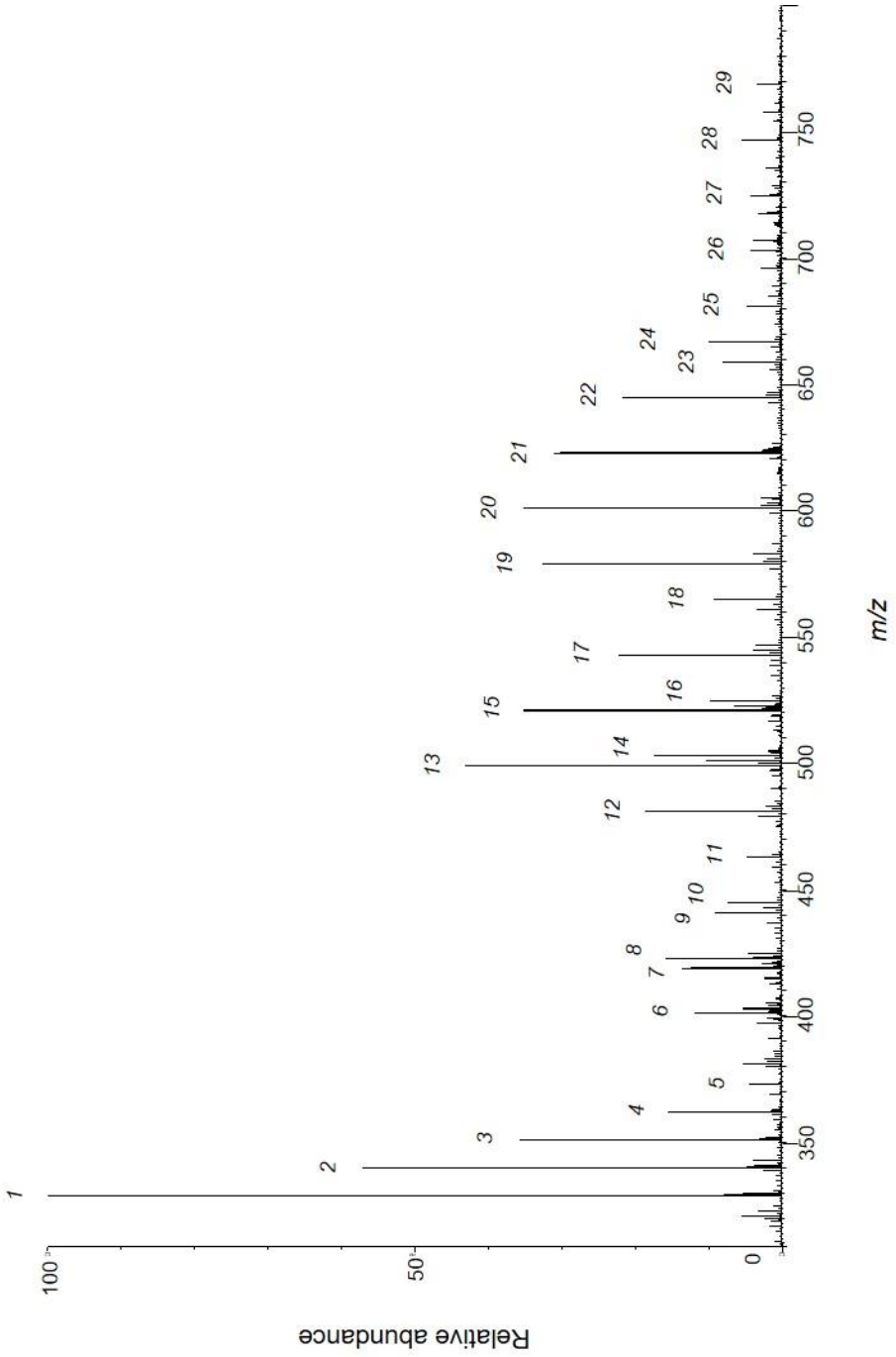

Figure 2.8: Mass spectrum of 0.5mM sodium phytate solution, following optimisation of sampling cone voltage to 20V. Figure shows intensity of peaks relative to the most abundant. The spectrum is a mean composite of 100 scans taken at a source voltage of -3.1kV. Peak identities are presented in Table 2.2.

Overall, these results shows that the fragmentation of phytate in electrospray ionisation is affected by both source voltage and cone voltage, with the greatest reduction in fragmentation achieved by reducing the cone voltage, thus reducing the frequency of dissociative collisions within the gas phase between charged ions and the nitrogen carrier gas. The differences observed between this work and that of McIntyre et al., (2017) for the effect of source voltage, and Cooper et al., (2006) for the effect of cone voltage, suggest that the fragmentation of phytate is highly variable and may be a function of many emergent factors unique to each experiment and the apparatus employed for its analysis.

At both the optimal cone voltage and source voltage identified in this system, whilst it was not possible to eliminate fragmentation, it was possible to dramatically reduce it. However, the continued presence of fragment ions that have coincidental m/z ratios with true hydrolysed inositol phosphates means that their quantitative measurement in solution is unlikely to be achieved by ESI-ToF-MS without their prior chromatographic separation and purification.

2.4.5 Application of ESI-ToF-MS to the analysis of the enzymatic dephosphorylation of phytate

An objective of this chapter was to test the ability of ESI-ToF-MS to analyse the dephosphorylation of phytate in real-time as true dephosphorylated IPs are generated by enzymatic hydrolysis. An analytical process was designed in which the molecular composition of the reaction between 0.5mM sodium phytate and 2FTU mL^{-1} phytase enzyme could be analysed in real-time. Upon addition of phytate to the phytase solution, the reaction mixture was drawn into the internal syringe of the mass spectrometer and was pumped continuously into the ESI source for mass spectrometric analysis. There was a small amount of day-to-day variation in optimisation settings, so minor optimisation procedures were carried out prior to each analysis. With the cone voltage set to 20V, a slightly more negative source voltage of -3.1kV was found to produce the least fragmentation on the day of the reaction, so was used for each analysis. A total of three 22-minute replicate reactions were run, amassing a total of 1320 scans for each, and from the resulting data set a mean trace for each IP was

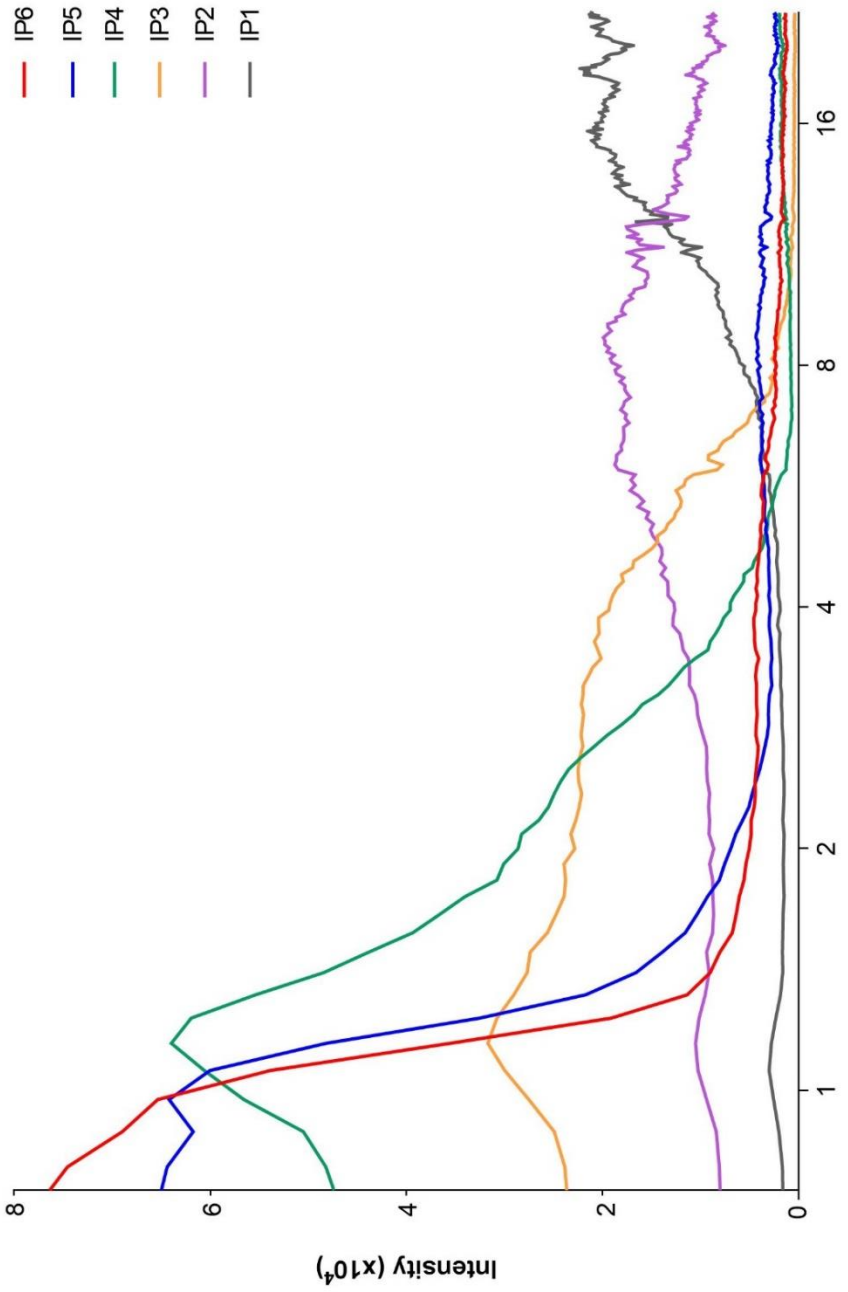

Figure 2.9: ESI-ToF-MS analysis of the dephosphorylation of 0.5mM sodium phytate by 2FTU mL-1 RONOZYME HiPhos phytase. Intensity of each inositol phosphate was calculated as the sum of each inositol phosphate and their respective sodium adducts. Data points are mean values of sets of 10 sequential scans. Figure is presented as a mean composite (n=3) over a total of 20 minutes. Time is presented in log2 scale to clarify the beginning of the reaction.

calculated by summing the peaks for each along with their respective sodium adducts over each scan. The data from sets of ten consecutive scans were then averaged to increase signal:noise ratios. A composite figure tracing the abundance of each IP over time was then produced by calculating an average from the three reactions (Figure 2.9). Standard error of the mean is presented separately for each IP in Figure 2.10. As much of the reaction occurs within the first two minutes of analysis, the reaction is presented on a log2 time scale for clarity. Due to the time taken for the reaction solution to reach the ESI source, and the initial very low signal:noise upon initial ionisation, the reaction is presented from 0.7 minutes (42 seconds).

Figure 2.9 shows the pattern of dephosphorylation of phytate measured in real-time by ESI-ToF-MS. Initially IP6 is the most prevalent ion in solution, along with substantial amounts of IP5 and IP4. Levels of IP6 and IP5 fall rapidly within the first 90 seconds of the reaction, accompanied by a rise in IP4 and IP3 to peaks at 1.14 minutes (68s). From this peak, IP4 falls to near zero by approximately 6 minutes. IP3 levels also fall, but at a slower rate than IP4 until IP4 levels are low at 4 minutes, at which point the rate of IP3 decline increases until it reaches near-zero at 8 minutes. IP2 levels remain stable from the beginning of the reaction, beginning to steadily rise as IP3 levels fall from 3 minutes, reaching a peak at approximately 9 minutes. IP1 levels remain near-zero until approximately 8 minutes when IP2 is the predominant IP remaining in the reaction. IP1 becomes the predominant IP in the reaction at approximately 13 minutes. IP2 levels continue to fall over the remainder of the analysis time, but IP2 is still present in solution at 22 minutes.

This analysis provides valuable qualitative information about the reaction, highlighting that the rate of dephosphorylation by the phytase enzyme is initially rapid for IP6 and IP5, but decreases for each of the remaining IPs, with a likely final product of IP1. No evidence was found for the existence of fully dephosphorylated *myo*-inositol (IP0) in the spectra. However, a quantitative interpretation of the reaction from this figure may be misleading, owing to the fragmentation of IP6 at the beginning of the reaction. As the fragment ions produced by the dissociation of $[PO_3]^-$ have a coincidental m/z ratio with the true products of enzymatic hydrolysis, it is not possible to distinguish between the two, and therefore it is not possible to account for the proportion of each IP trace that

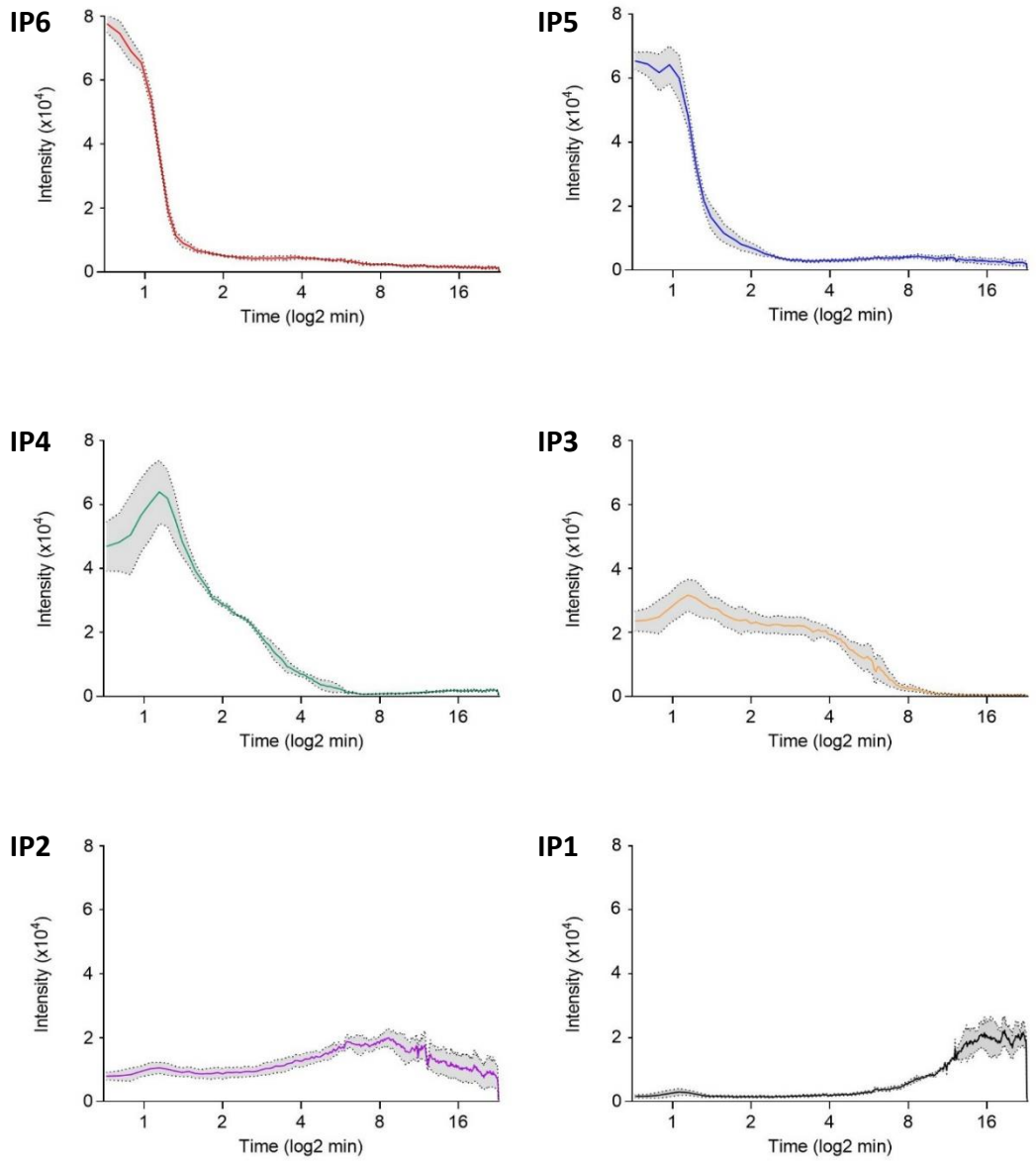

Figure 2.10: Mean intensity ± SEM for each separate inositol phosphate during the reaction between 0.5mM sodium phytate and 2FTU mL^{-1} RONOZYME HiPhos phytase (n=3).

is generated by in-source fragmentation. Furthermore, there is a distinct decrease in the overall ion intensity throughout the reaction, which could be interpreted as lower concentrations of the lower IPs than the initial IPs at the beginning of the reaction. However, as the initial reaction solution taken into the internal syringe pump is a fixed volume and the infusion rate is constant throughout, there should be no change in the total ion intensity throughout the reaction, despite changes in the composition of the reaction mixture. This suggests that the ionisation efficiency within ESI declines as IPs

become increasingly dephosphorylated. Each dephosphorylated IP is likely to be optimally ionised at different source voltages, so within the optimised reaction conditions of 3.1kV source voltage and 20V cone voltage, the ionisation efficiency of IP6 and IP5 is high, but this decreases with each further dephosphorylation as the conditions are sub-optimal for ionisation of the different IPs. The consequence of this is that the analytical conditions are not optimal for the quantification of all IPs in a single analysis.

2.5 Conclusions

In this chapter, it was demonstrated that the sensitivity and resolution of ^{31}P NMR is not sufficient for the determination of phytate or its dephosphorylated esters when they are present at low concentrations. ESI-ToF-MS is able to resolve phytate and all of its dephosphorylated esters, even at low concentrations. However, a significant amount of in-source fragmentation of phytate was encountered during electrospray ionisation, which produced a spectrum with fragment ions that have coincidental m/z ratios with lower IPs. This fragmentation could be reduced by reducing cone voltage, and increasing source voltage, but could not be eliminated. Via the generation of lower IPs by the enzymatic dephosphorylation of phytate, it was shown that it is not possible to quantify all IPs in a mixture, for two reasons. Firstly, there is no way to determine the amount of lower IP esters that are present in a sample as it is not possible to determine the proportion of that signal that has been erroneously generated by fragmentation. Secondly, the ionisation efficiency of each IP ester seems to vary, demonstrated by the successive loss of ion intensity through the reaction.

This evidence suggests that the simultaneous quantification of all IP esters within a single sample is not possible by ESI-ToF-MS. A potential alternative approach would be to separate the esters chromatographically, prior to detection by ESI-ToF-MS. If complete separation was achieved, then any peaks occurring within the spectra at coincidental m/z ratios with lower IPs could be confirmed as fragment ions. In a recent paper, McIntyre et al., (2019) described the development of a method for the quantification of phytate in manure and soil samples. They achieved separation of IP6 from IP5 and contaminants within the extractant solution by ion chromatography, and analysed eluate for the IP6 peak by ESI high resolution mass spectrometry.

Quantification of phytate by this method was well correlated with results by ^{31}P NMR but achieved a much-improved limit of detection, at 0.7mg kg^{-1} compared to >10mg kg^{-1} by ^{31}P NMR. This paper also suggests that chromatographic separation prior to IP analysis is necessary for the removal of contaminants from the extracts samples that interfere with ESI. However, the above work does not attempt to quantify lower inositol phosphates, and they are not identified in the chromatographic separation. In order to successfully quantify lower IPs, a method that achieved clear separation of each IP would be necessary, and further, the ionisation conditions within the mass spectrometer would need to be optimised separately for each fraction.

For these reasons, it was concluded that quantitative analysis of lower IPs is unlikely to be achievable in the complex environmental samples that are to be analysed in this thesis. Building upon a successful method developed within the lab for the analysis of P compounds in soil (Robertson, 2018), ^{31}P NMR will be used for the analyses undertaken in subsequent chapters. Despite the recognised limitations of ^{31}P NMR, it remains the most powerful technique for the analysis of phytate and other organic phosphates in environmental samples, and using this method, the results generated will be comparable with the majority of work in the wider field.

3: Analysis of phytate through an advanced anaerobic sludge treatment process

3.1 Summary

Like other monogastric animals, humans lack the production of endogenous phytase enzymes in our guts, meaning that we are unable to efficiently digest the phytate found in grains in our diets. Therefore, there is likely to be a high concentration of phytate entering the sludge treatment process in human excreta. Nearly 80% of digested sludge in the UK is spread on arable land, which returns valuable nutrients and organic matter to the soil. However, plants can only absorb P in its inorganic orthophosphate form, and there is evidence to suggest that due to the high charge density of phytate, it can become strongly adsorbed to the soil and preferentially accumulates as it is afforded a level of protection from microbial degradation. If phytate is abundant in the digested sludge that is applied to land, this would therefore represent a potential waste of valuable phytate-P.

Few studies have analysed the behaviour of phytate through the sludge treatment process, and there is conflicting evidence regarding the survival of P other than orthophosphate in anaerobic digestion. In this chapter, sludge samples from five stages throughout an advanced anaerobic sludge treatment process are analysed for total P, orthophosphate and phytate by both colorimetric methods, and solution ^{31}P NMR.

Total P concentration is found to increase through the process, reaching its greatest concentration following anaerobic digestion. Sludges are dominated by orthophosphate throughout, making up approximately 80% of extractable P. Phytate is found to be present in sludge, but at a relatively low proportion of approximately 4.5%. However, phytate does persist through the various stages of the treatment process, and is present in the final product, cake, which is spread to land.

3.2 Introduction

Global phosphate fertilizer demand for 2019 is forecast to stand at 45 million tonnes, with demand increasing annually by 2.2% between 2015 and 2020 (FAO, 2017). With the finite nature of phosphate rock sources widely recognised, and the possibility of a peak in phosphate production forecast within the next century (Cordell & White, 2014), it is essential for future global food production that alternative sources of P can be identified and adopted.

Municipal wastewater streams provide one such opportunity for resource recovery and reuse. Wastewater is rich in P , with an average typical P load of 1.5-2g per person entering the wastewater stream daily in Europe via inputs from human excreta, food residues and industrial outputs (Egle *et al*., 2015). The primary purpose of wastewater treatment is the removal of contaminants to produce water clean enough to be discharged to watercourses, whilst safeguarding both human and environmental health (DEFRA, 2012). This translates to a wide variety of processes that are designed to remove organic matter, pathogens, nutrients, chemicals and metals that are detrimental to both humans and the natural environment (Appels et al., 2008). The impacts of untreated wastewater entering the environment can range from hypoxia/anoxia and eutrophication of waterways due to the aerobic break down of organic matter and unnaturally elevated levels of nitrogen and P, through to health risks posed by pathogens such as *Escherichia coli.* In many countries a secondary purpose to wastewater treatment is evolving, as it is now commonly seen as a key intervention point for the recovery and recycling of valuable nutrient resources.

3.2.1 Wastewater treatment in the UK

A simplified wastewater treatment is depicted in Figure 3.1. The process begins with the inflow of raw wastewater from industry and households to a wastewater treatment plant (WWTP). Wastewater at the inlet stage is first screened for large debris that would not be readily degraded in the process, and sand and grit is settled out. Water then moves to primary settlement, in which organic solids sink to form a sludge layer and fats and oils float to the top. The middle layer of sewage water is then siphoned off to a secondary treatment stage. Secondary treatment effectively carries out the natural

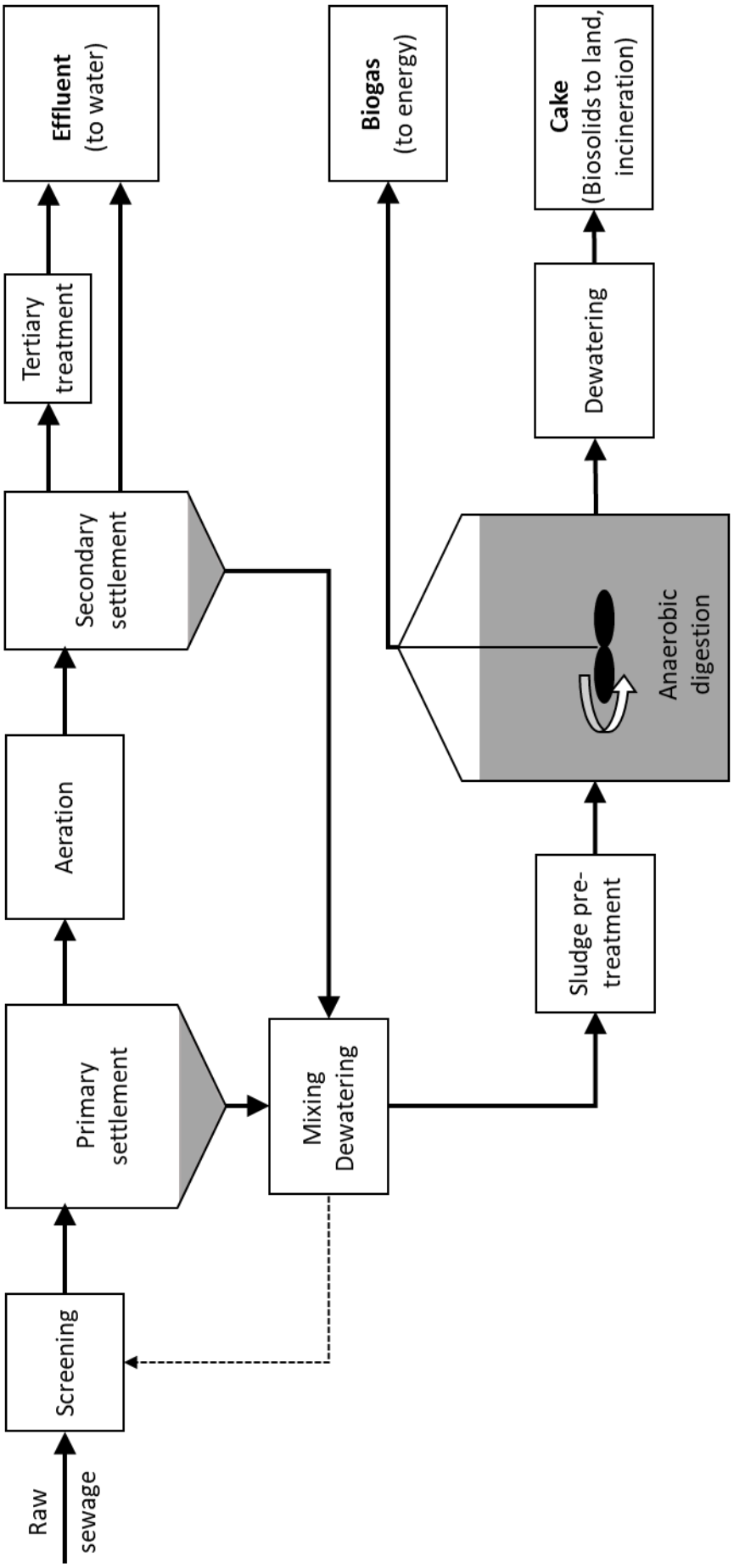

Figure 3.1: A schematic diagram of a typical wastewater treatment process with 'advanced' anaerobic digestion of sludge (including a pre-treatment step before anaerobic digestion).

aerobic breakdown of organic matter and contaminants in an artificially aerated and controlled process, rather than in water bodies where it may contribute to hypoxia and eutrophication. Organic debris settles out at this stage, after which the treated water is generally considered acceptable and is returned to a water body (Gerardi, 2003). In some instances, tertiary treatments are required, particularly in waste streams with specific pollutants, or if the effluent is to be discharged into an environment that is particularly sensitive. A consequence of both primary and secondary water treatment is the generation of large volumes of residual organic matter, or sewage sludge. Before the introduction of the EU Urban Waste Water Treatment Directive in January 1999, much of the sludge produced in the UK was dumped at sea, or sent to landfill (Table 3.1), but since 1999, sea disposal has ceased, landfill rates have decreased and the reuse of sludge by agriculture has increased from 440,000 tonnes per year in 1992 to 1,118,000 tonnes per year in 2010 (DEFRA, 2012).

Sludge generated by primary and secondary wastewater treatment is generally treated prior to its use in agriculture to reduce its volume and create a product that is free of pathogens such as *E. coli* and *Salmonella* spp. In the UK, sludge treatment predominantly involves anaerobic digestion, with 73% of sludge currently treated in this way. Alternative aerobic techniques include composting, thermal drying, or lime stabilisation, in which lime (CaO) is added to liquid sludge to produce an exothermic reaction which both dries and pasteurises the sludge (Haynes et al., 2009).

Table 3.1: UK sewage sludge disposal 1992-2010 (tonnes dry solids; from DEFRA, 2012)

Disposal Route	Sludge to Sea	Sludge Reuse		Sludge Disposal			Total
		Agriculture	Other	Landfill	Incineration	Other	
1992	281,588	440,137	32,100	129,748	89,800	24,300	*997,673*
2008	-	1,241,639	90,845	10,882	185,890	1,523	*1,530,779*
2010	-	1,118,159	23,385	8,787	259,642	2,863	*1,412,836*

3.2.2 Anaerobic digestion (AD) of sludge

AD is seen as an optimal treatment technique for sludge due to its ability to transform organic matter into methane-rich biogas, simultaneously reducing the volume of biosolids by 30-50%, destroying pathogens and reducing the environmental and

operational costs of sludge disposal (Gebreeyessus & Jenicek, 2016). Biogas can be used to fulfil the energy requirements of the process, and in larger plants can also contribute to national energy supplies (Appels *et al*., 2008).

Sludges from primary and secondary settlement are often combined before being dewatered, with the excess separated water returned to the inlet stage of the treatment process (Figure 3.1). AD requires tightly controlled anaerobic conditions and depends on a complex and delicate association between certain groups of microorganisms to convert organic matter into CO_2 and CH_4 (Gerardi, 2003). The AD process begins with the hydrolysis of insoluble organic material and high molecular weight lipids, proteins, polysaccharides and nucleic acids into soluble constituents, which are further degraded by acidogenic bacteria to produce volatile acids and alcohols, ammonia, CO_2 and H_2S. Organic acids and alcohols produced at this stage are then subject to acetogenesis, producing acetic acid, as well as CO_2 and H_2. The final stage, methanogenesis, is performed by two groups of methanogenic bacteria, producing methane either by the splitting of acetate, or the reduction of CO_2 by H_2 (Appels *et al*., 2008; Gerardi, 2003).

AD can be operated at both mesophilic temperatures (30-38°C) or thermophilic temperatures (50-57°C), with mesophilic AD most commonly used (Gerardi, 2003; Appels *et al*., 2008). Thermophilic AD is a quicker process than mesophilic digestion due to increased rates of reaction and produces fewer solid outputs and greater destruction of pathogens. However, as well as a greater energy requirement, it has a greater potential for odour production, produces a poor quality supernatant with higher dissolved solids, and is a much less stable process, with thermophilic bacteria much more sensitive to fluctuations in temperature than mesophilic bacteria (Appels *et al*., 2008). Despite the clear advantages presented by AD, there are some drawbacks to the process that can include insufficient decomposition of sludge, long retention times necessitating the use of large volume tanks, the vulnerability of the process to changes to conditions and inhibitors, impurities in the biogas produced, and the increased concentration of indigestible products in the final digestate (heavy metals, industrial organics, pharmaceuticals) due to the reduced volume of the digestate (Appels *et al*., 2008).

3.2.3 Sludge pre-treatment

Hydrolysis of the influent is commonly recognised as the rate-limiting step in AD (Li & Noike, 1992; Vavilin *et al*., 2008). During hydrolysis, cell walls are broken down to release organic constituents for acidogenesis, but cells are relatively unfavourable substrates for microbial degradation and are slowly degraded (Appels *et al*., 2008). In order to reduce AD solid retention times and increase the conversion of organic solids to methane, many processes are moving to 'advanced' AD, which incorporates a form of pre-treatment of the AD influent to hydrolyse cellular structures within the sludge, effectively bypassing the rate-limiting hydrolysis step (Figure 3.1; Carrère *et al*., 2010; Appels *et al*., 2008). Many different forms of pre-treatment exist, and include biological, mechanical, chemical and thermal processes that aim to enhance the hydrolysis process to complement AD. Of these processes, thermal hydrolysis is favoured due to its efficiency in sludge solubilisation and the resulting improvement of methane yield (Bougrier *et al*., 2008; Kim *et al*., 2003), and it has since become widely used, with many commercial thermal hydrolysis plants (THPs) currently in operation in the UK, including Cambi THP (Kepp *et al*., 2000) and *Bio*THELYS® (Veolia Water Technologies, 2015) which claims to produce 30-50% more biogas and 20-35% less dry solid waste than conventional digestion. Treatment temperatures of between 160-180°C are maintained by hot steam injection over a period of 30-60 minutes under pressures ranging from 600-2500kPa (Carrère *et al*., 2010; Bougrier *et al*., 2008) and these conditions have the additional advantage of effectively pasteurising sludge prior to AD.

3.2.4 Sludge phosphorus recovery and reuse

Municipal wastewater in central Europe contains a P load that could, if fully recovered and recycled, replace 40-50% of the annually applied rock-phosphate derived P fertilizers (Egle *et al*., 2016). Many technologies exist for P recovery, but these are often targeted at different P-containing flows (i.e effluent, anaerobic digester supernatant, digested sludge, and ash from incinerated sludge), and various treatments are favoured in different countries according to policy and regulations.

Anaerobically digested sewage sludge contains high levels of P and other nutrients. Various techniques are used to deal with the large amounts of sludge produced

depending on the priorities of the plant and government regulations. Some WWTPs opt for incineration, which yields further energy while destroying all pathogens and organic matter, greatly reducing the mass of the end product. However, P contained in sewage sludge ash is poorly available for uptake by plants and must be processed much in the same way as phosphate rock ore, but can yield a high quality P fertiliser with the added advantage of low heavy metal content once it has been processed (Egle et al., 2015). Alternatively, sewage sludge can be directly applied to agricultural land, where it is incorporated into the soil to provide nutrients and organic matter that can have positive benefits for soil health. In the UK, since the ban on dumping of sludge at sea, and discouragement of landfill disposal, this has become the most popular route for sewage sludge disposal (Table 3.1; DEFRA, 2012). However, despite its widespread use in the UK, the application of sludge to agricultural land is strictly controlled according to the 1989 UK 'Sludge (Use in Agriculture)' regulations, and the ADAS 'Safe Sludge Matrix' guidance in order to ensure high standards of food safety and livestock welfare (BRC et al., 2001). For example, it is stated that untreated sludge must not be spread on agricultural land used for food production. Treated sludge can be applied to land growing cereal crops, and may be spread on land growing vegetable crops, provided that 12 months has elapsed between sludge application and harvest. For salads that are eaten raw, this elapsed time is extended to 30 months. Furthermore, treated sludge may not be spread on grazed grassland, but may be used provided that it is injected deep into the soil at a minimum of three weeks prior to grazing (BRC et al., 2001).

The fate of P compounds in digested sludge is likely dependent on many factors, including the source of the wastewater (domestic/agricultural/industrial), digestion processes, and subsequent P recovery treatments. Phytate-P makes up the majority of P in grain, and is therefore abundant in human diets (Raboy, 2003). However, phytate cannot be directly absorbed and is not efficiently digested in the human gut, so a significant proportion passes through into excreta, with Joung et al., (2007) reporting faecal phytate-P concentrations between 4 – 11mg g^{-1}, equivalent to 24-54% of faecal phosphorus. This leads to the assumption that phytate should therefore be abundant in sludge, comprising a significant fraction of the total P in untreated sewage solids.

The fact that some papers have noted the persistence of phytate in the sludge effluent after AD (Smith et al., 2006; Annaheim et al., 2015) is important when considering that this sludge is often applied to agricultural soils. Phytate-P is not available for uptake by plants without prior dephosphorylation by phytase enzymes, but its high charge density means that it can become rapidly immobilised in soil via the formation of insoluble precipitates with metal cations, or interaction with the organic and clay fractions (Giles et al., 2011). This means that if phytate survives the wastewater treatment process intact and in abundance, a significant fraction of sludge P could be lost to the soil, potentially accumulating rather than being bioavailable for crops as would be intended. However, a recent paper observed the mineralisation of all orthophosphate monoesters during anaerobic digestion, with inorganic orthophosphate the only P compound present in ^{31}P NMR spectra of digested sludge extracts (Li et al., 2019). Despite phytate not being specifically measured in this study, it may indicate its mineralisation during AD. Furthermore, there are currently no papers that have measured phytate concentrations in WWTP processes that include a modern hydrolytic step. This is potentially important, as cell lysis could release phytate into the digester solution, where it would be more bioavailable for microbial degradation in AD, should there be a resident phytase-producing microbial population.

3.2.5 Aims and Objectives

The aim of this chapter therefore was to confirm the presence, abundance and persistence of phytate in sludge throughout an advanced anaerobic sludge treatment process through to the final cake destined for land application. Sludge total phosphorus concentration (P_T), and concentrations and proportions of orthophosphate-P and phytate-P in sludge extracts were measured at five consecutive stages in the treatment process. Solution ^{31}P NMR was used to measure orthophosphate-P and phytate-P, and data was compared to colorimetric measurements of identical samples using a phytase enzyme assay in order to assess the suitability of this less-expensive and higher-throughput method for future samples.

It was hypothesised that sludge P_T would be lowest in the primary sludge, increasing with the addition of secondary sludge, and peaking following anaerobic digestion due to

the inherent reduction in sludge mass. Orthophosphate was expected be the dominant P-fraction in all sludges, with phytate making up a smaller but significant fraction. There was expected to be good agreement between ^{31}P NMR and colorimetric data, but the measurement of phytase-labile P could overestimate phytate due to the broad substrate specificity of the enzyme.

Phytate was hypothesized to persist throughout the treatment process due to its lower bioavailability compared to orthophosphate, with little variation in its concentration and was expected to be present as a small (~10%) fraction of total extractable P in the final dewatered sludge.

3.3 Methods

3.3.1 Wastewater treatment plant (WWTP) & Sampling

Sludge samples were obtained from Esholt wastewater treatment plant near Bradford, UK. A schematic of the Esholt wastewater treatment process with sampling points is presented in Figure 3.2. The plant is owned and operated by Yorkshire Water Ltd, serving a population equivalent of 750,000 (350,000 people, and an equivalent of 400,000 designated to industry), and imports both liquid sludge and cake to the site (ratio imported:indigenous 34:66). The final sludge mixture following addition of secondary sludge comprises 70% primary sludge and 30% secondary sludge. The plant handles a maximum of 82 tonnes of dry-solid throughput per day, employing advanced AD with a BioThelys thermal hydrolysis plant (THP) supplied by Veolia Water Technologies. Within the THP, sludge is heated to 165°C at 6 bar pressure for 20 minutes, prior to introduction to digesters, in which mesophilic AD is carried out with a solid retention time of 11 days. There are currently no P removal or recovery techniques employed at the plant, (Personal communication, Yorkshire Water, 2019). Sludge was sampled on a single day in March 2019 at five successive points in the treatment process (Figure 3.2). These were primary sludge (PS), secondary sludge/THP feed (SS), digester feed (DF) digested sludge (DS), and dewatered cake (CK; Figure 3.2). At each sample point, a single 5L bucket of sludge was taken, transported to the University of Sheffield and refrigerated until use.

3.3.2 Sample Processing

A summary of the sample preparation and analysis procedures can be found in Figure 3.3. All samples apart from CK were in liquid form and had to be largely dewatered in the lab. Due to the high solids content of the samples, filtration was not a viable option for solid separation. Samples were instead split into 50mL falcon tubes and centrifuged at 4,700 x *g* for 5 minutes. Supernatant was discarded and solid material was removed and spread into large plastic weighing boats. Solid samples were then left to air dry for 2 days in a fume cupboard. Once dry, samples were broken up and ground. The fibrous and tacky nature of the samples meant that ball milling was not an adequate homogenisation method. Instead, coarsely ground samples were subsequently frozen

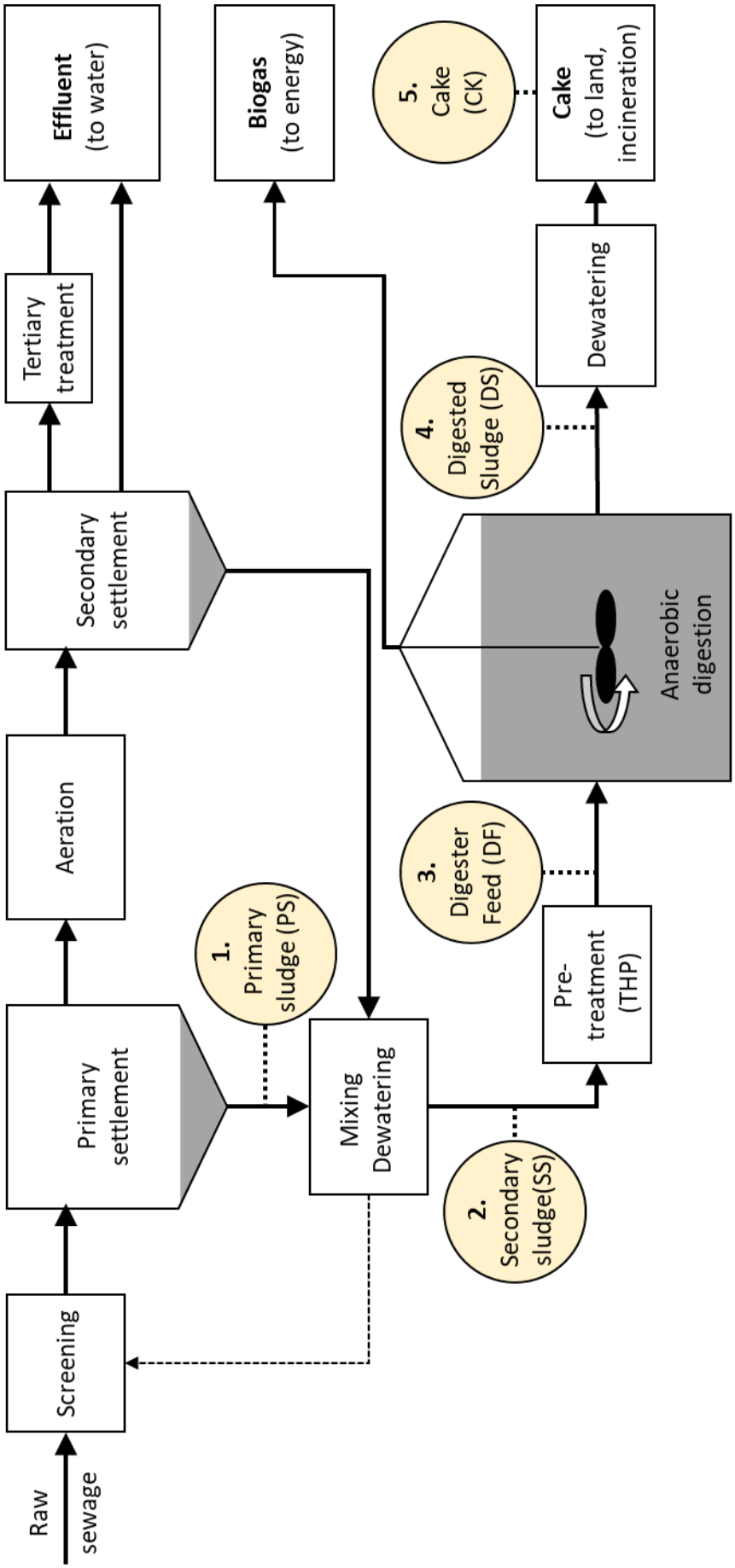

Figure 3.2: Schematic of the wastewater treatment process at Esholt WWTP near Bradford, UK. Circles show points at which samples were taken through the process, from Primary Sludge (PS), Secondary Sludge (SS), Digester Feed (DF), Digested Sludge (DS), and final dewatered Cake (CK).

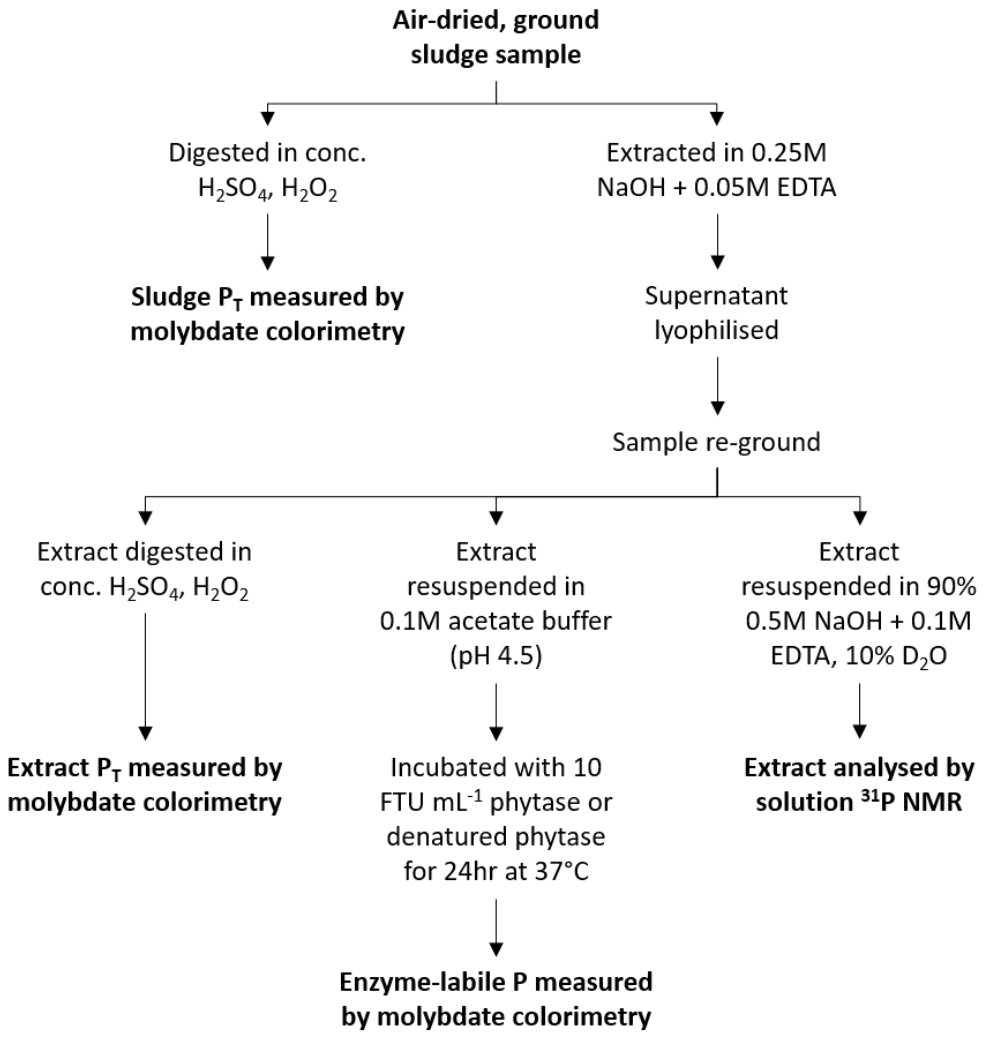

Figure 3.3: A schematic diagram of the methods used to determine Total P, Orthophosphate P and Phytate-P in sludge and extracts

under liquid nitrogen and homogenised with a pestle & mortar to pass a 2mm sieve. Homogenised samples were stored in 50mL falcon tubes at 5°C prior to use.

For each sampling point, three 1g replicates of each sludge were extracted in 50mL falcon tubes with 20mL 0.25M NaOH + 0.05M EDTA for 16 hours in an end-over-end shaker. Extracted samples were centrifuged for 10 minutes at 4700 x g, and the supernatant filtered through Whatman No. 1 filter paper into fresh tubes. These were then frozen at -80°C before lyophilisation with an Edwards Modulyo Freeze Dryer. Lyophilised extracts were re-ground with a pestle and mortar, weighed, and stored at 5°C.

3.3.3 Colorimetric Analyses

3.3.3.1 Sludge & Sludge Extract Total P (P_T) – P_T of sludge and 0.25M NaOH + 0.05M EDTA extracts were measured colorimetrically following a modified version of the acid-peroxide digestion protocol devised by Lindner, (1944). Three 20mg replicates of each dried sludge, and one 20mg replicate of each sludge extract were weighed into acid-washed digest tubes. Samples were then subject to acid-peroxide digestion and were subsequently measured for P_T by a modified version of the molybdate blue reaction (Murphy & Riley, 1962). 50mg samples were digested in 1mL concentrated H_2SO_4 for 30 minutes at 350°C under reflux. Tubes were then cooled and 0.2mL 30% H_2O_2 added to the tube, which were uncapped and returned to 350°C. Samples were heated until vapour production ceased, after which they were removed from the heat. H_2O_2 addition was repeated if necessary, before samples were left open overnight to cool. Digests were then diluted to 10mL with UHP water, transferred to 15mL falcon tubes and centrifuged for 5 minutes at 4700 x g. P_T was measured by the addition of the following to a 4mL cuvette: 0.5mL digest, 0.2mL 0.1M *L*-ascorbic acid, 0.5mL developer (ammonium molybdate antimony potassium tartrate in 2M H_2SO_4), 0.5mL 3.44M NaOH, and 2.1mL UHP water. Colour was left to develop for 40 minutes and absorbance measured at 882nm on a Cecil CE 1020 spectrophotometer.

3.3.3.2 Colorimetric determination of extract MRP & phytase-labile P – A bespoke method was designed in order to measure extract MRP and phytase-labile P based upon similar enzymatic quantification procedures (He et al., 2009; Menezes-Blackburn et al., 2014). 10mg samples of extracted sludge were resuspended in 10mL of 0.1M acetate buffer (pH 4.5). Each suspension was then split into two 5mL aliquots, to which was added 1mL of either 10 FTU mL^{-1} phytase enzyme, or 1mL of 10 FTU mL^{-1} denatured phytase enzyme that had been autoclaved in a Prestige 2100 Benchtop Autoclave with an 11min hold cycle at 121°C at 15 psi, then centrifuged for 5 minutes at 4,500 x *g* to remove precipitated protein. Mixtures were incubated at 37°C with shaking for 24 hours, before molybdate-reactive P (MRP) was measured by molybdate colorimetry. Extract P_I was estimated as MRP of the suspension treated with denatured enzyme. Phytase-labile P was calculated as the difference in MRP between phytase- and denatured phytase-treated suspensions. Each colorimetric sample was measured

against an identical sample in which colour development was prevented by replacing 100µL 0.1M L-ascorbic acid with 100uL UHP. Absorbance of this blank sample was subtracted from primary sample absorbance to account for the colour of the resuspended extract.

3.3.4 Solution ^{31}P NMR

Solution ^{31}P NMR was carried out according to the method developed by Robertson, (2018) according to the recommendations of Cade-Menun & Liu, (2014), for the quantitative analysis P compounds in soil samples. This method was adapted for use with sludge samples containing comparatively high P concentrations, and optimisation of the method was validated with a spike-recovery procedure.

3.3.4.1 Sample preparation – For solution ^{31}P NMR spectroscopy of 0.25M NaOH + 0.05M EDTA extracts of sewage sludge, 50mg of lyophilised extract was resuspended in 1mL of 1M NaOH + 0.1M EDTA. Due to the high P concentration of sludge extracts, and viscosity of the concentrated sample, 0.2mL of this resuspension was then added to a 1.5mL Eppendorf tube and diluted to 1mL with 0.7mL 1M NaOH + 0.1M EDTA and 0.1mL of 4mM methylene diphosphonate (MDP; internal standard) in D_2O for signal lock. Tubes were vortex mixed and left to settle for 5 minutes, before centrifuging at 9000rpm for 5 minutes. 0.5mL of the preparation was transferred to a 5mm NMR tube.

3.3.4.2 ^{31}P NMR parameters – ^{31}P NMR spectroscopy was performed on a Bruker Advance 500 Spectrometer with a mag1 console (Bruker, Germany). CK samples and spiked samples were analysed following an upgrade of the NMR mag1 console to an AvII console. This increased sensitivity and signal:noise ratio within spectra, but integration was not affected, and data were comparable. Spectra were recorded at a frequency of 202.456 MHz with a 5mm broadband probe at a temperature of 298 K (24.85°C). 10% D_2O was included in all samples as a signal lock. During each sample analysis, the following parameters were unchanged: acquisition time = 0.845s; pulse width of 22µs; pulse angle 90°; delay time = 1s; total number of scans = 16,384; pulse program = zgig. Peak areas of signals were integrated using Bruker Topspin 4.0.3, and calibrated to the peak area of the MDP internal standard for absolute quantification. Calculation of orthophosphate and phytate concentrations was achieved by integration of their peaks

at 6.0 - 5.6 ppm and 4.78 - 4.68ppm respectively, relative to the peak of the MDP internal standard at 17.19 - 16.92ppm, followed by correction to account for the proportion of signal observed for each compound at 1s relaxation delay. For phytate, the second peak was used for integration as this was the most clearly defined peak and was well separated from the orthophosphate peak. This peak accounts for 2 of the 6 P nuclei within the molecule, so the integral was multiplied by three.

3.3.4.3 ^{31}P NMR Optimisation - An optimisation procedure was carried out for sludge extract samples to provide a correction factor for integrals due to the insufficient but necessary relaxation delay time of 1s, and the method was validated with a spike-recovery assay.

As the delay time of 1s is insufficient to allow full relaxation of P compounds between scans, an optimisation procedure was carried out prior to integration in which delay time was increased. Sludge samples were analysed according to the parameters described above, but over 100 scans. In a series of seven analyses, delay time was set to 1, 2, 5, 10, 20, 30 and 40s. Integrals for each compound were plotted over increasing delay time to calculate the proportion of the signal produced with a delay time of 1s compared to the signal produced when nuclei are allowed to fully relax.

Spike & Recovery – Following sample analysis, three sludge sample extracts were selected, and spiked with 10uL of 7.25mM (0.0725 µmol) sodium dihydrogen orthophosphate, and 5uL of 15mM (0.45 µmol) phytic acid sodium salt dihydrate. Spiked samples originated from the original resuspensions and were analysed following the same ^{31}P NMR parameters to be directly comparable. Recovery of spiked compounds was calculated as the observed increase in concentration above un-spiked values, divided by the expected increase. The three replicates of CK sludges were spiked, as un-spiked samples for these sludges were also recorded after the machine console was updated, meaning that the analysis would be directly comparable.

3.3.5 Statistical Analysis

Concentrations of P_T, along with orthophosphate-P and phytate-P measured by both colorimetry and ^{31}P NMR were compared between sludge samples using one-way ANOVA. Absolute concentrations of orthophosphate and phytate-P were also converted

to percentage contribution to total extracted P. Percentage contributions were compared between sludge samples by one-way ANOVA. Where significant differences were present, one-way ANOVAs were followed by Tukey multiple comparison tests. Statistical analysis was performed using GraphPad Prism v.7.04 (GraphPad Software Inc, San Diego USA).

3.4 Results

3.4.1 Total Phosphorus of Sludge

P_T content of sludge was measured by H_2SO_4-H_2O_2 digestion, followed by molybdate blue colorimetry. There was a statistically significant difference between measured total P levels in each of the sludges (One-way ANOVA, $p < 0.0001$; Tukey multiple comparisons test, $\alpha=0.05$; Figure 3.4). P_T of PS was the lowest found throughout the process, with an average P content of 8118 µg P g^{-1} sludge. This increased sharply in SS to an average of 15971 µg P g^{-1} and increased again after THP in the DF sludge to 18765 µg P g^{-1}. The digested sludge (DS) collected after anaerobic digestion had the greatest level of P_T at 25997 µg P g^{-1}, which then fell slightly in dewatered cake (CK) to a final concentration of 23263 µg P g^{-1}.

3.4.2 Total Extractable Phosphorus

Total extractable P was measured by H_2SO_4-H_2O_2 digestion, followed by molybdate blue colorimetry of the lyophilised 0.25M NaOH + 0.05M EDTA sludge extracts. The extraction efficiency of sludge samples was high, with P recovery of between 81-93% of sludge P_T (Figure 3.5). Total extractable P therefore followed the same pattern of P concentration as unextracted sludge (PS < SS < DF < CK < DS). A statistically significant difference in P concentration of sludge extracts was observed between all sludge types (One-way ANOVA, $p < 0.0001$; Tukey multiple comparisons test, $\alpha=0.05$; Figure 3.5).

3.4.3 Colorimetric determination of sludge MRP and phytase-labile P

Absolute content of P compounds in sludge extracts were measured colorimetrically. Orthophosphate-P was estimated as molybdate-reactive P (MRP) in extracts, phytase-labile P was calculated as the increase in MRP after phytase incubation. The difference between total extractable P and the sum of MRP and phytase-labile P was designated as 'residual P' (Figure 3.6). There was a significant difference in the absolute concentration of MRP between sludges (One-way ANOVA, $p<0.0001$; Tukey multiple comparisons test, $\alpha=0.05$; Figure 3.6 A), which made up the largest fraction

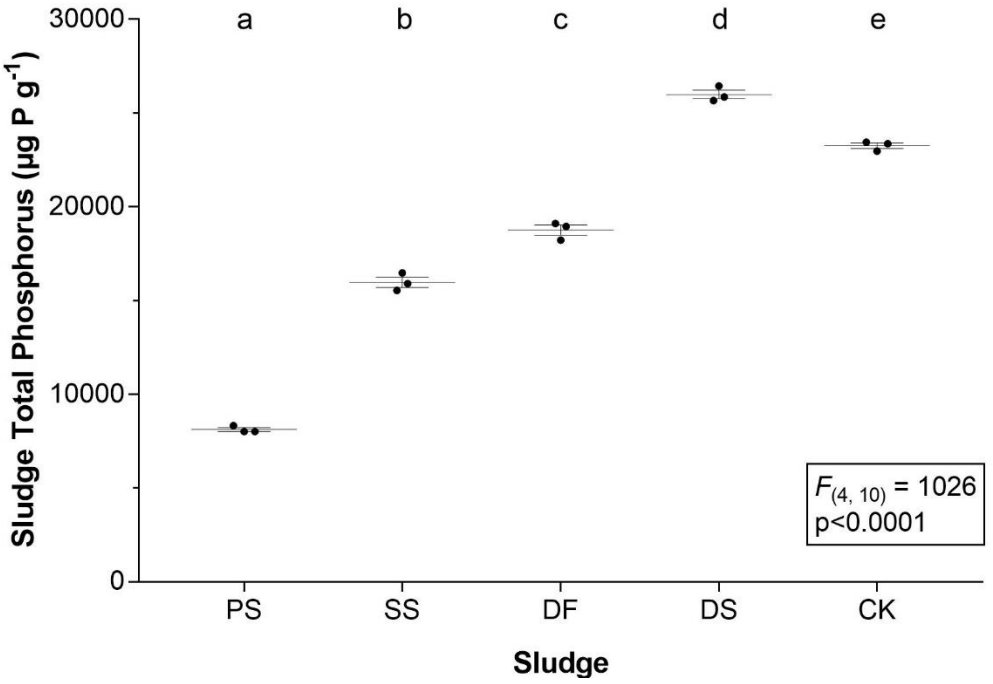

Figure 3.4: Sludge total phosphorus concentration (µg P g^{-1} sludge) measured by molybdate colorimetry. Samples are represented as individual points (n=3) with horizontal bars indicating mean ± SEM. Results of one-way ANOVA are inset. Significant differences are represented as different letters above bars (Tukey multiple comparison, α = 0.05).

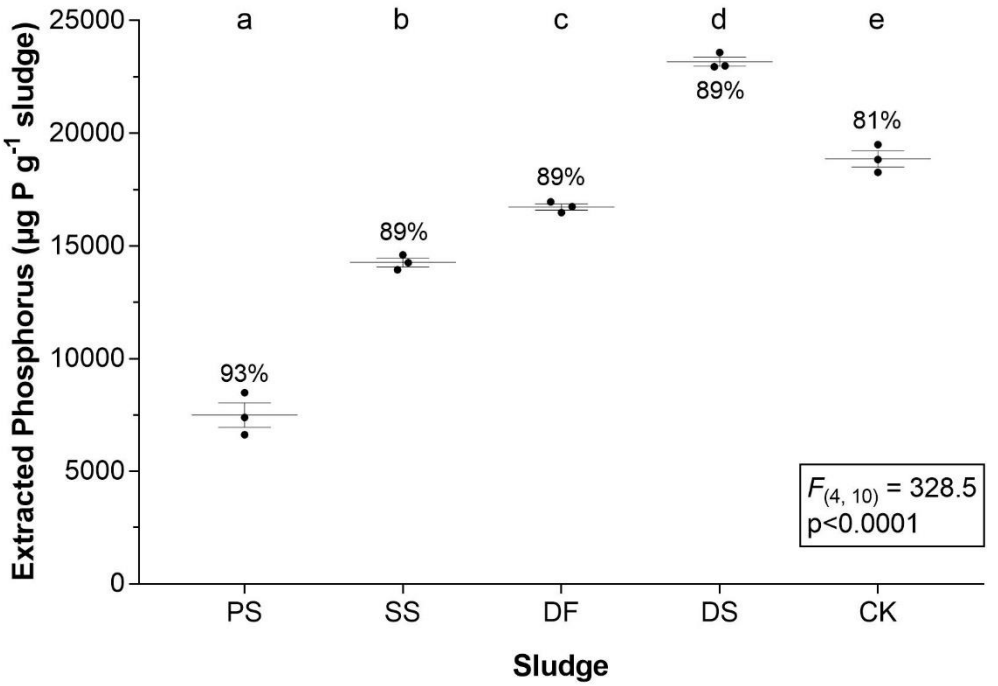

Figure 3.5: Extract total phosphorus (µg P g^{-1} sludge) measured by molybdate colorimetry. Mean extraction efficiency (%) is presented for each sludge. Samples are represented as individual points (n=3) with horizontal bars indicating mean ± SEM. Results of one-way ANOVA are inset. Significant differences are represented as different letters above bars (Tukey multiple comparison, α = 0.05).

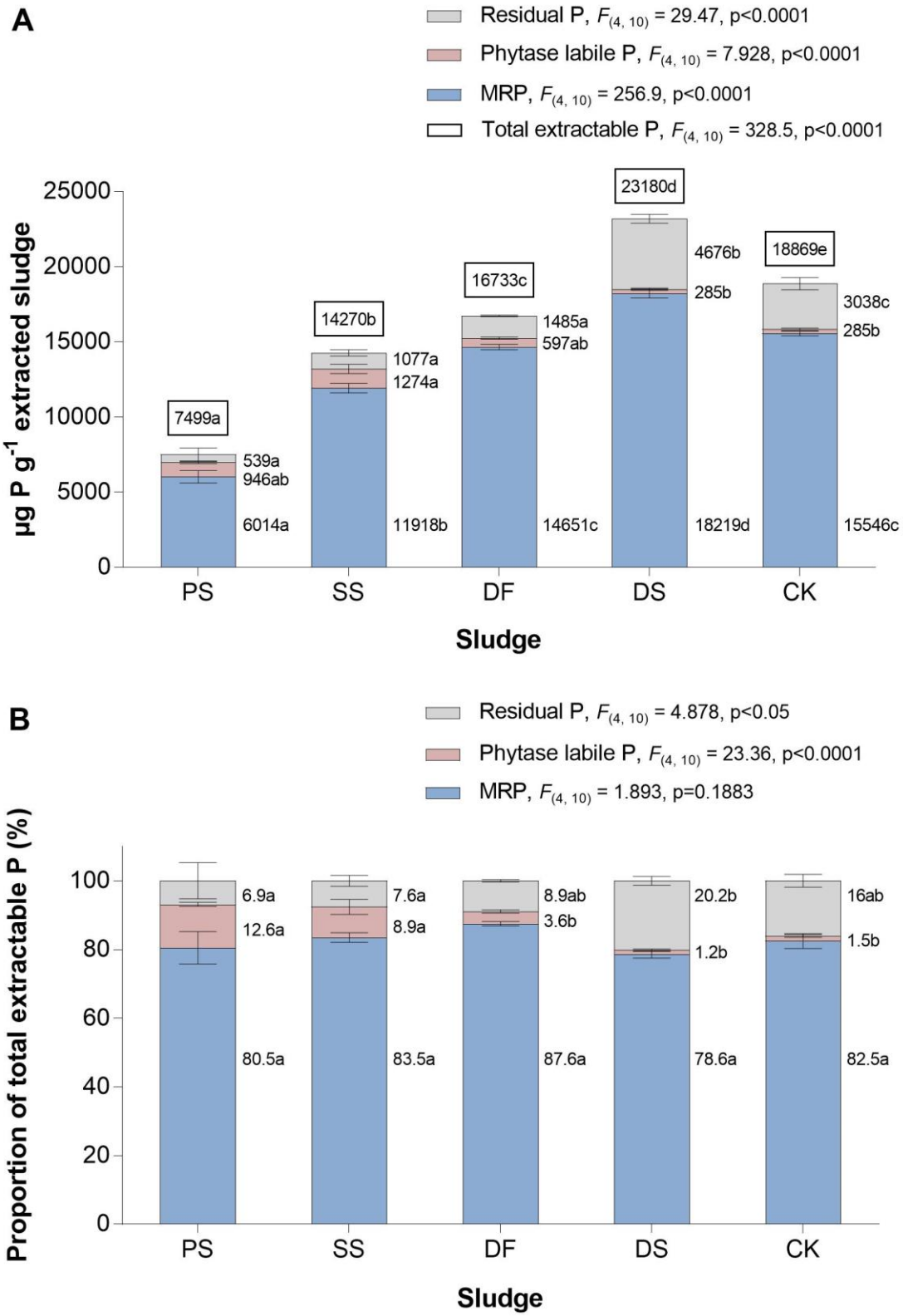

Figure 3.6: A: Mean absolute concentrations of P fractions in sludges measured colorimetrically (µg P g^{-1} extracted sludge ± SEM, n=3). Total extractable P is presented above each bar. **B:** Mean concentrations of P fractions in sludges as a proportion of total extractable P (% ± SEM, n=3). Results of one-way ANOVA are shown for each P fraction. Results of Tukey multiple comparison test for each fraction are shown with means to the right of bars (α = 0.05). Different letters indicate a significant difference between values for that P fraction.

of total extractable P in all samples increasing in the same pattern as total extractable P levels (PS < SS < DF < CK < DS).

The greatest concentration of phytase-labile P was found in SS, and a significant decrease was observed in DS and CK sludges following anaerobic digestion (One-way ANOVA, $p<0.0001$; Tukey multiple comparisons test, $\alpha=0.05$; Figure 3.6 A). No significant difference in calculated residual-P was observed between sludges prior to digestion. However, a sharp and significant increase was observed following anaerobic digestion in DS, which then fell slightly in the final CK sludge (One-way ANOVA, $p<0.0001$; Tukey multiple comparisons test, $\alpha=0.05$; Figure 3.6A).

Absolute levels of P were then expressed as a proportion of total extractable P (Figure 3.6 B). There was no significant difference in proportional levels of MRP, which made up approximately 80% of total extractable P in all sludge (One-way ANOVA, $p>0.05$). There was a significant difference in the proportion of phytase-labile P, which is greatest in the PS at 12.6% and SS at 8.9%, before falling significantly following THP treatment to 3.6% in DF. Following digestion, the proportion of phytase-labile P fell slightly to between 1.2-1.5% in DS and CK (One-way ANOVA, $p<0.0001$; Tukey multiple comparison test, $\alpha=0.05$). There was also a significant difference in the proportion of residual-P (One-way ANOVA, $p<0.05$), which increased slightly from 6.9-8.9% between PS < SS < DF, before making up 20.2% in DS, then falling slightly to 16% in CK (Tukey multiple comparison test, $\alpha=0.05$).

3.4.4 ^{31}P NMR Optimisation

Prior to the integration of NMR signals in sludge spectra, an optimisation procedure was carried out to calculate the proportion of the total signal that is produced using a 1s delay time, relative to the maximum signal produced when compounds can relax fully at longer delay times. Spiked samples were analysed with 100 scans at delay times of 1, 2, 5, 10, 20, 30 and 40s, for each compound, integrals were measured and presented as a percentage of the largest measured (Figure 3.7). Methylene diphosphonate (MDP) was used as an internal standard to represent a peak of 0.4 µmol P. In sludge samples, the MDP peak was found to increase to a plateau at a delay time of 5s, with the integral observed at 1s found to represent 81% of the fully

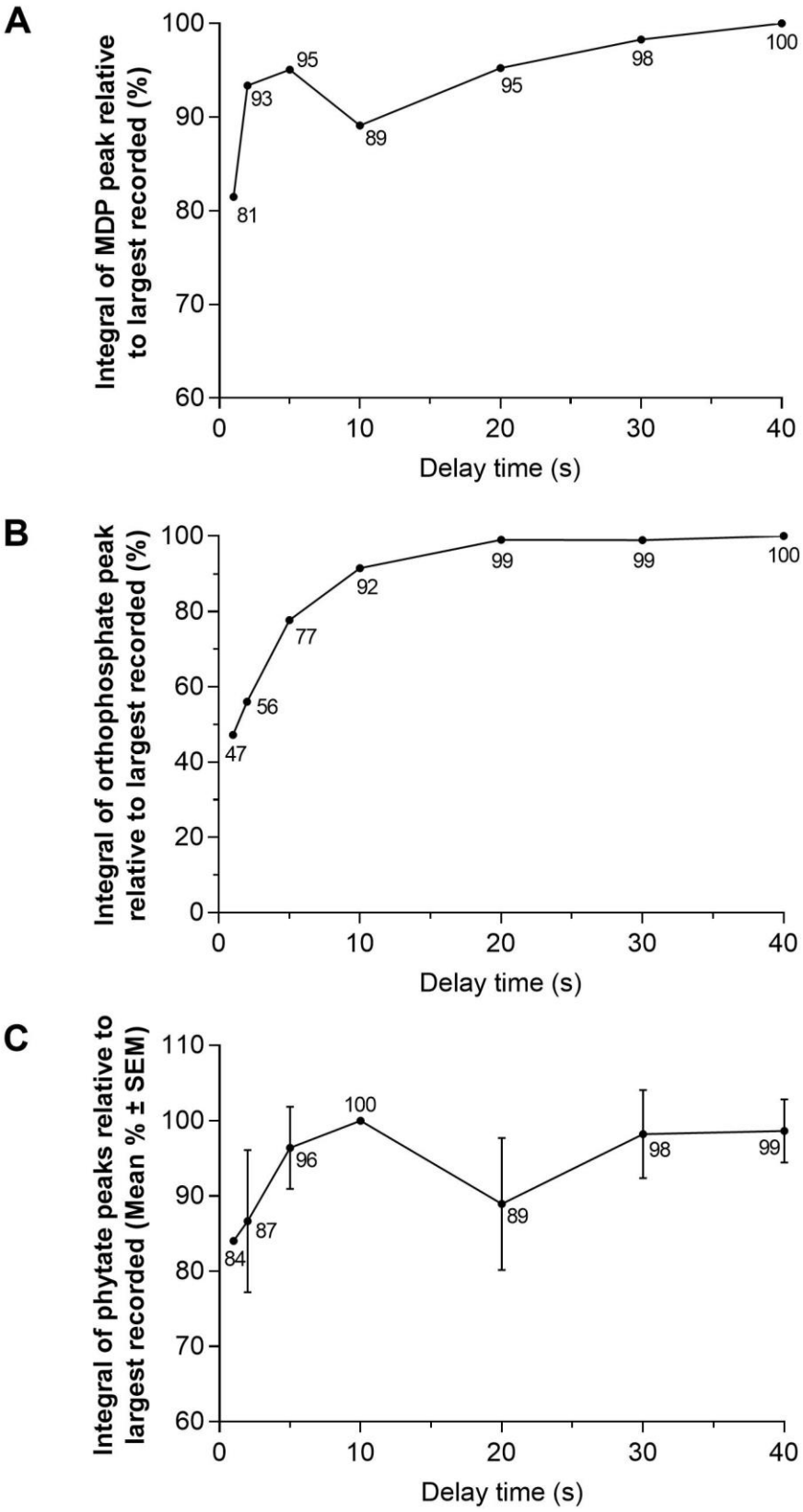

Figure 3.7: Integrals of ^{31}P NMR peaks relative to the largest of: **A**. MDP; **B**. Orthophosphate and **C**: Phytic acid, with increasing delay times. Figures A & B show relative integrals for the single peaks produced by each compound, figure C shows the mean relative integral of the four phytic acid peaks ± SEM. No error bars are present in the maximum integral as each replicate was set to 100.

relaxed signal (Figure 3.7A). For phosphate, the increase in integrals was a smooth curve reaching plateau by approximately 20s, with the signal at 1s representing 47% of the total signal (Figure 3.7B). For phytate, integrals were measured for each of the four spectral peaks, which were treated as replicates. The increase in integral area appears to reach maximum at 10s, with the 1s signal representing 84% of the total expected signal (Figure 3.7C). These percentages were used to adjust the integrals measured in each sample spectrum to correct for the loss of signal when using a 1s delay time. The method was validated in a spike-recovery assay on CK sludge. Percentage recovery of spiked orthophosphate and phytate in three CK sludge extracts by ^{31}P NMR were 103.78 ± 2.14% and 104.77 ± 5.17 % respectively (Figure 3.8).

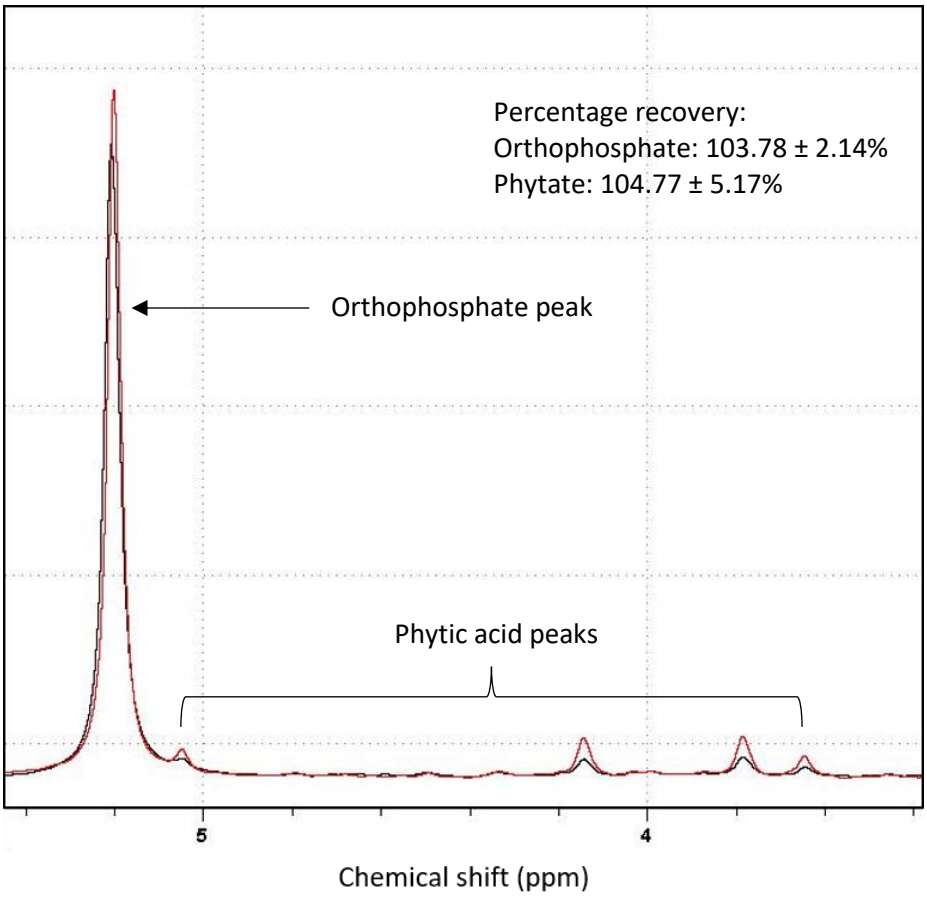

Figure 3.8: ^{31}P NMR spectra of **Black**: Sample CK-1; and **Red**: Sample CK-1 spiked with 5µL 7.25mM sodium dihydrogen orthophosphate and 5µL 15mM phytic acid sodium salt dihydrate. Integration of original and spiked samples enabled the calculation of percentage recovery. Mean percentage recovery ± SD for orthophosphate and phytate are shown in the figure (n=3). See Appendix A for remaining spike-recovery figures.

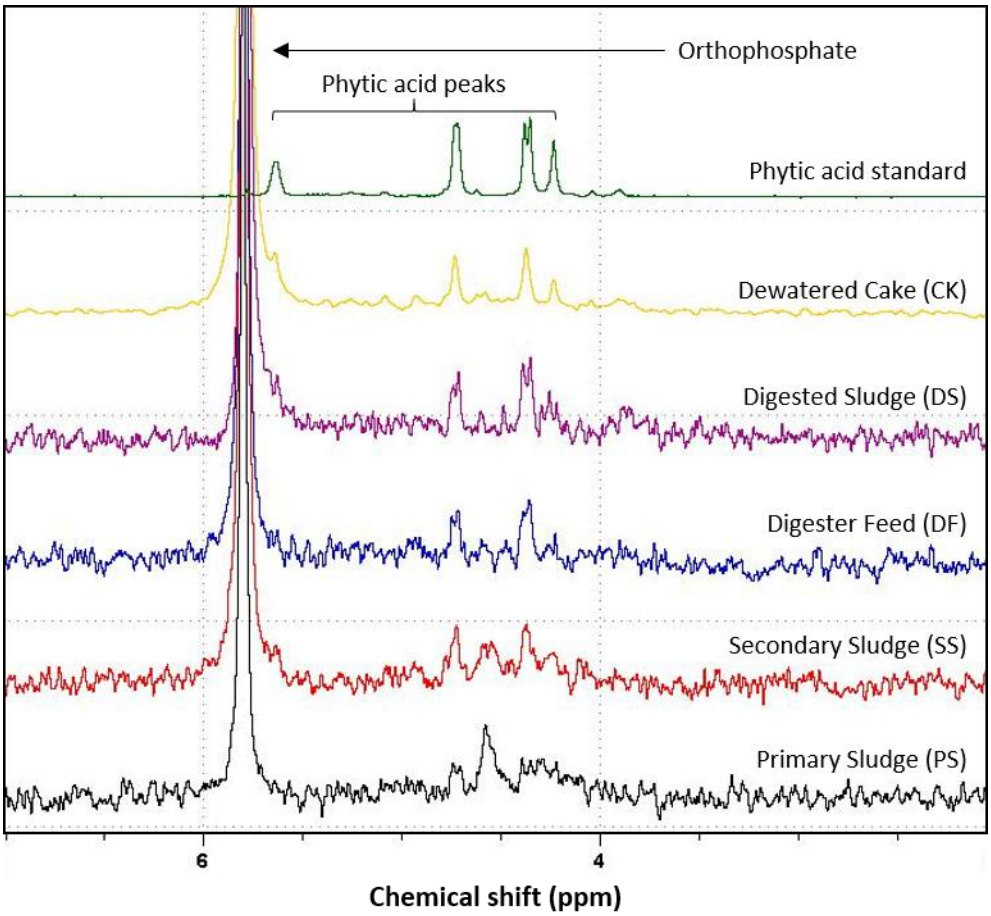

Figure 3.9: Selected ^{31}P NMR spectra of sludge extracts between 7ppm and 2ppm. A phytate standard is included to indicate phytate peaks. Sludge phytate was integrated using the second phytate peak, as this was at sufficient distance to avoid distortion by the large orthophosphate peak, and was the best separated from other peaks. Signal to noise ratio in CK was improved due to the installation of a new ^{31}P NMR console during the analysis period. Spectra for all samples are shown in Appendix A.

3.4.5 ^{31}P NMR determination of sludge orthophosphate and phytate

Typical spectra from a single replicate of each sludge sample are presented in Figure 3.9. Full spectra for each replicate are presented in Appendix A. Orthophosphate was found to be the most abundant P compound in ^{31}P NMR analysis of all sludge samples. There was a significant difference in absolute orthophosphate concentration between all sludge types (One-way ANOVA, $p<0.0001$), which increased from PS < SS < DF < CK < DS (Tukey multiple comparisons test, $\alpha=0.05$; Figures 3.10 & 3.12A). There was a strong positive linear relationship between orthophosphate concentrations measured by NMR and colorimetry ($R^2 = 0.98$, $p < 0.0001$; Figure 3.13A). As a proportion of total extractable P, orthophosphate comprised between 74.3% and 86.5% (Figure 3.12 B). Despite having the highest

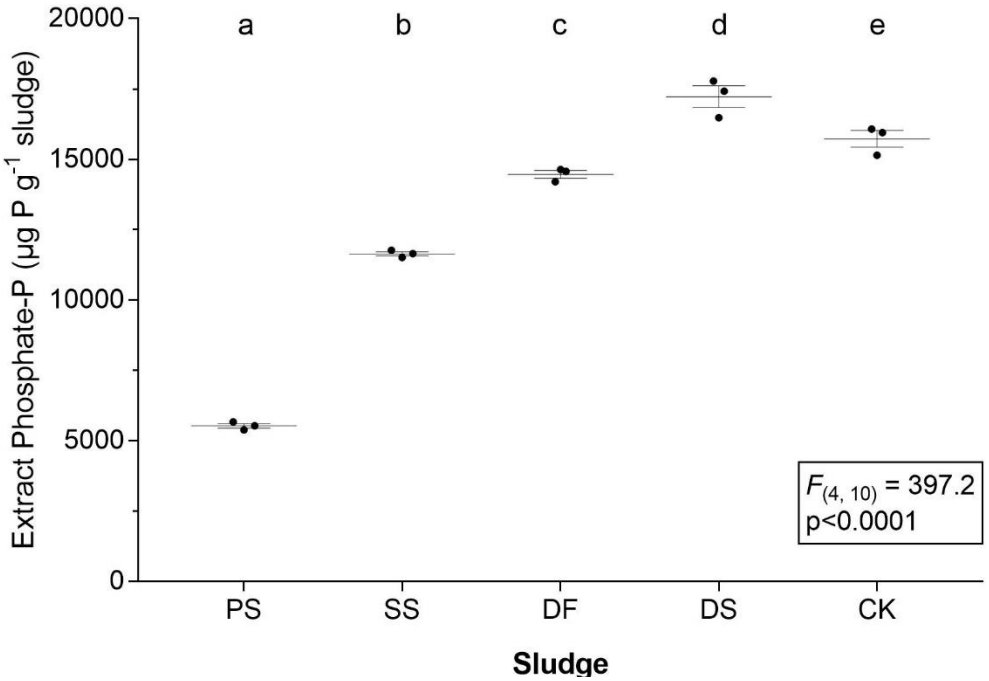

Figure 3.10: Concentration of orthophosphate-P measured by ^{31}P NMR of sludge extracts, expressed as µg P g^{-1} dry weight of sludge. Samples are represented as individual points (n=3) with horizontal bars indicating mean ± SEM. Results of one-way ANOVA are inset. Significant differences are represented as different letters above bars (Tukey multiple comparison, α = 0.05).

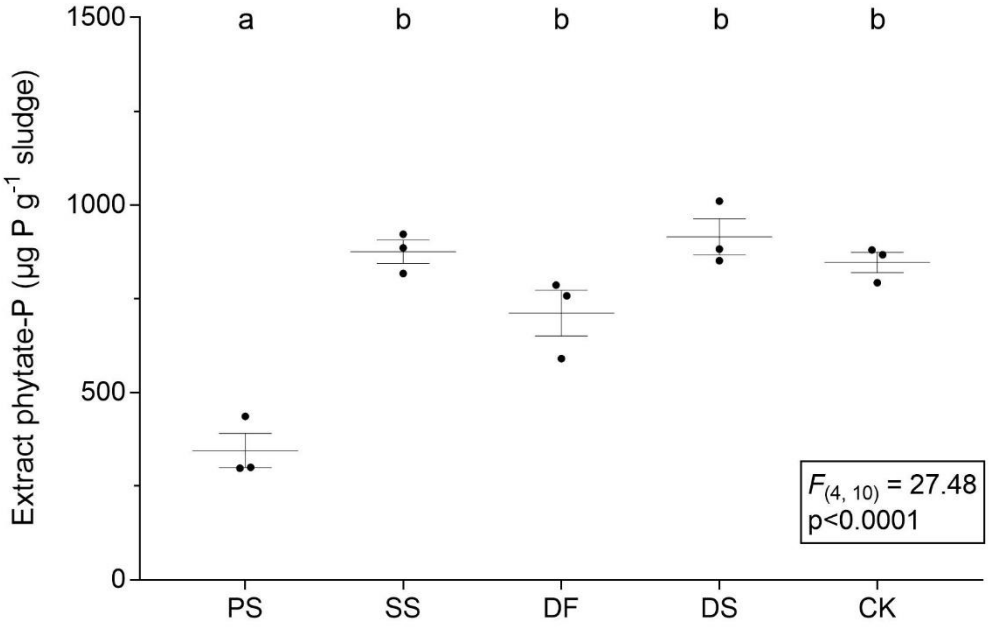

Figure 3.11: Concentration of phytate-P measured by ^{31}P NMR of sludge extracts, expressed as µg P g^{-1} dry weight of sludge. Samples are represented as individual points (n=3) with horizontal bars indicating mean ± SEM. Results of one-way ANOVA are inset. Significant differences are represented as different letters above bars (Tukey multiple comparison, α = 0.05).

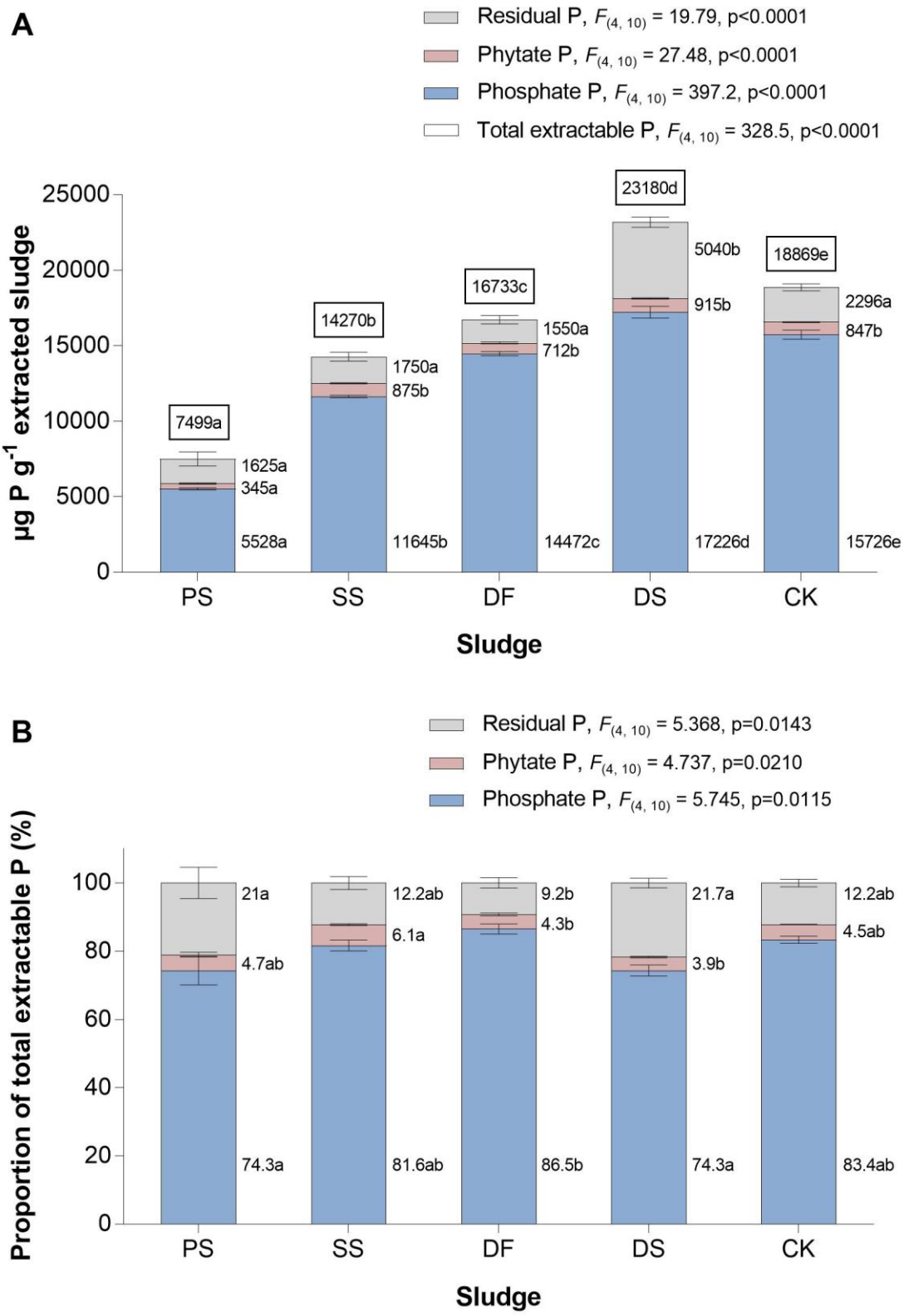

Figure 3.12: A: Mean absolute concentrations of P fractions in sludge extracts measured by ^{31}P NMR (µg P g^{-1} extracted sludge ± SEM, n=3). Total extractable P is presented above each bar. **B:** Mean concentrations of P fractions in sludges as a proportion of total extractable P (% ± SEM, n=3). Results of one-way ANOVA are shown for each P fraction. Results of Tukey multiple comparison test for each fraction are shown with means to the right of bars (α = 0.05). Different letters indicate a significant difference between values for that P fraction.

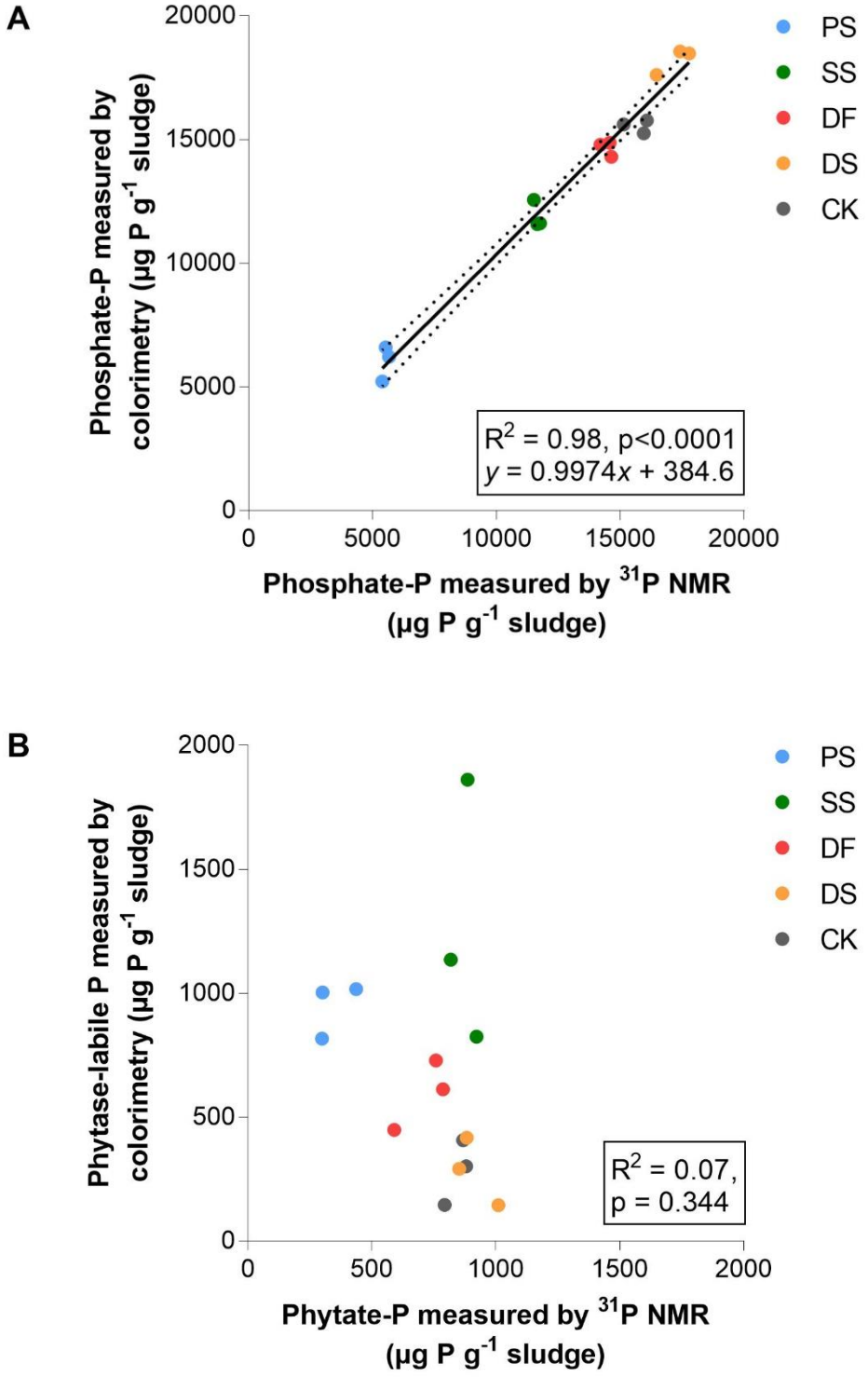

Figure 3.13: Linear regression of **A:** Phosphate-P of sludge extracts measured by molybdate colorimetry and ^{31}P NMR; and **B:** Phytate-P measured colorimetrically as phytase-labile P and by ^{31}P NMR. Points represent single samples. R^2 and p values presented on graphs. Where a linear relationship exists, the equation of the regression line is presented.

absolute orthophosphate concentration, the proportion of orthophosphate was joint lowest in DS, whereas the highest proportion was found in DF sludge (One-way ANOVA, $p<0.05$, Tukey multiple comparisons, $\alpha=0.05$).

Absolute phytate concentrations measured by ^{31}P NMR were much lower than orthophosphate levels and were lowest in PS at 345 µg P g^{-1}. There was a significant difference between phytate concentrations (One-way ANOVA, $p<0.0001$), with all other sludges having a significantly greater concentration than that found in PS, increasing between 712 and 915 µg P g^{-1} in the order DF < CK < SS < DS (Tukey multiple comparisons test, $\alpha=0.05$; Figures 3.11 & 3.12A). As a proportion of total extracted P, phytate-P ranged between 3.9% and 6.1% in the order DS < DF < CK < PS < SS (One-way ANOVA, $p<0.05$; Figure 3.12B). Interestingly, despite containing the highest absolute concentration of phytate-P, DS contained the lowest proportion of phytate-P of any sludge. There was no linear relationship between phytate levels measured by ^{31}P NMR and those measured colorimetrically as 'phytase-labile P' when measured by linear regression ($R^2 = 0.07$, $p = 0.34$; Figure 3.13B).

There was no significant difference observed in absolute residual-P levels calculated in PS, SS, DF, and CK which ranged between 1625 and 2296 µg P g^{-1} sludge (Figure 3.12A). However, levels in DS were significantly greater than all others, standing at 5040 µg P g^{-1} (One-way ANOVA, $p<0.0001$; Tukey multiple comparisons test, $\alpha=0.05$). This was also the highest proportion of residual P found in all sludges, at 21.7% of total extracted P, with the lowest proportion found in DF, and increasing through SS & CK <PS < DS (One-way ANOVA, $p<0.05$; Tukey multiple comparisons test, $\alpha=0.05$; Figure 3.12 B).

3.5 Discussion

This is the first study to employ a combination of colorimetric methods and solution ^{31}P NMR to specifically measure the concentrations and proportions of orthophosphate and phytate in sludge samples taken over five consecutive points in an advanced anaerobic digestion sludge treatment process. Overall it was found that orthophosphate makes up the greatest concentration and proportion of extractable sludge P, standing at approximately 80%, with good agreement between analytical techniques. Phytate-P measured colorimetrically as phytase-labile P was found to be initially high at ~12% in PS, but fell dramatically following digestion to 1.2%. However, when measured by ^{31}P NMR, phytate-P proportions were found to remain relatively stable throughout the process, and there was no linear relationship between results of the two methods. When compared to evidence from spike-recovery experiments with ^{31}P NMR, this suggests that colorimetric measurement of phytase-labile P in sludge samples may be inaccurate, both over- and under-estimating phytate levels depending on sludge sample**.** Persistence of phytate-P in the final digested sludge cake may have important impacts on soil P stoichiometry when applied to agricultural soil, which is the preferred route of disposal in the UK. The 4.5% fraction of total sludge-P measured as phytate-P is likely to become rapidly and irreversibly immobilised in soil, accumulating in a form inaccessible to crops.

3.5.1 Sludge Total Phosphorus & Extraction Efficiency

Sludge P_T concentration increased through consecutive stages of the wastewater treatment process, peaking in the product of anaerobic digestion (DS), before falling slightly in dewatered cake (CK). As there are no current P removal techniques used on sludge at Esholt, the change in P concentrations can be explained by looking at the changes within the sludge during processing. PS is the product of primary gravitational settlement of suspended solids in the wastewater, meaning that a portion of the P_T contained in the wastewater is settled out at this stage. However, the remainder, comprising unsettled suspended solids, dissolved organic matter and soluble P moves with water to secondary treatment, where it is stripped from the water and metabolized by aerobic microorganisms. The biological floc produced is settled out to produce

secondary waste-activated sludge, which is then returned to the sludge treatment process. At Esholt, sludge has a final ratio of 64:36% primary:secondary sludge when mixed. The increase in P_T from PS to SS can therefore be explained by the addition of the nutrient-rich activated sludge to the mix.

P_T was greatest in DS, following anaerobic digestion. Over a retention time of 15 days, sludge solids undergo mesophilic digestion, resulting in the production of methane gas, and a reduction in sludge mass of approximately 50% on a dry solids basis (personal communication, Yorkshire Water Ltd, 2019). This therefore coincides with an increase in concentration of P within the solids fraction to its peak at almost 26000 μg P g^{-1} sludge. P_T concentration then decreased slightly with dewatering to 23263 μg P g^{-1} in CK. P_T content of Esholt sludge is similar to concentrations found in other studies. Smith et al., (2006) measured P_T of undigested sludge, digested sludge and cake at 9000, 21000 and 16000 μg P g^{-1} respectively, whereas the concentration of P in dried anaerobically digested sewage sludge measured by Annaheim et al., (2015) was slightly higher at 33200 μg P g^{-1}. Phosphorus concentration of sludge extracts followed the same pattern as that of sludge P_T, and extraction efficiency was high, ranging between 81% in CK to a high of 93% in PS. This indicates that the range of P compounds and their proportions within the extract are likely to be highly representative of the actual range within unextracted sludge.

3.5.2 ^{31}P NMR Optimisation

To improve the signal:noise ratio of ^{31}P NMR spectra, it is necessary to increase the number of scans to increase the amount of signal. Background noise is random, and improvement of sensitivity is proportional to the square root of the number of scans (Bünemann et al., 2011). This means that to double the signal:noise, the number of scans must be quadrupled, leading to long analysis times.

With a relaxation delay time of 1s and 20,000 scans, analysis time was over 8 hours per sludge sample. This delay time is insufficient for the full relaxation of compounds between scans but is necessary, as any longer delay would have meant unacceptable analysis time. The level of relaxation achieved for each separate compound is dependent of their individual relaxation constants, or T1 values, which decrease with increasing size

of molecules. Using a relaxation time that does not enable full relaxation causes a proportional underestimation of signal obtained for each compound, depending on the level of relaxation achieved. For example, whereas full relaxation would produce 100% of the expected signal, 50% relaxation would result in 50% of the expected signal. When comparing the signals of multiple compounds with different T1 times, this may lead to overestimation of one compound compared to one that has not been allowed to relax to the same degree. To overcome this issue, the proportion of signal achieved by the three compounds of interest (MDP standard, orthophosphate and phytate) was measured in spectra over relaxation times ranging between 1 – 40 seconds, enabling the calculation of a correction factor for integration and absolute quantification. Previous work in this lab found T1 times for solutions of orthophosphate and phytate of 9.04 and 1.09s respectively (Robertson, 2018). As the smallest compound of interest, orthophosphate has the longest T1, and this was reflected in the finding that a delay time of 1s recovered only 47% of the total orthophosphate signal. MDP and phytate, being larger molecules, were able to relax to a greater degree at 1s, but the signal generated was found to be only 81% and 84% of total signal respectively. The analysis of spiked sludge samples produced recovery values for orthophosphate of 103.78 ± 2.14%, and for phytate of 104.77 ± 5.17 % when using this method to adjust integrals according to relaxation delay times. This indicates that the above technique successfully enables the absolute quantification of these compounds within sludge extracts.

3.5.3 Orthophosphate-P in sludge treatment

Orthophosphate-P was identified as the major P constituent in all 5 sludges with both the colorimetric assay and ^{31}P NMR, comprising approximately 80% of total extracted P. The observed domination of the ^{31}P NMR spectra by orthophosphate is typical of anaerobically digested sludges, and similar to the patterns reported by Hinedi et al., (1989) and Escudey et al., (2004) in anaerobically digested sludges. Furthermore, these results agree with those of Smith et al., (2006), who measured the orthophosphate fraction at between 66–78% of total extracted P in both undigested sludge and anaerobically digested sludges from the same process.

There was a positive linear relationship between orthophosphate concentration measured by molybdate colorimetry and ^{31}P NMR (Figure 3.13A), and both methods indicated that absolute orthophosphate concentrations increase with consecutive sludges from lowest in PS to greatest in DS, before falling slightly in CK. This pattern reflects that of both sludge P_T and sludge total extractable P concentrations. Despite absolute orthophosphate concentration peaking in DS, when expressed as a proportion of total extractable P, the orthophosphate fraction is in fact lower in DS than in DF, significantly so according to ^{31}P NMR data, and is accompanied by an increase in the fraction designated as 'residual P'. In this work, residual P is calculated as the difference between total extractable P and the sum of orthophosphate and phytate-P, and represents the contribution of other P compounds that might include polyphosphates, non-phytate monoester P and diester P. The increase in residual P during digestion may be explained as an increase in diesters such as phospholipids and DNA resulting from the metabolism of orthophosphate by the rich microbial community within the digester (Smith et al., 2006). Between DS and CK, the absolute concentration of orthophosphate remains relatively stable, but increases proportionally as the residual P fraction falls. It is possible that this is due to the loss of microbial-P in the dewatering of DS by centrifugation, which would indicate that much of the orthophosphate is bound within the solid-phase of the digested material as it was not lost in solution.

3.5.4 Phytate-P in sludge treatment

Whilst orthophosphate was by far the most abundant P compound in all sludge extracts, phytate P was detectable in all extracts by both colorimetric and ^{31}P NMR methods. Within the literature that has attempted to identify and measure P compounds within various sludges, phytate (Annaheim et al., 2015; Smith et al., 2006), or orthophosphate monoesters that could include phytate (Huang & Tang, 2015; Escudey et al., 2004) have been detected in anaerobically digested sludges. Evidence for the loss of orthophosphate monoesters during anaerobic digestion was presented in recent work by Li et al., (2019), but it is impossible to say whether this was due to the loss of phytate or the loss of more bioavailable monoesters during AD, as no attempt to was made to identify specific compounds.

Faecal phytate concentrations have been measured at between 4000-11000 µg P g^{-1} (Joung et al., 2007), and can constitute between 24-54% of faecal P_T (Joung et al., 2007; Kim et al., 2009), so it was expected that phytate levels would be abundant in primary and secondary sludges (PS & SS). From its initial levels in PS and SS, phytate was expected to persist throughout the treatment process due to its relatively lower bioavailability in comparison to the abundant orthophosphate. As a proportion of total extracted P, phytate was expected to comprise approximately 10% of total extractable P throughout the process, reflecting the findings of similar work by Annaheim et al., (2015) and Smith et al., (2006).

3.5.4.1 Phytase-labile P – Figure 3.6 A & B show the fractions of P measured by molybdate colorimetry. Phytate content was estimated as phytase-labile P, and was calculated as the increase in molybdate-reactive P following 24 hours incubation of the extract with a phytase enzyme. The absolute concentration of phytase-labile P was calculated at 946 µg P g^{-1} in PS, increasing to its highest recorded concentration in SS at 1274 µg P g^{-1}. From this peak, phytase-labile P then fell in DF, and fell again following digestion to its lowest concentration of 285 µg P g^{-1} in both DS and CK. As a proportion of total extracted P, phytase-labile P was greatest in PS at 12.6% of P, and fell to 8.9% in SS. This trend continued again in DF, which exhibited a significant reduction in phytase-labile P at just 3.6%, accompanied by an increase in the orthophosphate-P fraction. However, phytate fractions were lowest following digestion, making up just 1.2% and 1.5% of total extracted P in DS and CK respectively. These results indicate that phytate is initially abundant in undigested sludge, but is negatively affected both by sludge pre-treatment by thermal hydrolysis, explaining the decrease in concentration between SS and DF, and by anaerobic digestion, causing a 10.5x decrease in the proportion of phytase-labile P between PS and DS.

These results would suggest that rather than phytate remaining relatively constant throughout the process as observed in similar studies, phytate is actually degraded in this treatment process, causing a significant drop in terms of both concentration and proportion. However, there is no positive linear relationship between phytate concentrations of identical samples when measured by molybdate colorimetry and by ^{31}P NMR (Figure 3.13B, $R^2 = 0.07$).

3.5.4.2 ^{31}P NMR – The absolute phytate concentration of sludge extracts was measured by integration of the second of the four phytate peaks present in the orthophosphate monoester region of ^{31}P NMR spectra. According to this data, absolute phytate concentration was lowest in PS at 345 µg P g^{-1} sludge, increasing to 875 µg P g^{-1} sludge in SS after the addition of sludge from secondary settlement. Phytate levels then remained relatively constant throughout the process, with no significant difference between concentrations in SS, DF, DS or CK. As a proportion of total extractable P, the phytate fraction constitutes between 3.9% and 6.1% in DS and SS respectively (Figure 3.12B). Taken together, the ^{31}P NMR data indicates that phytate levels increase from PS to SS but fall slightly upon thermal hydrolysis pre-treatment in the DF sludge. The proportional reduction of phytate from DF to DS is not reflected by the absolute concentration of phytate, which increases, but is instead caused by the contribution of the large proportional increase in the residual-P fraction to the increase in total extractable P during anaerobic digestion.

The ^{31}P NMR data is consistent with the work of Smith et al., (2006), who found phytate levels to remain constant between undigested and digested sludge. However, at 10% of total extracted P, the sludges studied by Smith et al., (2006) and Annaheim et al., (2015) had over twice the level of phytate as the Esholt sludges studied in this work.

3.5.4.3 Methodological comparison – With no positive linear relationship existing for the measurement of phytate-P between colorimetric and ^{31}P NMR methods, it is not possible to conclude how phytate behaves in the wastewater treatment process without further evidence.

Under ideal conditions, ^{31}P NMR enables the user to identify specific compounds within a sample and allows their quantification, as the area under the compounds peak(s) are directly proportional to the number of P nuclei in a particular molecular configuration (Cade-Menun, 2005). Analysis of spiked sludge samples by ^{31}P NMR showed an average recovery of spiked orthophosphate of 103.78 ± 2.14%, and of spiked phytate of 104.77 ± 5.17 %. These values indicate that the quantification of the orthophosphate and phytate concentrations within sludge extracts is highly accurate by the ^{31}P NMR method,

with only a slight underestimation of absolute concentrations occurring for both compounds.

By comparison, measurement of phytate by enzymatic dephosphorylation and subsequent colorimetric quantification of the released orthophosphate is a less direct approach. In this chapter, phytase-mediated quantification of phytate was tested in order to assess whether it could provide a reliable, cheaper and less time and labour-intensive method to estimate levels of phytate in sludge, compared to traditional ^{31}P NMR. Within the sludge extracts, colorimetric estimation of inorganic orthophosphate was achieved by measurement of MRP in extracts incubated with denatured phytase and agreed well with the ^{31}P NMR determination of orthophosphate. Molybdate unreactive P (MUP), the difference between extract total P and MRP, contains a wide variety of organic P forms including orthophosphate monoesters (phytates, sugar phosphates), diester P (DNA), organic condensed phosphates and phosphonates, as well as inorganic polyphosphates (George et al., 2018; Turner et al., 2003a). It was expected that a phytase enzyme could be used to dephosphorylate phytate, enabling its quantification as the measurement of phytase-labile P. However, the disparity between the ^{31}P NMR results, and colorimetric results for phytate quantification indicate that this is not the case. It is likely that there are many factors that cause the apparent overestimation of phytate in PS and SS, and underestimation in DS and CK by phytase-mediated quantification when compared to ^{31}P NMR.

Commercially produced phytase enzymes such as that used in this study often belong to the histidine-acid phosphatase (HAP) family of phytases. HAPs have a broad substrate specificity for phytate and can sequentially dephosphorylate the five equatorial phosphate groups of phytate to produce a final product of *myo*-inositol monophosphate, but they can also dephosphorylate various other phosphate esters (Wyss et al., 1999; Oh et al., 2004). Other phytase enzymes such as the alkaline phytases, exhibit a strict substrate specificity for phytate, but are often only able to partially dephosphorylate phytate to *myo*-inositol trisphosphate (Oh et al., 2004).

The use of HAP phytases with broad substrate specificity is an advantage for commercial feed enzymes, allowing greater dephosphorylation of phytate in the gastrointestinal

tract. This characteristic may however be disadvantageous for its use in quantitative assays, as the tendency to act not only upon phytate, but other orthophosphate monoesters like sugar phosphates and α and β glycerophosphates, means that 'phytase-labile P' does not just constitute phytate, but these other compounds as well. It's likely that in PS and SS, the overestimation of phytate by this method is due to this broad specificity and the degradation of other phytase-labile compounds. In ^{31}P NMR spectra of PS and SS sludge extracts, there is a large broad peak present directly between the 2nd and 3rd phytate peak (Figure 3.9). Whilst this peak was not specifically identified, it lies within the orthophosphate monoester region of the spectrum, and may be derived from the products of phospholipid hydrolysis in the alkaline extraction, glycerophosphates (Doolette et al., 2009). With its broad substrate specificity, the phytase enzyme is likely to be able to dephosphorylate glycerophosphate as well as phytate (Wyss et al., 1999), and this may help to explain the overestimation of phytate observed.

In contrast to the overestimation of phytate observed in PS and SS, there was a distinct underestimation of phytate with this method in DS and CK following anaerobic digestion. It is possible that many of the alternative substrates that phytase enzymes can target have been hydrolysed during thermal pre-treatment, or metabolized during anaerobic digestion. Li et al., (2019) noted a complete loss of detectable monoester P ^{31}P NMR spectra of an anaerobically digested sludge, suggesting that this loss resulted from their hydrolysis and degradation due to their greater bioavailability during AD. In this study, the peak tentatively assigned to glycerophosphate in PS and SS is no longer present in DF, DS and CK sludge extracts (Figure 3.9), which might indicate that phospholipids are degraded and metabolized within the thermal hydrolysis and AD processes. Additionally, phytase activity within extract solutions may be inhibited due to the difference in the chemical composition of digested sludge. Due to the loss of solids mass within the digester, the concentration of metal cations is likely to be greater in digested sludge. Igamnazarov et al., (1999) studied the effect of elevated metal cation concentration on extracellular *Bacterium* sp. phytase enzymes, and found that 2mM concentrations of Cu^{2+} and Fe^{3+} reduced phytase activity to 8% and 29% of their original activities. Wyss et al., (1999) noted a similar inhibitory effect of metal cations on phytase

activity, and suggested that this is most likely due to the formation of poorly soluble phytate-metal salts rather than direct binding of cations to the phytases. It therefore appears that this method of enzyme-mediated estimation of phytate concentration is unsuitable for use in the complex chemical environments of sewage sludge, due to reasons including the presence of additional substrates, and the potential effect of increased concentrations of inhibitory agents such as metal cations later in the process.

3.5.5 Implications for soils amended with AD sludge

As of 2010, 79% of the sludge derived biosolids produced in the UK are applied directly to the land (DEFRA, 2012). Being rich in macronutrients and organic matter, they can both reduce the requirement for chemical fertilizer inputs, and have been demonstrated to increase productivity (Singh & Agrawal, 2008; Haynes et al., 2009).

Analysis of the extract of anaerobically digested and dewatered biosolids produced at Esholt (sample CK) revealed it to contain a P_T concentration of almost 19000 µg P g^{-1}. 83% of this was present as orthophosphate, which is typical of other anaerobically digested sludges (Smith et al., 2006; Escudey et al., 2004; Annaheim et al., 2015), whereas in aerobically treated sludge the content of organic P compounds, including orthophosphate monoesters and diesters, can be nearer to 50% of P_T (Hinedi et al., 1989). Smith et al., (2006) measured the levels of bicarbonate-extractable (phytoavailable) P of sludges through the sewage treatment process and noted that whilst phytoavailable P was highest in anaerobically digested sludge, the vast majority was actually removed during the dewatering step that followed. The slight decrease in absolute phosphate concentration observed between DS and CK in this work may indicate that soluble, phytoavailable phosphate is being lost in the same manner. The majority of the orthophosphate remaining in the final cake is not immediately phytoavailable, being bound to minerals and cations including ferrihydrite and aluminium hydroxides, hydroxyapatite and calcium phosphates (Haynes et al., 2009). In a study combining sequential fractionation, ^{31}P NMR and XANES, more labile orthophosphate forms in sludge included calcium- and some aluminium-phosphates, whereas iron- and most aluminium-phosphates were recalcitrant (Ajiboye et al., 2007). These phosphate-cation complexes are inherently less phytoavailable when they are

applied to the soil, as they must first be solubilised and mineralised before they can be taken up by plants.

Only a slight reduction of the absolute phytate concentration was observed in this study during the dewatering step between digested sludge (DS) and final cake product (CK), and this may be due to the loss of soluble phytate in the sludge solution. The retention of the vast majority of phytate-P indicates that phytate is also bound within sludge, either within organic constituents, or associated or precipitated with metal cations. When applied to the soil, orthophosphate, non-phytate monoester P and diester P are more phytoavailable than phytate (Smith et al., 2006). For phytate-P to be absorbed by plants and microbes, the surrounding phosphate groups must first be enzymatically cleaved from the inositol ring by phytase enzymes. Due to the presence of 6 phosphate groups, phytate has a high charge density and thus a high sorption capacity, forming strong associations within insoluble salts of Ca, Fe and Al, and adsorbing to clay particles in the soil (Turner et al., 2002). Therefore, it's likely that the phytate present in land-applied biosolids is rapidly immobilized, whereas other phosphates and phosphate monoesters are more mobile and susceptible to microbial metabolism, resulting in a preferential accumulation of an unreactive phytate fraction over time. This was demonstrated by Smith et al., (2006) in the repeated analysis of sludge amended soils by ^{31}P NMR, where phytate concentrations were found to have stabilized in the soil 81 days after amendment, in which time concentration of DNA and other monoesters had fallen.

Biosolids contain approximately twice as much nitrogen (N) as P, but agricultural crops typically sequester four times as much N than P (Haynes et al., 2009). This leads to an overall accumulation in the amount of P relative to N, and importantly, increases the risk of leaching and eutrophication once the soil P sorption capacity has been exceeded. A net accumulation of P compounds from this input-output imbalance may reinforce the tendency for phytate accumulation, as high levels of more labile P compounds such as orthophosphate and monoester/diester P will discourage the production of phytate-degrading enzymes by the microbial population, which are often only produced in response to P limitation (Giles et al., 2011).

Assuming the CK phytate concentration of 847 µg P g^{-1} is typical of all UK sludge, based on 2010 levels of land application (DEFRA, 2012), 947 tonnes of phytate-P is applied to soil every year in sludge amendments. This is of course dwarfed by the application of 17,584 tonnes of orthophosphate-P applied in sludge under the same assumptions, but is nevertheless a significant amount of P, much of which is likely to become immobilised and accumulate in soil.

3.6 Conclusions

Understanding the abundance of the key P compounds orthophosphate and phytate in anaerobically digested sludge is important considering that the vast majority of sludge produced in the UK is returned to agricultural soils. Sludge P_T is lowest in primary sludge, increasing through the process to a peak of almost 26000 µg P g^{-1} after anaerobic digestion, likely due to the reduced mass of sludge resulting from the digestion process. P_T then falls slightly to 23263 µg P g^{-1} after dewatering in the final sludge cake. Using ^{31}P NMR and colorimetric techniques, orthophosphate was identified as the major P-containing compound in all sludges sampled through the advanced sludge treatment process of Esholt WWTP, making up approximately 80% of total extractable P, and good agreement was achieved between results of the two methods.

Phytate levels were measured by both ^{31}P NMR and as phytase-labile P, but there was no linear relationship between results. With supportive evidence from spike-recovery analysis in ^{31}P NMR, it was concluded that phytase-labile P is likely to be an unsuitable method for phytate estimation in sludge samples. This method has the potential to both overestimate phytate, owing to the broad substrate specificity of the enzyme, and underestimate phytate due to inhibition by metal cations in the extract (Igamnazarov et al., 1999; Wyss et al., 1999).

^{31}P NMR analysis revealed that the proportion of phytate-P relative to total extractable P remains relatively stable throughout the sludge treatment process, comprising 4.5% of total extractable P in the final dewatered sludge cake. This suggests that phytate is able to withstand both the high temperature and pressure of thermal hydrolysis pre-treatment, and the 15-day mesophilic anaerobic digestion process. If phytate-P comprises 4.5% of the final land-spread product, this means that in the UK, 947 tonnes of phytate-P are spread to agricultural land every year (according to 2010 data for the mass of sludge spread to land (Water UK, 2010)). Much of this phytate is likely to become rapidly immobilised in soil and could preferentially accumulate relative to other P compounds due to its high charge density and tendency to adsorb to clays and precipitate with metal cations. In Chapter 4, a variety of soils with varied land-use histories will be analysed, to assess the effect that land use history has on phytate

concentration. Of particular interest will be the analysis of an agricultural soil from a field that has recently been converted from an arable soil to a pig pen, and as such receives high input of phytate-rich monogastric manure.

4: Measurement of phytate in soils with varied land-use history

4.1 Summary

Phytate can enter the soil in organic amendments such as plant residues, animal manure and human wastewater sludge, and is often the most abundant organic P compound identified in ^{31}P NMR analyses of soil extracts, leading to the assumption that phytate is preferentially stabilised and accumulates. However, some work has also demonstrated the rapid degradation of phytate when applied to the soil, indicating that the tendency of phytate to accumulate may be affected by a wide range of soil factors. The types and quantities of P species in soil are governed by local environmental factors and land management, with agricultural practices such as cultivation, fertilisation and harvesting having a major effect on soil health and natural P cycling. In this chapter, a combination of ^{31}P NMR and colorimetric techniques are applied for the analysis of orthophosphate and phytate content of a range of UK agricultural and grassland soils, to understand how land-use can affect P speciation.

Vast differences exist in P speciation between the natural grassland soils and agricultural soils. In grassland soils, less than half of the P_T content is comprised of orthophosphate, with P forms other than orthophosphate and phytate making up the greatest proportion, which is reflected by the high organic matter content of these soils. In contrast, agricultural soils including arable, pasture, and a pig pen soils are dominated by orthophosphate, making up approximately 80% in each. Phytate levels are lowest in the arable soil, likely due to detrimental intensive management practices, which have denuded the soil also of organic matter. Phytate concentration increases in pasture soil but is greatest in the pig pen soil. The high phytate concentration of the pig pen soil is of most interest, as it may indicate an accumulation of phytate derived from inputs of pig manure and suggests a recovery of the soil since its conversion from arable land.

4.2 Introduction

4.2.1 Phytate accumulation in soil

Phytate enters the soil in sludge, manure and plant residues, and is often the most abundant organic P compound in soils (Jørgensen et al., 2015; Turner et al., 2002). With six phosphate groups, phytate has a high charge density, and thus has a propensity to adsorb to surfaces in soils via electrostatic interactions and form insoluble precipitates with polyvalent metal cations (Turner et al., 2002). This high charge density means that phytate often undergoes stronger interactions than other P forms, with phytate sorption capacity in the region of four times greater than that of orthophosphate (Celi & Barberis, 2006; Richardson et al., 2006). This strong adsorptive capacity, and the relative abundance of phytate when compared to most other organic P species in the soil, has led to the general conclusion that phytate preferentially accumulates in soils as it is not immediately available for plant or microbial uptake, has low lability, and is afforded a degree of protection from enzymatic degradation in its adsorbed form (Turner et al., 2002; Menezes-Blackburn et al., 2013).

However, two studies that assessed soil P speciation after phytate addition show that this is not always the case. When phytate in manure (Leytem et al., 2006) and in solution (Doolette et al., 2010) was added to calcareous soils, no accumulation was observed after many weeks, suggesting phytate had become rapidly degraded in the soil. Similarly, in more acidic soils, Annaheim et al., (2015) found no evidence of accumulation of P species in soils receiving a range of organic amendments despite variation in P speciation within the amendments applied. This suggests that the tendency of phytate and wider organic P forms to accumulate in soil is not universal, and accumulation is likely to be governed by a wide range of soil and environmental factors such as soil chemistry and pH, metal cation and clay content, organic matter content, moisture, microbial diversity and land-use history.

4.2.2 Land-use history

The speciation and quantity of P forms in soil are governed by biological, chemical, and physical factors which themselves can be influenced by environmental factors and land use history (Condron et al., 2005). Land use history has a major effect on soil P speciation

and accumulation, particularly in agricultural soils (Stutter et al., 2015). These soils can often be subject to large inputs of chemical fertilisers, which add large amounts of phytoavailable orthophosphate (HPO_4^{2-} and $H_2PO_4^-$), and can also receive organic amendments such as manure and sludge solids, which also predominantly add orthophosphate, but include other complex inorganic and organic P forms, including phytate (See Figure 1.2) which are not immediately phytoavailable (Cade-Menun et al., 2017).

Organic P compounds are formed within biomass, and enter the soil via the decomposition of plant detritus, animal wastes, and soil microbiota (Nash et al., 2014). In arable soils, these natural processes are often vastly reduced, as P absorbed by crops is removed from fields during harvest and is replenished by the addition of predominantly inorganic orthophosphate fertilisers to the soil. Furthermore, arable soils can also experience disruptive management practices including soil cultivation and fallow periods which may have a significant impact on the soil microbial mineralisation processes (Liu et al., 2018). In an analysis of 32 UK soils, Stutter et al., (2015) found that arable soils were dominated by orthophosphate and exhibited no accumulation of organic P forms. This is likely due to the predominant addition of inorganic P fertilisers, and the promotion of organic matter degradation via the aeration of soil during tillage (McLauchlan, 2006). Liu et al., (2018) found that genes encoding phytase and phosphoesterase enzymes were abundant in arable soils, which may indicate that microbial populations adapt to the high temporal variability in bioavailable P in these soils by degrading organic P in P-limited or fallow periods.

Liu et al., (2018) recently found a greater concentration of phytate, along with its stereoisomer forms; *scyllo*-, *neo*-, and *D-chiro*- inositol hexakisphosphate in cattle grazed grassland soils compared to arable soil. According to Nash et al., (2014), up to 85% of P absorbed by plants in grazed pastures is returned to the soil in manure. Despite being ruminant animals with phytase enzymes present in their gut, phytate digestion in cattle is surprisingly inefficient (Menezes-Blackburn et al., 2014), so a large amount of phytate is likely to enter the soil from manure in grazed pastures. As these soils suffer a lower degree of inorganic P inputs, and less structural disturbance from tillage, the cycling of P is likely to be more representative of natural soils, with P derived

predominantly from manure and plant litter, and driven by plant and microbial P demands (Liu et al., 2018). Stutter et al., (2015) also recorded higher proportions of orthophosphate monoesters in intensively grazed soils than in cultivated arable soils. However, they also found that orthophosphate diesters such as DNA and RNA, and polyphosphates like ATP, which are indicators of healthy microbial turnover, were only abundant in more natural, extensively grazed grasslands, indicating that the natural ability of the soil to cycle organic P is negatively affected by both chemical fertilisation and intensive organic manure fertilisation (Stutter et al., 2015). This loss is even more prominent in arable soils, where crop monocultures have been shown to reduce microbial diversity (Stutter & Richards, 2012).

4.2.3 Aims & Objectives

It's clear therefore that the accumulation of phytate is dependent on many factors. In this chapter, both the orthophosphate and phytate content of UK soils with varied land-use histories and physiochemical characteristics were compared. Three agricultural soils (arable, pasture, and pig pen) and two natural grassland soils (acidic and calcareous grassland) were analysed by solution ^{31}P NMR to investigate how various agricultural land management practices influence both orthophosphate levels and phytate accumulation in comparison to more natural systems. Enzymatic hydrolysis was also assessed as a potential alternative to ^{31}P NMR, to see whether it can provide more accuracy in soil extract samples than was found in sludge extract samples.

Of particular interest was the pig pen soil, which was previously an arable field under a similar management regime to that of the nearby permanently arable field, but was converted to a pig pen in 2016. Since that date, the field has experienced no cultivation, no crop monocultures, no harvest and no chemical fertilisation, with the sole nutrient input to this soil therefore derived from pig manure. Pigs are monogastric livestock with similar digestive systems to humans, and Liang et al., (2018) recently measured pig manure orthophosphate-P and phytate-P content at 90.7% and 8.5% of total manure P respectively. Proportionally, these proportions are similar to the digested sludge measured in Chapter 3, in which orthophosphate-P made up 83.4% and phytate-P made up 4.5% of total extractable sludge P. This soil therefore was expected to provide useful

insight to the recovery and accumulation of P stocks and organic matter when organic amendments similar to sewage sludges are applied to a previously arable field.

It was hypothesised that land-use history would have a major effect on orthophosphate and phytate content of soils. Arable soils were expected to be dominated by orthophosphate due to inorganic fertiliser inputs, but would have the lowest concentration of phytate of all soils due to low organic P inputs, regular harvest outputs, and conventional cultivation practices, which would also result in low organic matter content. In contrast, pasture soils with greater organic matter were expected to have an intermediate level of phytate due to regular inputs of organic livestock manures, absence of cultivation and lack of significant P outputs, with orthophosphate content lower in this soil. The pig pen soil was expected to contain an organic matter concentration intermediate between the arable and pasture soils as an indicator of recovery, and would contain the greatest total P concentration of all soils, due to regular inputs of P-rich organic fertiliser and lack of significant outputs. Phytate levels in this soil were considered likely to be the greatest measured in all soils due to the monogastric nature of pigs, coupled with the legacy of low microbial turnover due to its use as an arable soil.

Compared to agricultural soils, acidic and calcareous grasslands were expected to have a much greater organic matter content due to the natural cycling in this soil. Grassland soils would have lower total P due to the historical lack of P inputs to these soils. Organic P (calculated in this chapter as phytate-P and residual-P) was expected to form a greater proportion of total P than orthophosphate due to the natural plant and microbial P cycling in these soils. With this greater proportion of organic P, intermediate levels of phytate-P were expected in these soils. Between the adjacent acidic and calcareous grasslands, overall proportions of orthophosphate and phytate were expected to be be similar between the soils, but could be greater in acidic soils, due to the increased cycling of P in the greater aboveground biomass in acidic soil.

4.3 Methods

4.3.1 Soil sampling

A total of five soils with varying land-use history were sampled in autumn 2018. Three agricultural soils were sampled from the University of Leeds Spen Farm, Tadcaster, UK (53°51'45.3"N 1°20'37.2"W; Figure 4.1A). Two extensively grazed permanent grassland soils were sampled from Wardlow Hay Cop, a conical hill in the Cressbrook Dale National Nature Reserve in the Peak District National Park, Derbyshire, UK (53°15'45.0"N 1°43'59.4"W; Figure 4.1B). Sampling sites were chosen primarily due to their use as long-term study sites with well documented land-use histories. For agricultural soils, difficulty was encountered in locating a suitable soil that had received anaerobically digested sludge amendments. Spen Farm, whilst not incorporating sludge amendments, has the advantage of holding detailed historical records on crop history and fertiliser inputs, and exhibits a variety of land-uses within a small geographical area, enabling more straightforward comparison between soils. Spen Farm also has an outdoor pig facility that has been recently converted from an intensively managed arable soil. Pig manure has been shown to contain comparable concentrations of P_T, phytate-P and orthophosphate-P to anaerobically digested sludge (Turner, 2004; Liang et al., 2018), so this soil was selected as a suitable proxy for a soil receiving human sludge amendment. Wardlow Hay Cop was selected to represent a comparatively natural grassland ecosystem, which experiences only sparse, extensive grazing by sheep and cattle. Wardlow also has the unique advantage of having contiguous calcareous and acidic grasslands, enabling the comparison of P dynamics within adjacent but contrasting natural grassland soils.

Spen farm is a commercial mixed pasture and arable farm, with brown earth soils of the Aberford series of Calcaric Endoleptic Cambisols (Cranfield University, 2019; Holden et al., 2019), underlain by dolomitic limestone of the Cadeby formation. Soils are a sandy calcareous loam, composed of a boulder clay parent material, limestone residue and sandy millstone grit and reach a total depth of between 50-90cm (Holden & Gell, 2009). Soils were sampled as a single mass in each field with an area of 50cm^2 and depth of 15cm. The first was an Arable Soil (SAra) which had supported crops since at least 2001 and had been sown with a monoculture crop of winter wheat two months prior to

sampling. The second was a permanent pasture soil (SPas) which was dominated by perennial ryegrass grazed intensively by both sheep and cattle, which had not been cropped for at least 40 years. The final Spen soil was obtained from a pig pen (SPig), which contained no vegetation due to intensive pig foraging. This field had been used as a pig pen since 2016, before which it was an arable field supporting a range of crops since at least 2001. SAra and SPig soils exhibited no soil horizons due to their history of heavy transformation by total inversion ploughing. In SPas soil, the upper 30cm horizon is a sandy clay loam, becoming finer below 30cm as the soil extends to the limestone bedrock (Holden & Gell, 2009). Each field was surrounded by hedgerows dominated by Hawthorn (*Crataegus monogyna)*, Elder (*Sambucus nigra)* and Holly (*Ilex aquifolium;* (Holden et al., 2019). Crop history for Spen Farm soils is presented in Table 4.1.

Wardlow soils are well drained silty soils underlain by the Monsal Dale Limestone Formation (BGS, 2019). The site has the unique advantage of having a shallow calcareous (WCal) grassland adjacent to a deeper acidic (WAc) grassland, which receive no nutrient inputs other than that provided by sparse sheep and cattle grazing and atmospheric nitrogen deposition. The acidic grassland is located on the south-eastern slope of Wardlow Hay Cop, and it's soil is a paleo-argillic brown earth in the Nordrach series of chromic endoleptic luvisols (Cranfield-University, 2019; Basto et al., 2015), derived from wind-blown loess deposited following the last glaciation (O'Sullivan et al., 2011) that reaches up to 70cm in depth. The upper soil surface horizon reaches 12-15cm deep and is a dark brown, humus rich, stoneless silty loam, and the lower mineral horizon extends to the bedrock, containing clay and sesquioxides in an almost stoneless, silty clay loam matrix (O'Sullivan et al., 2011). Due to the thickness of this soil and high precipitation levels, the limestone bedrock does not have an effect on soil surface pH, which is therefore extremely acidic due to acid rainfall (Basto et al., 2015). The acidic soil supports a *Festuca-Agrostis-Galium* grassland, which is the most common type of unimproved acidic grassland community in the UK, supporting approximately 9 higher plant species per square metre (O'Sullivan et al., 2011). The calcareous grassland is located adjacent to the acidic grassland on the south western slope of Wardlow Hay Cop and extends to a depth of just 10cm to the limestone bedrock. The soil has a sandy loam texture and was a humic rendzina of the Lulsgate Complex, but is transitioning to a

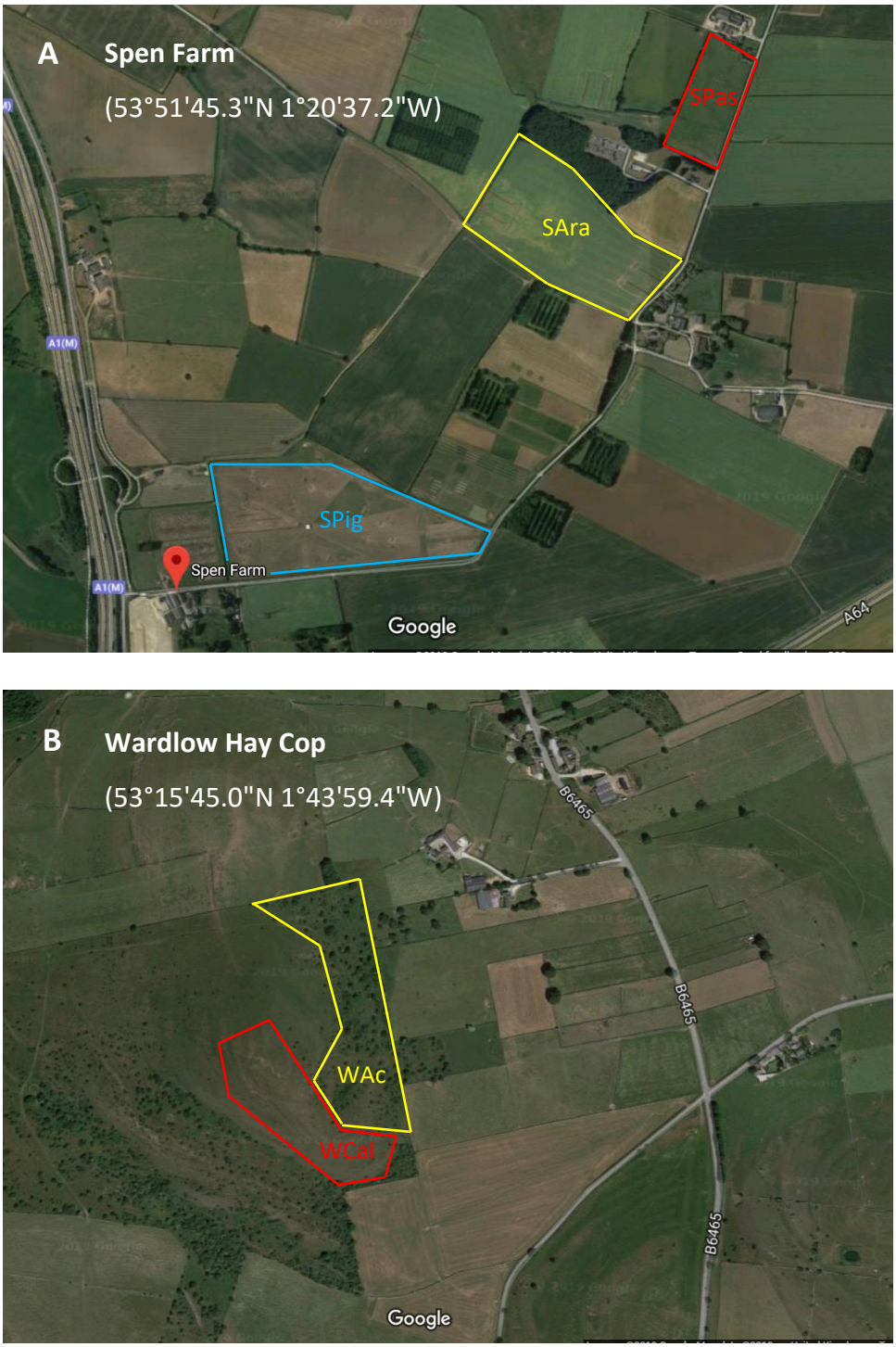

Figure 4.1: Aerial view of sampling sites. A: Spen Farm, Tadcaster, UK. SAra = Arable soil, SPas = Permanent Pasture soil, SPig = Pig pen. B: Wardlow Hay Cop, Derbyshire, UK. WAc = Acidic grassland, WCal = Calcareous Grassland. (Google Maps, July 2019).

ranker of the Wetton series due to acid deposition (Phoenix et al., 2019). This soil supports a species-rich *Festuca-Avenula* grassland comprised of a rich mixture of grasses, sedges, forbs and herbaceous legumes (O'Sullivan et al., 2011). Both Wardlow grassland soils were sampled in November 2018 as a single mass with an area of 50cm^2.

In WAc, sampling depth was 15cm, but in WCal, sampling depth was up to 10cm due to the shallow nature of the soil.

4.3.2 Sample processing

Soils were transported to the lab and stored at 5°C until processing. Soils were separated from the turf layer (if present) which was discarded, after which five cores of 4cm width and 10cm depth were taken from each soil mass. Cores for each soil were crumbled to pass through a 5mm sieve to remove stone and root debris, and were then mixed thoroughly and left to air-dry for 5 days. Once air dried, each soil was milled to a fine powder in a Fritsch Pulverisette Ball Mill and passed through a 2mm sieve. Subsamples were taken and oven-dried at 80°C for 24 hours to obtain dry weight.

Soil pH was measured according to the method of Hendershot et al., (2008). Briefly, three 10g replicates of each air-dried soil was suspended in 20mL distilled water, and pH measured with a Jenway PHM6 pH meter after 30 minutes of intermittent stirring, followed by 1 hour settling time. Organic matter was estimated using the loss on ignition

Table 4.1: Spen Farm crop history of sampled fields from 2001-2019

Harvest Year	**Field** SAra	SPas	SPig
2001	Winter Wheat	Pasture	Spring Barley
2002	Potato	Pasture	Sugar Beet
2003	Winter Wheat	Pasture	Winter Wheat
2004	Oilseed Rape	Pasture	Oilseed Rape
2005	Winter Wheat	Pasture	Winter Wheat
2006	Sugar Beet	Pasture	Peas
2007	Winter Wheat	Pasture	Winter Wheat
2008	Winter Wheat	Pasture	Winter Wheat
2009	Potato	Pasture	Oilseed Rape
2010	Winter Wheat	Pasture	Winter Wheat
2011	Oilseed Rape	Pasture	Winter Wheat
2012	Winter Wheat	Pasture	Potatoes
2013	Peas	Pasture	Winter Wheat
2014	Winter Wheat	Pasture	Peas
2015	Winter Wheat	Pasture	Winter Wheat
2016	Summer Barley	Pasture	*Pig*
2017	Winter Barley	Pasture	*Pig*
2018	Oilseed Rape	Pasture	*Pig*
2019	Winter Wheat	Pasture	*Pig*

method (Karam, 2008). Air-dried soils were desiccated overnight in an 80°C oven, after which 2g was weighed into dried porcelain crucibles. Soils were then heated in a Carbolite AAF 1100 muffle furnace at 450°C for 4 hours. Once cool, samples were stored in a desiccator jar before weighing was repeated. The reduction in mass was taken as an approximation of the organic content of soil. For each soil, three 1g replicates of air-dried, milled soil were extracted in 20mL of 0.25M NaOH + 0.05M EDTA, then lyophilised and re-ground as described in Section 3.3.2.

4.3.3 Colorimetric Analyses

4.3.3.1 Soil & Soil extract total phosphorus (P_T)

Soil P_T and soil extract P_T were measured as described in detail in Section 3.3.3.1. For each soil, three 30mg samples of air-dried, milled soil were digested in 1mL concentrated H_2SO_4 and oxidized with H_2O_2. Acid digested samples were then diluted to 10mL with UHP water before measurement of P by molybdate blue colorimetry. For each of the three extracts of each soil, a single 20mg sample of dried homogenised extract was subject to acid digestion and measured for extract P_T by molybdate colorimetry according to the same method.

4.3.3.2 Colorimetric determination of extract molybdate-reactive P (MRP) & phytase-labile P

Due to the lower P concentration of soil extracts than those of sludge, 100mg extract samples were resuspended in 10mL 0.1M acetate buffer (pH 4.5). Samples were then split into two 5mL aliquots and measured for molybdate-reactive P and phytase-labile P as described in Section 3.3.3.2.

4.3.4 Solution ^{31}P NMR

For solution ^{31}P NMR spectroscopy of 0.25M NaOH + 0.05M EDTA extracts of soil, 100mg samples of lyophilised extracts in 1.5mL Eppendorf tubes were resuspended in 1mL of a mixture containing a 9:1 (v:v) of 0.5M NaOH + 0.1M EDTA, and 4mM methylene diphosphonate internal standard (MDP) in D_2O. Tubes were vortex mixed and left for 5 minutes, before centrifuging at 9000rpm for 5 minutes. 0.5mL of this preparation was then transferred to a clean 5mm NMR tube. ^{31}P NMR spectroscopy was performed on a Bruker Advance 500 Spectrometer with a mag1 console (Bruker, Germany) according to

the parameters described in Section 3.3.4.2. The following parameters were unchanged for all samples: acquisition time = 0.845s; pulse width 22µs; pulse angle 90°; delay time = 1s; total number of scans = 16,384; pulse program = zgig. Peak integration was performed in Bruker Topspin 4.0.3 and calibrated to the peak area of the MDP internal standard. Due to the existence of a broad peak in the orthophosphate monoester region, to avoid overestimation, phytate was measured by integration of the first phytate peak (5.7-5.65ppm) which represents the phosphate group at Carbon 2 of the inositol ring, and lies outside of the region of this broad peak, whilst being clearly separated from the orthophosphate peak. The integral for this peak was multiplied by 6, as it represents one of the six P nuclei of the phytate molecule (Turner, 2004).

Peak areas were corrected to account for the underestimation of peak areas due to the necessary but insufficient relaxation delay time of 1s, according to the method developed by Robertson, (2018). Correction factors were calculated by running a series of analyses in which soil extracts from one Spen soil (SPas2) and one Wardlow soil (WCal3), both spiked with 10uL of 5mM phytic acid sodium salt hydrate, were analysed over 100 scans with delay times of 1, 2, 5, 10, 20, 30 & 40s. Integrals in each spectrum were then plotted over time to calculate the proportion of signal produced at 1s compared to that produced when P nuclei can fully relax. A single delay time analysis was carried out for each of the two sampling locations. SPas was used to represent Spen soils, and WCal was used for Wardlow soils. Due to their production of a single peak in the spectrum, a single integral was taken at each delay time for MDP and orthophosphate. For phytate, a mean integral could be calculated from the four phytate peaks.

To validate ^{31}P NMR determination using this method, three soil samples (SAra, SPas & WCal) were used in a spike-recovery analysis. Resuspensions of soil extracts were spiked with 10uL of 7.25mM (0.0725 µmol) sodium dihydrogen orthophosphate, and 5µL of 5mM (0.15 µmol) phytic acid sodium salt dihydrate and analysed in an identical manner to the original un-spiked samples. Recovery was calculated as the observed increase in concentration over expected increase.

4.3.5 Statistical Analysis

Concentrations of P_T and total extractable P, and both colorimetric and ^{31}P NMR measurements of orthophosphate and phytate concentrations were compared between soils using one-way ANOVAs. Where significant differences existed, one-way ANOVAs were followed by Tukey multiple comparisons tests (α=0.05). Measurements of orthophosphate-P and phytate-P by both techniques were compared using simple linear regressions. Statistical analysis was performed in GraphPad Prism v7.04 (GraphPad Software Inc, San Diego, USA).

4.4 Results

4.4.1 Soil properties (pH and organic matter)

Soil pH of the three Spen Farm soils was 6.94 ± 0.01, 7.1 ± 0.01 and 5.38 ± 0.01 in SAra, SPas & SPig respectively. In Wardlow soils, pH was measured at 4.25 ± 0.01 in WAc, and 6.54 ± 0.01 in WCal (Table 4.2). Organic matter was markedly lower in Spen Farm soils than in Wardlow soils, ranging between 4.36% in SAra to 8.17% in SPig and reaching 12.38% in SPas. In Wardlow soils, organic matter content was over double that of the SPas soil, at 29.57% in WCal and 35.96% in WAc (Table 4.2).

Table 4.2: pH and organic matter content of Spen and Wardlow soils

	Soil				
	SAra	SPas	SPig	WAc	WCal
pH	6.94 ± 0.01	7.10 ± 0.01	5.38 ± 0.01	4.25 ± 0.01	6.54 ± 0.01
Organic matter (%)	4.36 ± 0.067	12.383 ± 0.155	8.17 ± 0.169	35.96 ± 0.143	29.57 ± 0.266

4.4.2 Total Phosphorus of Soil

There was a statistically significant difference between P_T of soils measured by molybdate-blue colorimetry (One-way ANOVA, $p<0.0001$; Figure 4.2). P_T of WAc was lowest, with an average of 728 µg P g^{-1}, and was closely followed by SAra, which contained on average 765 µg P g^{-1}. WCal and SPas contained intermediate levels of P, averaging at 860 µg P g^{-1} and 887 µg P g^{-1} respectively. SPig had the greatest concentration of P_T of any of the soils studied, at 1167 µg P g^{-1} (Tukey multiple comparisons test, $\alpha=0.05$; Figure 4.2).

4.4.3 Total Extractable Phosphorus

There was a statistically significant difference between total extractable P of 0.25M NaOH + 0.05M EDTA extracts of soil (One-way ANOVA, $p<0.0001$; Figure 4.3). Extraction efficiency ranged from a low of 43.9% of total soil P in SAra to a high of 60.8% in SPas soil. Mean extract P_T was lowest in SAra at 335.6 µg P g^{-1} soil and increased in the order SAra < WAc < WCal < SPas to the greatest concentration of 612.2 µg P g^{-1} soil in SPig (Figure 4.3).

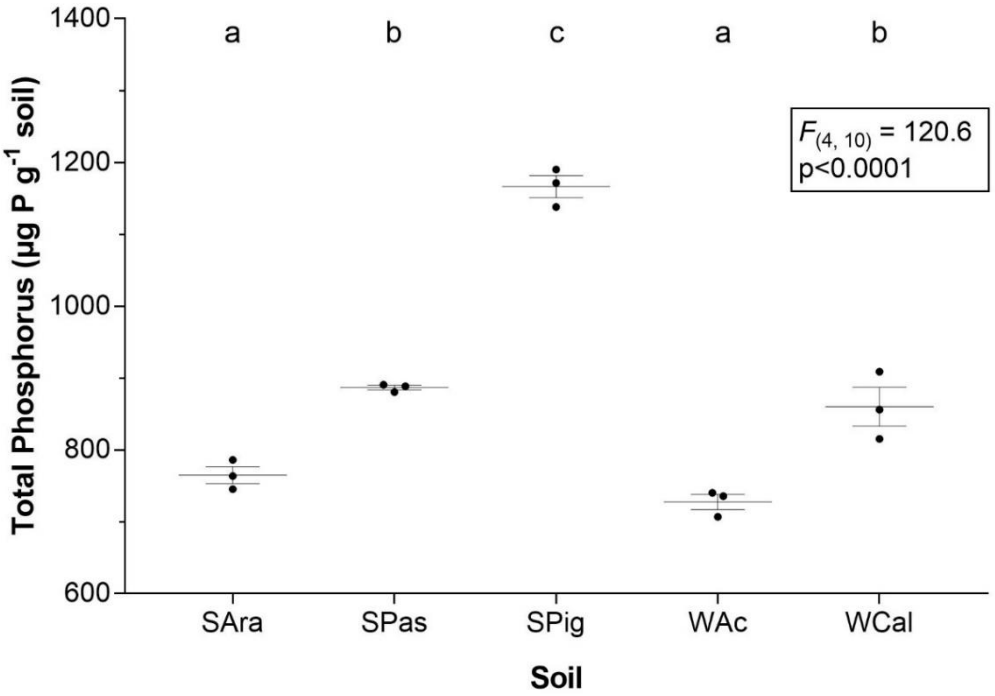

Figure 4.2: Soil total phosphorus concentration (µg P g^{-1} soil) measured by molybdate colorimetry. Samples are represented as individual points (n=3) with horizontal bars indicating mean ± SEM. Results of one-way ANOVA are inset. Significant differences are represented as different letters above bars (Tukey multiple comparison, α = 0.05).

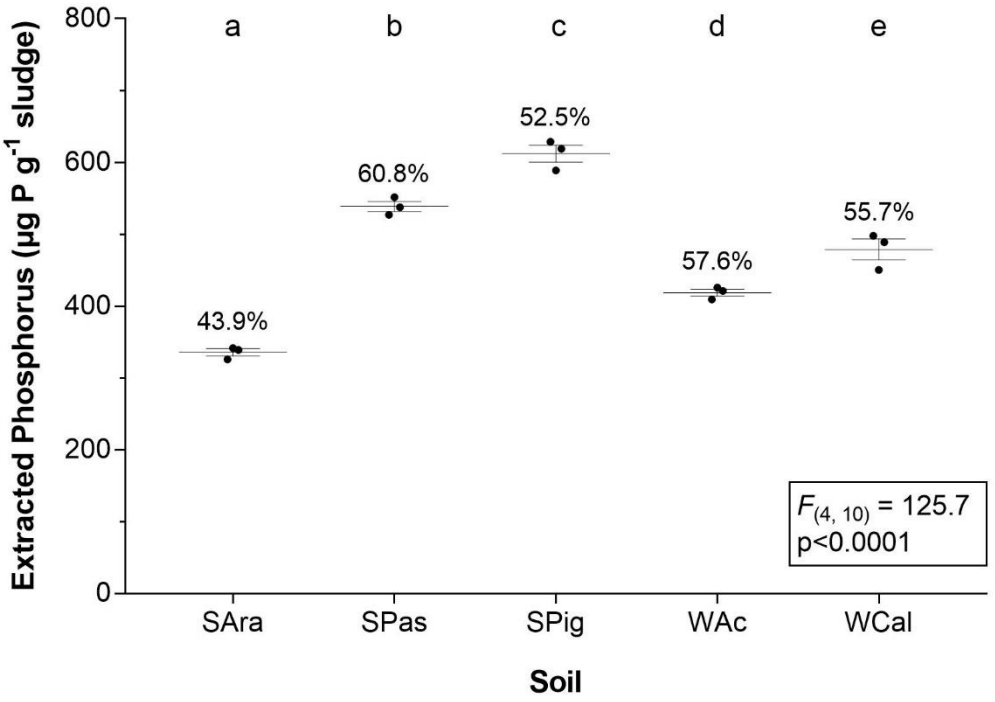

Figure 4.3: Extract total phosphorus (µg P g^{-1} soil) measured by molybdate colorimetry. Mean extraction efficiency (%) is presented for each soil Samples are represented as individual points (n=3) with horizontal bars indicating mean ± SEM. Results of one-way ANOVA are inset. Significant differences are represented as different letters above bars (Tukey multiple comparison, α = 0.05).

4.4.4 Colorimetric measurement of MRP and phytase-labile P

Absolute concentration of orthophosphate and phytate was measured colorimetrically as MRP and phytase-labile P. The difference between total extractable P and the sum of MRP and phytase-labile P was designated as 'residual P' (Figure 4.4A). There was a statistically significant difference between MRP concentrations in soil extracts (One-way ANOVA, $p<0.0001$). Values for MRP concentration were significantly different between Spen Farm soils, with absolute concentration of extractable MRP increasing from lowest in SAra at 210 µg P g^{-1} to greatest at 421 µg P g^{-1} in SPig (Tukey multiple comparisons test, $\alpha=0.05$). There was no significant difference between the absolute concentration of MRP in WCal and WAc, which were the lowest of all soils tested at 80 and 72 µg P g^{-1} of extracted soil respectively (Tukey multiple comparisons test, $\alpha=0.05$; Figure 4.4A). There was also a significant difference between absolute concentrations of phytase-labile P in soil extracts (One-way ANOVA, $p<0.0001$). Phytase-labile P was greatest in WAc, WCal and SPas at 149, 138 and 132 µg P g^{-1} extracted soil. SPig contained an intermediate level of 93 µg P g^{-1}, with the lowest value of all soils found in SAra at 56 µg P g^{-1} (Tukey multiple comparisons test, $\alpha=0.05$). There was also a statistically significant difference in residual P concentration between soils, increasing from lowest at 70 µg P g^{-1} in SAra < SPig < SPas < WAc to the highest concentration in WCal at 260 µg P g^{-1} (One-way ANOVA, $p<0.0001$; Tukey multiple comparisons test, $\alpha=0.05$; Figure 4.4A).

There was a significant difference in the proportional contribution of MRP to total extractable P between all Spen Farm soils (One-way ANOVA, $p<0.0001$). MRP was found to constitute the largest P fraction in each Spen soil, increasing in the order SPas < SAra < SPig and making up 47, 62.6 & 68.8% of total extractable P respectively (Tukey multiple comparisons test, $\alpha=0.05$; Figure 4.4B). There was a significant reduction in the proportion of MRP from Spen soils to Wardlow soils, but no significant difference was found between the two Wardlow soils, in which MRP constituted 16.8 and 17.3% of total extractable P in WAc and WCal respectively (Tukey multiple comparisons test, $\alpha=0.05$). There was a significant difference in the proportions of phytase-labile P (One-way ANOVA, $p<0.0001$), which was greatest in WAc soil at 35.5%, decreasing through WAc > WCal > SPas > SAra > SPig, in which it made up 15.3% of total extractable P (Tukey multiple comparisons test, $\alpha=0.05$; Figure 4.4B). The residual P fraction was greatest in

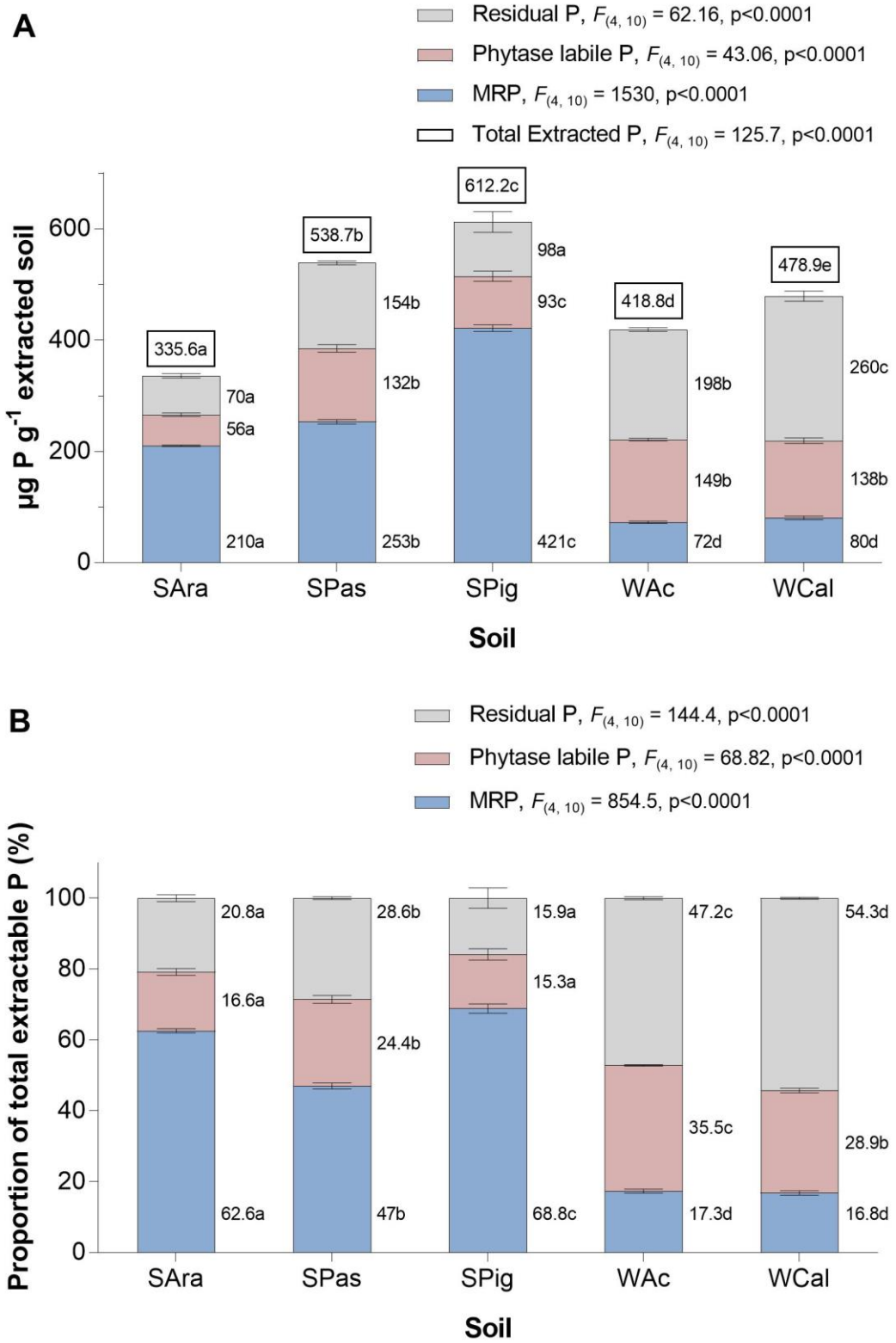

Figure 4.4: **A:** Mean absolute concentrations of P fractions in soils measured colorimetrically (µg P g^{-1} extracted soil ± SEM, n=3). Total extractable P is presented above each bar. **B:** Mean concentrations of P fractions in soils as a proportion of total extractable P (% ± SEM, n=3). Results of one-way ANOVA are shown for each P fraction. Results of Tukey multiple comparison test for each fraction are shown, with means to the right of bars (α = 0.05). Different letters indicate a significant difference between values for that P fraction.

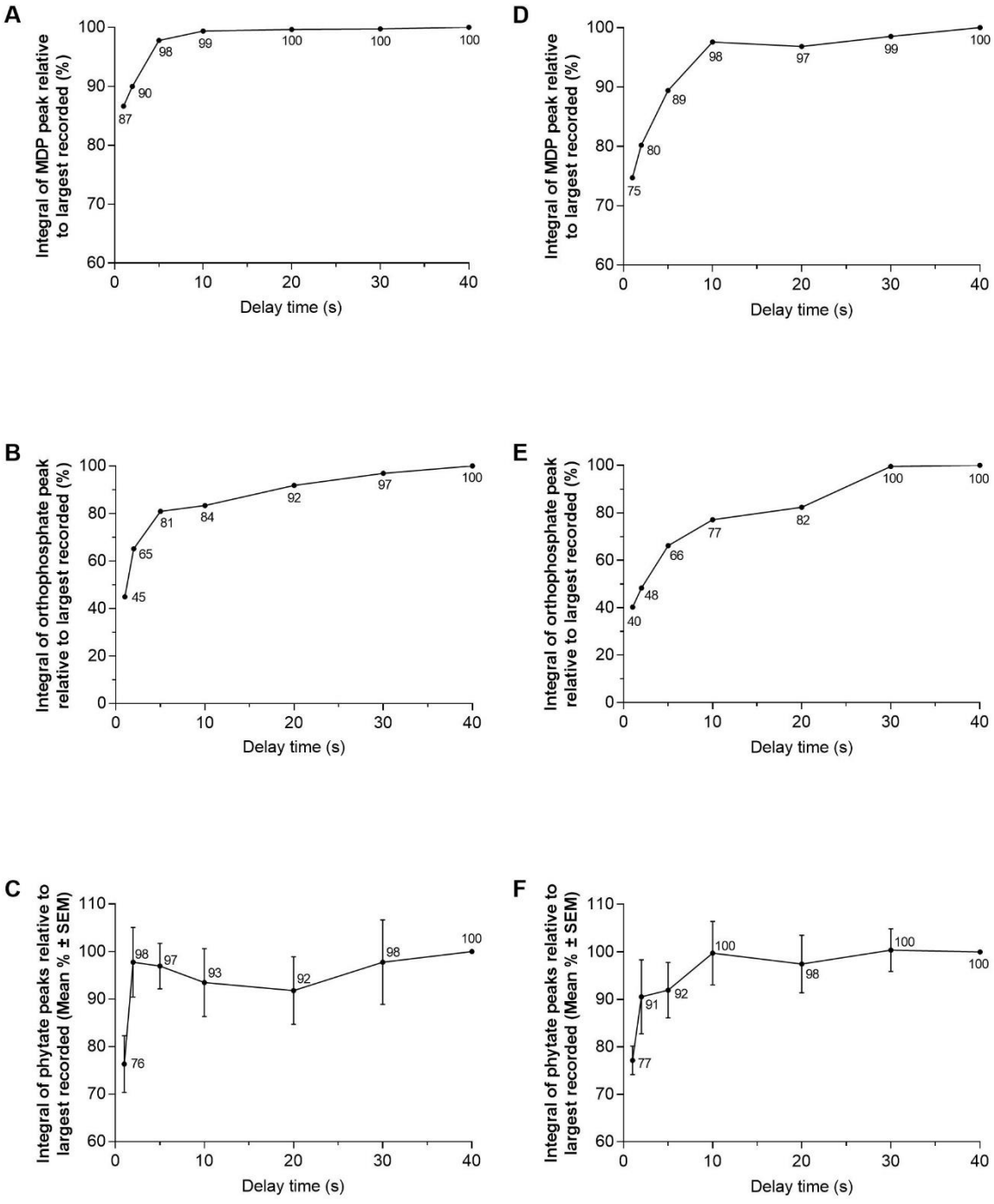

Figure 4.5: Integrals of ^{31}P NMR peaks relative to the largest of: **A**. MDP (Spen); **B**. Orthophosphate (Spen); **C**. Phytate (Spen); **D**. MDP (Wardlow); **E**. Orthophosphate (Wardlow) and **F**. Phytate (Wardlow), with increasing delay times. For MDP and Orthophosphate, relative integrals for the single peaks produced by each compound are presented, for phytate, the mean relative integral of the four phytate peaks ± SEM is presented. No error bars are present in the maximum integral as each replicate was set to 100.

WCal at 54.3% of total extractable P, which was closely followed by WAc at 47.2%. In Spen soils, SPas had the greatest fraction of residual P at 28.6%, with SAra and SPig containing 20.8 and 15.9% residual P respectively (One-way ANOVA, $p<0.0001$; Tukey multiple comparisons test, $\alpha=0.05$; Figure 4.4B).

4.4.5 ^{31}P NMR Optimisation

Before soil NMR spectra were integrated, an optimisation procedure was undertaken to calculate the proportion of the total signal that is produced using a 1s delay time, relative to the maximum signal produced when compounds can relax fully at longer delay times. A spiked sample from a Spen soil and a Wardlow soil were analysed with 100 scans at delay times of 1, 2, 5, 10, 20, 30 and 40s, and for each compound, integrals were measured and presented as a percentage of the largest measured according to the

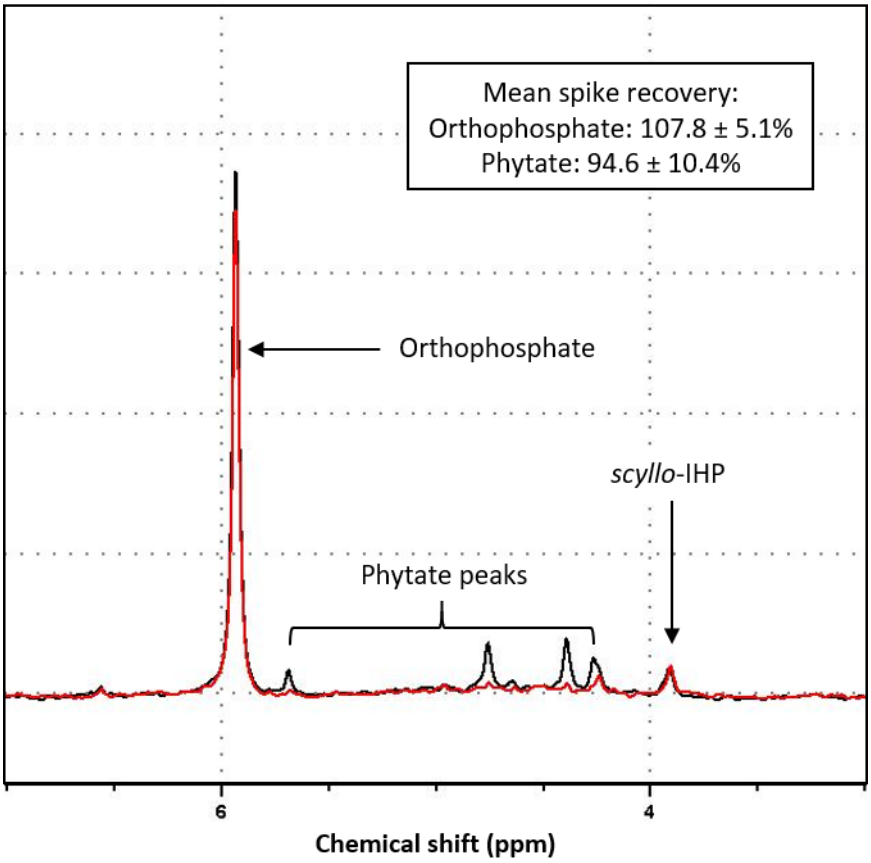

Figure 4.6: Example spectrum of spiked soil extract. Red: Sample SAra1; and Black: SAra1 spiked with 5µL of 5mM phytic acid sodium salt hydrate and 10µL of 7.25mM sodium dihydrogen orthophosphate. Integration of original and spiked sample enabled the calculation of percentage recovery. In total, three soil extracts (SAra, SPas and WCal) were spiked in this way. Mean percentage ± SD is presented in the figure (n=3).

method of Robertson, (2018) (Figure 4.5). At 1s, the MDP peak represents 87% and 75% of the total signal measured with delay time of 40s for Spen and Wardlow soil respectively (Figure 4.5, A & D). For orthophosphate, the peak produced with 1s delay time represents just 45% and 40% of the total potential signal for Spen and Wardlow soils (Figure 4.5, B & E). At 1s delay time, the phytate signal produced represents 76% and 77% of the total expected signal for Spen and Wardlow soil respectively (Figure 4.5, C & F). Spike-recovery analysis of three soils (SAra, SPas & WCal) revealed a mean recovery for spiked orthophosphate at 107.8 ± 5.1%, and for phytate at 94.6 ± 10.4%. (Figure 4.6)

4.4.6 ^{31}P NMR Determination of Soil Orthophosphate and Phytate

A single spectrum for each soil is presented in Figure 4.7 along with a spectrum for a phytic acid sodium salt hydrate standard. Spectra for all replicates are presented in Appendix B. In all soils, the orthophosphate peak at 6.02 - 5.85 ppm was large and well separated from other peaks. The four phytate peaks could be clearly seen for all extracts, apart from SAra where signal:noise ratio was low. In these spectra, peaks could be seen when intensity scale was increased for integration. In all extracts, the first phytate peak at 5.7 - 5.65 ppm was used for integration and multiplied by six. This is because this peak lies outside of the characteristic 'humic P' broad peak that exists in soils within the monoester area (Figure 4.7), meaning that the potential for overestimation is reduced. As well as the four characteristic phytate peaks, a large single peak was observed in all spectra at 3.95 - 3.85 ppm, which is tentatively identified as the stereoisomer of phytate, *scyllo*-inositol hexakisphosphate (Turner & Richardson, 2004).

4.4.6.1 Orthophosphate-P

There was a strong positive linear relationship between levels of orthophosphate measured by ^{31}P NMR, and MRP measured colorimetrically (R^2 = 0.95, $p<0.0001$; Figure 4.8A). According to ^{31}P NMR analysis of extracts, there is a significant difference in the absolute concentration of orthophosphate between extracts of different soils (One-way ANOVA, $p<0.0001$; Figures 4.9 & 4.10A). There was no significant difference in orthophosphate-P between the two Wardlow soils, which had lower concentrations than Spen Farm soils (Tukey multiple comparisons test, $\alpha=0.05$). Within the three Spen

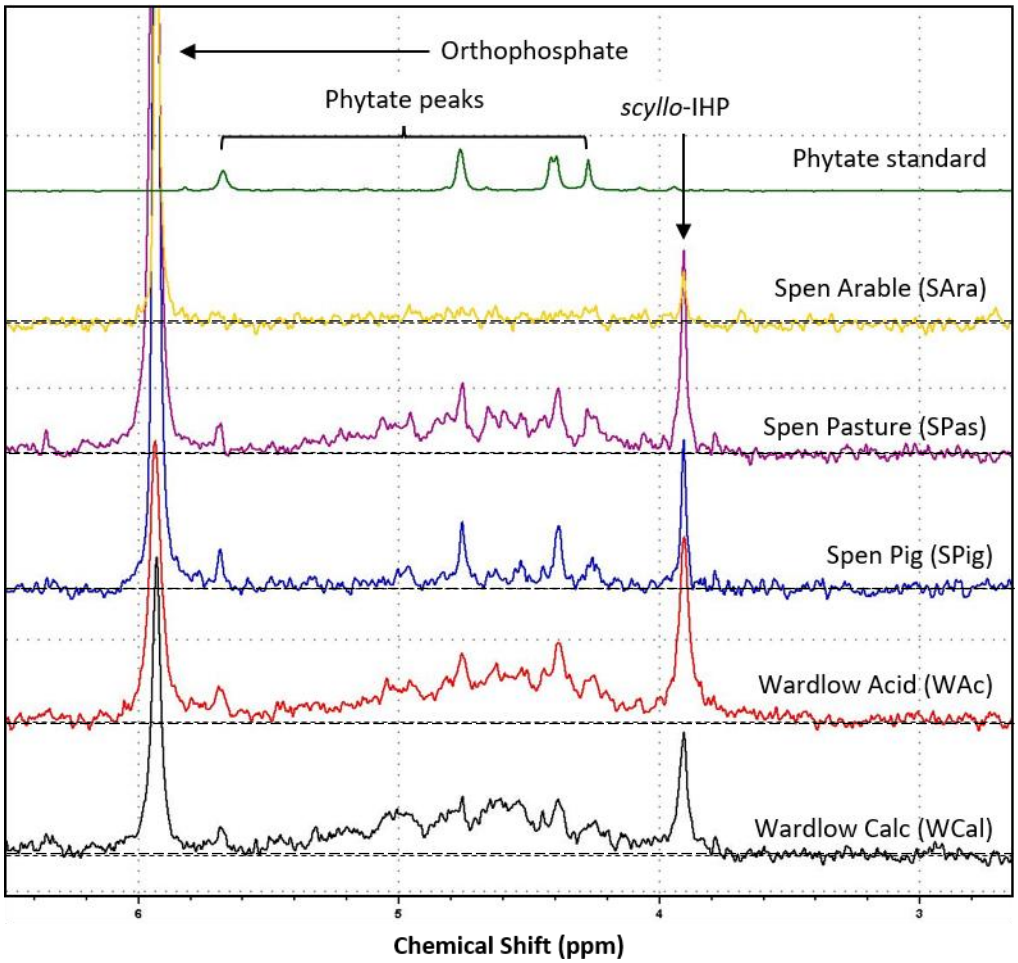

Figure 4.7: Selected ^{31}P NMR spectra of soil extracts between 6.5ppm and 2.6ppm. A phytate standard is included to indicate phytate peaks. Soil phytate was integrated using the first phytate peak, as this was at sufficient distance to avoid distortion by the large orthophosphate peak, and avoided the large humic peak seen in SPas, WAc and WCal between 5.4ppm and 4ppm. Dashed lines are overlaid to indicate baselines. Spectra are shown at the same intensity for each soil. SAra intensity was increased for peak identification. Spectra for all samples are presented in Appendix B.

Farm soils, there was a significant difference between each of the soils, with average orthophosphate concentrations increasing from 253 µg P g^{-1} in SAra to 401 µg P g^{-1} in SPas, and peaking at 538 µg P g^{-1} extracted soil in SPig (Tukey multiple comparisons test, α=0.05; Figure 4.9 & 4.10A). As a proportion of total extractable P, there was no significant difference between the orthophosphate fraction in Spen soils, which made up between 75-88%. In Wardlow soils, the orthophosphate fraction made up approximately 32% of total extractable P in both WAc and WCal (Tukey multiple comparisons test, α=0.05; Figure 4.10B).

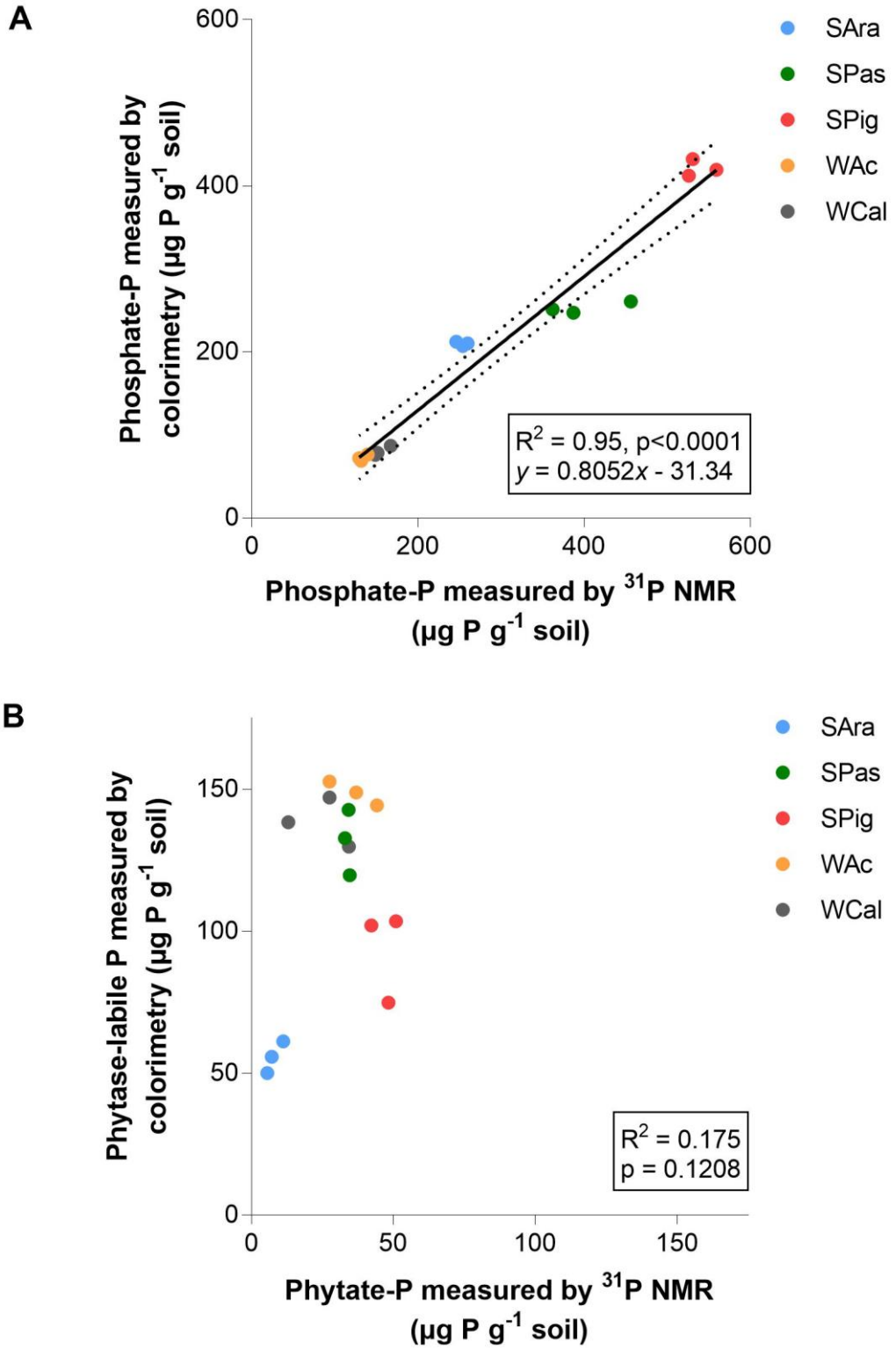

Figure 4.8: Linear regression of **A:** Phosphate-P of soil extracts measured by molybdate colorimetry and ^{31}P NMR; and **B:** Phytate-P measured colorimetrically as phytase-labile P and by ^{31}P NMR. Points represent single samples. R^2 and p values presented on graphs. Where a linear relationship exists, the equation of the regression line is presented.

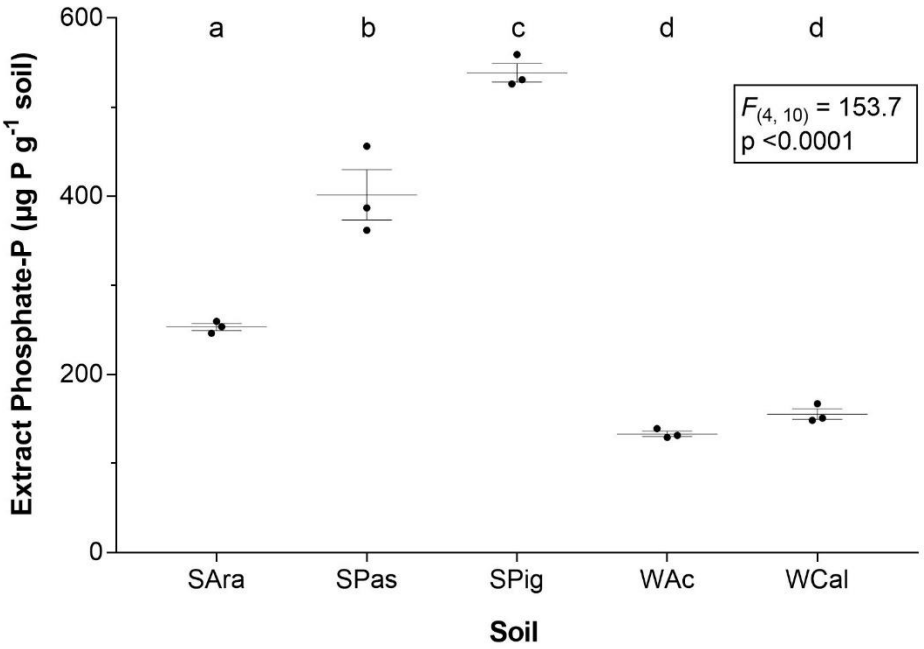

Figure 4.9: Concentration of orthophosphate-P measured by ^{31}P NMR of soil extracts, expressed as µg P g^{-1} dry weight of soil. Samples are represented as individual points (n=3) with horizontal bars indicating mean ± SEM. Results of one-way ANOVA are inset. Significant differences are represented as different letters above bars (Tukey multiple comparison, α = 0.05).

4.4.6.2 Phytate-P

There was no linear relationship observed between phytate-P data obtained colorimetrically as phytase-labile P and by ^{31}P NMR (R^2 = 0.175, p = 0.1208; Figure 4.8B). There was a statistically significant difference in absolute phytate concentration between soils according to ^{31}P NMR analysis (One-way ANOVA; p<0.005; Figures 4.10A & 4.11). Phytate-P was lowest in SAra with an average phytate-P concentration of just 8 µg P g^{-1} extracted soil, increasing through WCal < SPas < WAc to a greatest concentration of 47 µg P g^{-1} in SPig (Tukey multiple comparisons test, α=0.05; Figures 4.10A & 4.11). As a proportion of total extractable P, the phytate-P fraction was smallest in SAra at just 2.4%. This increased from WCal < SPas < SPig to WAc, which had the greatest mean proportion of phytate-P at 8.7% (Tukey multiple comparisons test, α=0.05; Figure 4.10B).

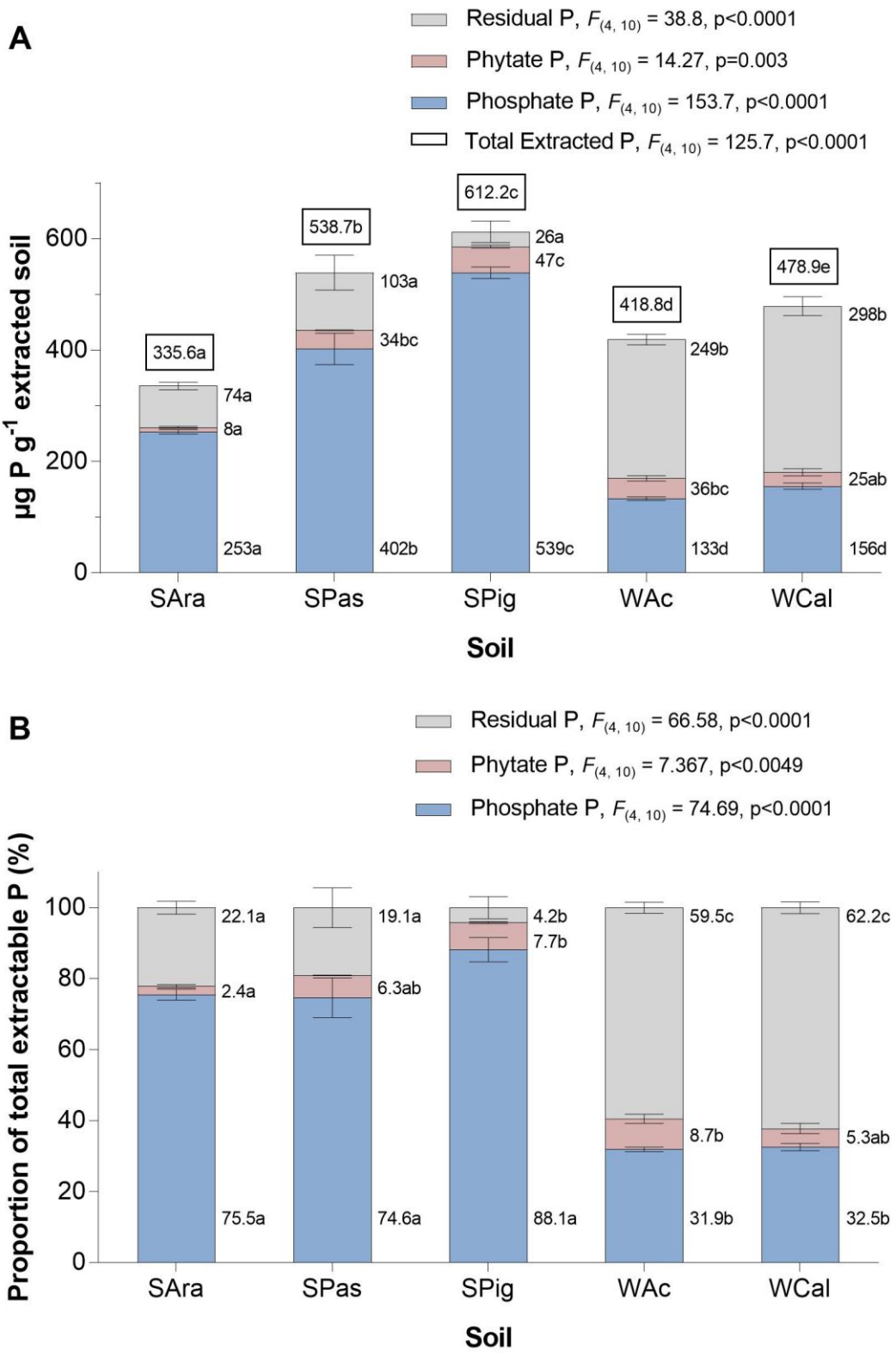

Figure 4.10: **A:** Mean absolute concentrations of P fractions in soil extracts measured by ^{31}P NMR (µg P g^{-1} extracted soil ± SEM, n=3). Total extractable P is presented above each bar. **B:** Mean concentrations of P fractions in soils as a proportion of total extractable P (% ± SEM, n=3). Results of one-way ANOVA are shown for each P fraction. Results of Tukey multiple comparison test for each fraction are shown with means to the right of bars (α = 0.05). Different letters indicate a significant difference between values for that P fraction.

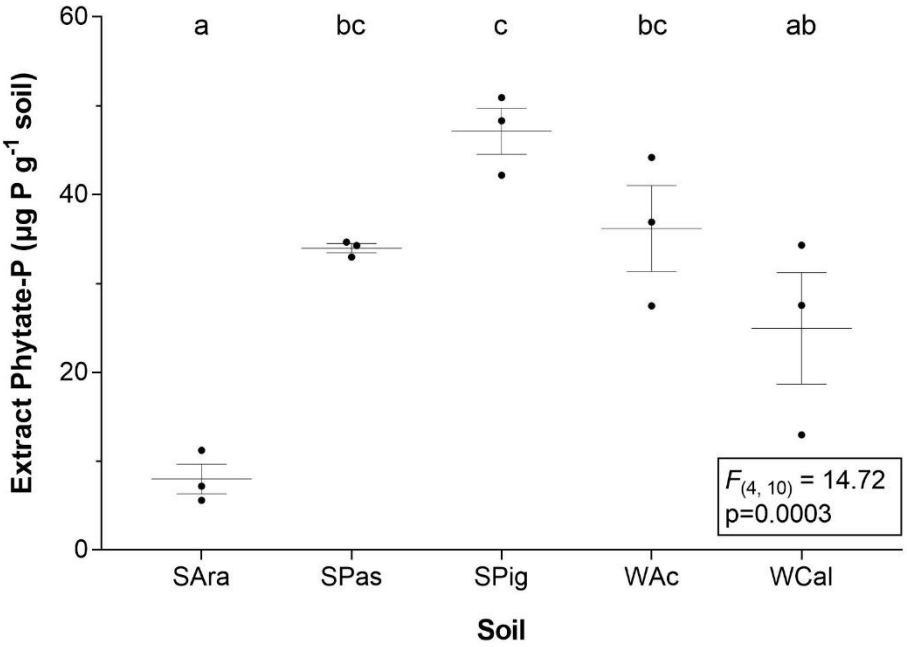

Figure 4.11: Concentration of phytate-P measured by ^{31}P NMR of soil extracts, expressed as µg P g^{-1} dry weight of soil. Samples are represented as individual points (n=3) with horizontal bars indicating mean ± SEM. Results of one-way ANOVA are inset. Significant differences are represented as different letters above bars (Tukey multiple comparison, α = 0.05).

4.4.6.3 Residual-P

The residual-P fraction was calculated as the P remaining after the subtraction of orthophosphate-P and phytate-P from total extractable P. There was a significant difference in residual-P concentration between soils (One-way ANOVA, $p<0.0001$; Figure 4.10A). However, there was no significant difference between the absolute residual-P of individual Spen soils, nor between the two Wardlow soils, but Wardlow soils were comprised of a significantly higher concentration of residual-P than Spen soils, at between 249-298 µg P g^{-1} extracted soil (Tukey multiple comparisons test, α=0.05). As a proportion of total extractable P, residual-P is lowest in SPig at 4.2%. Residual P is approximately 20% in SAra and SPas but comprises a much higher 60-62% of total extractable P in Wardlow soils (Figure 4.10B).

4.5 Discussion

This is the first study to use a combination of colorimetric analysis and solution ^{31}P NMR to determine the concentrations and proportions of phytate and orthophosphate in a variety of British agricultural soils and natural acidic and calcareous grassland soils.

Large differences in P fractions were observed between the agricultural and grassland soils, indicating that land-use history has a significant impact on P speciation. Orthophosphate was found to dominate Spen Farm soils, whereas Wardlow soils were instead dominated by organic P, with orthophosphate making up only 32% of extractable P. This likely reflects a more natural state in Wardlow soils relative to Spen soils, where intensive agricultural practices have disrupted natural soil P cycling. Application of pig manure, and a cessation in cultivation since its use as an arable soil seems to have caused a recovery in soil organic matter in SPig soil, accompanied by an increase in P_T, orthophosphate and phytate concentrations. The observed differences in P speciation in SPig relative to SAra supports the hypothesis that phytate-P derived from organic inputs accumulates in soil.

4.5.1 Soil pH & organic matter

Within Spen Farm soils, SAra and SPas soil pH was found to be near neutral, with pH values of 6.94 and 7.1 respectively. The SPig soil, which had been a permanent arable soil prior to three successive years as a pig pen before sampling, was more acidic than SAra and SPas at pH 5.6. Although the SPig soil was not sampled prior to its transition from arable land to pig pen, the fact that this soil is appreciably more acidic than the nearby arable soil suggests that its conversion and resulting recipience of pig excreta has caused a reduction in pH of the topsoil. A similar trend was reported by de Oliveira et al., (2014), who found that pig slurry application reduced pH of the top layer of an arable soil, suggesting that this could be due to increased organic acid production from the biodegradation of applied organic matter. Its therefore possible that the increased acidity of SPig soil compared to SAra is caused by microbial degradation of the organic matter excreted onto SPig soils. SAra had by far the lowest organic matter content of all soils, at just 4.36% by mass, which is likely to be a symptom of the intensive treatment of the soil. The repeated growth and harvest of annual crops means that little organic

matter is returned to arable soil in plant residues. Frequent tillage also aerates the soil, increasing the rate of decomposition of organic matter, as well as disrupting aggregates which can expose previously inaccessible organic matter to microbial degradation (McLauchlan, 2006). It's probable that the cessation of arable farming on the SPig soil and the resulting lack of tillage, as well input of pig excreta are the underlying causes of the elevated organic matter content in this soil, and it's recovery is remarkable considering it has occurred over only three years. As a permanent grassland, with an absence of tillage and regular grazing, it is unsurprising that SPas had the greatest organic matter in Spen soils.

In Wardlow soils, organic matter content was much greater, between 29.57% and 35.96% by mass in WCal and WAc soils. In the same soils, pH was 6.54 in WCal and 4.25 in WAc. Organic matter is much greater in these soils due to the natural state of the grasslands relative to Spen farm soils, with no recorded cultivation of the soil, and light grazing by sheep and cattle. This means there are few outputs from the soil, enabling the natural accumulation of soil organic matter via inputs from plant material. Such a stark difference in the pH of the adjacent grasslands at Wardlow is primarily due to the difference in soil thickness. The WCal grassland soil is a 5-10cm deep soil meaning that the shallow limestone bedrock has a significant influence on soil pH, whereas in the WAc grassland, the soil depth reaches 70cm, with the limestone bedrock having little to no effect on the pH in the surface layer (Basto et al., 2015).

The availability of phosphate compounds to plants and microbes in the soil is highly dependent on the soil pH. The generally accepted view is that on a scale of soil pH between pH 3 and pH 9, there are two points of maximum P solubility at approximately pH 4.5 and pH 6.5 (Appendix C; Penn & Camberato, 2019). According to this model, at very low pH (<pH 4), much of the soil P is fixed in association with iron. Between pH 5 and pH 6, P is predominantly fixed by aluminium, and above pH 7, P is increasingly fixed by calcium in the soil. P can be removed from the soil solution into the labile and non-labile pools by a variety of mechanisms. These processes are very similar for both inorganic phosphates and organic phosphates like phytate, however the strength of phytate sorption is greater than that of the orthophosphate anion, owing to the number of orthophosphate moieties that are able to interact with a surface (Gerke, 2015). By

testing a range of inositol phosphates with varied degrees of phosphorylation, McKercher & Anderson, (1989) showed that sorption capacity for inositol phosphates increases with the number of phosphate esters bound within the compound, and competitive isotherm studies have further shown that phytate can competitively desorb phosphate bound to the soil solid phase (Berg & Joern, 2006).

The negatively charged phosphate anion can associate with a positively charged surface such as those of Fe and Al oxides and hydroxides via anion exchange (Penn & Camberato, 2019). At low pH, these surfaces have a positive charge, which decreases with increasing solution pH, meaning that the surface can retain less anionic phosphate. P adsorption can also occur with Al and Fe oxides and hydroxides, and the edges of aluminosilicate clay minerals via ligand exchange. Unlike anion exchange, this mechanism does not depend on the surface charge, and instead involves a strong covalent bond between the phosphate and surface metal ions, in which the phosphate moiety displaces either an H_2O or OH^- group. This mechanism is favoured at lower pH, as the surface functional groups tend to carry H_2O groups rather than OH^- groups, which are less easily displaced. OH^- groups are also more competitive for surfaces than the phosphate anion, so with increasing pH and hence increasing OH^- concentration, the frequency of phosphate ligand exchange decreases (Penn & Camberato, 2019).

At higher pH, and in soils with appreciable concentrations of calcium, precipitation of calcium phosphate compounds occurs when the solution becomes saturated with dissolved P and $Ca2^+$ (Penn & Camberato, 2019). At high pH, calcium phosphates are insoluble, and effectively remove phosphate from solution into the non-labile pool, rendering it unavailable for uptake until it is dissolved by a reduction in soil pH. Phosphates can also precipitate with Fe and Al when pH is very low, and the concentration of phosphates are very high. Decreased pH promotes the dissolution of Fe and Al oxides and hydroxides by hydrolysis resulting in free Fe^{3+} and Al^{3+} ions in solution which can then interact directly with phosphate to produce insoluble Fe and Al phosphates (Penn & Camberato, 2019).

According to this model, in the neutral SAra and SPas soils, at pH 6.94 and 7.10 respectively, P solubility is likely to be increasingly influenced by calcium concentration,

and thus phosphate and phytate may be more bound within calcium phosphates. In the SPig soil, at the more acidic pH 5.38, P sorption is more likely influenced by anion- and ligand-exchange with Fe and Al oxides and hydroxides. Interestingly, the WAc and WCal soils, at pH 4.36 and pH 6.54 respectively, each sit at one of the two points of maximal P solubility, at pH 4.5 and pH 6.5 (Penn & Camberato, 2019). However, in the Wardlow soils, P solubility may be further impacted by the vastly greater organic matter content. Orthophosphate and phytate in the soil solution bind to humic surfaces via Fe or Al bridging cations, and in the case of phytate, can bind very strongly due to the interaction of multiple phosphate groups. Over time, phytate can become incorporated into the humic matrix, affording it protection from mobilisation and rendering it all but non-labile. This pool of immobilised phytate is not easily extracted with current methods, and is often speculated to comprise part of a so called humic peak that is often observed in solution ^{31}P NMR spectra of soil samples (Doolette et al., 2010).

4.5.2 Soil total phosphorus & extraction efficiency

P_T varied greatly between soils. Within Spen Farm soils, P_T was lowest in SAra, slightly higher in SPas, and much higher in SPig (Figure 4.2). Within the SAra soil, it is likely that soil P_T varies widely throughout the year, due to fertiliser inputs and uptake by intensive cropping. Samples were taken in the autumn of 2018, two months after the simultaneous sowing of a crop of Winter Wheat, and application of phosphate fertiliser at a rate of 63.67 kg ha^{-1}, meaning that much of the soil P may have been absorbed by germinating crops. In SPas, a permanent pasture, soils receive nutrient input from grazing cattle and sheep, and there is colloquial evidence for an application of pig slurry in 2016 (Robertson, 2018). Pasture fields at Spen Farm are also mown up to twice a year for silage which, along with grazing, is the only significant nutrient output from the soil. It is unsurprising that the SPig soil had the highest levels of P_T of all soils. Swine manure is high in P, with a P_T concentrations of 10.4 mg P g^{-1} and 14.62 mg P g^{-1} measured by Liang et al., (2018) and Turner, (2004) respectively. Since its transition from an arable field to pig pen in 2016, inputs to the soil have come from this high P swine manure, with outputs minimised due to the low plant biomass within the pig pens, and an absence of harvesting.

Of the soils measured in this study, WAc soil was found to have the lowest P_T, slightly lower than was found in SAra soil. WCal contained more P than WAc and had comparable levels to SPas soil from Spen. Light grazing of the grasslands by cattle and sheep may present an input of P to the soil via excreta, but this is expected to be small and relatively similar between the two grasslands. The difference in P_T concentrations between the adjacent grasslands may be attributed again to the soil depth, as well as the biomass cycling. In the WCal soil, with a shallow depth of up to 10cm, the limestone bedrock has a greater influence on the soil chemistry than in the WAc grassland, where soil depth can reach 70cm. Weathering of exposed bedrock in the WCal grassland may therefore lead to a slow accumulation in soil P_T over time, which would have a smaller impact in the top layers of the WAc soil. Furthermore, WAc soils support a greater above-ground biomass, which will in turn lead to greater uptake of P from the soil, explaining the difference in P_T observed.

Extraction efficiency of soils was found to range between 43.9% and 60.8% of soil P_T, which is a much lower recovery than was found for sludge samples in Chapter 3. Excluding WAc, the calcareous nature of the soils studied might explain this low rate of recovery. Turner et al., (2003b) reported recovery values between 12-45% of soil P_T in a range of calcareous arable soils. In calcareous soils, P compounds can precipitate with calcium ions to form insoluble calcium phosphate salts. When extracted in alkaline solvents, such as the 0.25M NaOH + 0.05M EDTA solvent used in this work, these precipitates remain insoluble, meaning that they are not efficiently extracted from the soil. However, this doesn't explain the low extraction efficiency from WAc soil. With these rates of recovery, the total extractable P concentrations ranged between a low of 335.6 µg P g^{-1} of extracted soil in SAra, and high of 612.2 µg P g^{-1} of extracted soil in SPig (Figure 4.3).

4.5.3 Soil ^{31}P NMR optimisation

Due to the low P concentration of soil extracts, to generate an acceptable signal to noise ratio in solution ^{31}P NMR spectra, a total of 16,384 scans were performed per sample, meaning that a short delay time of 1s was required for acceptable analysis times. Correction factors were calculated for both soils to account for the underestimation of

peak integrals that are generated with an insufficient 1s delay time. MDP represented 87% and 75% of the full signal in Spen (SPas) and Wardlow (WCal) soil extracts respectively. Orthophosphate, a smaller compound with a longer T1 time (Robertson, 2018), represented 45% and 40% of the full signal, with phytate representing 76 and 77% of the full signal for Spen and Wardlow soils respectively. The relative integral at 1s for MDP and orthophosphate is greater in Spen soil than Wardlow soil, indicating that in the Spen extract, molecules could relax at a slightly faster rate. It's possible that this was caused by a higher concentration of paramagnetic ions (eg. Fe^{3+}, Mn^{2+}, Co^{2+} & Cu^{2+}) in the Spen extract, which are known to reduce the time required for relaxation (Cade-Menun & Liu, 2014), thereby increasing the signal at 1s delay relative to the fully relaxed signal.

When analysed by ^{31}P NMR, the recovery of orthophosphate-P and phytate-P spiked into soil extracts stood at 107.8 ± 5.1%, and 94.6 ± 10.4% respectively (Figure 4.6), showing that the ^{31}P NMR analysis coupled with the delay time correction provides an accurate quantification of orthophosphate-P and phytate-P in soil extracts from both sampling locations.

4.5.4 Colorimetric analysis of soil P

According to the colorimetric data, SAra had the lowest concentration of orthophosphate, calculated as MRP, in the Spen Farm soil extracts, and was closely followed by SPas, with SPig having by far the greatest concentration. However, SPas had the lowest MRP as a proportion of total extractable P at 47%, with SAra and SPig extracts containing 62.6 and 68.8% orthophosphate-P respectively. In Wardlow soils, absolute concentrations of MRP were significantly lower than those of Spen Farm soils, and orthophosphate made up approximately 17% of total extractable P in both Wardlow soils (Figure 4.4 A & B). Despite the existence of a positive linear relationship between the colorimetric and ^{31}P NMR data for orthophosphate, the colorimetric values were consistently lower than those of ^{31}P NMR (Figure 4.8A), an issue that wasn't observed in sludge extracts in Chapter 2. This discrepancy could be explained by the tendency of phosphate to associate with humic substances. Molybdate colorimetry measures free orthophosphate in solution, but some orthophosphate is bound within humic-metal

complexes in soil, and a proportion of this is not hydrolysed by the acidity of the colorimetric assay, so cannot react with ammonium molybdate in solution and hence is not measured colorimetrically (Turner et al., 2005a; Gerke, 2010). This leads therefore to an underestimation of orthophosphate-P in samples containing high levels of humic substances. It is telling that SAra soils showed a lower degree of underestimation than other soils (Figure 4.8A), as the organic matter content is lowest in this soil, meaning that there is a lower concentration of humic substances with which orthophosphate could complex.

Colorimetric determination indicated that phytase-labile P was relatively abundant in soil extracts, making up between 15.3 and 24.4% of total extractable P in Spen soils, and 28.9-35.5% in Wardlow soils. SAra had the lowest absolute concentration, followed by SPig, with the greatest concentration in Spen soils found in SPas with over double the amount of phytase-labile P of SAra. Absolute concentrations in Wardlow soils were similar to those found in SPas, at 138 and 149 µg P g^{-1} soil. However, as described in Chapter 3, section 3.5.4.3, the reliability of these results is questionable when compared to the results obtained by ^{31}P NMR on the same extract samples, as phytate can be overestimated due to the tendency of phytase enzymes to catalyse the dephosphorylation of not only phytate, but other P compounds too (Oh et al., 2004). There was also no significant linear relationship between phytate concentrations calculated by the two methods (Figure 4.8B). Coupled with the spike-recovery data carried out on ^{31}P NMR samples (Figure 4.6), this suggests that ^{31}P NMR provides a more accurate and reliable method for phytate determination than phytase hydrolysis. However, a message that can be taken from the colorimetric data is that, proportionally, the pool of phytase-labile P is smaller in arable (SAra) or recently arable soils (SPig), than in soils with higher organic matter content, which indicates that the current or past intensive treatment of these soils has caused them to have a lower concentration and variety of P compounds than more natural grassland soils.

4.5.5 Solution ^{31}P NMR analysis of soil P

4.5.5.1 Major features of soil ^{31}P NMR spectra

Due to the much lower P concentration of soil, signal to noise ratio in ^{31}P NMR spectra of soil extracts was lower than was observed in sludge extracts (Figure 4.7). Peaks were clearly visible in all spectra apart from SAra where, due to the very low phytate concentration, potential peaks were visible only when the intensity scale was increased. In SAra, a spiked sample was used to confirm the existence and identity of the phytate peak used for integration (Figure 4.6). For all extracts, the first phytate peak, representing the phosphate group at carbon-2 of the inositol ring, was used for integration and calculation of phytate. This overcomes the potential overestimation of phytate that can be caused by the existence of a broad peak underlying the orthophosphate monoester region of the spectra, a feature which can be clearly seen in SPas, WAc and WCal spectra (Figure 4.7). A broad monoester peak is commonly observed in ^{31}P NMR spectra of soil extracts, and made up 14-23% of total extractable P in a calcareous soil studied by Doolette et al., (2010). There has been much discussion over the identity of the unresolved molecules that make up this broad peak, with various authors describing it as monoester P associated with humic compounds (Doolette et al., 2010), large molecular weight materials (Jarosch et al., 2015) and soil organic matter (McLaren et al., 2014). A recent investigation of the molecular structure of the broad peak compounds, based on their transverse relaxation (T2) times in ^{31}P NMR, found that the broad peak decayed rapidly compared to sharper peaks in the monoester region, indicating the presence of high molecular weight macromolecules, with which phosphate monoesters are associated (McLaren et al., 2019). It is notable that in the ^{31}P NMR spectra of SAra and SPig, in which organic matter content is lowest due to the intensive treatment of the soil, this broad macromolecular peak is far less apparent than in the soils with higher organic matter content (Figure 4.7).

A further notable feature of spectra for all soil extracts was the presence of a sharp peak at ~3.9 ppm (Figure 4.7), which was tentatively assigned to the stereoisomer of phytate, *scyllo*-inositol hexakisphosphate (*scyllo*-IHP), based on the peak library produced by (Cade-Menun, 2015). Whilst *scyllo*-IHP is relatively abundant in soils, and is regularly

identified in ^{31}P NMR spectra, little is known about its origin and behaviour in the soil (Turner & Richardson, 2004). It often produces a clear strong peak in spectra as, unlike phytate, the chemical environment around each phosphate group is identical, meaning that the single *scyllo*-IHP peak represents all 6 phosphate groups in the molecule. Although *scyllo*-IHP concentration was not measured in this work, we can see from figure 4.7 that peak size is smallest in SAra, relatively similar in SPig and WCal, and greatest in WAc and SPas, and seems to make up a significant proportion of extractable P in each soil. Little is known about the origin or bioavailability of *scyllo*-IHP in soil, but evidence from phytase assays suggests that it has a degree of resistance to phytase hydrolysis owing to the lack of an axial phosphate group (Cosgrove, 1966). However, when Turner et al., (2005b) analysed *scyllo*-IHP in pasture soils, they found ryegrass growth reduced its concentration in nutrient limited soils, but increased its concentrations in nutrient rich soils, suggesting that under P-limitation, organisms that can degrade *scyllo*-IHP are favoured, whereas in nutrient rich soils, microbial synthesis of *scyllo*-IHP is favoured (Turner et al., 2005b). If *scyllo*-IHP is readily degraded by the phytase enzyme used in this chapter, it may also partially explain the observed overestimation of phytate measured as phytase-labile P.

4.5.5.2 Spen Farm Soils

^{31}P NMR data showed consistently higher concentrations of orthophosphate, and lower levels of phytate-P than the colorimetric approach (Figure 4.10A). In Spen farm soils, orthophosphate constituted the majority of P in all extracts, making up between 74.6 – 88.1% of total extractable P. Phytate concentration was lowest in SAra, making up just 2.4% of total extractable P, with SPig containing the greatest phytate concentration in Spen soils, making up a proportion of total extractable P three times greater than that of SAra. Despite the overall low P_T concentration found in arable soil, the dominance of orthophosphate in this soil was expected due to the intensive use of this land for cropping and the regular application of inorganic mineral phosphate fertiliser. In an analysis of soils conducted by Stutter et al., (2015), arable soils were found to contain an average orthophosphate-P concentration of 695 ± 328 µg P g^{-1}, making up an average 74% of total NaOH-EDTA extractable P. The SAra soils, containing an average of 253 µg orthophosphate-P g^{-1} are much less orthophosphate-rich, but extracts proportionally

contain over 75% orthophosphate-P. Whilst the soils sampled by Stutter et al., (2015) were sampled in spring 2008, no information is provided as to whether this was before or after application of P fertilisers to the soil. SAra soils were sampled in November 2018, following the sowing of a crop of Winter Wheat. The field had received an input of triple superphosphate fertiliser in early August at a rate of 63.67 kg P_2O_5 ha^{-1} (Dr. George Sorensen, personal communication), so the very low phosphate concentration detected by ^{31}P NMR is surprising. However, with plants having grown on the fertilised soil for three months, there was likely to have been significant absorbance of fertiliser P by young plants, and there is also the possibility that phosphate had become precipitated in alkaline salts, which would be under-represented in alkaline extracts due to their insolubility. SAra contained the lowest concentration of phytate in Spen soils, at just 8 µg P g^{-1}, which made up just 2.4% of total extractable P. With regular harvests, and application of inorganic P fertilisers, there is likely to be very little input of phytate to arable soils from plant residue and manure, and there is no evidence for manure applications to this field. Further, conventional arable practices do not promote the persistence or accumulation of organic phosphates in soil, as tillage is known to decrease the organic matter content by dispersing soil aggregates and aerating the soil, promoting microbial degradation (McLauchlan, 2006). It's also a possibility that, as the SAra soil seems so P-limited, over the fallow winter months there is a competitive advantage for soil microbiota that can metabolize P from organic sources due to P limitation, meaning that levels of organic P, including phytate may be depleted year on year.

Soil total P and total extractable P were greater in SPas than SAra, and absolute concentrations of orthophosphate-P and phytate-P were both significantly greater than those of SAra. However, the proportional contributions of both orthophosphate and phytate were not significantly different to those of SAra, with 74.6% of total extractable P present as orthophosphate-P, and 6.3% present as phytate-P. In the intensive grassland environment of a permanent pasture field, it is perhaps surprising that organic P compounds do not make up a greater proportion of the total extractable P. In pasture soils, past work has shown the organic P fraction to dominate. Turner et al., (2003b) used solution ^{31}P NMR to characterise the P speciation in 29 UK pasture soils, finding

that orthophosphate monoesters were the dominant P forms, constituting 29-60% of extractable P. In a similar study, Stutter et al., (2015) measured orthophosphate monoesters making up between 17-36% of extractable P in 10 intensive grassland soils in which orthophosphate-P made up an average of just 39% of extractable P. The greater presence of organic P observed in these studies is likely to result from the less intensive land use of these soils. An absence of regular cultivation, as well lower outputs from crop harvests means that organic P can more readily persist and accumulate in the soil. It is estimated that between 60-95% of P absorbed by plants in grazed pastures is returned to the soil in plant residue and animal excreta, and between 30-60% of P in plants exists in organic form (Condron et al., 2005). Higher organic P in the pasture soils mentioned above may therefore result from low output, and regular input of organic P. However, in this work, pasture soil was found to be dominated by orthophosphate-P, with just 6.3% made up of phytate-P, and 19% assigned as 'residual' P, which is likely to be comprised of unmeasured orthophosphate monoesters, diesters, polyphosphates and any P associated with humic macromolecules. The reason for the lower than expected values of organic P, and higher than expected values of orthophosphate is unclear, but there is colloquial evidence that SPas has received applications of pig slurry from the onsite pig facility at Spen in the past (Robertson, 2018). Data for the amount and frequency of application is not available, but pig manure is known to be highly concentrated in orthophosphate, with concentrations of 7272.9 µg P g^{-1} measured by Liang et al., (2018), and 11,200 µg P g^{-1} measured by Turner, (2004) making up approximately 90% of extractable P in both studies. If the pasture soil has received applications of pig slurry in the past, this might explain the dominance of orthophosphate over organic P in this soil.

Having received a high continuous application of pig manure from its use as a pig pen, SPig soil unsurprisingly contains the highest concentration of total P, orthophosphate-P and phytate-P of all the soils analysed. With an average phytate-P concentration of 680.7 µg P g^{-1}, making up 8.5% of extractable P (Liang et al., 2018), pig manure is rich in phytate, due to their predominantly grain-based diet, and inefficient digestion by phytase enzymes (Abioye et al., 2014). Proportionally, SPig is dominated by orthophosphate-P, which makes up over 88% of extractable P, and also contains the

highest proportion of phytate-P of Spen soils, at the expense of the 'residual P' fraction. With P outputs from this soil reduced to a minimum due to the observed lack of plant biomass in the SPig field, continual inputs of orthophosphate-P and phytate-P to this field in pig excreta are the likely cause of this accumulation. Prior to 2016, SPig had been an arable field since at least 2001 (Table 4.1), but soil was unfortunately not sampled prior to its conversion. If SAra is considered an acceptable proxy soil for comparison, then in three years since pig pen conversion, SPig has seen an 82% increase in soil P_T concentration, a 113% increase in orthophosphate-P concentration, and a near 5x increase in phytate-P concentration compared to SAra.

4.5.5.3 Wardlow Soils

The P speciation of Wardlow soils was vastly different to those of Spen Farm soils (Figure 4.10A), but between WAc and WCal, the only significant difference observed was for soil total P, and total extractable P, with no significant differences observed for absolute concentrations or proportions of orthophosphate-P, phytate-P or residual-P. Orthophosphate-P concentration in these soils is lower than in Spen soils, and makes up approximately 32% of total extractable P. Phytate concentrations were similar in these soils, making up 8.7 and 5.3% of extractable P in WAc and WCal respectively. Extractable P is instead dominated by the 'residual P' fraction, which in this study is comprised of all soil P other than orthophosphate and phytate, so includes other orthophosphate monoesters, diesters, phosphonates and inorganic polyphosphates, for which specific concentrations were not measured. The dominance of the organic P fraction in Wardlow soils, which in this work is calculated as non-orthophosphate-P, is reflective of these soils as extensively grazed grasslands, in a more natural state than Spen Farm soils. These soils receive minimal P inputs from excreta, and have minimal output from grazing, so the majority of P cycling occurs through plant P uptake and subsequent soil replenishment with organic P from plant litter. Organic P in this soil is likely to be heavily influenced by the soil microbial population. Bünemann et al., (2012) showed that microbial uptake and immobilisation of P dominates P fluxes in grassland soils with low P inputs. The finding that extensive grassland soils contain greater concentrations of diester-P and polyphosphates, which are indicative of high P turnover and an active microbial population, supports this conclusion (Stutter et al., 2015). Despite this

microbial immobilisation of inorganic P, P-limited grasslands often exhibit high levels of biodiversity (Lambers et al., 2010), and recent work on the Wardlow calcareous grassland has demonstrated that co-occurring grassland plant species are able to acquire P from varied P sources, including diester-P (DNA), soluble orthophosphate and calcium bound phosphates to varying extents (Phoenix et al., *in press*). Although phytate was not analysed in this study, its relative abundance in Wardlow soils suggests that it may play an important role alongside the 'residual P' fraction in plant P-acquisition in P-limited soils.

4.5.6 P Accumulation of phytate in pig pen soil

The results obtained from ^{31}P NMR analysis of Spen soils tentatively suggest that phytate can accumulate in previously arable soils that receive P inputs from monogastric pig manure. If the P concentrations found in SAra can be assumed to be representative of the SPig soil prior to its conversion from permanent arable soil in 2016, then the cessation of intensive arable practices and application of pig manure has almost doubled organic matter levels, and has increased P_T, orthophosphate and phytate concentrations by 82%, 113% and 489% respectively. Pig manure was measured by Liang et al., (2018) to contain a P_T concentration of 10,400 µg P g^{-1}, and orthophosphate and phytate made up 90.7% and 8.5% of total extractable P respectively. Whilst this total P concentration is lower than that found in anaerobically digested sludge in Chapter 3, the proportion of orthophosphate and phytate found in digested sludge, at 83.4% and 4.5% of extractable P, is remarkably similar to pig manure. Its therefore probable that when applied to arable soils, anaerobically digested sludge behaves much in the same way as pig excreta, increasing overall P concentrations, and increasing the proportion of phytate-P in the soil.

The potential for phytate accumulation in soils is likely to be dependent on many factors, including abiotic stabilisation, the microbial processes of immobilisation and mineralisation, soil pH, organic matter content and the abundance of P sorption sites (Stutter et al., 2015; Dou et al., 2009). Microbial mineralisation of phytate via the production of exogenous phytase enzymes is promoted in response to P deficiency in soil (Richardson & Simpson, 2011). However, in SPig where phytate has been applied

alongside large concentrations of more labile orthophosphate, this microbial degradation may be suppressed. Furthermore, competitive isotherm studies in controlled conditions have shown that phytate is strongly and preferentially sorbed in soil compared to glucose-6-phosphate, ATP and orthophosphate, and may even compete with orthophosphate for sorption sites when applied in low concentrations (Berg & Joern, 2006). Saturation of P sorption sites by phytate in soil could culminate in elevated P run-off to water bodies, where it can then contribute to eutrophication (Dou et al., 2009). Accumulation of phytate from application of pig manure and anaerobically digested sludge therefore presents two problems, the first due to its potential to promote environmental P pollution and eutrophication, and the second, the likely avoidable loss of phytate-P from the agricultural P cycle due to its strong and irretrievable sorption to the soil. It therefore stands to reason that the elimination of phytate from anaerobically digested sludge amendments would be beneficial for P resource recovery and environmental protection, and the use of exogenous phytase enzymes for its dephosphorylation may be a solution.

4.6 Conclusions

Overall, this work has highlighted the stark difference in soil P speciation between farmed soils and natural grassland soils in the UK, and that there is large variation within farmed soils depending on their land use history. ^{31}P NMR analysis has revealed that farmed soils are dominated by inorganic orthophosphate, whereas extensively grazed grassland soils exhibit much greater organic matter and are instead dominated by organic phosphates, which may indicate greater microbial influence on soil P dynamics and greater soil health.

The addition of monogastric pig manure in SPig has caused a small but significant recovery in soil organic matter, accompanied by an increase in P_T, and concentrations and proportions of orthophosphate and phytate over three years since its conversion from arable soil, when SAra soil is used for comparison. With the similarity in P composition between pig manure and anaerobically digested sludge from human waste, it is likely that a similar accumulation would be seen in soils amended with sludge. Ideally, this would be confirmed with future work to assess changing P speciation in sludge-amended soils over a number of years. However, the evidence presented in this chapter strongly suggests that phytate can accumulate in amended soils, which may represent both wastage of valuable P resources, and an environmental risk from the elevated potential for runoff and eutrophication. The use of phytase enzymes could present an opportunity to address this problem, and the following chapter will look into the dephosphorylation of phytate by one such commercially available enzyme, to assess its potential for the breakdown of phytate in environmental samples.

5: Phytase-mediated liberation of phytoavailable phosphate from phytate in a model substrate

5.1 Summary

In order to reduce the need for inputs of unsustainable chemical P fertilisers to arable land, strategies to provide phytoavailable orthophosphate from stabilised P in soils and amendments are required. Phytate is commonly identified as the most abundant organic P compound in soil extracts, so is a prime candidate compound for such mobilisation. One approach involves the inoculation of soils and manures with phytase-producing microbial strains, but this suffers from poor long-term persistence of inoculant strains. Alternatively, genetic engineering can be used to introduce or improve phytase exudation from the roots of plants. While this approach has had some recent success, there remain legislative and social barriers to the use of transgenic crops in food production. Microbial phytase enzymes are now produced on a commercial scale for use as supplements in the diets of monogastric livestock, but their application as potential bio-fertilisers is not well-studied.

In this chapter, the performance of a commercially produced, microbially-derived phytase enzyme was assessed for its use in the dephosphorylation of phytate and provision of phytoavailable orthophosphate to plants grown in model substrates. Due to the tendency of phytase activity to be lost in soils due to the adsorption of both phytate and phytase to the soil solid phase, enzyme performance was assessed in two substrates, one containing a mixture of sand and peat, and one with a higher adsorption capacity containing clay, sand and peat. Overall, no consistent evidence was found to support the hypothesis that the treatment of phytate-fertilised substrates with phytase would result in phytate dephosphorylation, provision of phytoavailable P to plants, and improved plant performance. This was the case in both substrates, indicating that phytase activity was lost in both substrates regardless of clay content, most likely due to the adsorption of both phytate and phytase to the substrate solid phase.

5.2 Introduction

5.2.1 Phytate dephosphorylation by phytases in environmental samples

Anaerobic digestion of sewage sludge is purported to lead to mineralisation of key nutrients, such as N and P, making them bio-available as potential fertilisers. In contrast to this received wisdom, it was shown in in Chapter 3 that phytate is still present in the anaerobically digested sludge that is commonly spread to arable land. Phytate applied to the soil in such organic amendments may become preferentially stabilised due to its high charge density and is often identified in soil extracts as the most abundant organic P compound (Jørgensen et al., 2015). Moreover, the prior use of land for rearing monogastric animals can generate high residual levels of soil phytate, for example in pig pens (Chapter 4). Consequently, it is now clear that phytate concentration in the soil can depend on land-use history. As part of a future sustainable and efficient model for the use of limited P resources, there will be a need for strategies that enable the mobilisation and mineralisation of P from stabilised phytate in the soil, in order to reduce the use of unsustainable chemical P fertilisers.

Some approaches have attempted to increase the ability of a soil to mineralise phytate-P via inoculation of manure or soil with phytase-producing microbes, and commercial bioinoculants designed to exploit soil legacy P are already in existence (Owen et al., 2015). Menezes-Blackburn et al., (2016) inoculated cattle manure with a phytase-producing *Bacillus* species, and found that inoculated manure had a greater concentration of inorganic orthophosphate than uninoculated manures. However, the survival of bio-inoculants is a major obstacle to their widespread use. Whilst inoculation can provide an initial abundance of beneficial microbes, they often have poor survival and are outcompeted by the native soil microorganisms (Martínez-Viveros et al., 2010; Menezes-Blackburn et al., 2017). This was observed in the above cattle manure study of Menezes-Blackburn et al., (2016), in which the prevalence of their *Bacillus* sp. inoculum decreased over the six day incubation due to competition with the natural manure microbiota.

An alternative to microbial inoculants is the enhancement of crops for increased phytase exudation from roots. Most plants have intrinsic P mobilising traits, but there is an

assumption within the literature that in modern crops, these traits have become either insufficiently expressed or even lost due to the successive breeding of crops in high nutrient environments with the application of fertilisers (Menezes-Blackburn et al., 2017). Studies such as that by George et al., (2005b), in which *Nicotiana tabacum* plants were genetically modified to express *Aspergillus niger* phytase, have had some success. In this study, transgenic plants were found to accumulate 3.7-fold more P than wildtype controls when grown on sterile agar. This effect was lost when plants were grown on P-deficient soil, but was regained somewhat when soils were amended with phytate, indicating that a limiting factor is the availability of phytate as a substrate for the enzyme (George et al., 2005b). Since then, with increased understanding of rhizosphere biochemistry has come an appreciation of the role of low molecular weight (LMW) organic acids such as citrate, which are exuded by both plants and microbes to mobilise phytate that has become adsorbed within the soil by occupying soil sorption sites (Richardson et al., 2009). Recent work has shown that *N. tabacum* plants engineered to express both phytase and citrate exudation accumulated more P from a P-limited soil than plants expressing either alone (Giles et al., 2017). Despite the promise of this approach, there remains large legislative and societal obstacles to the use of genetically modified crops, particularly in Europe, and wider collaborations between academia and social and political scientists will be required to overcome these before they can be widely adopted (Menezes-Blackburn et al., 2017; Horton et al., 2017).

Microbial phytase enzymes have been isolated and are commonly produced commercially for use as supplements to aid phytate digestion in the grain-based diets of monogastric livestock (Jorquera et al., 2008). Despite their widespread availability, there has been relatively little work investigating their activity when applied to organic matrices such as manure and soil. Menezes-Blackburn et al., (2014) found that amending soil with a cattle manure treated with a stabilised feed-additive phytase enzyme resulted in a significant increase in soil phytoavailable P, and increased plant P concentrations by 39%. Similarly, Gujar et al., (2013) found that when added to a phytate-amended soil, *A. niger* phytase supplementation reduced soil phytate content by 30%, and simultaneously increased phytoavailable phosphate levels by 1.18%. However, the addition of enzymes directly to the soil can result in their rapid

immobilisation via adsorption to soil solid phase constituents such as clays, metals and metal oxides, which when coupled with the tendency of phytate to similarly adsorb, can result in a rapid loss of enzyme activity (George et al., 2005a).

5.2.2 Aims and Objectives

Microbial phytase enzymes are widely commercially available, yet are under-studied with respect to their ability for use as a biofertilizer in crop production. The aim of this chapter was therefore to assess the performance of a commercially available microbially derived feed-supplement phytase enzyme for the provision of phytoavailable phosphate from phytate in model substrates with varied adsorptive capacities. To test whether the performance of the enzyme was affected by adsorption to the substrate solid phase, two substrates were used, the first containing a mixture of 50% quartz sand and 50% peat, and the second with an increased sorption capacity containing 40% quartz sand, 10% bentonite clay, and 50% peat. Spring onion plants were treated with a nutrient solution containing either no P, orthophosphate-P or phytate-P, with half in each treatment provided with a dose of phytase enzyme following fertilisation. Plants were then analysed for total biomass, total P uptake and P concentration, and substrates analysed for both total and phytoavailable P following harvest.

P treatment was expected to have a major effect on overall plant performance, with plants treated with phosphate showing the greatest P uptake, concentration and biomass, and those receiving no P having the lowest P uptake, concentration and biomass, and there was expected to be no effect of the phytase enzyme within these treatments. Clay content in the substrate could also have an overall effect on plant performance due to the tendency of P to adsorb to clay surfaces, so plants in the 10% clay substrate were considered likely to show a lower P uptake, P concentration and biomass compared to those in 0% clay substrate. Within phytate-treated plants, it was hypothesised that the application of phytase would cause a degree of phytate dephosphorylation in the non-clay substrate, resulting in increased biomass, total P uptake, and P concentration in plants, along with an increase in phytoavailable P in the substrate compared to plants receiving no phytase. It was postulated that this increased P uptake from the soil could result in decreased substrate P_T compared to substrates

receiving no enzyme, as phytate-P cannot be absorbed by plants without prior dephosphorylation. Any effect of the enzyme in 0% clay substrate was expected to be depressed or absent in the 10% clay substrate, in which greater adsorption of both phytate and phytase would result in the loss of enzyme activity.

5.3 Methods

5.3.1 Experimental set-up

A fully factorial greenhouse experiment was designed to test ability of a commercial phytase enzyme for liberating phosphate from phytate spiked in a model soil substrate, and to test whether substrate clay content might affect this. Spring onion plants were grown in 150cm^3 of one of two substrates (Figure 5.1). The first substrate ('0% Clay') contained (by volume) 50% Irish Peat Moss and 50% quartz sand, and the second substrate ('10% Clay') contained 50% Irish Peat Moss, 40% quartz sand, and 10% Bentonite clay (Honeywell Fluka) by volume. Substrates were balanced by mass of the organic Irish peat moss fraction but differed in total dry mass equivalent. 150cm^3 of '0% Clay' contained approximately 127.5g substrate (dry mass per pot), whereas 150cm^3 of '10% Clay' contained approximately 107g (dry mass per pot) owing to clay having a lower mass than the sand it replaced. Nutrient content is expressed as mass per pot, rather than mass per gram of substrate. The two substrates were tested for available P concentration (See Section 5.5.3) prior to seedling transplant. '0% Clay' contained a total of 1034µg of phytoavailable P per pot, and '10% Clay' contained 1511µg of phytoavailable P per pot, indicating that the bentonite clay contained a phosphate impurity. To balance available P budgets in the experiment, pots containing '0% Clay'

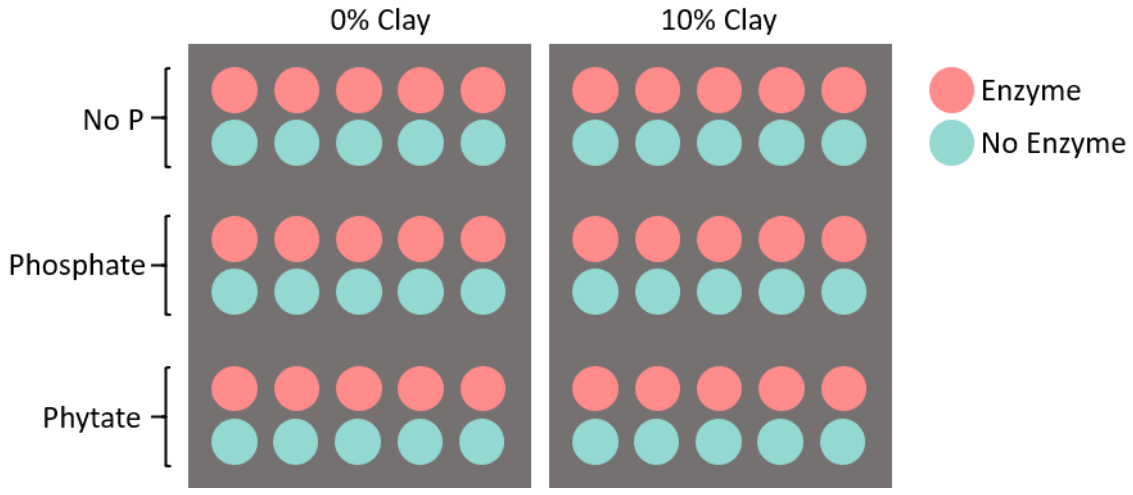

Figure 5.1: Schematic diagram of the experimental set up. Plant in two clay treatments were treated with one of three phosphorus treatments. Within each phosphorus treatment, half of plants were treated with phytase enzyme, half were not.

received 477 µg P per pot as 19.1mL of 25 µg P mL^{-1} sodium dihydrogen orthophosphate, and were left for 5 days prior to receiving transplanted seedlings.

Spring onion seeds (var. White Lisbon; Mr Fothergills Seeds, UK) were sown in 100% Irish peat moss at a depth of 1.5cm. 7 days after first germination, the sixty strongest seedlings were transplanted equally into 60 individual pots containing either substrate. Plants were watered with UHP water every 2-3 days as required. One week following transplantation, to promote P limitation, pots were each provided with 20mL of a modified nitrogen (N) and potassium (K)-rich Hoagland's nutrient solution containing no P (No P; Table 5.1). All nutrient solutions were adjusted to pH 4.5 via the dropwise addition of 1M H_2SO_4.

Plants were grown in a greenhouse chamber at the Arthur Willis Environment Centre, University of Sheffield, with a 16-hour day length, daytime temperature of 20°C and night-time temperature of 15°C. 42 days following germination, plants in each substrate were split into three sub-groups according to the nutrient treatment they were to receive (Figure 5.1). Nutrient treatments consisted of three modified Hoagland's solutions (No P (negative control), phosphate-P (positive control) and phytate-P; Table 5.1). Each nutrient solution was balanced for NPK with a molar ratio of 15:3:8, apart from No-P which was 15:0:8. 20mL of No P contained 0 µg P, phosphate-P contained 1858 µg P as sodium dihydrogen orthophosphate, and phytate-P contained 1858 µg of phytase-labile P as phytic acid dipotassium salt (Santa Cruz Biotechnology, Germany; Table 5.1). As phytate dephosphorylation by the enzyme is incomplete, releasing 5 of the 6 phosphate groups, and giving a final product of *myo*-inositol monophosphate, phytate concentration was increased in order to balance the phytase-labile P in 'phytate-P' with the phytoavailable orthophosphate in 'phosphate-P' solution. Pots each received 20mL of their respective nutrient solution at 42 days and were left for three days before the addition of enzyme treatments. Substrate pH was measured in pots of surplus substrate without plants, which had been treated in an identical manner to the experimental substrates. pH was measured following nutrient treatment, according to the method outlined in Chapter 4, section 4.2.2 (Hendershot et al., 2008). pH of 0% clay was measured at pH 4.25 ± 0.01, and pH of 10% clay was measured at pH 4.93 ± 0.01.

Half the pots within each P-treatment group in each substrate then received 20mL of 50 FTU mL^{-1} phytase enzyme (Ronozyme HiPhos, DSM Nutritional Products, Switzerland) or 20mL of denatured enzyme at the same concentration. Enzyme was denatured by autoclaving in a Prestige 2100 Benchtop autoclave with an 11 minute hold cycle at 121°C under 15psi of pressure. The enzyme is a commercially produced *Citrobacter braakki* phytase expressed in *Aspergillus oryzae* and is used as a feed additive for monogastric livestock under the name RONOZYME HiPhos (DSM Agricultural Products, Switzerland). *C. braakii* is an enterobacterium, with the enzyme having a broad activity over the range of pH 2 – 6 (Brejnholt et al., 2011; Lichtenberg et al., 2011), but an optimal range of at least 80% optimal activity between pH 3 and pH 4.5 (Menezes-Blackburn et al., 2015).

Table 5.1: Modified Hoagland's nutrient solutions for plant phosphorus treatments. All solutions contained 1mL L^{-1} of micronutrient solution providing 0.5ppm Boron, 0.5ppm Manganese, 0.05ppm Zinc, 0.02ppm Copper & 0.01ppm Molybdenum

Treatment	Macronutrient salt	Concentration (g L^{-1})	Nitrogen (µg 20mL^{-1})	Phosphorus (µg 20 mL^{-1})	Potassium (µg 20 mL^{-1})
No P Molar ratio: 15:0:8	KNO3	0.505	1401	-	3910
	$Ca(NO_3)_2$	0.820	2801	-	-
	KCl	0.224	-	-	2346
	$MgSO_4$	0.241	-	-	-
	Total:		***4202***	***0***	***6256***
Phosphate-P *Molar ratio: 15:3:8*	KNO_3	0.505	1401	-	3910
	$Ca(NO_3)_2$	0.820	2801	-	-
	KH_2PO_4	0.408	-	1858	2346
	$MgSO_4$	0.241	-	-	-
	Total:		***4202***	***1858***	***6256***
Phytate-P *Molar ratio: 15:3:8*	KNO_3	0.505	1401	-	3910
	$Ca(NO_3)_2$	0.820	2801	-	-
	KCl	0.134	-	-	1408
	$MgSO_4$	0.241	-	-	-
	K_2-Phytate	0.442	-	1858	938
	Total:		***4202***	***1858***	***6256***

5.3.2 Sample Processing

Plants were grown for 14 days following enzyme treatment before harvest. Plants were harvested by separating shoots from roots at the base of the bulb. Roots were then separated from the substrate over a 5mm sieve and washed clean. Roots and shoots were placed in individual paper envelopes and dried at 80°C for 3 days. Dried root and shoot samples were weighed, then placed into 2mL extraction tubes with a small ball-bearing for homogenisation. Milling of samples was performed on a QUIAGEN TissueLyser for 5 minutes.

Substrates were placed in tinfoil vessels and placed in a fume cupboard for 5 days to air-dry. Once dried, substrates were weighed and milled to pass a 2mm sieve in a Fritsch Pulverisette Ball Mill. A 1g subsample of each milled substrate was dried at 80°C for 3 days to determine the residual moisture content of air-dried substrates.

5.5.3 Sample Analysis

Air-dried milled root and shoot samples and final substrates were subject to acid digestion and total P determination using a modified version of the Murphy & Riley, (1962) molybdate blue colorimetric assay as described in Chapter 3, section 3.3.3. For root and shoot samples, due to the high P concentration in plant tissue, just 20mg of milled sample was digested in 1mL of concentrated H_2SO_4 and H_2O_2, followed by P determination.

Sodium bicarbonate extractable P was calculated both before the experiment and after as a measure of substrate available P according to the method of Olsen et al., (1954). 1g samples of air-dried substrate were extracted for 30 minutes in 20mL of 0.5M $NaHCO_3$ adjusted to pH 8.5 on a reciprocating shaker at 120 strokes per minute. Extracts were then filtered through Whatman No. 40 filter paper into clean 50mL falcon tubes. Phosphorus content of the extracts was determined using a modified version of the molybdate blue colorimetric assay (Murphy & Riley, 1962). For each sample, a 4mL cuvette was prepared containing 0.5mL extract, 0.5mL developer solution containing ammonium molybdate antimony potassium tartrate in 2M H_2SO_4, 0.2mL of 0.1M *L*-ascorbic acid, and 2.6mL UHP. Absorbance was measured after 40 minutes at 882nm on a Cecil CE 1020 spectrophotometer. Blank cuvettes were prepared alongside samples in

which 0.1M *L*-ascorbic acid was replaced with UHP. Absorbance was again measured at 882nm after 40 minutes to measure the contribution of the extract colour to the absorbance reading.

5.3.4 Statistical analyses

The effect of clay content, P treatment and enzyme treatment on the measured variables of plant biomass, total plant P uptake, plant P concentration, substrate phytoavailable P and substrate total P was investigated using three-way ANOVAs (α = 0.05). A series of two-way ANOVAs were then run on the phytate-treated samples to test for an effect of, or interaction between, clay treatment and phytase treatment. Finally, in each substrate, the single effect of enzyme addition on phytate-treated plants was assessed using unpaired students t-tests (α = 0.05). Statistical analyses were performed in SPSS Statistics v.23 (IBM Corp, Armonk, USA). Figures were produced in GraphPad Prism 7.04 (GraphPad Software Inc, San Diego, USA).

5.4 Results

5.4.1 Plant Biomass

Clay treatment was the only factor to have a significant effect on overall plant biomass, with plants grown in 10% clay substrate having a significantly greater biomass at harvest than those grown in 0% clay substrate. There was no significant effect of P treatment or enzyme treatment, and no two-way or three-way interactions between treatments (Three-way ANOVA; $\alpha = 0.05$; Figure 5.2; Table 5.2). In phytate-treated plants alone, there was a significant effect of clay treatment on plant biomass, but no independent significant effect of enzyme treatment. However, there was a significant interaction between clay and enzyme treatment (Two-way ANOVA, $\alpha = 0.05$; Table 5.3A). Students t-tests revealed that there was no significant difference between biomass of phytate treated plants in 0% clay, but in 10% clay, phytate-treated plants that received no enzyme treatment had a greater biomass than those that received phytase (Unpaired t-test, $p < 0.05$; Figure 5.2).

5.4.2 Total Plant P uptake

There was a statistically significant effect of P treatment on total plant P uptake, with plants that received P in the form of inorganic orthophosphate exhibiting the greatest uptake in both clay treatments (Figure 5.3, Table 5.4). There was also a significant effect of clay treatment on P uptake, and a two-way interaction between the two factors. In 0% clay substrate, plants receiving 'No P' contained more P than those grown in 10% clay. Plants receiving phosphate-P contained similar amounts of P in both clay treatments, but plants receiving phytate-P absorbed more P when grown in 0% clay substrate than in 10% clay substrate. There was no overall significant effect of enzyme treatment on total absorbed P, as well as no two-way interactions involving enzyme treatment. No three-way interaction between treatments was present. (Three-way ANOVA; $\alpha = 0.05$; Figure 5.3; Table 5.4). In phytate-treated plants, there was a significant effect of clay treatment on total plant P uptake, but no significant effect of enzyme, and no two-way clay-enzyme interaction (Two-way ANOVA, $\alpha = 0.05$; Table 5.3B). This was confirmed by unpaired student t-tests in phytate-treated plants in each substrate, which

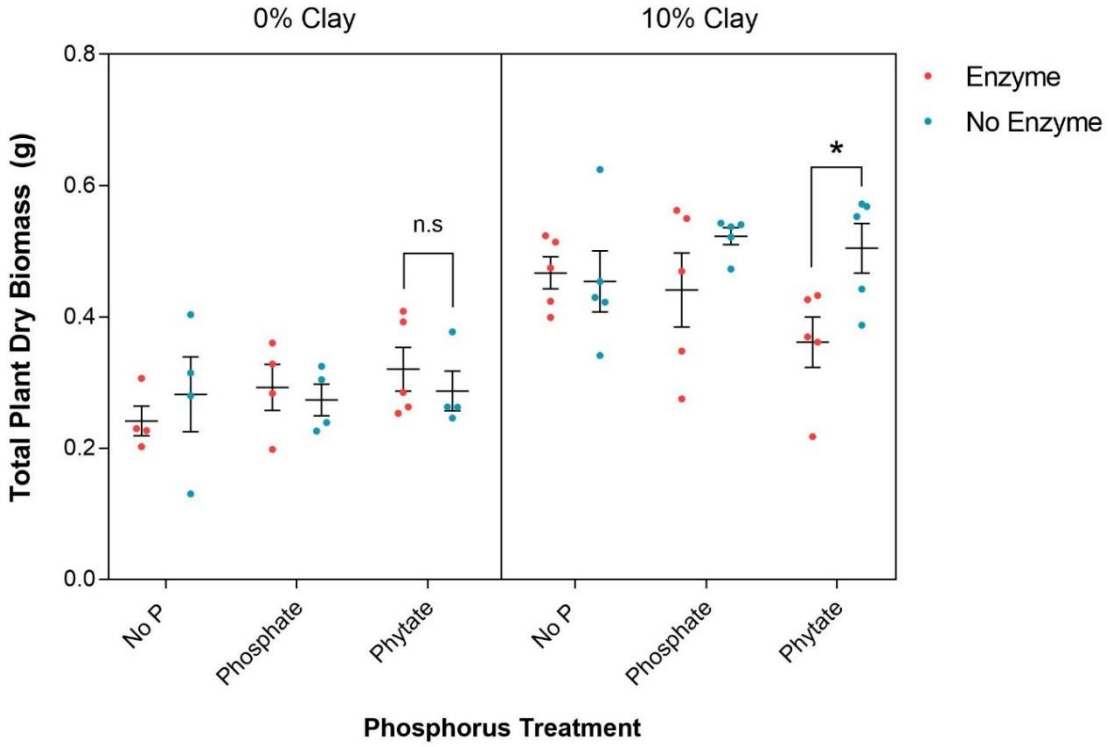

Figure 5.2: The effect of clay content, phosphorus treatment and enzyme addition on final plant biomass. The results of a three-way ANOVA to test the effect of treatments and their interactions is presented in Table 5.2. Points represent individual plants (n = 4-5). Horizontal lines represent means ± SEM. The results of unpaired t-tests for phytate-treated plants with and without enzyme in each substrate are shown above phytate columns, (n.s) = not significant, (*) = significant at $p < 0.05$.

Table 5.2: Results of three-way ANOVA for final plant biomass

Source	Type III Sum of Squares	df	Mean Square	*F*	p value
Clay	0.420	1	0.420	64.406	<0.001*
Phosphorus	0.004	2	0.002	0.320	0.728
Enzyme	0.015	1	0.015	2.336	0.134
Clay × Phosphorus	0.015	2	0.007	1.146	0.328
Clay × Enzyme	0.019	1	0.019	2.903	0.096
Phosphorus × Enzyme	0.004	2	0.002	0.297	0.745
Clay × Phosphorus × Enzyme	0.031	2	0.016	2.383	0.104
Residual	0.280	43	0.007		
Total	8.704	55			

revealed no significant difference in total plant P uptake between plants that received enzyme and those that did not (Unpaired t-test, $p > 0.05$; Figure 5.3).

5.4.3 Plant P Concentration

Clay treatment had a significant effect on plant P concentration, with plants grown in 10% clay having a lower P concentration than those grown in 0% clay. Phosphorus treatment also had a significant effect, with plants receiving P as orthophosphate having the greatest P concentrations within each clay treatment. There was no significant effect of enzyme treatment, and no two-way or three-way interaction between treatments (Three-way ANOVA; $\alpha = 0.05$; Figure 5.4; Table 5.5). Within the phytate-treated plants, there was a significant effect of clay on plant P concentration, but again no significant effect of enzyme, and no two-way interaction (Two-way ANOVA, $\alpha = 0.05$; Table 5.3C). However, an unpaired t-test revealed that there was a significant

Table 5.3: Results of two-way ANOVA for measured parameters in phytate-treated plants. Significant factors or interactions are highlighted with an asterisk (*), α=0.050.

	Source	Type III Sum of Squares	df	Mean Square	*F*	p value
A Plant Biomass	Clay	0.079	1	0.079	12.920	<0.050*
	Enzyme	0.014	1	0.014	2.330	0.148
	Clay × Enzyme	0.037	1	0.037	5.998	<0.050*
	Residual	0.091	15	0.006		
B Plant P Uptake	Clay	1.538×10^6	1	1.538×10^6	60.760	<0.001*
	Enzyme	4.68×10^2	1	4.68×10^2	0.018	0.894
	Clay × Enzyme	1.535×10^3	1	1.535×10^3	0.067	0.809
	Residual	3.797×10^5	15	2.531×10^4		
C Plant P Concentration	Clay	3.271×10^7	1	3.271×10^7	109.800	<0.001*
	Enzyme	1.462×10^4	1	1.462×10^4	0.049	0.828
	Clay × Enzyme	1.090×10^6	1	1.090×10^6	3.661	0.075
	Residual	4.468×10^6	15	2.979×10^5		
D Substrate phyto-available P	Clay	1.936×10^5	1	1.936×10^5	20.930	<0.001*
	Enzyme	3.476×10^4	1	3.476×10^4	3.757	0.072
	Clay × Enzyme	6.377×10^3	1	6.377×10^3	0.689	0.419
	Residual	1.387×10^5	15	9.251×10^3		
E Substrate Total Phosphorus	Clay	2.108×10^6	1	2.108×10^6	7.615	<0.050*
	Enzyme	1.807×10^6	1	1.807×10^6	6.528	<0.050*
	Clay × Enzyme	2.656×10^3	1	2.656×10^3	0.010	0.923
	Residual	4.153×10^6	15	2.769×10^5		

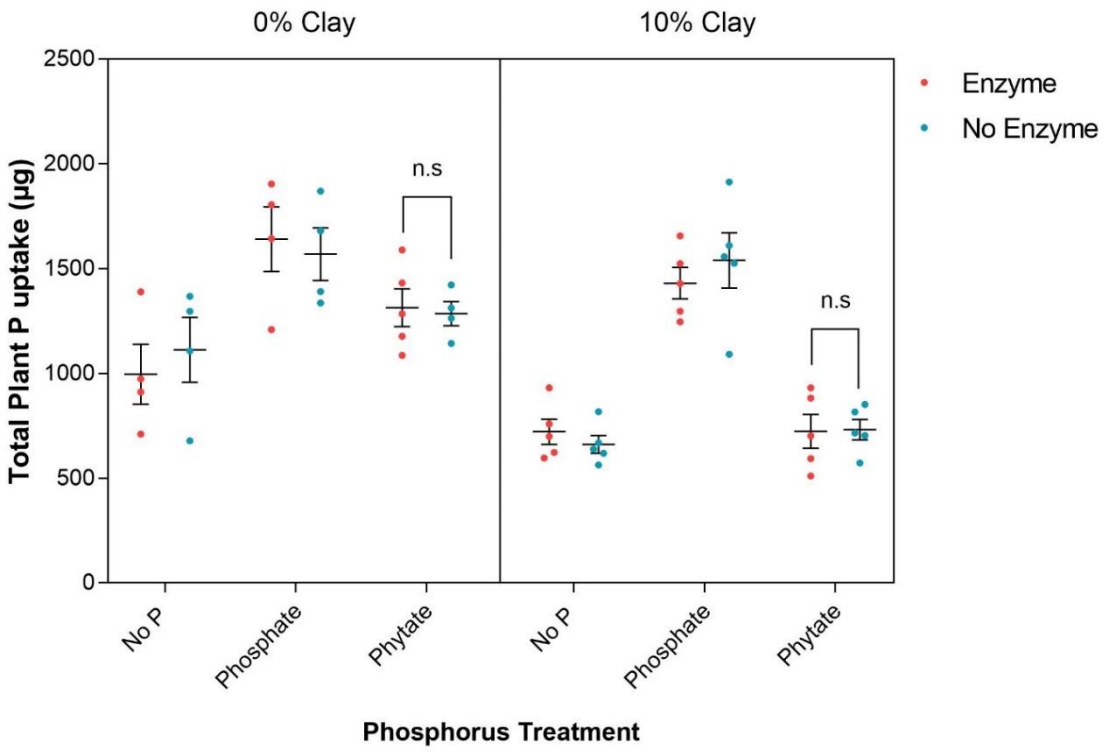

Figure 5.3: The effect of clay content, phosphorus treatment and enzyme addition on total plant P uptake. The results of a three-way ANOVA to test the effect of treatments and their interactions is presented in Table 5.4. Points represent individual plants (n = 4-5). Horizontal lines represent means ± SEM. The results of unpaired t-tests for phytate-treated plants with and without enzyme in each substrate are shown above phytate columns, (n.s) = not significant, (*) = significant at $p < 0.05$.

Table 5.4: Results of three-way ANOVA for total plant P uptake. Significant factors or interactions are highlighted with an asterisk (*), α=0.050.

Source	Type III Sum of Squares	df	Mean Square	*F*	p value
Clay	1.677×10^6	1	1.677×10^6	37.043	<0.001*
Phosphorus	4.484×10^6	2	2.242×10^6	49.503	<0.001*
Enzyme	2.038×10^3	1	2.038×10^3	0.045	0.833
Clay × Phosphorus	4.670×10^5	2	2.335×10^5	5.156	<0.050*
Clay × Enzyme	5.853×10^2	1	5.853×10^2	0.013	0.910
Phosphorus × Enzyme	3.597×10^3	2	1.798×10^3	0.040	0.961
Clay × Phosphorus × Enzyme	7.159×10^4	2	3.579×10^4	0.790	0.460
Error	1.947×10^6	43	4.529×10^4		
Total	7.886×10^7	55			

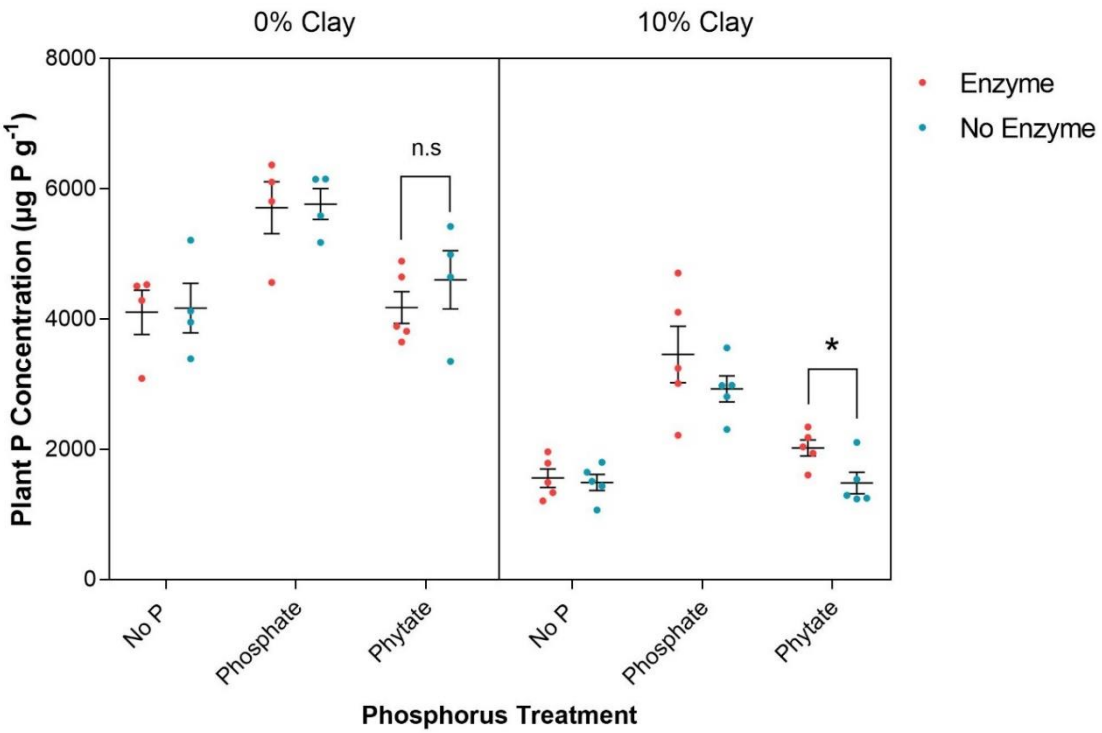

Figure 5.4: The effect of clay content, phosphorus treatment and enzyme addition on plant P concentration. The results of a three-way ANOVA to test the effect of treatments and their interactions is presented in Table 5.5. Points represent individual plants (n = 4-5). Horizontal lines represent means ± SEM. The results of unpaired t-tests for phytate-treated plants with and without enzyme in each substrate are shown above phytate columns, (n.s) = not significant, (*) = significant at $p < 0.05$.

Table 5.5: Results of three-way ANOVA for plant P concentration. Significant factors or interactions are highlighted with an asterisk (*), α=0.05.

Source	Type III Sum of Squares	df	Mean Square	*F*	p value
Clay	9.167×10^7	1	9.167×10^7	254.778	<0.001*
Phosphorus	2.782×10^7	2	1.391×10^7	38.667	<0.001*
Enzyme	1.289×10^5	1	1.289×10^5	0.358	0.553
Clay × Phosphorus	1.989×10^4	2	9.947×10^3	0.028	0.973
Clay × Enzyme	1.062×10^6	1	1.062×10^6	2.953	0.093
Phosphorus × Enzyme	1.368×10^5	2	6.845×10^4	0.190	0.827
Clay × Phosphorus × Enzyme	3.971×10^5	2	1.986×10^5	0.552	0.580
Error	1.547×10^7	43	3.598×10^5		
Total	7.454×10^8	55			

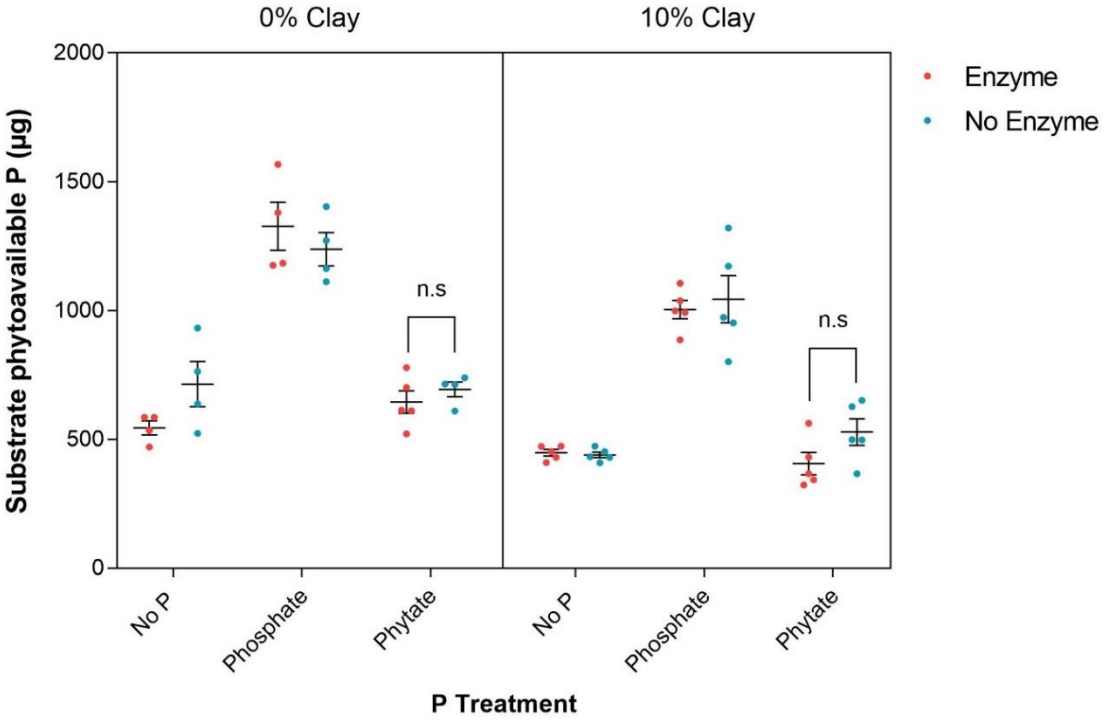

Figure 5.5: The effect of clay content, phosphorus treatment and enzyme addition on substrate phytoavailable P. The results of a three-way ANOVA to test the effect of treatments and their interactions is presented in Table 5.6. Points represent individual plants (n = 4-5). Horizontal lines represent means ± SEM. The results of unpaired t-tests for phytate-treated plants with and without enzyme in each substrate are shown above phytate columns, (n.s) = not significant, (*) = significant at $p < 0.05$.

Table 5.6: Results of three-way ANOVA for substrate phytoavailable P. Significant factors or interactions are highlighted with an asterisk (*), α=0.05.

Source	Type III Sum of Squares	df	Mean Square	*F*	p value
Clay	6.308×10^5	1	6.308×10^5	45.979	<0.001*
Phosphorus	4.322×10^6	2	2.161×10^6	157.511	<0.001*
Enzyme	3.049×10^4	1	3.049×10^4	2.222	0.143
Clay × Phosphorus	1.278×10^4	2	6.388×10^3	0.466	0.631
Clay × Enzyme	2.251×10^2	1	2.251×10^2	0.016	0.899
Phosphorus × Enzyme	3.489×10^4	2	1.745×10^4	1.272	0.291
Clay × Phosphorus × Enzyme	6.005×10^4	2	3.002×10^4	2.189	0.124
Error	5.899×10^5	43	1.372×10^4		
Total	3.569×10^7	55			

difference between phytate treated plants in 10% clay substrate, with plants receiving enzyme having a greater P concentration than those without enzyme (Unpaired t-test, $p < 0.05$; Figure 5.4), though this effect was not mirrored in the 0% clay substrate (Figure 5.4).

5.4.4 Substrate phytoavailable P

Clay treatment had a statistically significant effect on substrate bicarbonate-extractable (phytoavailable) P, with phytoavailable P slightly lower in 10% clay substrate than in 0% clay substrate. Phosphorus treatment also had a significant effect on phytoavailable P, with substrates receiving phosphate-P containing more phytoavailable P than those receiving either no P or phytate-P. There was no significant interaction between clay and P treatment, with no difference in the effect of P treatment between the two clay treatments. Furthermore, there was no significant effect of enzyme treatment on substrate phytoavailable P, and no significant two-way or three-way interactions between treatments (Three-way ANOVA; $\alpha = 0.05$; Figure 5.5; Table 5.6). In phytate-treated pots, only clay had a significant effect on substrate phytoavailable P, with no effect of enzyme treatment, and no two-way interaction (Two-way ANOVA, $\alpha = 0.05$; Table 5.3D). This was confirmed in unpaired t-tests, which showed there was no significant difference in phytoavailable P in phytate-treated substrates that received enzyme or no enzyme.

5.4.5 Substrate total P

Clay treatment had a significant effect on final substrate P_T, with P_T greater overall in 10% clay substrates. As mentioned in section 5.3.1, P_T of substrates was greater in 10% clay owing to a P impurity in the clay. However, substrates were balanced for phytoavailable P rather than total P content, so this clay effect is to be expected. Phosphorus treatment also had a significant effect on substrate P_T, with substrates receiving P in either phosphate or phytate form having greater P_T than substrates receiving no P, which is to be expected. Overall, no significant effect of enzyme addition was found, and again, no significant two-way or three-way interactions between treatments were found for substrate P_T (Three-way ANOVA; $\alpha = 0.05$; Figure 5.6; Table 5.7). Within the phytate treated plants, there was a significant effect of clay treatment and enzyme treatment on substrate P_T, but no interaction

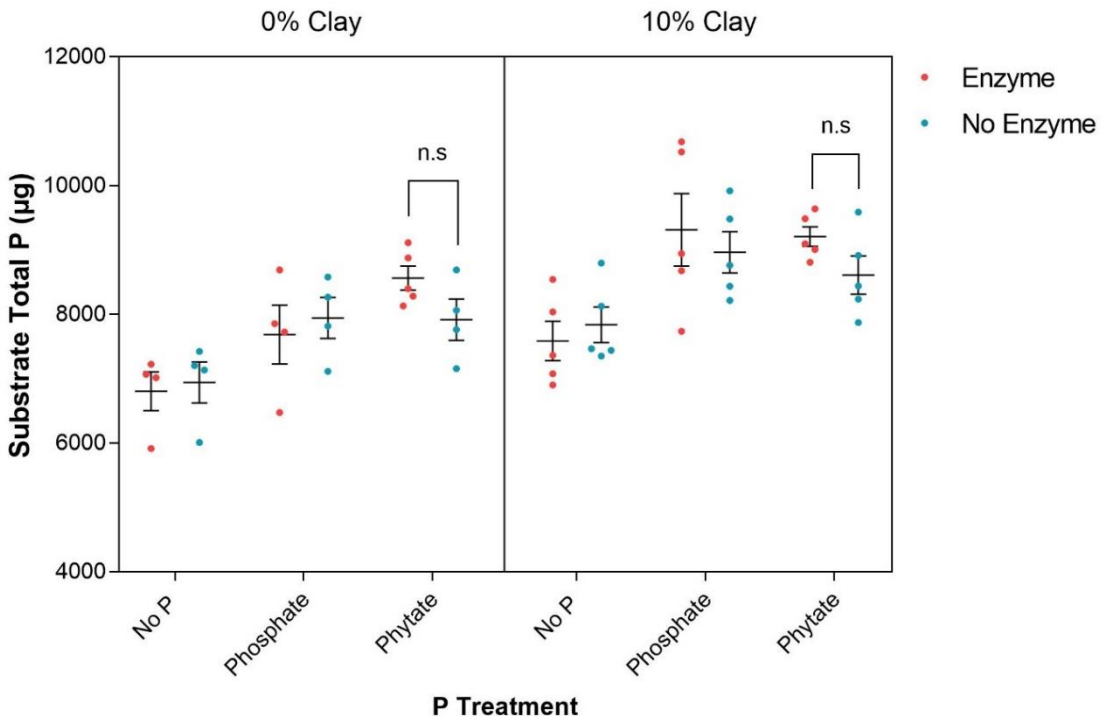

Figure 5.6: The effect of clay content, phosphorus treatment and enzyme addition on substrate total P. The results of a three-way ANOVA to test the effect of treatments and their interactions is presented in Table 5.7. Points represent individual plants (n = 4-5). Horizontal lines represent means ± SEM. The results of unpaired t-tests for phytate-treated plants with and without enzyme in each substrate are shown above phytate columns, (n.s) = not significant, (*) = significant at $p < 0.05$.

Table 5.7: Results of three-way ANOVA for substrate total P. Significant factors or interactions are highlighted with an asterisk (*), α=0.05.

Source	Type III Sum of Squares	df	Mean Square	*F*	p value
Clay	1.208×10^7	1	1.208×10^7	23.590	<0.001*
Phosphorus	1.831×10^7	2	9.157×10^6	17.888	<0.001*
Enzyme	3.366×10^5	1	3.366×10^5	0.658	0.422
Clay × Phosphorus	1.041×10^6	2	5.206×10^5	1.017	0.370
Clay × Enzyme	7.475×10^4	1	7.475×10^4	0.146	0.704
Phosphorus × Enzyme	1.608×10^6	2	8.039×10^5	1.570	0.220
Clay × Phosphorus × Enzyme	3.570×10^5	2	1.785×10^7	0.349	0.708
Error	2.201×10^7	43	5.119×10^5		
Total	3.731×10^9	55			

between these factors (Table 5.3). From Figure 5.6, there appears to be a trend in phytate-treated plants in both substrates whereby P_T of enzyme-treated substrate is greater than non-enzyme substrate. However, unpaired t-tests suggest that these differences are not significant (Figure 5.6, $p > 0.05$).

5.5 Discussion

This experiment is the first to attempt to investigate the application of a commercially available phytase enzyme for the mobilisation of phytate-P in controlled artificial soil substrates with varying clay content. Overall, it was found that both clay content and P fertiliser had a major effect on plant growth over all treatments, however any effect of phytase treatment was inconsistent.

Phytase treatment was only expected to have an effect in plants treated with phytate. Within phytate-fertilised plants, whilst some significant effects of enzyme were found, these are generally inconsistent and do not support the hypothesis that phytase application would result in phytate dephosphorylation. Instead, it is possible that both phytate and phytase have become adsorbed within the substrate, resulting in a lack of phytase activity and phosphate liberation in either clay treatment.

5.5.1 Overall effects of clay, phosphorus and enzyme treatments

A series of three-way ANOVAs were used to look at the overall effects of clay, P and enzyme treatments on plant performance parameters and substrate P. The only factors to have a significant effect on overall plant performance were clay treatment and P treatments. Plants grown in 10% clay substrate had a greater overall biomass than those grown on 0% clay substrate (Figure 5.2). Concurrently, clay treatment had a significant effect on plant total P uptake, with plants in 10% clay absorbing a slightly lower amount of P than those in 0% clay across all treatments (Figure 5.3). This resulted in plants grown in 10% clay having a substantially lower P concentration in their biomass than those in 0% clay.

The substrates were balanced for phytoavailable P, and took up relatively similar amounts, so the stark difference in final biomass between the substrates is intriguing. It's possible that this difference could have been caused by an elevated macronutrient content introduced with clay. Substrate nutrient content was only measured for phytoavailable P prior to the experiment, but it is possible that there was an elevated concentration of N and K in clay substrates that enabled more vigorous growth, although all plants received an input of 'No P' nutrient solution at the beginning of the experiment providing N and K to encourage P limitation. Alternatively, plants in 10% clay may have

benefitted from the increased water holding capacity of that substrate. Clay soils have a higher water holding capacity than sandy soils due to the large surface area created by their fine particulate structure (Mana et al., 2017). Whilst pots received the same amount of water every 2-3 days, and were not droughted, the 0% clay substrate was likely to be less water retentive, and experienced greater evaporation than the 10% clay substrate.

However, the most likely cause of the stark difference in biomass between plants grown in the two substrates is the difference in substrate pH. Peat moss is naturally acidic, with pH commonly between 3.2 and 4.0 due predominantly to cation exchange with the soil solution, in which the moss absorbs cations including calcium and magnesium, whilst releasing H^+ ions into the soil solution (Clymo, 1984). The 0% clay substrate used in this experiment contained a mix of 50% sand and 50% peat moss and had a pH of 4.25. This is a highly acidic pH and may have inadvertently depressed the growth of the spring onion plants. At this pH, plants can suffer from toxicity due to high concentrations of H^+ and Al^{3+} ions in the soil, which can cause root growth inhibition and nutrient deficiencies (Kobayashi et al., 2013). In mineral soils, aluminium toxicity is dominant as the acidic pH liberates free Al^{3+} ions into the soil solution. In organic soils, and in the 0% clay substrate with high organic matter content, toxicity is more likely caused by a high concentration of H^+ ions, and the lack of significant buffering capacity in these soils means that in some cases, pH can fall to below pH 3. In this experiment, the addition of 10% bentonite clay increased the substrate pH to 4.93. It is likely that this was caused by the addition of calcium carbonates, oxides and hydroxides to the substrate as impurities within the clay. When these dissolve in the acidic conditions, free OH^- and HCO_3^- ions react with and remove free H^+ from the soil solution, reducing acidity of the soil solution. Ca^{2+} ions also act to reduce the negative charge of the root plasma membrane, thereby reducing electrostatic attraction of Al^{3+} cations, and can therefore reduce the toxicity caused by high Al^{3+} concentrations in the soil solution (Kobayashi et al., 2013). Furthermore, whilst many plant species are adapted to life in acidic soils, in a study of pH optima of a range of crop species, Islam et al., (1980) found an optimal pH between pH 5.5 and 6.5 at which all plants exhibited near optimal growth. For onion crops in particular, Kane et al., (2006) reported that those grown at pH 6.5 yielded significantly greater edible biomass than

those grown at pH 5.8, indicating that for onions, a near-neutral soil pH is optimal for biomass production.

It is unsurprising that P treatment had a significant effect on total P uptake and plant P concentration, owing to the inclusion of phosphate-P treatment as a positive control. As phosphate is immediately phytoavailable, it was expected that plants receiving this treatment would have a greater P uptake than other treatments, with the potential exception of phytate-fertilised plants treated with phytase. A curious result, however, is the significant two-way interaction between clay treatment and P treatment on total P uptake (Table 5.5, Figure 5.4). This result owes to the seemingly elevated P uptake in phytate treated plants in 0% clay substrate relative to their counterparts in 10% clay substrate (Figure 5.3). The fact that this effect was observed regardless of enzyme treatment is unexpected, as enzyme treated phytate-receiving plants were expected to show greater P concentration than non-enzyme treated plants. A potential explanation could be contamination of the phytate treatment with phytoavailable orthophosphate, though this is unlikely owing to the absence of the same effect in 10% clay substrate. Alternatively, elevated P uptake in these treatments could be caused by microbial degradation of phytate-P in 0% clay. Substrates were not sterilised prior to this experiment in order to avoid a potential negative effect on enzyme activity due to the dissolution of tannins from the sphagnum peat during autoclaving. Tannins such as lignin-like phenolics are found in high concentration in the partially degraded organic matter of peat, and when solubilised are able to inactivate extracellular enzymes (Bengtsson et al., 2018). Therefore, it is possible that phytase-producing microbes are present in the substrates, and are able to exude microbial phytase enzymes to dephosphorylate phytate in the 0% clay substrate. In this substrate, added phytate is assumed to become less strongly bound than in the 10% clay substrate, where the highly charged phytate molecules interact strongly with clay surfaces lending them physical protection from enzymatic degradation (Doolette, 2010). If microbial degradation is indeed occurring, then the physical protection provided in the 10% clay substrate might explain the absence of the same microbial effect in that substrate. Phytase-producing microbes can also exude metabolites such as LMW organic acids that lower the pH within the soil microenvironment, making phytate more readily soluble and creating

more optimal conditions for enzymatic dephosphorylation (Drouillon & Merckx, 2003). However, if there was a microbial phytase effect occurring, this should also be reflected by an increase in phytoavailable phosphate in the substrate. No difference was observed for this parameter between substrates treated with 'No P' and 'Phytate-P' in either clay treatment (Figure 5.5), and there was no significant interaction between clay treatment and P treatment for this factor. Lacking this evidence, and without further work to quantify the naturally occurring microbial phytase activity of the substrates, it cannot be comprehensively concluded that microbial phytases are to blame for the discrepancy in total P uptake in phytate-treated plants.

Substrate phytoavailable P was measured as bicarbonate-extractable P. Both clay treatment and P treatment independently had a significant effect on phytoavailable P, but there was no interaction, and again no enzyme effect (Figure 5.5, Table 5.6). 10% clay substrates had a lower phytoavailable-P across all treatments than 0% clay substrates, which could be due either to greater P uptake by plants in that substrate, and lower P lability due to its binding to the clay surfaces in that substrate. Phosphorus treatment had a significant effect owing to the increased phytoavailable P of the phosphate-P treatment, but contrary to the hypothesis that enzyme treatment would increase phytoavailable P, no increase was found in phytate-P treated plants that received phytase compared to those without enzyme, in either substrate.

Finally, there was a significant overall effect of clay treatment and P treatment on substrate total P (Figure 5.6, Table 5.7). However, these effects are easily explained, as despite being balanced for phytoavailable P, 10% clay substrates had a greater total P content at the beginning of the experiment due to P contamination within the clay. This has translated to greater total P content at the end of the experiment across all treatments within the 10% clay substrate. Phosphate-P and phytate-P treated substrates also had greater total P than those receiving the 'No P' treatment, which is to be expected.

5.5.2 Effect of Clay and Enzyme in phytate-treated plants

An effect of enzyme treatment would only be expected to occur in substrates that have been fertilised with phytate. In order to assess the enzyme effect in these substrates

alone, a series of two-way ANOVAs were run to test for an interaction between clay and enzyme, and a series of t-tests were run within each clay treatment to test for differences caused by the enzyme alone.

The results of a series of two-way ANOVAs are presented in Table 5.3 A-E. For all parameters measured, there was an independent significant effect of clay treatment, but no independent significant effect of enzyme treatment, apart from for substrate total P. However, there was a significant interaction between clay and enzyme treatment on the biomass of phytate treated plants (Table 5.3 A), meaning that there was an effect of enzyme in one substrate that was not replicated in the other. Further investigation was carried out using unpaired t-tests on phytate treated plants in each substrate, revealing that in the 10% clay substrate, there was a significant difference in biomass between enzyme and no-enzyme treatments, but rather surprisingly it was the plants receiving no enzyme that had a greater biomass than those that did receive phytase (Figure 5.2). It is unclear why this is the case, as any enzyme effect would be expected to increase biomass via the release of phytoavailable P, rather than negatively affect growth. In the same plants, there was no significant difference in plant P uptake (Figure 5.3), but there was a significant difference in plant P concentration, with enzyme-treated plants having a greater P concentration than non-enzyme treated plants (Figure 5.4; unpaired t-test, $p<0.05$). Due to the lack of any difference in total P uptake, rather than an enzyme effect here, it's probable that the difference in P concentration is instead caused by the difference in total biomass between these plants. In other words, enzyme treated plants have a greater P concentration because they have a smaller biomass than non-enzyme plants yet absorbed the same amount of P from the soil, but the reason for this difference in biomass remains unclear.

In this experiment, it was hypothesized that the application of phytase enzyme to phytate-treated substrates would result in its dephosphorylation, causing a modest increase in plant biomass, P uptake, and plant P concentration, and increasing phytoavailable P levels in substrates. This effect was expected to be depressed or absent in the 10% clay substrate due to the potential for adsorption of both phytate and phytase to clay surfaces, inhibiting dephosphorylation. However, the only treatment that exhibited the expected effect was that of plant P concentration in 10% clay

substrate (Figure 5.4), and for the reasons stated above, this is likely to be due to the difference in biomass, rather than any enzyme effect, as there was no difference in P uptake from the substrate, and no increase in bioavailable substrate P resulting from the enzyme treatment.

In phytate-treated plants, both clay type and enzyme addition had a significant effect on substrate total P (Table 5.3 E). In Figure 5.6 there is a trend for increased total P in phytate-treated plants that received phytase. However, in both substrates, no significant difference was found between enzyme and non-enzyme treated plants in either substrates when analysed by unpaired t-tests, likely due to the low replication. The trend for increased substrate total P in enzyme-treated plants is unexpected however, as if the enzyme was dephosphorylating phytate, then phytoavailable P in the soil should be increased and P uptake from the soil should be increased, which would result in a reduction in overall substrate total P.

Overall, these results suggest that simply adding a soluble commercial phytase to the substrates did not result in significant dephosphorylation of phytate and subsequent release of phytoavailable phosphate, regardless of the substrate clay content. Two main factors govern the activity of the phytase enzyme in substrates and soil. The first is the availability of phytate for enzymatic dephosphorylation, that is, whether the phytate is free or easily mobilised in soil solution or is strongly bound within the substrate matrix and therefore unavailable for dephosphorylation. The second is the favourability of the complex substrate environment for the persistence and performance of the active enzyme. For example, phytase enzymes may also become adsorbed to surfaces in the substrate, can be inhibited by interactions with organic components like lignin and tannins in the soil solution, or can be degraded by microbes and protease enzymes. The fact that no evidence of phytate dephosphorylation has been found in this experiment likely owes to one or both of these factors, and these are discussed further in the following sections.

5.5.3 Phytate adsorption

With a high charge density from its six phosphate moieties, phytate can interact strongly with the soil solid phase via surface complexation with organic matter, metal cations,

and clay minerals. McKercher & Anderson, (1989) showed that the adsorption of phytate is stronger than that of orthophosphate, and that even the adsorption of inositol trisphosphate was greater, indicating that the strength of adsorption is related to the degree of phosphorylation. In this experiment, substrates were designed to differ in phytate-binding capacity due to the inclusion of a substrate containing 10% clay in place of quartz sand. Clays have a fine particulate structure, with an average particle diameter of 2μm and thus have a very high surface area in soils (Ulusoy et al., 2003). The bentonite clay used in this experiment is dominated by montmorillonite clay minerals, which are common in soils and sediments (Grim & Kulbicki, 1961). Clays are generally layered structures, and bentonite in particular is made up of octahedral sheets of aluminium, sandwiched between tetrahedral sheets of silica (Grim & Kulbicki, 1961; Hebbar et al., 2014). The silicate layers in the structure give bentonite an overall negative charge, but this is offset by the association of exchangeable cations with the clay surfaces (Hebbar et al., 2014). Phytate and orthophosphate, carrying negative charges, can form complexes with unsaturated aluminium cations at the edge of the octahedral sheets via electrostatic interaction (Shang et al., 2013), and also adsorb to specific exchange spots that have unbalanced charges (e.g. excess aluminium) within the lattice structure (Ulusoy et al., 2003). As phytate carries six phosphate moieties, a single molecule can form multiple interactions, which explains its greater adsorption capacity.

As well as clays, phytate can adsorb strongly to iron and aluminium oxides in the soil via ligand exchange with the H_2O and ^-OH groups on the surface of minerals (Celi & Barberis, 2006). The interaction with these metal oxides involves multiple phosphate groups, and those that aren't bound impart a strong negative charge on the complex, which can impede the approach of other molecules by electrostatic repulsion (Shang et al., 1990). The abundance of calcium in the soil also has a major impact on phytate immobilisation, as phytate can both adsorb to, and precipitate with calcium to form insoluble salts (Celi et al., 2000). Finally, phytates in soils can be retained by organic matter via direct adsorption to the surface, or via polyvalent bridging cations to form organic matter-metal-phytate complexes (Celi & Barberis, 2006). The association of P with metal cations at the humic surface is similar to the association of P with Al and Fe oxides, whereby the

orthophosphate anion replaces ^{-}OH or H_2O groups bound to the cations via ligand exchange (Gerke, 2010).

In this experiment, to make the substrates more representative of real soil systems, phytate-P nutrient solution was applied three days prior to the phytase treatment to allow the stabilisation and interaction of phytate within the substrate to occur, and phytate was expected to form stronger associations in 10% clay substrates due to the increased adsorptive capacity provided by the clay. However, it's possible that during this stabilisation period, phytate has become largely removed from the substrate solution via surface interactions in both substrates, and hence no effect of enzyme application was observed in either. A study by Gujar et al., (2013) reported a 76% increase in P assimilation of wheat plants compared to controls when phytate fertilized soils were treated with phytase, but a caveat of this work is that phytase was applied to soil immediately after phytate application, meaning that the potential limitations of soil-phytate interactions on the reaction were much reduced, a situation that does not reflect natural soil dynamics. In contrast to that study, it's possible that in this experiment, much of the phytate applied in the nutrient solution has become bound to the organic matter in the peat fraction of the 0% clay substrate, and the enzyme is therefore unable commence dephosphorylation.

Phytase-producing microbes in soil environments are able to overcome this phytate limitation to a degree via the exudation of LMW organic acids into the soil environment (Huang et al., 2003), which can remobilise bound phytate into the soil solution via the exchange of their carboxyl functional groups with adsorbed phosphate moieties (Waithaisong et al., 2015). LMW organic acids can also release phosphate groups from organic matter by dissolving humic molecules and by competing for sorption sites with phosphate groups via ligand exchange, and P is more easily mobilised from its interaction with organic matter than it is with metal oxides (Gerke, 2010). With the application of phytase in this experiment, there was no concurrent manipulation of LMW organic acid concentration, so any phytate that is adsorbed is unlikely to be efficiently dephosphorylated in the presence of the enzyme alone.

5.5.4 Phytase enzymes in soil & substrate matrices

Enzymes show an affinity for the interface between soil solid and solution phases due to both intermolecular and intramolecular forces generated by the structural properties of their complex amino acid chains (Quiquampoix et al., 2002), and these properties also make them susceptible to adsorption to soil surfaces. As with phytate, the large surface area of clays, and heterogenous surfaces of organic matter are likely to be the main surfaces with which extracellular enzymes associate.

Clay-enzyme interactions can take many forms. Firstly, strong electrostatic interactions can occur between hydroxyl groups at the edges of clays and charged groups in the amino acid side chains of enzymes (Quiquampoix et al., 2002). Additionally, weaker van der Waals interactions may occur when enzymes approach clay molecules, in which the charge distribution of the molecules can vary to produce polarity and net electrostatic attraction between the two (Quiquampoix et al., 2002). Hydrophobic interactions may also provide strong adsorption of proteins to clays despite the hydrophilic nature of clay surfaces. The exchange of hydrophilic cations that are associated with the clay surface exposes the hydrophobic silica sheet, with which the hydrophobic amino acid groups can thus interact (Quiquampoix et al., 2002). Enzymes also interact with soil organic matter and humic substances, and the heterogenous nature of organic matter can lend itself to adsorption by providing an abundance of macropores in which enzymes can become embedded (Yang & Chen, 2017). Interactions may occur via hydrogen bonding (George et al., 2006), for example between acidic protons in humic tannins and polar amino acid side chains (McRae et al., 2010), or alternatively via the formation of strong and irreversible covalent bonds (George et al., 2006).

Adsorption can have negative consequences for enzyme activity due to the removal of the enzyme from the soil solution, and enzymes can subsequently become deactivated and denatured. Adsorption can, however, also provide protection for enzymes within soil, maintaining their activity and longevity in the soil environment (Naidja et al., 2000). George et al., (2005a) assessed the behaviour of an *Aspergillus niger* phytase when applied to three soils with different sorption capacities. When added to a soil suspension, phytase activity was largely lost within ten minutes in all soil types, whereas activity was maintained in non-soil controls, suggesting that phytase was rapidly inactivated by soil constituents. However, phytase activity was found to be recoverable

from the soil solid phase, and actually decayed at a slower rate than in non-soil controls. Enzymes can be metabolised by microbes as nutrient sources, and adsorption can provide some protection against this and the action of proteases. Degradation involves conformational change of the enzyme, and takes place at exposed amino acid structures on the enzyme surface, so adsorption provides some protection for the enzyme by limiting the access of degradative substances via steric hinderance (George et al., 2006). Interestingly, different phytase enzymes exhibit varying levels of susceptibility to microbial degradation, as George et al., (2007) demonstrated when a *Peniophora lycii* phytase was active for longer in sterile soil compared to unsterile soil, whereas an *Aspergillus niger* phytase was unaffected by microbial presence.

In this experiment, any effect of enzyme addition was expected to be depressed in 10% clay substrate, due to the greater surface area and strong adsorptive properties of the clay. This adsorption to mineral soil surfaces can cause conformational changes in the enzyme, leading to unfolding of the protein and deactivation of the enzyme (George et al., 2005a; Leprince & Quiquampoix, 1996). However, no effect of enzyme addition was found in either soil, so phytase could be becoming readily immobilised in the organic matter of the 0% clay substrate too. Yang & Chen, (2017) measured the distribution of phytase activity in soil and found that the phytase-sorption capacity of soils containing both clay and organic matter was 2-5 times greater than the same soils following the removal of clay. However, their results also indicated that the adsorptive capacity of organic matter alone was greater than that of clay alone. This stronger adsorption has been attributed to the greater heterogeneity of organic matter surfaces and the relative abundance of macropores in which enzymes can embed (Yang & Chen, 2017; Naidja et al., 2000). It therefore stands to reason that in this experiment, phytase that was added to the substrates could have become adsorbed by the organic matter of the peat fraction, which made up 50% by volume in each substrate. Despite the increased adsorptive capacity of the combined organic matter and clay mixture in 10% clay substrate, the adsorptive capacity of 0% clay substrate may have been sufficient to bind the phytase added, masking any effect of clay content on enzyme activity.

The phytase enzyme used in this experiment was a commercially available phytase isolated from the enterobacterium *Citrobacter braakii*, and expressed in *Aspergillus*

oryzae, and as such is optimal for use in the digestive tract of monogastric livestock (Pontoppidan et al., 2012). The resilience of phytase enzymes to adsorption in soil matrices seems to be dependent on their natural functional environments. For example, an intracellular wheat germ phytase was found to be completely inhibited by adsorption to clay, whereas two extracellular phytases from *Aspergillus niger* and *Hebeloma cylindrosporum* were able to retain catalytic properties, regardless of their degree of adsorption (Matumoto-Pintro & Quiquampoix, 1997). Whilst the *C. braakii* phytase used in this experiment is an extracellular enzyme, its properties are optimal for its survival in the gastrointestinal tract of monogastric animals, a quite different chemical environment to soils. The active pH range of the *C. braakii* phytase is broad, between pH 2 - 6, but is optimal between pH 3 - 4.5 (Menezes-Blackburn et al., 2015), which is close to the pH range measured for both substrates (0% clay: pH 4.25; 10% clay: pH 4.93). However, many possible factors in the substrate, such as the adsorptive capacity of the substrate constituents, the presence of inhibitory tannins and metal cations, and the susceptibility of the enzyme to degradation by microbes and protease enzymes may have all negatively impacted the ability of this phytase enzyme in the catalysis of phytate degradation.

5.6 Conclusions

This experiment attempted to assess the performance of a commercially available phytase enzyme on the provision of phytoavailable phosphate from phytate in model soil substrates that varied in adsorptive capacity. However, no effect of enzyme treatment was found on plant performance, P uptake or substrate available P. There are many possible reasons for this result, none of which are mutually exclusive. Firstly, the highly acidic pH of the 0% clay substrate likely depressed growth of these plants when compared to those grown in 10% clay, which benefitted from a less acidic substrate pH due to the addition of calcium within the clay. It's quite possible that this growth depression masked any potential advantage these plants had over their 10% clay counterparts, had there been an effect of clay content on the mobility of phytate or the enzyme in the substrate solution. In follow-up experiments, the pH of the 0% clay substrate could be raised via the addition of lime to match the pH of the 10% clay substrate which should serve to alleviate the inhibitory effect on 0% clay plants.

Phytate may have been removed from the substrate solution via adsorption or precipitation interactions with organic matter, clay minerals, and metal cations. The enzyme may also have experienced adsorption, which may have caused temporary or destructive inactivation. Alternatively, the enzyme may have experienced inhibition from substrate constituents including tannins or metal cations, or the chemical environment within the substrates may simply have not been conducive to enzyme catalysis of phytate dephosphorylation, due to the enzyme being optimal for use in the gastrointestinal tract of monogastric livestock. Taken together, it can be concluded that the simple addition of this commercial extracellular phytase enzyme is ineffective for phytate degradation in this model substrate environment, which is a simple matrix in comparison to the complex heterogenous nature of soil.

Plant roots and microbes exude LMW organic acids alongside phosphatase enzymes in response to P limitation, with LMW organic acids increasing phytate mobilisation via ligand exchange with the soil solid phase (Drouillon & Merckx, 2003). In future experiments, it would be valuable to investigate whether the addition of LMW organic acids to substrates alongside phytase would benefit dephosphorylation by remobilising

phytate into the substrate solution phase. If the enzyme is also becoming adsorbed, the addition of LMW organic acids may also improve enzyme solubility, as has been demonstrated with acid phosphatase enzymes (Huang et al., 2003). Adjustment of the substrate pH may also positively affect phytase solubility, as George et al., (2005a) suggested that the slightly less acidic microenvironment of rhizosphere soil was able to maintain phytase activity in solution due to changes in the electrostatic interactions between proteins and soil solids.

Finally, widely available and cheaply produced commercially available phytase enzymes are predominantly used in the gastrointestinal tract of livestock, and as such are likely sub-optimal for use in soil or substrate environments. Future work may benefit from the use of enzyme isolates from soil microbes, which are likely to exhibit more suitable properties for performance in soils.

6: General Discussion

6.1 Phosphorus Sustainability

P is increasingly recognised as a scarce resource and one which is used inefficiently in agricultural systems. There is approximately 259 years of phosphate rock supply remaining, but demand is increasing annually, and this estimate has been revised down from approximately 300 years in 2016 due to increasing demand (Blackwell et al., 2019). Morocco alone controls 71% of the global phosphate rock reserves (Jasinski, 2019), and this monopoly raises concerns considering recent geopolitical instability in the region, and the fact that much of these reserves are located in Western Sahara, which Morocco has illegally occupied since the late 20th century (Blackwell et al., 2019).

Current anthropogenic use of P is a largely linear process (Figure 6.1A), with vast amounts of chemical fertiliser P spread to land each year. Depending on the type of soil and its health, it is estimated that just 8% of this fertiliser P is absorbed by crops (Blackwell et al., 2019), with the remainder stabilised in soil or lost to water bodies, contributing to eutrophication and hypoxia (Cordell et al., 2009). Once crops are harvested and consumed, much of the absorbed P passes into animal manure and human excreta, with a calculation based on P flows developed by Cordell et al., (2009) approximating that 54% of P in manure and excreta is lost to the wider environment in landfill, non-arable soils or water bodies every year. These P losses, along with the stabilisation of P in soil in plant-unavailable forms, result in the insufficient replenishment of soils with P, meaning that the fraction of freely dissolved phytoavailable orthophosphate is depleted annually, and requires further inputs of fertiliser P to maintain subsequent crop yields.

In response to the potential scarcity of P and the effect of its inefficient use on future food security, much work over the past decade has sought to develop strategies to close the anthropogenic P cycle, to recycle and reuse P resources, and reduce the requirement for chemical P inputs in order to maintain or increase yields. A schematic is presented in Figure 6.1B envisaging a more sustainable anthropogenic P cycle. Such a system would involve refinement of chemical fertiliser dosing, with a greater understanding of the P requirements of specific crops in order to feed the plant, rather than the soil (Blackwell

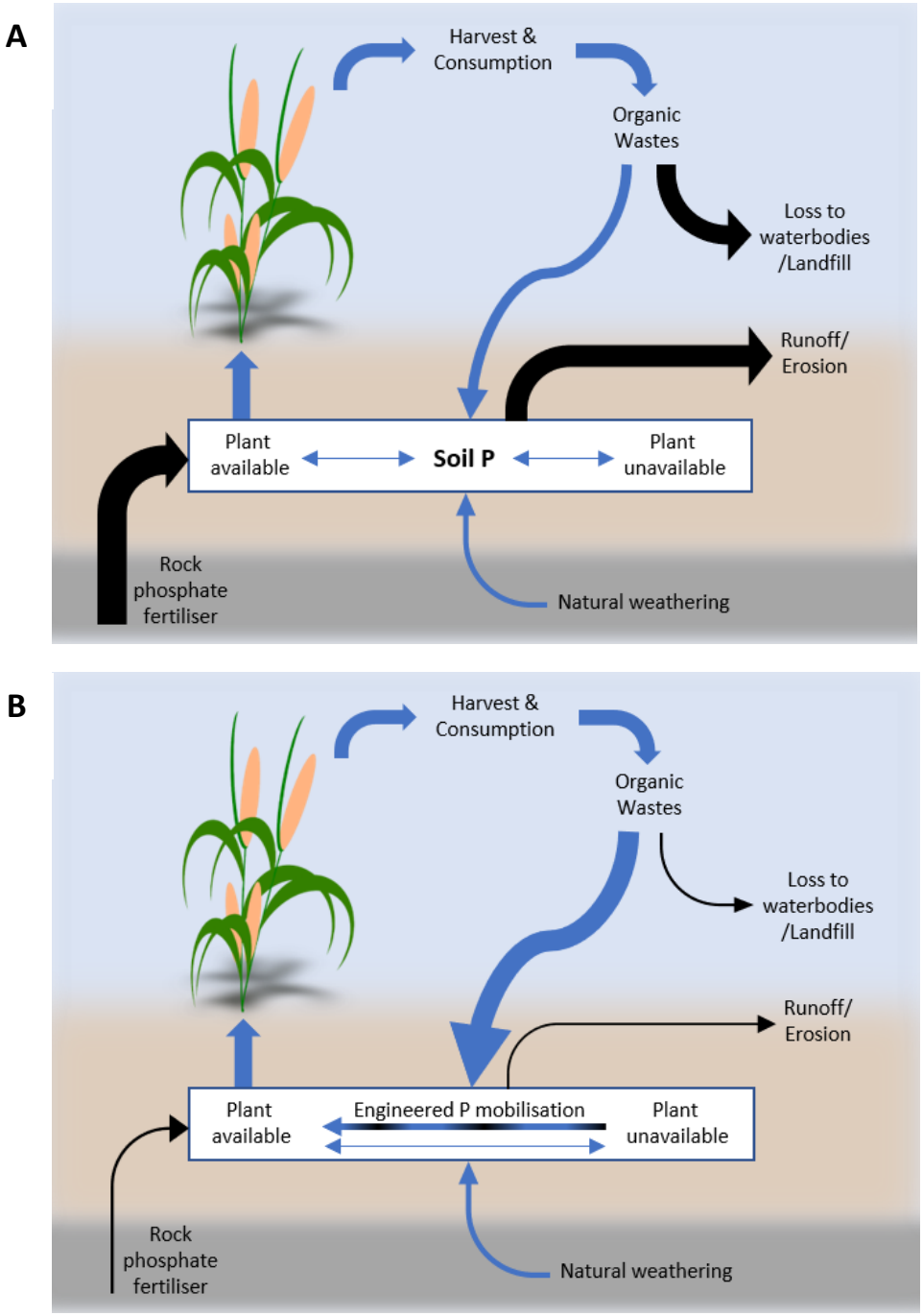

Figure 6.1: Current and future anthropogenic P cycles. Black arrows represent anthropogenic flows of P, Blue arrows represent natural flows of P. **A:** The current linearised anthropogenic P cycle. Large amounts of phosphate fertiliser are spread on land to increase crop harvests, with large amounts of P permanently lost from the cycle to the wider environment. **B:** A more efficient and sustainable anthropogenic P cycle. Small amounts of phosphate fertiliser are spread to land based on optimal crop requirements. Losses after consumption are minimised with nutrients largely returned to arable land. Soil management practices are improved to maintain soil health and minimise soil erosion. A greater understanding of microbial P cycling and engineering of rhizosphere processes enable greater mineralisation of accumulated unavailable P to provide phytoavailable phosphate.

et al., 2019). Stemming the loss of organic wastes such as manure and excreta, and also food waste and animal by-products (Darch et al., 2019) to the wider environment and instead directing it to P deficient soils, would retain P within the food production cycle and replenish soils with other valuable nutrients and organic materials, simultaneously improving soil health and reducing losses by soil erosion. Finally, a greater understanding of rhizosphere soil biochemical and physical processes will enable the engineering and manipulation of natural mineralisation processes to increase the mobilisation of stabilised soil P to phytoavailable dissolved inorganic forms, further reducing the requirement for inputs of exogenous chemical P fertilisers (Figure 6.1B).

This thesis focussed on the organic P compound phytate, which is a compound synthesised in plants as the main P storage compound in grains (Gerke, 2015). Phytate is not efficiently digested by humans or other monogastric animals and so can pass into excreta, which can then enter the soil in organic amendments. However, phytate is not available for uptake by plants, and due to its high recalcitrance in the soil, it is often the most abundant organic P compound identified by ^{31}P NMR in soil extracts (Jørgensen et al., 2015). Its widespread presence in organic amendments and soils therefore makes phytate a prime candidate for strategies that aim to remobilise phytoavailable phosphate from stabilised P for crops.

In the UK, the majority of anaerobically digested sewage sludge is applied to agricultural land (DEFRA, 2012), but whether phytate, which can make up 34-54% of the P content in human faeces (Joung et al., 2007), can survive the sludge treatment process to comprise a significant proportion of sludge total P was unclear until now. When in the soil, the effect of land-use history on the concentration of phytate and its tendency to accumulate is not fully understood. If phytate does accumulate, then there is scope for the use of biofertilisation strategies, namely the use of phytase enzymes, to drive the mobilisation and use of phytate-P by crops, which could reduce the need for the application of chemical phosphate fertilisers, improving the efficiency of P use and sustainability. This General Discussion will bring together the main findings presented in this thesis to address the following research questions:

1. *Is phytate present in sewage sludge, does it persist through the stages of a modern advanced anaerobic digestion sludge treatment process, and does it constitute a substantial fraction of total P in the final sludge 'cake' that is spread on land?*
2. *How does the land-use history of agricultural and grassland soils affect the concentrations of phytate in soil? Does phytate accumulate in a previously arable soil that has been converted to a pen housing monogastric swine?*
3. *Can a commercially available feed-supplement phytase enzyme be used to release phytoavailable phosphate from phytate in a simple soil substrate, and how does clay content affect this ability?*

6.2 Evaluating and optimising the available analytical methods for quantifying different chemical species of P

While solution ^{31}P NMR has over the past two decades become the field standard method for P analysis in environmental samples, and has significantly advanced our knowledge of P speciation and quantification in these samples (Cade-Menun & Liu, 2014), this method does have limitations. ^{31}P NMR can suffer from issues of sensitivity and resolution, particularly if P forms are present in low concentrations, which results in long analysis times to increase signal to noise ratios, and means that these less abundant P forms are often overlooked. With this in mind, there is growing interest in the development of more sensitive techniques that can be used to identify and quantify these compounds, which include the lower inositol phosphates (IP5-IP1) that are produced by the enzymatic hydrolysis of phosphate from phytate. In Chapter 2, the use of Electrospray ionisation time-of-flight Mass Spectrometry (ESI-ToF-MS) was investigated to assess its value in the analysis of phytate and the lower IPs in mixed samples. Whilst this method was able to detect lower IPs at their specific m/z ratios, significant dissociation of phytate was encountered during ESI that produced fragment ions sharing coincidental m/z ratios with true lower IPs, making their quantitation impossible. Other papers have tried to optimise the ESI step by varying either the cone voltage (Cooper et al., 2006), or source voltage (McIntyre et al., 2017), and in Chapter 2, fragmentation was indeed decreased by optimisation of both, but it could not be

eliminated. It is apparent that fragmentation is likely a universal feature of phytate analysis in ESI-ToF-MS, which therefore precludes the simultaneous analysis of multiple inositol phosphates in a sample. However, if IPs can be separated prior to their analysis by mass spectrometry, then any appearance of peaks at coincidental m/z ratios with lower IPs could be identified as fragment ions with confidence. A very recent paper by McIntyre et al., (2019) has demonstrated the quantification of phytate in NaOH-EDTA extracts of soil samples in this way, by purifying phytate using anion-exchange chromatography and detection with ESI-ToF MS. They found good correlation between quantification with their method and with ^{31}P NMR, along with an improved detection limit of 0.7mg P kg^{-1} relative to >10mg P kg^{-1} with ^{31}P NMR. Whether this method can be extended to the quantification of lower IPs remains to be seen, but this work highlights the promise of Mass Spectrometry for the sensitive analysis of P in environmental samples.

Solution ^{31}P NMR analysis was instead used to quantify phytate and orthophosphate in sludge and soil extracts in Chapters 3 & 4. Over 16,000 scans were used to improve the signal to noise ratio of spectra, so a relaxation delay time of 1s was necessary to keep the analysis time to a manageable 8 hours. However, when using a 1 second relaxation delay time, P nuclei within different compounds in the sample are unable to relax fully to thermal equilibrium after pulsing, and relax to different degrees, with P nuclei in larger molecules (e.g. phytate) able to relax to a greater degree than those in small molecules (e.g. orthophosphate). This means that the peaks generated in the spectra do not quantitatively represent their respective compounds, with smaller compounds underestimated relative to larger (Cade-Menun & Liu, 2014). Using long relaxation delay times can ensure that all P relaxes to thermal equilibrium, but this can lead to long analysis times. For example, McLaren et al., (2015) used relaxation delay times of up to 36s between scans of a soil extract to permit full orthophosphate relaxation, resulting in analysis times reaching 32 hours. However, such long analysis time makes ^{31}P NMR a low throughput and expensive procedure and would not have been suitable for use in this project. Instead, to ensure accurate quantitative analysis of soil extracts when using a low, 1 second relaxation time, a preliminary analysis building upon on the procedure developed by Robertson, (2018) was carried out to calculate a correction factor for

underestimated peaks. This involved measuring the peaks of a sample spiked with orthophosphate and phytate over a range of increasing relaxation times to calculate the maximum peak area that could be achieved when fully relaxed. Peaks measured at 1s delay times could be then scaled-up to these ratios to correct for the insufficient signals generated. This procedure was carried out in both Chapters 3 & 4 and was verified in each using a spike recovery assay. In sludge, using this method, an average recovery of 103.78 ± 2.14% and 104.77 ± 5.17% was achieved for spiked orthophosphate and spiked phytate respectively. In soils, an average recovery of 107.8 ± 5.1% and 94.6 ± 10.4% was achieved for spiked orthophosphate and spiked phytate respectively, suggesting that this method enables an increased signal to noise ratio without loss of accuracy. This method is uncommon in experiments involving solution ^{31}P NMR, but as was shown in this thesis, it is useful for experiments which aim to quantify a small number of compounds to a high degree of accuracy, and will be particularly advantageous for the analysis of 'dirty' samples such as soil and sludge which often suffer from poor spectral resolution. The increase in signal to noise ratio that is produced by analysing a sample over a very high number of short scans results in a high resolution ^{31}P NMR spectrum with clearly defined peaks, which when interpreted with the pre-determined correction factor, allows highly accurate quantification of specific compounds within a shorter analysis time.

6.3 Phytate survives anaerobic sludge treatment

As part of a closed anthropogenic P cycle, P contained in organic wastes should be efficiently recycled back to the soil to stem the leakage of P and its permanent loss to the wider environment. There is a wealth of work that has studied and quantified the P forms in manure (Cade-Menun, 2005; Giles & Cade-Menun, 2014; Cade-Menun, 2011), and this is widely accepted as a source of nutrients for the soil, but less work has been carried out on human waste. With phytate-P making up between 24-54% of human faecal P (Joung et al., 2007), it was hypothesized that phytate would make up a large proportion of P in sewage sludge prior to its treatment. In the UK, human excreta is often treated in advanced wastewater treatment processes, which generate large amounts of sludge that undergo anaerobic digestion in order to reduce its mass, and extract energy in the form of methane. Since the enforcement of the EU Urban Wastewater Treatment

Directive in 1999, the vast majority of treated sludge is returned to arable land (DEFRA, 2012). However, the P speciation and contribution of phytate to sludge P is not well studied. Anaerobically digested sludge has been shown to be dominated by orthophosphate, and there is some evidence that phytate persists through digestion (Annaheim et al., 2015; Smith et al., 2006). If phytate is also abundant, then when applied to soil, it may be unavailable for absorption by plants and may preferentially accumulate, representing somewhat of a dead-end for the cycling of P.

In Chapter 3, using solution ^{31}P NMR it was shown that phytate is present in sewage sludge, and persists throughout an advanced anaerobic sludge treatment process to make up 4.5% of total P in the final dewatered sewage sludge cake. The analysis of total P, orthophosphate and phytate concentrations in Chapter 3 provides a clear picture of the overall P dynamics through the system. Total P becomes successively more concentrated through the process, and is most concentrated in digested sludge, before falling slightly with dewatering in the final cake. Orthophosphate P is by far the most dominant P form throughout the process, making up close to 80% of total P throughout, whilst the proportion of phytate remains relatively stable, making up an average 4.7% of total P throughout. The apparent survival of phytate in this process is supported by the work of Smith et al., (2006) and Annaheim et al., (2015), who found phytate in anaerobically digested sewage sludges at approximately 10% of total P. The lower proportion of phytate in this study is likely representative of lower phytate levels in the wastewater solids at the beginning of the process, as there was no major loss of phytate at any treatment stage. Li et al., (2019) measured P speciation in sludge before and after anaerobic digestion. Interestingly, they found that orthophosphate monoesters were completely lost during anaerobic digestion. Whilst phytate was not specifically measured, it may be that phytate was absent or at very low concentrations in their samples, with other monoesters being eliminated during the digestion process. Furthermore, it is possible that the sensitivity and resolution of their spectra were not sufficient for phytate identification and quantification as signal to noise ratios are very low.

The finding that phytate persists through anaerobic sludge treatment is important considering that according to DEFRA, (2012) 79% of sludge is spread on land in the UK.

By this estimate, and the concentration of phytate found in cake in Chapter 3, 947 tonnes of phytate-P is spread on UK soil annually from sludge application. That is equivalent to 1.15% of the 81,968 tonnes of P applied to UK soils as chemical fertilisers in 2017 (FAO, 2019). Whilst this seems an insignificant amount, it is important due to the behaviour of phytate in the soil. When phytate is applied to soils, the high charge density afforded to the molecule by its six phosphate groups means that it has a tendency to become preferentially stabilised in soil and can accumulate by forming strong interactions with soil P sorption sites (Menezes-Blackburn et al., 2013). Indeed, it was shown in Chapter 4 that a previously arable soil that had been converted to a pig pen, and thus received large inputs of monogastric pig manure, had a phytate concentration almost six times greater than that of a nearby permanently arable soil. This recalcitrance has negative impacts, because the saturation of P-sorption sites in the soil by phytate can lead to decreased retention of P applied to soils in fertilisers (Sharpley, 1995; Kleinman, 2017), which in turn can lead to leaching of P into water bodies and eutrophication. Furthermore, the application of phytate to soil in this way represents an inefficient use of P resources, as P is applied in a form unavailable for uptake by crops. A potential approach to alleviating this issue could be to apply an intervention step following sludge digestion and prior to its land application, in which phytase enzymes could be used to dephosphorylate phytate to eliminate its application to soil. However, there are numerous obstacles to this approach, the first being that a large part of the P in digested sludge is adsorbed within the sludge solids with metals such as aluminium and iron, or is precipitated with calcium (Shober et al., 2006; Ajiboye et al., 2007), and is therefore likely to be poorly available as a substrate for a phytase enzyme. This idea is supported in Chapter 3 by the fact that very little phytate was lost from digested sludge during its dewatering, indicating that little phytate was dissolved in solution (Figure 3.12). Secondly, the chemical environment within sludge is likely to be unfavourable for phytase activity. For example, Igamnazarov et al., (1999) showed that 2mM concentrations of Cu^{2+} and Fe^{3+} reduced the activity of *Bacterium* sp. phytase to 8% and 29% of their initial activity respectively. Heavy metals in the digested sludge are present in high concentrations due to the reduction of organic mass during AD (Gerardi, 2003), so these may inhibit any phytase enzyme that is applied. A further consideration is whether the benefits of mobilising such a small fraction of P, when 83%

of P is already present as orthophosphate, would outweigh the cost of both the phytase enzyme and the infrastructure that would be required for its use. Finally, there is the question of who would bear these costs, as farmers are unlikely to be willing to pay for this intervention when the orthophosphate concentration in sludge is already so high. Overall, if the concentration of phytate in sludge measured in Chapter 3 is representative of concentrations throughout the UK, then such an intervention is unlikely to be feasible, meaning that this phytate fraction is destined to be applied to soils. Further work to measure phytate concentrations in both pre- and post-AD sludges at multiple locations would be useful to measure the locational variation in sludge phytate concentration, and whether it varies according to the size of the population served by the WWTP. For example, it may be the case that phytate concentrations are greater in WWTPs that serve a greater proportion of households relative to industry, in which case, a phytase-based intervention may prove more valuable in certain situations than in others. Furthermore, despite the potentially unfavourable conditions for phytase-mediated dephosphorylation of phytate within the sludge treatment process, a lab-based experiment, in which an external commercial phytase enzyme or phytase-producing microbe was introduced to sludge in a bench-top AD treatment process, has not been carried out before, and may yet have an effect on phytate concentrations at the end of the process.

6.4 Land use has a major effect on soil P and phytate concentrations

The accumulation of phytate in the soil is not universal and is likely to be influenced by many factors. For example, the application of phytate to calcareous soils in solution (Doolette et al., 2010) and in manure (Leytem et al., 2006) did not result in its preferential accumulation in soil over a number of weeks, whereas in other soils, manure applications have been shown to increase phytate concentrations (Gatiboni & Brunetto, 2013; Hansen et al., 2004). In Chapter 4, phytate and orthophosphate concentrations were measured in a range of agricultural and grassland soils to assess the effect of land-use on P speciation and phytate accumulation. Agricultural soils, which included a permanently arable soil, a pasture soil and a pig pen soil, were dominated by orthophosphate, whereas grassland soils were dominated by the 'residual P', which was P other than orthophosphate or phytate. These differences were mirrored by soil

organic matter content, which made up between 29.5 - 36% of grassland soil, but only between 4.3 – 12.4% of agricultural soils.

Among the agricultural soils, arable soils surprisingly had the lowest total P concentration, which increased in pasture soil, and was greatest in the pig pen soil. Arable soil also had the lowest phytate concentration of all soils, which is symptomatic of its intensive use over the past 20 years. The soil has received only chemical fertiliser inputs, and is harvested and cultivated regularly, disrupting the natural cycling of P. Pasture soil was expected to contain a greater proportion of organic P forms, including phytate. However, it was similarly dominated by orthophosphate, which made up almost 75% of total P in this soil, with phytate making up 6.3%. The most interesting finding was that of the pig pen soil. This soil had been a permanently arable soil prior to its conversion to a pig pen three years prior to sampling, in which time, it had received no chemical fertilisers, experienced no cultivation, and produced no crops for harvest. Receiving nutrient inputs only from pig manure, this soil had the greatest total P content, along with the greatest orthophosphate and phytate content of all soils analysed. The pig pen soil contained almost six-fold more phytate than the permanently arable soil. Pigs are monogastric animals and cannot produce their own phytase enzymes to break down phytate in the gut, but do harbour phytase-producing microflora in their hindgut that degrade phytate to a degree (Dersjant-Li et al., 2015). Liang et al., (2018) found pig manure to contain a P concentration of 10,400 µg P g^{-1}, made up of 90.7% orthophosphate-P, and 8.5% phytate-P. Whilst it cannot be unequivocally confirmed, it is highly likely that prior to its conversion, P content of this soil more closely resembled that of the arable soil, and therefore the current high phytate content of the pig pen soil results from an accumulation of phytate from manure inputs since its conversion. Whether this accumulation is representative of what happens to phytate applied to arable soil remains to be seen. Annaheim et al., (2015) found no evidence of accumulation of organic P forms including phytate from 62 years of manure and dried sewage sludge applications to conventionally managed arable soil. Whilst Chapter 4 may indicate accumulation of phytate in the pig pen, this soil is no longer subject to the intensive cultivation and crop harvesting of an arable soil, so may favour accumulation over degradation. Further experiments using real human sludge on agricultural soils

would provide more conclusive evidence for the accumulation of phytate following soil amendment than was possible in Chapter 4. Ideally, these experiments would assess the changing P dynamics following sludge application over both the short-term, and over a period of years. Whilst pig manure was successfully used as a proxy in this thesis, there may be key differences between the mobility of P in manure and AD sludge matrices, and these could have major impacts on the ability of plants to access any added P. Furthermore, long term studies with AD sludge would enable further research on the unintended consequences of sludge application, such as the co-addition of pharmaceutical compounds or heavy metal contaminants, which at high concentrations can be toxic to microbial populations, and can be absorbed and accumulated by plants from where they may enter the food chain (Haynes et al., 2009).

6.5 Phytase catalytic activity is lost when applied directly to substrate

Despite the uncertainty around the factors that affect phytate accumulation, it remains true that phytate is often identified in ^{31}P NMR as the most abundant organic P compound in soil extracts (Cade-Menun et al., 2010; Liu et al., 2018). In order to reduce the requirement for chemical P fertiliser applications in sustainable systems, techniques will be necessary to increase the mineralisation of soil P that is stabilised and thus unavailable for absorption by plants. Many of the strategies in development involve the genetic manipulation of plants to improve the exudation of phytate-hydrolysing enzymes, phytases, from roots. Whilst this has seen some success (Giles et al., 2017), there are currently political and social limitations to the use of genetically engineered crops (Lei et al., 2013), particularly in Europe. An alternative solution could be the application of phytase enzymes directly to the soil. Phytase enzymes are already produced on a commercial scale to supplement the grain-based feed of monogastric livestock and have reduced both the need for supplemental inputs of phosphate to diets, and can reduce levels of P in monogastric excreta by 30-50% (Jorquera et al., 2008). In Chapter 5, an experiment was designed to test the ability of one such commercially produced phytase enzyme to dephosphorylate phytate in the setting of an artificial soil substrate, and further, to assess the effect of clay content on its performance. However, there were no consistent effects of the enzyme observed in either substrate on parameters including biomass, P uptake and substrate available P, which indicated that

phytase activity was lost in both substrates. It is probable that this was due to adsorption of the phytate or the enzyme to the substrate solid phase, regardless of clay content. Similar loss of activity has been observed in other approaches to phytase application. For example, when *Nicotiana tabacum* plants were engineered to express a fungal extracellular *Aspergillus niger* phytase, plants grown in sterile phytase-rich agar accumulated 3.7 fold more P than control plants, but this advantage was lost when plants were grown in P-deficient soil (George et al., 2005b). Greater understanding of rhizosphere chemistry has revealed that low molecular weight organic acids such as citrate can play a key complementary role in soil phytase activity, by mobilising phytate via ligand exchange with soil sorption sites. Recently, Giles et al., (2017) showed that *N. tabacum* plants engineered to express both phytase and citrate from their roots accumulated more P than plants expressing only one of the two traits, demonstrating the importance of low molecular weight organic acids for enzyme activity. Many commercial phytases, such as that used in this thesis, have an optimal activity at acidic pH (Menezes-Blackburn et al., 2014). Organic acid exudation in plants has been shown to cause reductions in rhizosphere soil pH (Adeleke et al., 2017), so their exudation may also provide more optimal biochemical conditions for phytase activity in soils. In future experiments, it would therefore be interesting to investigate whether co-application of one or more low molecular-weight organic acid with phytase would have a positive effect on enzyme activity by decreasing the adsorption of both enzyme and phytate in the substrate.

In this experiment, the pH of the two substrates differed according to the clay content, with the 0% clay substrate having a very low pH of 4.25, and the 10% clay substrate having a higher pH at 4.93. The clay content of the substrate was found to have a significant effect on the biomass of plants, with those grown in 10% clay consistently having greater biomass. It is possible that this difference was caused by the elevated substrate pH, and this may have masked any beneficial effect of the enzyme treatment on plant performance. Despite the lack of any significant observed effect of the commercial phytase enzyme on plant growth, further experiments are warranted to observe it's performance in substrates of the same pH, where the baseline biomass of plants is the same, and where any effect of the enzyme, or lack thereof, could be more

easily observed. Experiments could also be undertaken on substrates in the absence of plants to investigate the behaviour of phytate in substrate or soil systems. Substrates or soils could be treated with a known amount of phytate, the concentration of which could be measured by solution ^{31}P NMR, before soils are incubated with phytase, and again analysed for phytate concentration to observe any enzyme-induced change. This would remove the reliance on plant-performance indicators and provide direct quantitative data on any effect of the enzyme. This could then be followed up by varying substrate conditions such as pH, adsorptive capacity, organic acid concentration, clay and organic matter content to understand how these factors influence phytase dynamics. Alternatively, in a plant-based system, plants could be fertilised with a ^{33}P radiolabelled phytate prior to phytase addition, after which simple radio-imaging and scintillation counting could be used to measure plant uptake of ^{33}P following phytate dephosphorylation by phytase. This would require the generation of pure radiolabelled phytate free from phosphate contamination, which could be achieved by chromatographic or anion exchange separation following it's synthesis according to the methods described by either Robertson, (2018), or Whitfield et al., (2018).

Furthermore, future experiments may benefit from investigating the use of a range of phytase enzymes for phytate dephosphorylation in soils and substrates. The phytase enzyme used in this thesis was provided by DSM Nutritional Products, and is derived from the enterobacterium *Citrobacter braakii* for use in the dephosphorylation of phytate in the gut of monogastric livestock. Whilst the active pH range of this phytase is broad, between pH 2 – 6, and is optimal between pH 3 – 4.5 (Menezes-Blackburn et al., 2015), the complex and heterogenous conditions of the soil may inhibit the activity of enzymes not optimised for those conditions. Greater success may therefore be achieved by using phytase enzymes that have been isolated from soil-based microbes.

6.6 Conclusion

The recycling of P in organic wastes to arable land is an essential component of a sustainable model for agriculture. This thesis has shown that anaerobically digested sludge is P-rich and dominated by orthophosphate, but contains a substantial amount of phytate, which is spread to land in organic amendments. It was also shown that soil

P speciation varies with land-use history, with agricultural soils dominated by orthophosphate, but more natural grassland soils dominated by organic P forms. Conventional land management has depleted arable soil of phytate, but recovery and accumulation of phytate seems to occur when these land management practices are ceased and soil is amended with swine manure, which is accompanied by a recovery in soil organic matter. Long-term experiments are required to assess whether this is also the case when arable soils are amended with anaerobically digested sludge, and whether phytate accumulation is affected by the conventional cultivation, cropping and harvesting processes characteristic of these soils.

A key contribution to reducing requirements for chemical P fertiliser inputs is the mobilisation of stabilised, plant-unavailable P that is already in the soil. With phytate often identified as the most abundant organic P form in soil extracts by solution ^{31}P NMR, biofertilisation strategies involving the enzyme phytase are likely to prove pivotal for phytate mineralisation in soil, mirroring the established success of phytases as supplements for the grain-based feed of monogastric livestock. Many strategies are currently in development for this use, including the genetic engineering of crops for increased phytase exudation from roots (Giles et al., 2017), or the inoculation of manures and soils with phytase-producing microbes (Menezes-Blackburn et al., 2016). In this thesis, the direct application of a commercially available phytase enzyme was found to be ineffective for phytate dephosphorylation in a soil-like substrate, likely due to adsorption of phytate and phytase to the substrate solid-phase. A greater understanding of the rhizosphere biochemistry has elucidated the key role that low molecular weight organic acids play in the maintenance of both enzyme and phytate in solution, so future experiments involving the complementary application of these may yield improved results.

Regarding the wider development of sustainable and efficient use of P resources, there is a need firstly for more accurate and extensive testing of soil P levels, and greater understanding of optimal crop-specific P requirements, so that P can be applied to soil in a needs-based manner (Blackwell et al., 2019). Further efforts are also required to identify opportunities for nutrient recovery and recycling. Whilst manure and sludge are commonly recognised as straightforward intervention points, recent work has shown

that a fertiliser product derived from abattoir waste can provide comparable or improved yields versus a rock phosphate derived fertiliser (Darch et al., 2019), highlighting that there are opportunities for nutrient recovery in all corners of the food production industry. Furthermore, whilst a large amount of valuable scientific research has been undertaken, the integration of new strategies and biotechnology into a sustainable and efficient agricultural model will require a system-wide approach with input from all of the stakeholders involved in food production and consumption, to ensure that both societal and environmental concerns are addressed (Horton et al., 2017). For example, the use of genetically engineered crops is a complex societal and political issue, meaning that the integration of crop varieties engineered for increased phytase and organic acid exudation will require input from all parties to understand and overcome these obstacles. Such integrated thinking will furthermore enable the use of advanced life cycle analyses on proposed sustainable models (Horton et al., 2017; Goucher et al., 2017), which may highlight areas in which further research is required, and may help to mitigate adverse unintended consequences that may be encountered upon the application of new strategies.

This thesis contributes to our understanding of phytate dynamics in sewage sludge and soil, and how phytase enzymes could be used in future to enable its mobilisation for crop P nutrition, thereby reducing inputs of unsustainable phosphate fertilisers. However, a huge amount of work remains to be undertaken across academic, industrial and societal realms in pursuit of sustainable food production. With the human population increasing, and phosphate rock reserves becoming rapidly depleted, time is of the essence.

References

Abioye, S., Ige, D., Akinremi, O., Nyachoti, M. & Flaten, D. (2014). Characterizing Fecal and Manure Phosphorus from Pigs Fed Phytase Supplemented Diets. *Journal of Agricultural Science*. 2 (4). p.pp. 3–12.

Adeleke, R., Nwangburuka, C. & Oboirien, B. (2017). Origins, roles and fate of organic acids in soils: A review. *South African Journal of Botany*. 108. p.pp. 393–406.

Ajiboye, B., Akinremi, O.O., Hu, Y. & Flaten, D.N. (2007). Phosphorus Speciation of Sequential Extracts of Organic Amendments Using Nuclear Magnetic Resonance and X-ray Absorption Near-Edge Structure Spectroscopies. *Journal of Environment Quality*. 36 (6). p.p. 1563.

Annaheim, K.E., Doolette, A.L., Smernik, R.J., Mayer, J., Oberson, A., Frossard, E. & Bünemann, E.K. (2015). Long-term addition of organic fertilizers has little effect on soil organic phosphorus as characterized by 31P NMR spectroscopy and enzyme additions. *Geoderma*. 257–258. p.pp. 67–77.

Appels, L., Baeyens, J., Degrève, J. & Dewil, R. (2008). Principles and potential of the anaerobic digestion of waste-activated sludge. *Progress in Energy and Combustion Science*. 34 (6). p.pp. 755–781.

Banerjee, S. & Mazumdar, S. (2012). Electrospray Ionization Mass Spectrometry: A Technique to Access the Information beyond the Molecular Weight of the Analyte. *International Journal of Analytical Chemistry*. p.pp. 1–40.

Basto, S., Thompson, K., Phoenix, G., Sloan, V., Leake, J. & Rees, M. (2015). Long-term nitrogen deposition depletes grassland seed banks. *Nature Communications*. 6. p.pp. 1–6.

Batstone, D.J., Hülsen, T., Mehta, C.M. & Keller, J. (2015). Platforms for energy and nutrient recovery from domestic wastewater: A review. *Chemosphere*. 140 (November). p.pp. 2–11.

Bengtsson, F., Rydin, H. & Hájek, T. (2018). Biochemical determinants of litter quality in 15 species of Sphagnum. *Plant and Soil*. 425. p.pp. 161–176.

Berg, A.S. & Joern, B.C. (2006). Sorption dynamics of organic and inorganic phosphorus compounds in soil. *Journal of Environmental Quality*. 35. p.pp. 1855–1862.

BGS (2019). *British Geological Survey - Geology of Britain*. [Online]. 2019. Available from: https://www.bgs.ac.uk/discoveringGeology/geologyOfBritain/viewer.html. [Accessed: 30 July 2019].

Blackwell, M., Darch, T. & Haslam, R. (2019). Phosphorus use efficiency and fertilizers: future opportunities for improvements. *Frontiers of Agricultural Science and Engineering*.

Bougrier, C., Delgenès, J.P. & Carrère, H. (2008). Effects of thermal treatments on five

different waste activated sludge samples solubilisation, physical properties and anaerobic digestion. *Chemical Engineering Journal*. 139. p.pp. 236–244.

Bowman, R.A. & Moir, J.O. (1993). Basic EDTA as an extractant for soil organic phophorus. *Soil Science Society of America Journal*. 57. p.pp. 1516–1518.

BRC, Water UK & ADAS (2001). *The Safe Sludge Matrix: Guidelines for the application of sewage sludge to agricultural land.* [Online]. 2001. Available from: www.adas.co.uk/matrix. [Accessed: 14 May 2019].

Brejnholt, S.M., Dionisio, G., Glitsoe, V., Skov, L.K. & Brinch-Pedersen, H. (2011). The degradation of phytate by microbial and wheat phytases is dependent on the phytate matrix and the phytase origin. *Journal of the Science of Food and Agriculture*. 91. p.pp. 1398–1405.

Bünemann, E.K., Oberson, A. & Frossard, E. (2011). *Phosphorus in Action - Biological Processes in Soil Phosphorus Cycling*.

Bünemann, E.K., Oberson, A., Liebisch, F., Keller, F., Annaheim, K.E., Huguenin-Elie, O. & Frossard, E. (2012). Rapid microbial phosphorus immobilization dominates gross phosphorus fluxes in a grassland soil with low inorganic phosphorus availability. *Soil Biology and Biochemistry*. 51. p.pp. 84–95.

Cade-Menun, B. (2011). Characterizing phosphorus in animal waste with solution 31P-NMR spectroscopy. In: Z. He (ed.). *Environmental Chemistry of Animal Manure*. pp. 275–299.

Cade-Menun, B. & Liu, C.W. (2014). Solution phosphorus-31 nuclear magnetic resonance spectroscopy of soils from 2005 to 2013: A review of sample preparation and experimental parameters. *Soil Science Society of America Journal*. 78. p.pp. 19–37.

Cade-Menun, B.J. (2005). Characterizing phosphorus in environmental and agricultural samples by 31P nuclear magnetic resonance spectroscopy. *Talanta*. 66. p.pp. 359–371.

Cade-Menun, B.J. (2015). Improved peak identification in 31P-NMR spectra of environmental samples with a standardized method and peak library. *Geoderma*. 257–258. p.pp. 102–114.

Cade-Menun, B.J., Carter, M.R., James, D.C. & Liu, C.W. (2010). Phosphorus Forms and Chemistry in the Soil Profile under Long-Term Conservation Tillage: A Phosphorus-31 Nuclear Magnetic Resonance Study. *Journal of Environmental Quality*. 39. p.pp. 1647–1656.

Cade-Menun, B.J., Doody, D.G., Liu, C.W. & Watson, C.J. (2017). Long-term Changes in Grassland Soil Phosphorus with Fertilizer Application and Withdrawal. *Journal of Environmental Quality*. 46. p.pp. 537–545.

Cade-Menun, B.J. & Preston, C.M. (1996). A Comparison of Soil Extraction Procedures for 31P NMR Spectroscopy. *Soil Science*. 161 (11). p.pp. 770–785.

Carrère, H., Dumas, C., Battimelli, A., Batstone, D.J., Delgenès, J.P., Steyer, J.P. &

Ferrer, I. (2010). Pretreatment methods to improve sludge anaerobic degradability: A review. *Journal of Hazardous Materials*. 183. p.pp. 1–15.

Celi, L. & Barberis, E. (2006). Abiotic Reactions of Inositol Phosphates in Soil. In: B. L. Turner, A. E. Richardson, & E. J. Mullaney (eds.). *Inositol Phosphates: Linking Agriculture and the Environment*. pp. 207–220.

Celi, L., Lamacchia, S. & Barberis, E. (2000). Interaction of inositol phosphate with calcite. *Nutrient Cycling in Agroecosystems*. 57. p.pp. 271–277.

Celi, L., Presta, M., Ajmore-Marsan, F. & Barberis, E. (2001). Effects of pH and Electrolytes on Inositol Hexaphosphate Interaction with Goethite. *Soil Science Society of America Journal*. 65. p.pp. 753–760.

Choi, B.K., Hercules, D.M. & Houalla, M. (2000). Characterization of polyphosphates by electrospray mass spectrometry. *Analytical Chemistry*. 72 (20). p.pp. 5087–5091.

Clymo, R.S. (1984). Sphagnum-dominated peat bog: a naturally acid ecosystem. *Philosophical Transactions of the Royal Society B: Biological Sciences*. 305. p.pp. 487–499.

Condron, L.M., Turner, B.L. & Cade-Menun, B.J. (2005). Chemistry and dynamics of soil organic phosphorus. In: J. T. Sims & A. N. Sharpley (eds.). *Phosphorus, Agriculture and Environment - American Society of Agronomy*. pp. 87–121.

Cooper, W.T., Heerboth, M. & Salters, V.J.M. (2006). High-performance Chromatographic Separations of Inositol Phosphates and Their Detection by Mass Spectrometry. In: B. L. Turner, A. Richardson, & E. Mullaney (eds.). *Inositol Phosphates: Linking Agriculture and the Environment*. pp. 23–40.

Cordell, D., Drangert, J.O. & White, S. (2009). The story of phosphorus: Global food security and food for thought. *Global Environmental Change*. 19 (2). p.pp. 292–305.

Cordell, D. & White, S. (2014). Life's Bottleneck: Sustaining the World's Phosphorus for a Food Secure Future. *Annual Review of Environment and Resources*. 39. p.pp. 161–188.

Cordell, D. & White, S. (2011). Peak Phosphorus: Clarifying the Key Issues of a Vigorous Debate about Long-Term Phosphorus Security. *Sustainability*. 3 (12). p.pp. 2027–2049.

Cosgrove, D.J. (1966). Synthesis of the hexaphosphates of myo-, scyllo-, neo- and D-inositol. *Journal of the Science of Food and Agriculture*. 17. p.pp. 550–554.

Cranfield-University (2019). *The Soils Guide*. [Online]. 2019. Available from: www.landis.org.uk. [Accessed: 30 July 2019].

Dao, T.H. (2004). Ligands and Phytase Hydrolysis of Organic Phosphorus in Soils Amended with Dairy Manure. *Agronomy Journal*. 96. p.pp. 1188–1195.

Darch, T., Dunn, R.M., Guy, A., Hawkins, J.M.B., Ash, M., Frimpong, K.A. & Blackwell, M.S.A. (2019). Fertilizer produced from abattoir waste can contribute to

phosphorus sustainability, and biofortify crops with minerals. *PLoS ONE*. 14 (9). p.pp. 1–16.

DEFRA (2012). *Waste water treatment in the United Kingdom*.

Dersjant-Li, Y., Awati, A., Schulze, H. & Partridge, G. (2015). Phytase in non-ruminant animal nutrition: A critical review on phytase activities in the gastrointestinal tract and influencing factors. *Journal of the Science of Food and Agriculture*. 95 (5). p.pp. 878–896.

Dodd, R.J. & Sharpley, A.N. (2015). Recognizing the role of soil organic phosphorus in soil fertility and water quality. *Resources, Conservation and Recycling*. 105. p.pp. 282–293.

Doolette, A. (2010). *Thesis: Improved Techniques for the Characterisation of Soil Organic Phosphorus Using 31P Nuclear Magnetic Resonance Spectroscopy and Their Application to Australian Soils*.

Doolette, A.L. & Smernik, R.J. (2011). Soil Organic Phosphorus Speciation Using Spectroscopic Techniques. In: E. K. Bünemann, A. Oberson, & E. Frossard (eds.). *Phosphorus in Action*. pp. 3–36.

Doolette, A.L., Smernik, R.J. & Dougherty, W.J. (2010). Rapid decomposition of phytate applied to a calcareous soil demonstrated by a solution 31P NMR study. *European Journal of Soil Science*. 61 (4). p.pp. 563–575.

Doolette, A.L., Smernik, R.J. & Dougherty, W.J. (2009). Spiking Improved Solution Phosphorus-31 Nuclear Magnetic Resonance Identification of Soil Phosphorus Compounds. *Soil Science Society of America Journal*. 73 (3). p.p. 919.

Dou, Z., Ramberg, C.F., Toth, J.D., Wang, Y., Sharpley, a. N., Boyd, S.E., Chen, C.R., Williams, D. & Xu, Z.H. (2009). Phosphorus Speciation and Sorption-Desorption Characteristics in Heavily Manured Soils. *Soil Science Society of America Journal*. 73 (1). p.p. 93.

Drouillon, M. & Merckx, R. (2003). The Role of Citric Acid as a Phosphorus Mobilization Mechanism in Highly P-Fixing Soils. *Gayana. Botánica*. 60 (1). p.pp. 55–62.

Edelson-Averbukh, M., Pipkorn, R. & Lehmann, W.D. (2006). Phosphate group-driven fragmentation of multiply charged phosphopeptide anions. Improved recognition of peptides phosphorylated at serine, threonine, or tyrosine by negative ion electrospray tandem mass spectrometry. *Analytical Chemistry*. 78 (4). p.pp. 1249–1256.

Egle, L., Rechberger, H., Krampe, J. & Zessner, M. (2016). Phosphorus recovery from municipal wastewater: An integrated comparative technological, environmental and economic assessment of P recovery technologies. *Science of the Total Environment*. 571. p.pp. 522–542.

Egle, L., Rechberger, H. & Zessner, M. (2015). Overview and description of technologies for recovering phosphorus from municipal wastewater. *Resources, Conservation and Recycling*. 105. p.pp. 325–346.

Escudey, M., Galindo, G., Avendaño, K., Borchardt, D., Chang, A. & Briceño, M. (2004). Distribution of phosphorus forms in Chilean soils and sewage sludge by chemical fractionation and 31P-NMR. *Journal of the Chilean Chemical Society*. 49 (2). p.pp. 107–111.

European Commission (2013). Consultative Communication on the Sustainable Use of Phosphorus. *Communication from the Commission to the European Parliament, the Council, the European Economic and Social Committee and the Committee of the Regions*.

FAO (2019). *FAOStat*. [Online]. 2019. Available from: http://www.fao.org/faostat/en/#data/RFN. [Accessed: 14 September 2019].

FAO (2009). *How to Feed the World in 2050*. [Online]. 2009. Available from: http://www.fao.org/wsfs/forum2050/wsfs-forum/en/.

FAO (2017). *World fertilizer trends and outlook to 2020*.

Fenn, J.B., Mann, M., Meng, C.K., Wong, S.F. & Whitehouse, C.M. (1989). Electrospray ionization for mass spectrometry of large biomolecules. *Science*. 246 (4926). p.pp. 64–71.

Gatiboni, L.C. & Brunetto, G. (2013). Spectroscopic quantification of soil phosphorus forms by 31P-NMR after nine years of organic or mineral fertilization. *Revista Brasileira de Ciência do Solo*. 37. p.pp. 640–648.

Gebreeyessus, G. & Jenicek, P. (2016). Thermophilic versus Mesophilic Anaerobic Digestion of Sewage Sludge: A Comparative Review. *Bioengineering*. 3 (2). p.p. 15.

George, T.S., Giles, C.D., Menezes-Blackburn, D., Condron, L.M., Gama-Rodrigues, A.C., Jaisi, D., Lang, F., Neal, A.L., Stutter, M.I., Almeida, D.S., Bol, R., Cabugao, K.G., Celi, L., Cotner, J.B., Feng, G., Goll, D.S., Hallama, M., Krueger, J., Plassard, C., Rosling, A., Darch, T., Fraser, T., Giesler, R., Richardson, A.E., Tamburini, F., Shand, C.A., Lumsdon, D.G., Zhang, H., Blackwell, M.S.A., Wearing, C., Mezeli, M.M., Almås, Å.R., Audette, Y., Bertrand, I., Beyhaut, E., Boitt, G., Bradshaw, N., Brearley, C.A., Bruulsema, T.W., Ciais, P., Cozzolino, V., Duran, P.C., Mora, M.L., de Menezes, A.B., Dodd, R.J., Dunfield, K., Engl, C., Frazão, J.J., Garland, G., González Jiménez, J.L., Graca, J., Granger, S.J., Harrison, A.F., Heuck, C., Hou, E.Q., Johnes, P.J., Kaiser, K., Kjær, H.A., Klumpp, E., Lamb, A.L., Macintosh, K.A., Mackay, E.B., McGrath, J., McIntyre, C., McLaren, T., Mészáros, E., Missong, A., Mooshammer, M., Negrón, C.P., Nelson, L.A., Pfahler, V., Poblete-Grant, P., Randall, M., Seguel, A., Seth, K., Smith, A.C., Smits, M.M., Sobarzo, J.A., Spohn, M., Tawaraya, K., Tibbett, M., Voroney, P., Wallander, H., Wang, L., Wasaki, J. & Haygarth, P.M. (2018). Organic phosphorus in the terrestrial environment: a perspective on the state of the art and future priorities. *Plant and Soil*. 427 (1–2). p.pp. 191–208.

George, T.S., Quiquampoix, H., Simpson, R.J. & Richardson, A.E. (2006). Interactions between phytases and soil constituents: Implications for the hydrolysis of inositol phosphates. In: B. L. Turner, A. E. Richardson, & E. J. Mullaney (eds.). *Inositol Phosphates: Linking Agriculture and the Environment*. pp. 221–241.

George, T.S., Richardson, A.E. & Simpson, R.J. (2005a). Behaviour of plant-derived

extracellular phytase upon addition to soil. *Soil Biology and Biochemistry*. 37 (5). p.pp. 977–988.

George, T.S., Simpson, R.J., Gregory, P.J. & Richardson, A.E. (2007). Differential interaction of Aspergillus niger and Peniophora lycii phytases with soil particles affects the hydrolysis of inositol phosphates. *Soil Biology and Biochemistry*. 39 (3). p.pp. 793–803.

George, T.S., Simpson, R.J., Hadobas, P.A. & Richardson, A.E. (2005b). Expression of a fungal phytase gene in Nicotiana tabacum improves phosphorus nutrition of plants grown in amended soils. *Plant Biotechnology Journal*. 3 (1). p.pp. 129–140.

Gerardi, M.H. (2003). *The Microbiology of Anaerobic Digesters*. 1st Ed. Wiley-Interscience.

Gerke, J. (2010). Humic (organic matter)-Al(Fe)-phosphate complexes: An underestimated phosphate form in soils and source of plant-available phosphate. *Soil Science*. 175 (9). p.pp. 417–425.

Gerke, J. (2015). Phytate (Inositol Hexakisphosphate) in Soil and Phosphate Acquisition from Inositol Phosphates by Higher Plants. A Review. *Plants*. 4 (2). p.pp. 253–266.

Giaveno, C., Celi, L., Cessa, R.M.A., Prati, M., Bonifacio, E. & Barberis, E. (2008). Interaction of Organic Phosphorus With Clays Extracted From Oxisols. *Soil Science*. 173 (10). p.pp. 694–706.

Giles, C., Cade-Menun, B. & Hill, J. (2011). The inositol phosphates in soils and manures: Abundance, cycling, and measurement. *Canadian Journal of Soil Science*. 91 (3). p.pp. 397–416.

Giles, C.D. & Cade-Menun, B.J. (2014). Phytate in Animal Manure and Soils: Abundance, Cycling and Bioavailability. In: Z. He & H. Zhang (eds.). *Applied Manure and Nutrient Chemistry for Sustainable Agriculture and Environment.* pp. 163–190.

Giles, C.D., George, T.S., Brown, L.K., Mezeli, M.M., Richardson, A.E., Shand, C.A., Wendler, R., Darch, T., Menezes-Blackburn, D., Cooper, P., Stutter, M.I., Lumsdon, D.G., Blackwell, M.S.A., Wearing, C., Zhang, H. & Haygarth, P.M. (2017). Does the combination of citrate and phytase exudation in Nicotiana tabacum promote the acquisition of endogenous soil organic phosphorus? *Plant and Soil*. 412 (1–2). p.pp. 43–59.

Giles, C.D., Richardson, A.E., Druschel, G.K. & Hill, J.E. (2012). Organic anion-driven solubilization of precipitated and sorbed phytate improves hydrolysis by phytases and bioavailability to Nicotiana tabacum. *Soil Science*. 177 (10). p.pp. 591–598.

Goucher, L., Bruce, R., Cameron, D.D., Lenny Koh, S.C. & Horton, P. (2017). The environmental impact of fertilizer embodied in a wheat-to-bread supply chain. *Nature Plants*. 3. p.pp. 1–5.

Grim, R.E. & Kulbicki, G. (1961). Montmorillonite: High Temperature Reactions and Classification. *The American Mineralogist*. 46. p.pp. 1329–1369.

Gujar, P.D., Bhavsar, K.P. & Khire, J.M. (2013). Effect of phytase from Aspergillus niger on plant growth and mineral assimilation in wheat (Triticum aestivum Linn.) and its potential for use as a soil amendment. *Journal of the Science of Food and Agriculture*. 93 (9). p.pp. 2242–2247.

Hansen, J.C., Cade-Menun, B.J. & Strawn, D.G. (2004). Phosphorus speciation in manure-amended alkaline soils. *Journal of environmental quality*. 33 (4). p.pp. 1521–1527.

Haynes, R.J., Murtaza, G. & Naidu, R. (2009). *Inorganic and Organic Constituents and Contaminants of Biosolids. Implications for Land Application*. 1st Ed. Elsevier Inc.

He, Z., Honeycutt, C.W., Xing, B., Mcdowel, R.W., Pellechia, P.J., Zhang, T., Kulakovskaya, T. V., Lichko, L.P. & Ryazanova, L.P. (2007a). Solid-State Fourier Transform Infrared and 31P Nuclear Magnetic Resonance Spectral Features of Phosphate Compounds. *Biochemistry*. 172 (7). p.pp. 1602–1614.

He, Z., Honeycutt, C.W., Zhang, T., Pellechia, P.J. & Caliebe, W.A. (2007b). Distinction of metal species of phytate by solid-state spectroscopic techniques. *Soil Science Society of America Journal*. 71 (3). p.pp. 940–943.

He, Z., Olk, D.C. & Cade-Menun, B.J. (2011). Forms and Lability of Phosphorus in Humic Acid Fractions of Hord Silt Loam Soil. *Soil Science Society of America Journal*. 75 (5). p.pp. 1712–1722.

He, Z., Waldrip, H.W., Honeycutt, C.W., Erich, M.S. & Senwo, Z.N. (2009). Enzymatic Quantification of Phytate in Animal Manure. *Communications in Soil Science and Plant Analysis*. 40. p.pp. 566–575.

Hebbar, R.S., Isloor, A.M. & Ismail, A.F. (2014). Preparation and evaluation of heavy metal rejection properties of polyetherimide/porous activated bentonite clay nanocomposite membrane. *RSC Advances*. 4 (88). p.pp. 47240–47248.

Hendershot, W.H., Lalande, H. & Duquette, M. (2008). Soil Reaction and Exchangeable Acidity. In: M. R. Carter & E. G. Gregorich (eds.). *Soil Sampling and Methods of Analysis*. pp. 173–178.

Hinedi, Z.R., Chang, A.C. & Lee, R.W.K. (1989). Characterization of Phosphorus in Sludge Extracts Using Phosphorus-31 Nuclear Magnetic Resonance Spectroscopy. *Journal of Environment Quality*. 18 (3). p.p. 323.

Holden, J. & Gell, K.F. (2009). Morphological characterization of solute flow in a brown earth grassland soil with cranefly larvae burrows (leatherjackets). *Geoderma*. 152 (1–2). p.pp. 181–186.

Holden, J., Grayson, R.P., Berdeni, D., Bird, S., Chapman, P.J., Edmondson, J.L., Firbank, L.G., Helgason, T., Hodson, M.E., Hunt, S.F.P., Jones, D.T., Lappage, M.G., Marshall-Harries, E., Nelson, M., Prendergast-Miller, M., Shaw, H., Wade, R.N. & Leake, J.R. (2019). The role of hedgerows in soil functioning within agricultural landscapes. *Agriculture, Ecosystems and Environment*. 273. p.pp. 1–12.

Horton, P., Banwart, S.A., Brockington, D., Brown, G.W., Bruce, R., Cameron, D., Holdsworth, M., Lenny Koh, S.C., Ton, J. & Jackson, P. (2017). An agenda for

integrated system-wide interdisciplinary agri-food research. *Food Security*. 9 (2). p.pp. 195–210.

Huang, Q., Zhao, Z. & Chen, W. (2003). Effects of several low-molecular weight organic acids and phosphate on the adsorption of acid phosphatase by soil colloids and minerals. *Chemosphere*. 52 (3). p.pp. 571–579.

Huang, R. & Tang, Y. (2015). Speciation Dynamics of Phosphorus during (Hydro)Thermal Treatments of Sewage Sludge. *Environmental Science and Technology*. 49 (24). p.pp. 14466–14474.

Igamnazarov, R.P., Tillaeva, Z.E. & Umarova, G.B. (1999). Effect of metal ions on the activity of extracellular phytase of Bacterium sp. *Chemistry of Natural Compounds*. 35 (6). p.pp. 661–664.

Islam, A.K.M.S., Edwards, D.G. & Asher, C.J. (1980). pH optima for crop growth - Results of a flowing solution culture experiment with six species. *Plant and Soil*. 54 (3). p.pp. 339–357.

Ivell, D.M. (2012). Phosphate fertilizer production - From the 1830's to 2011 and beyond. *Procedia Engineering*. 46. p.pp. 166–171.

James, T.L. (1998). *Fundamentals of NMR*.

Jarosch, K.A., Doolette, A.L., Smernik, R.J., Tamburini, F., Frossard, E. & Bünemann, E.K. (2015). Characterisation of soil organic phosphorus in NaOH-EDTA extracts: A comparison of 31P NMR spectroscopy and enzyme addition assays. *Soil Biology and Biochemistry*. 91. p.pp. 298–309.

Jasinski, S.M. (2019). Mineral Commodity Summaries, Phosphate Rock. *U.S. Geological Survey*. p.pp. 122–123.

Jasinski, S.M. (2008). Mineral Commodity Summaries, Phosphate Rock. *U.S. Geological Survey*. p.pp. 124–125.

Jørgensen, C., Turner, B.L. & Reitzel, K. (2015). Identification of inositol hexakisphosphate binding sites in soils by selective extraction and solution 31P NMR spectroscopy. *Geoderma*. 257–258. p.pp. 22–28.

Jorquera, M., Martínez, O., Maruyama, F., Marschner, P. & de la Luz Mora, M. (2008). Current and future biotechnological applications of bacterial phytases and phytase-producing bacteria. *Microbes and environments*. 23 (3). p.pp. 182–191.

Joung, H., Jeun, B.Y., Li, S.J., Kim, J., Woodhouse, L.R., King, J.C., Welch, R.M. & Paik, H.Y. (2007). Fecal phytate excretion varies with dietary phytate and age in women. *Journal of the American College of Nutrition*. 26 (3). p.pp. 295–302.

Kane, C.D., Jasoni, R.L., Peffley, E.P., Thompson, L.D., Green, C.J., Pare, P. & Tissue, D. (2006). Nutrient solution and solution pH influences on onion growth and mineral content. *Journal of Plant Nutrition*. 29 (2). p.pp. 375–390.

Karam, A. (2008). Chemical Properties of Organic Soils. In: M. R. Carter & E. G. Gregorich (eds.). *Soil Sampling and Methods of Analysis*. pp. 331–340.

Kemme, P.A., Lommen, A., De Jonge, L.H., Van Der Klis, J.D., Jongbloed, A.W., Mroz, Z. & Beynen, A.C. (1999). Quantification of inositol phosphates using 31P nuclear magnetic resonance spectroscopy in animal nutrition. *Journal of Agricultural and Food Chemistry*. 47 (12). p.pp. 5116–5121.

Kepp, U., Machenbach, I., Weisz, N. & Solhelm, O.E. (2000). Enhanced Stabilisation of Sewage Sludge through Thermal Hydrolysis - Three Years of Experience with Full Scale Plant. *Water Science & Technology*. 42 (9). p.pp. 89–96.

Kim, J., Park, C., Kim, T.-H., Lee, M., Kim, S., Kim, S.-W. & Lee, J. (2003). Effects of Various Pretreatments for Enhanced Anaerobic Digestion with Waste Activated Sludge. *Journal of Bioscience and Bioengineering*. 95 (3). p.pp. 271–275.

Kim, J., Woodhouse, L.R., King, J.C., Welch, R.M., Li, S.J., Paik, H.Y. & Joung, H. (2009). Relationships between faecal phytate and mineral excretion depend on dietary phytate and age. *British Journal of Nutrition*. 102 (6). p.pp. 835–841.

Kleinman, P.J.A. (2017). The Persistent Environmental Relevance of Soil Phosphorus Sorption Saturation. *Current Pollution Reports*. 3 (2). p.pp. 141–150.

Kobayashi, Y., Kobayashi, Y., Watanabe, T., Shaff, J.E., Ohta, H., Kochian, L. V., Wagatsuma, T., Kinraide, T.B. & Koyama, H. (2013). Molecular and physiological analysis of Al3+ and H+ rhizotoxicities at moderately acidic conditions. *Plant Physiology*. 163 (1). p.pp. 180–192.

Konietzny, U. & Greiner, R. (2004). Bacterial phytase: Potential application, in vivo function and regulation of its synthesis. *Brazilian Journal of Microbiology*. 35 (1–2). p.pp. 11–18.

Lambers, H., Brundrett, M.C., Raven, J.A. & Hopper, S.D. (2010). Plant mineral nutrition in ancient landscapes: High plant species diversity on infertile soils is linked to functional diversity for nutritional strategies. *Plant and Soil*. 334. p.pp. 11–31.

Lei, X.G., Weaver, J.D., Mullaney, E., Ullah, A.H. & Azain, M.J. (2013). Phytase, a New Life for an “Old” Enzyme. *Annual Review of Animal Biosciences*. 1 (1). p.pp. 283–309.

Leprince, F. & Quiquampoix, H. (1996). Extracellular enzyme activity in soil: Effect of pH and ionic strength on the interaction with montmorillonite of two acid phosphatases secreted by the ectomycorrhizal fungus Hebeloma cylindrosporum. *European Journal of Soil Science*. 47 (4). p.pp. 511–522.

Leytem, A.B., Kwanyuen, P., Plumstead, P.W., Maguire, R.O. & Brake, J. (2008). Evaluation of Phosphorus Characterization in Broiler Ileal Digesta, Manure, and Litter Samples: 31P-NMR vs. HPLC. *Journal of Environment Quality*. 37. p.pp. 494–500.

Leytem, A.B., Smith, D.R., Applegate, T.J. & Thacker, P.A. (2006). The Influence of Manure Phytic Acid on Phosphorus Solubility in Calcareous Soils. *Soil Science Society of America Journal*. 70 (5). p.pp. 1629–1638.

Leytem, A.B. & Thacker, P.A. (2008). Fecal Phosphorus Excretion and Characterization from Swine Fed Diets Containing a Variety of Cereal Grains. *Journal of Animal and*

Veterinary Advances. 7 (2). p.pp. 113–120.

Li, L., Pang, H., He, J. & Zhang, J. (2019). Characterization of phosphorus species distribution in waste activated sludge after anaerobic digestion and chemical precipitation with Fe3+ and Mg2+. *Chemical Engineering Journal*. 373. p.pp. 1279–1285.

Li, M., Tang, Y., Lu, X.Y., Zhang, Z. & Cao, Y. (2018). Phosphorus speciation in sewage sludge and the sludge-derived biochar by a combination of experimental methods and theoretical simulation. *Water Research*. 140. p.pp. 90–99.

Li, Y.Y. & Noike, T. (1992). Upgrading of anaerobic digestion of waste activated sludge by thermal pretreatment. *Water Science & Technology*. 26 (3–4). p.pp. 857–866.

Liang, X., Jin, Y., He, M., Niyungeko, C., Zhang, J., Liu, C., Tian, G. & Arai, Y. (2018). Phosphorus speciation and release kinetics of swine manure biochar under various pyrolysis temperatures. *Environmental Science and Pollution Research*. 25 (26). p.pp. 25780–25788.

Lichtenberg, J., Pedersen, P.B., Elvig-Joergensen, S.G., Skov, L.K., Olsen, C.L. & Glitsoe, L. V. (2011). Toxicological studies on a novel phytase expressed from synthetic genes in Aspergillus oryzae. *Regulatory Toxicology and Pharmacology*. 60 (3). p.pp. 401–410.

Lindner, R.C. (1944). Rapid Analytical Methods for Some of the More Common Inorganic Constituents of Plant Tissues. *Plant Physiology*. 19 (1). p.pp. 76–89.

Liu, J., Cade-Menun, B.J., Yang, J., Hu, Y., Liu, C.W., Tremblay, J., LaForge, K., Schellenberg, M., Hamel, C. & Bainard, L.D. (2018). Long-term land use affects phosphorus speciation and the composition of phosphorus cycling genes in agricultural soils. *Frontiers in Microbiology*. 9. p.pp. 1–14.

Lott, J.N.A., Ockenden, I., Raboy, V. & Batten, G.D. (2000). Phytic acid and phosphorus in crop seeds and fruits: a global estimate. *Seed Science Research*. (10). p.pp. 11–33.

Lu, Z., Chai, Y., Guo, C., Sun, C. & Pan, Y. (2013). H2O loss in the fragmentation of deprotonated N-o-tolylamides in tandem mass spectrometry. *Journal of Mass Spectrometry*. 48 (9). p.pp. 1010–1014.

Mana, S.C.A., Hanafiah, M.M. & Chowdhury, A.J.K. (2017). Environmental characteristics of clay and clay-based minerals. *Geology, Ecology, and Landscapes*. 1 (3). p.pp. 155–161.

Martínez-Viveros, O., Jorquera, M.A., Crowley, D.E., Gajardo, G. & Mora, M.L. (2010). Mechanisms and practical considerations involved in plant growth promotion by Rhizobacteria. *Journal of Soil Science and Plant Nutrition*. 10 (3). p.pp. 293–319.

Matumoto-Pintro, P.T. & Quiquampoix, H. (1997). La phase solide des sols comme contrainte au fonction-nement des enzymes sécrétés par les microorganismes: comparaison de phytases intra et extracellularies. In: *Microbiologie Industrielle et Environnement. Société Française de Microbiologie, Paris, France*. pp. 195–204.

McIntyre, C.A., Arkell, Jennifer, J.L., Arthur, C.J., Lawrence, P.G., Butts, C.P., Lloyd, C.E.M., Johnes, P.J. & Evershed, R.P. (2019). Identification and quantification of myo-inositol hexakisphosphate in complex biological and environmental matrices using ion chromatography and high-resolution mass spectrometry in comparison to 31P NMR spectroscopy. *Talanta*. In Press. p.pp. 1–33.

McIntyre, C.A., Arthur, C.J. & Evershed, R.P. (2017). High resolution mass spectrometric analysis of myo-inositol hexakisphosphate using electrospray ionisation Orbitrap. *Rapid Communications in Mass Spectrometry*. 31. p.pp. 1681–1689.

McKercher, R.B. & Anderson, G. (1989). Organic phosphate sorption by neutral and basic soils. *Communications in Soil Science and Plant Analysis*. 20 (7–8). p.pp. 723–732.

McLaren, T.I., Smernik, R.J., Guppy, C.N., Bell, M.J. & Tighe, M.K. (2014). The Organic P Composition of Vertisols as Determined by P NMR Spectroscopy. *Soil Science Society of America Journal*. 78 (6). p.p. 1893.

McLaren, T.I., Smernik, R.J., Simpson, R.J., McLaughlin, M.J., McBeath, T.M., Guppy, C.N. & Richardson, A.E. (2015). Spectral sensitivity of solution 31 P NMR spectroscopy is improved by narrowing the soil to solution ratio to 1:4 for pasture soils of low organic P content. *Geoderma*. 257–258. p.pp. 48–57.

McLaren, T.I., Verel, R. & Frossard, E. (2019). The structural composition of soil phosphomonoesters as determined by solution 31P NMR spectroscopy and transverse relaxation (T2) experiments. *Geoderma*. 345. p.pp. 31–37.

McLauchlan, K. (2006). The Nature and Longevity of Agricultural Impacts on Soil Carbon and Nutrients: A Review. *Ecosystems*. 9 (8). p.pp. 1364–1382.

McRae, J.M., Falconer, R.J. & Kennedy, J.A. (2010). Thermodynamics of grape and wine tannin interaction with polyproline: Implications for red wine astringency. *Journal of Agricultural and Food Chemistry*. 58 (23). p.pp. 12510–12518.

Mehta, N.C., Legg, J.O., Goring, C.A.I. & Black, C.A. (1954). Determination of Organic Phosphorus in Soils. I. Extraction Method. *Soil Science Society of America Journal*. 16 (4). p.pp. 443–449.

Menezes-Blackburn, D., Gabler, S. & Greiner, R. (2015). Performance of Seven Commercial Phytases in an in Vitro Simulation of Poultry Digestive Tract. *Journal of Agricultural and Food Chemistry*. 63 (27). p.pp. 6142–6149.

Menezes-Blackburn, D., Giles, C., Darch, T., George, T.S., Blackwell, M., Stutter, M., Shand, C., Lumsdon, D., Cooper, P., Wendler, R., Brown, L., Almeida, D.S., Wearing, C., Zhang, H. & Haygarth, P.M. (2017). Opportunities for mobilizing recalcitrant phosphorus from agricultural soils: A review. *Plant and Soil*. 427 (1–2). p.pp. 5–16.

Menezes-Blackburn, D., Inostroza, N.G., Gianfreda, L., Greiner, R., Mora, M.L. & Jorquera, M.A. (2016). Phytase-producing Bacillus sp. inoculation increases phosphorus availability in cattle manure. *Journal of Soil Science and Plant Nutrition*. 16 (1). p.pp. 200–210.

Menezes-Blackburn, D., Jorquera, M., Gianfreda, L., Rao, M., Greiner, R., Garrido, E. & De la Luz Mora, M. (2011). Activity stabilization of Aspergillus niger and Escherichia coli phytases immobilized on allophanic synthetic compounds and montmorillonite nanoclays. *Bioresource Technology*. 102 (20). p.pp. 9360–9367.

Menezes-Blackburn, D., Jorquera, M.A., Gianfreda, L., Greiner, R. & de la Luz Mora, M. (2014). A novel phosphorus biofertilization strategy using cattle manure treated with phytase-nanoclay complexes. *Biology and Fertility of Soils*. 50 (4). p.pp. 583–592.

Menezes-Blackburn, D., Jorquera, M.A., Greiner, R., Gianfreda, L. & De La Luz Mora, M. (2013). Phytases and phytase-labile organic phosphorus in manures and soils. *Critical Reviews in Environmental Science and Technology*. 43 (9). p.pp. 916–954.

Murphy, J. & Riley, J.P. (1962). A modified single solution method for the determination of phosphate in natural waters. *Analytica Chimica Acta*. 27. p.pp. 31–36.

Naidja, A., Huang, P.M. & Bollag, J.-M. (2000). Enzyme-Clay Interactions and Their Impact on Transformations of Natural and Anthropogenic Organic Compounds in Soil. *Journal of Environment Quality*. 29 (3). p.p. 677.

Nash, D.M., Haygarth, P.M., Turner, B.L., Condron, L.M., McDowell, R.W., Richardson, A.E., Watkins, M. & Heaven, M.W. (2014). Using organic phosphorus to sustain pasture productivity: A perspective. *Geoderma*. 221–222. p.pp. 11–19.

Neset, T.-S., Cordell, D., Mohr, S., VanRiper, F. & White, S. (2016). Visualizing Alternative Phosphorus Scenarios for Future Food Security. *Frontiers in Nutrition*. 3. p.pp. 1–13.

O'Sullivan, O.S., Horswill, P., Phoenix, G.K., Lee, J.A. & Leake, J.R. (2011). Recovery of soil nitrogen pools in species-rich grasslands after 12 years of simulated pollutant nitrogen deposition: A 6-year experimental analysis. *Global Change Biology*. 17 (8). p.pp. 2615–2628.

Oh, B.C., Choi, W.C., Park, S., Kim, Y.O. & Oh, T.K. (2004). Biochemical properties and substrate specificities of alkaline and histidine acid phytases. *Applied Microbiology and Biotechnology*. 63 (4). p.pp. 362–372.

de Oliveira, D.A., Pinheiro, A. & da Veiga, M. (2014). Effects of Pig Slurry Application on Soil Physical and Chemical Properties and Glyphosate Mobility. *Revista Brasileira de Ciência do Solo*. 38. p.pp. 1421–1431.

Olsen, S.R., Cole, C. V., Watanabe, F.S. & Dean, L.A. (1954). Estimation of Available Phosphorus in Soils by Extraction with Sodium Bicarbonate. *US Depaartment of Agriculture Circular*. 939. p.pp. 1–19.

Owen, D., Williams, A.P., Griffith, G.W. & Withers, P.J.A. (2015). Use of commercial bio-inoculants to increase agricultural production through improved phosphrous acquisition. *Applied Soil Ecology*. 86. p.pp. 41–54.

Palumbo, A.M., Smith, S.A., Kalcic, C.L., Dantus, M., Stemmer, P.M. & Reid, G.E. (2011). Tandem Mass Spectrometry Strategies for Phosphoproteome Analysis. *Mass*

Spectrometry Reviews. 30. p.pp. 600–625.

Paraskova, J. V., Jørgensen, C., Reitzel, K., Pettersson, J., Rydin, E. & Sjöberg, P.J.R. (2015). Speciation of inositol phosphates in lake sediments by ion-exchange chromatography coupled with mass spectrometry, inductively coupled plasma atomic emission spectroscopy, and 31P NMR spectroscopy. *Analytical Chemistry*. 87 (5). p.pp. 2672–2677.

Peng, X.L., Chen, L., Lv, Z.W., Hao, G.J. & Fang, H.L. (2010). Characterization of phosphorus in sewage sludge from different sources by 31Phosphorus nuclear magnetic resonance spectroscopy. *Communications in Soil Science and Plant Analysis*. 41 (10). p.pp. 1237–1244.

Penn, C.J. & Camberato, J.J. (2019). A critical review on soil chemical processes that control how soil ph affects phosphorus availability to plants. *Agriculture (Switzerland)*. 9 (6). p.pp. 1–18.

Peñuelas, J., Poulter, B., Sardans, J., Ciais, P., van der Velde, M., Bopp, L., Boucher, O., Godderis, Y., Hinsinger, P., Llusia, J., Nardin, E., Vicca, S., Obersteiner, M. & Janssens, I. a (2013). Human-induced nitrogen-phosphorus imbalances alter natural and managed ecosystems across the globe. *Nature Communications*. 78. p.pp. 19–37.

Phoenix, G.K., Johnson, D.A., Muddimer, S.P., Leake, J.R. & Cameron, D.D. (2019). Niche differentiation and plasticity in soil phosphorus acquisition among co-occurring plants. *Nature Plants*. In Press.

Pontoppidan, K., Glitsoe, V., Guggenbuhl, P., Quintana, A.P., Nunes, C.S., Pettersson, D. & Sandberg, A.-S. (2012). In vitro and in vivo degradation of myo-inositol hexakisphosphate by a phytase from Citrobacter braakii. *Archives of Animal Nutrition*. 66 (6). p.pp. 431–444.

Potter, P., Ramankutty, N., Bennett, E.M. & Donner, S.D. (2010). Characterizing the Spatial Patterns of Global Fertilizer Application and Manure Production. *Earth Interactions*. 14. p.pp. 1–22.

Ptáček, P. (2016). Phosphate Rocks (Chapter 7). In: *Apatites and their Synthetic Analogues - Synthesis, Structure, Properties and Applications*. pp. 335–381.

Quiquampoix, H., Servagent-Noinville, S. & Baron, M.H. (2002). Enzyme adsorption on soil mineral surfaces and consequences for the catalytic activity. In: R. G. Burns & R. P. Dick (eds.). *Enzymes in the Environment*. pp. 285–306.

Raboy, V. (2003). myo-Inositol-1,2,3,4,5,6-hexakisphosphate. *Phytochemistry*. 64 (6). p.pp. 1033–1043.

Ray, P.P., Shang, C., Maguire, R.O. & Knowlton, K.F. (2012). Quantifying phytate in dairy digesta and feces: alkaline extraction and high-performance ion chromatography. *Journal of Dairy Science*. 95 (6). p.pp. 3248–3258.

Reijnders, L. (2014). Phosphorus resources, their depletion and conservation, a review. *Resources, Conservation and Recycling*. 93. p.pp. 32–49.

Richardson, A.E., George, T.S., Jakobsen, I. & Simpson, R.J. (2006). Plant Utilization of Inositol Phosphates. In: *Turner, B., Richardson, A., Mullaney, E. (eds). Inositol Phosphates: Linking Agriculture and the Environment.* pp. 242–260.

Richardson, A.E., Hocking, P.J., Simpson, R.J. & George, T.S. (2009). Plant mechanisms to optimise access to soil phosphorus. *Crop and Pasture Science*. 60 (2). p.pp. 124–143.

Richardson, A.E. & Simpson, R.J. (2011). Soil microorganisms mediating phosphorus availability. *Plant physiology*. 156 (3). p.pp. 989–996.

Robertson, I.G. (2018). *Thesis: Organic Phosphorus (P) in Agricultural Soil and the Ability of Wheat to Use this as a P Source*. University of Sheffield.

Robinson, J.R. (1969). 33P: A superior radiotracer for phosphorus? *The International Journal Of Applied Radiation And Isotopes*. 20 (7). p.pp. 531–540.

Rugova, A., Puschenreiter, M., Santner, J., Fischer, L., Neubauer, S., Koellensperger, G. & Hann, S. (2014). Speciation analysis of orthophosphate and myo-inositol hexakisphosphate in soil- and plant-related samples by high-performance ion chromatography combined with inductively coupled plasma mass spectrometry. *Journal of Separation Science*. 37 (14). p.pp. 1711–1719.

Ruttenberg, K.C. (1993). Reassessment of the oceanic residence time of phosphorus. *Chemical Geology*. 107 (3–4). p.pp. 405–409.

Ruttenberg, K.C. (2003). The global phosphorus cycle. *Treatise on Geochemistry 8*. p.pp. 585–643.

Shang, C., Huang, P.M. & Stewart, J.W.B. (1990). Kinetics of Adsorption of Organic and Inorganic Phosphates by Short-Range Ordered Precipitate of Aluminum. *Canadian Journal of Soil Science*. 70. p.pp. 461–470.

Shang, C., Zelazny, L.W., Berry, D.F. & Maguire, R.O. (2013). Orthophosphate and phytate extraction from soil components by common soil phosphorus tests. *Geoderma*. 209–210. p.pp. 22–30.

Sharpley, A.N. (1995). Dependence of runoff phosphorus on extractable soil phosphorus. *Journal of Environmental Quality*. 24 (5). p.pp. 920–926.

Shen, J., Yuan, L., Zhang, J., Li, H., Bai, Z., Chen, X., Zhang, W. & Zhang, F. (2011). Phosphorus Dynamics: From Soil to Plant. *Plant Physiology*. 156 (3). p.pp. 997–1005.

Shober, A.L., Hesterberg, D.L., Sims, J.T. & Gardner, S. (2006). Characterization of phosphorus species in biosolids and manures using XANES spectroscopy. *Journal of Environmental Quality*. 35 (6). p.pp. 1983–1993.

Singh, R.P. & Agrawal, M. (2008). Potential benefits and risks of land application of sewage sludge. *Waste Management*. 28 (2). p.pp. 347–358.

Smil, V. (2000). Phosphorus in the Environment: Natural Flows and Human Interferences. *Annual Review of Energy and the Environment*. 25. p.pp. 53–88.

Smith, M.T.E., Cade-Menun, B.J. & Tibbett, M. (2006). Soil phosphorus dynamics and phytoavailability from sewage sludge at different stages in a treatment stream. *Biology and Fertility of Soils*. 42 (3). p.pp. 186–197.

Steward, J.H. & Oades, J.M. (1976). The Determination of Organic Phosphorus in Soils. *Journal of Soil Science*. 23 (1). p.pp. 38–49.

Stutter, M.I. & Richards, S. (2012). Relationships between soil physicochemical, microbiological properties, and nutrient release in buffer soils compared to field soils. *Journal of Environmental Quality*. 41. p.pp. 400–409.

Stutter, M.I., Shand, C.A., George, T.S., Blackwell, M.S.A., Dixon, L., Bol, R., MacKay, R.L., Richardson, A.E., Condron, L.M. & Haygarth, P.M. (2015). Land use and soil factors affecting accumulation of phosphorus species in temperate soils. *Geoderma*. 257–258. p.pp. 29–39.

Talboys, P.J., Heppell, J., Roose, T., Healey, J.R., Jones, D.L. & Withers, P.J.A. (2016). Struvite: a slow-release fertiliser for sustainable phosphorus management? *Plant and Soil*. 401 (1–2). p.pp. 109–123.

Toor, G.S., Cade-Menun, B.J. & Sims, J.T. (2005). Establishing a linkage between phosphorus forms in dairy diets, feces, and manures. *Journal of environmental quality*. 34 (4). p.pp. 1380–91.

Turner, B., Cade-Menun, B., Condron, L. & Newman, S. (2005a). Extraction of soil organic phosphorus. *Talanta*. 66 (2). p.pp. 294–306.

Turner, B.L. (2004). Optimizing Phosphorus Characterization in Animal Manures by Solution Phosphorus-31 Nuclear Magnetic Resonance Spectroscopy. *Journal of Environment Quality*. 33. p.pp. 757–766.

Turner, B.L., Cade-Menun, B.J. & Westermann, D.T. (2003a). Organic Phosphorus Composition and Potential Bioavailability in Semi-Arid Arable Soils of the Western United States. *Soil Science Society of America Journal*. 67 (4). p.pp. 1168–1179.

Turner, B.L., Cheesman, A.W., Godage, H.Y., Riley, A.M. & Potter, B.V.L. (2012). Determination of neo- and D-chiro-inositol hexakisphosphate in soils by solution 31P NMR spectroscopy. *Environmental Science & Technology*. 46 (9). p.pp. 4994–5002.

Turner, B.L., Mahieu, N., Condron, L.M. & Chen, C.R. (2005b). Quantification and bioavailability of scyllo-inositol hexakisphosphate in pasture soils. *Soil Biology and Biochemistry*. 37 (11). p.pp. 2155–2158.

Turner, B.L., McKelvie, I.D. & Haygarth, P.M. (2003b). Characterisation of water-extractable soil organic phosphorus by phosphatase hydrolysis. *Soil Biology and Biochemistry*. 34 (1). p.pp. 27–35.

Turner, B.L., Newman, S. & Reddy, K.R. (2006). Overestimation of organic phosphorus in wetland soils by alkaline extraction and molybdate colorimetry. *Environmental Science and Technology*. 40 (10). p.pp. 3349–3354.

Turner, B.L., Paphazy, M.J., Haygarth, P.M. & Mckelvie, I.D. (2002). Inositol phosphates

in the environment. *Philosophical Transactions of the Royal Society B: Biological Sciences*. 357 (1420). p.pp. 449–469.

Turner, B.L. & Richardson, A.E. (2004). Identification of scyllo-Inositol Phosphates in Soil by Solution Phosphorus-31 Nuclear Magnetic Resonance Spectroscopy. *Soil Science Society of America Journal*. 68 (3). p.pp. 802–808.

Ulrich, A.E. (2019). Cadmium governance in Europe's phosphate fertilizers: Not so fast? *Science of the Total Environment*. 650. p.pp. 541–545.

Ulusoy, U., Şimşek, S. & Ceyhan, Ö. (2003). Investigations for modification of polyacrylamide-bentonite by phytic acid and its usability in Fe3+, Zn2+ and UO2 2+ adsorption. *Adsorption*. 9 (2). p.pp. 165–175.

Vaccari, D.A. (2009). Phosphorus: A looming crisis. *Scientific American*. 300 (6). p.pp. 54–59.

Vavilin, V.A., Fernandez, B., Palatsi, J. & Flotats, X. (2008). Hydrolysis kinetics in anaerobic degradation of particulate organic material: An overview. *Waste Management*. 28 (6). p.pp. 939–951.

Veolia Water Technologies (2015). *Bio Thelys ^{TM} batch thermal hydrolysis*. [Online]. 2015. Available from: http://technomaps.veoliawatertechnologies.com/processes/lib/municipal/3474-150497_VWT_Mkt_Municipal_BioThelys_.pdf. [Accessed: 10 May 2019].

Waithaisong, K., Robin, A., Martin, A., Clairotte, M., Villeneuve, M. & Plassard, C. (2015). Quantification of organic P and low-molecular-weight organic acids in ferralsol soil extracts by ion chromatography. *Geoderma*. 257–258. p.pp. 94–101.

Walan, P. (2013). *Modeling of Peak Phosphorus: A Study of Bottlenecks and Implications*.

Water UK (2010). *Recycling of Biosolids to Agricultural Land*. [Online]. 2010. Available from: https://assuredbiosolids.co.uk/wp-content/uploads/2018/05/Recycling-Biosolids-to-Agricultural-Land.pdf. [Accessed: 14 May 2019].

Waters (2015). *Mass data terminology, considerations, and interpretation*. [Online]. 2015. Available from: https://www.waters.com/webassets/cms/events/docs/us_events/2015_us_events/QDa_QRC_Mass_Data_Terminology_Considerations_Interpretation.pdf. [Accessed: 27 August 2019].

Watson, F.T., Smernik, R.J. & Doolette, A.L. (2019). Thermal degradation of phytate produces all four possible inositol pentakisphosphates as determined by ion chromatography and 1H and 31P NMR spectroscopy. *Phosphorus, Sulfur and Silicon and the Related Elements*. In Press. p.pp. 1–9.

Whitfield, H., Riley, A.M., Diogenous, S., Godage, H.Y., Potter, B.V.L. & Brearley, C.A. (2018). Simple synthesis of32P-labelled inositol hexakisphosphates for study of phosphate transformations. *Plant and Soil*. 427 (1–2). p.pp. 149–161.

Wyss, M., Brugger, R., Kronenberger, A., Rémy, R., Fimbel, R., Oesterhelt, G., Loon,

A.P.G.M. Van, Re, R. & Lehmann, M. (1999). Biochemical Characterization of Fungal Phytases (myo-Inositol Hexakisphosphate Phosphohydrolases): Catalytic Properties. *Applied and Environmental Microbiology*. 65 (2). p.pp. 367–373.

Yan, Z., Caldwell, G.W., Jones, W.J. & Masucci, J.A. (2003). Cone voltage induced in-source dissociation of glucuronides in electrospray and implications in biological analyses. *Rapid Communications in Mass Spectrometry*. 17 (13). p.pp. 1433–1442.

Yang, X.Z. & Chen, L.J. (2017). Distribution of exogenous phytase activity in soil solid–liquid phases and their effect on soil organic P hydrolysis. *Journal of Plant Nutrition and Soil Science*. 180 (1). p.pp. 39–48.

Appendix A

Solution ^{31}P NMR Spectra of Sludge Extracts

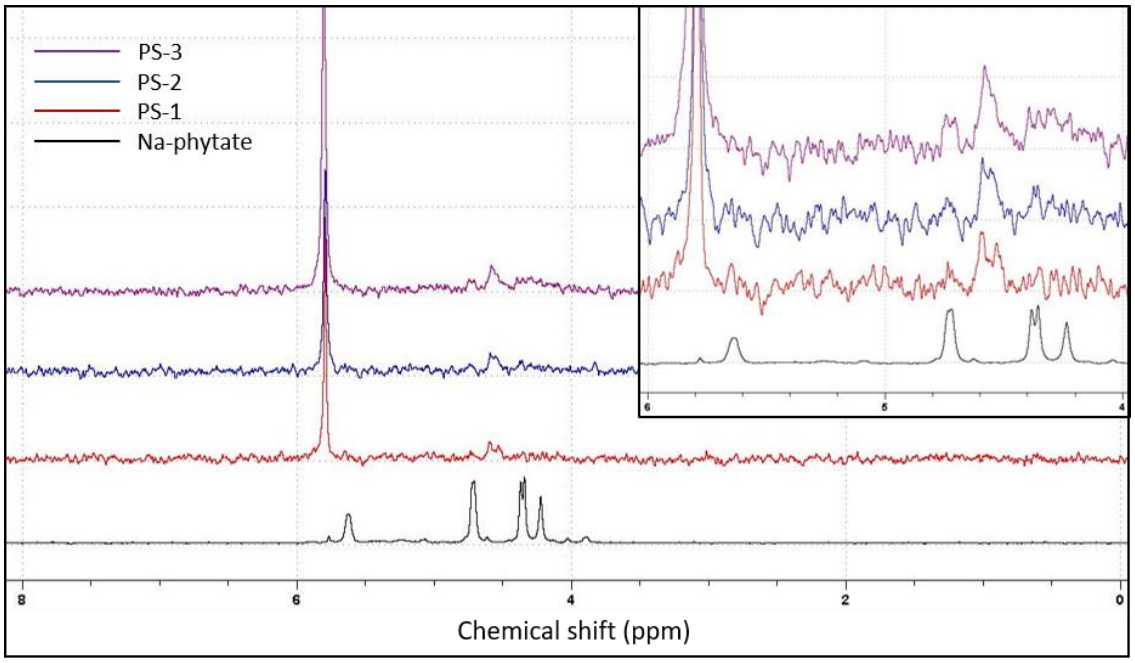

Figure A.1: Solution ^{31}P NMR spectra of 0.25M NaOH + 0.05M EDTA extracts of Primary Sludge (PS; n=3). Spectrum is presented between 8 – 0 ppm. **Inset:** Close-up of the orthophosphate monoester region with phytate peaks. Na-phytate (Black) is included for reference. Orthophosphate was measured by integration of the single phosphate peak (~5.8 ppm), and Phytate was measured by integration of the second phytate peak (~4.75 – 4.7 ppm) with comparison to an internal standard of 4mM methylene diphosphonate (MDP; not shown). 100mg of extract was dissolved in 1mL of a mix containing 9 volumes 1M NaOH + 0.1M EDTA, and 1 volume 4mM MDP in D_2O. For PS-1 and PS-2 samples, 100uL of this was then diluted to 1mL in the same solution. For PS-3 analysis, and all subsequent analyses, 200µL of suspension was diluted to 1mL to increase signal:noise ratio.

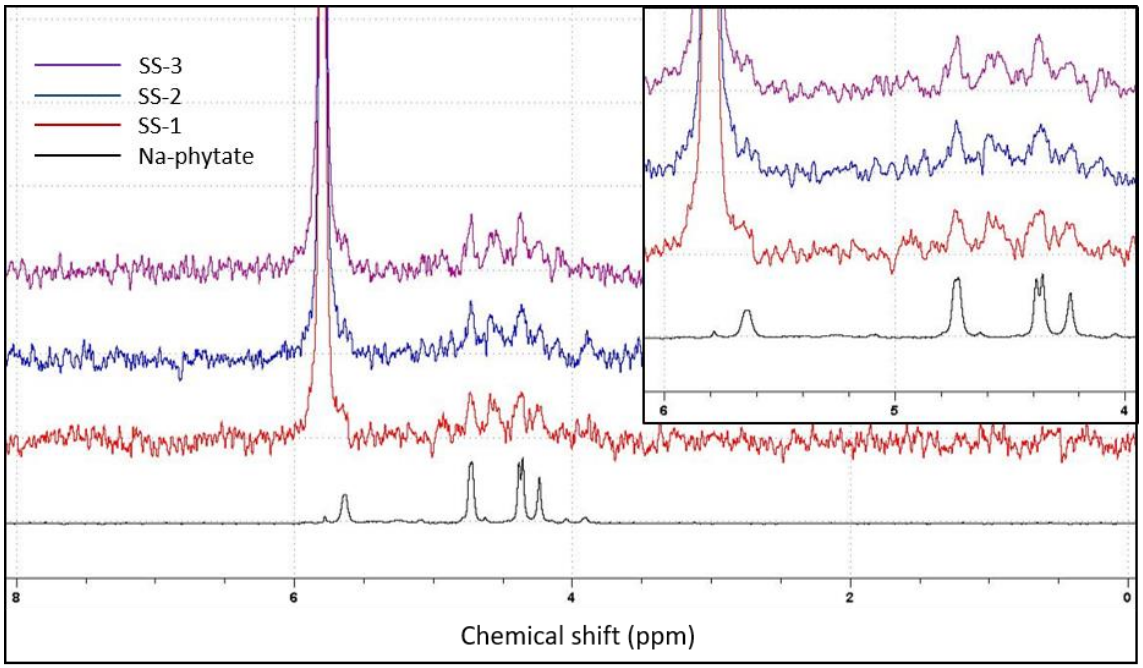

Figure A.2: Solution ^{31}P NMR spectra of 0.25M NaOH + 0.05M EDTA extracts of Secondary Sludge (SS; n=3). Spectrum is presented between 8 – 0 ppm. **Inset:** Close-up of the orthophosphate monoester region with phytate peaks. Na-phytate (Black) is included for reference. Orthophosphate was measured by integration of the single phosphate peak (~5.8 ppm), and Phytate was measured by integration of the second phytate peak (~4.75 – 4.7 ppm) with comparison to an internal standard of 4mM methylene diphosphonate (MDP; not shown). 100mg of extract was dissolved in 1mL of a mix containing 9 volumes 1M NaOH + 0.1M EDTA, and 1 volume 4mM MDP in D_2O, and 200µL of suspension was diluted to 1mL.

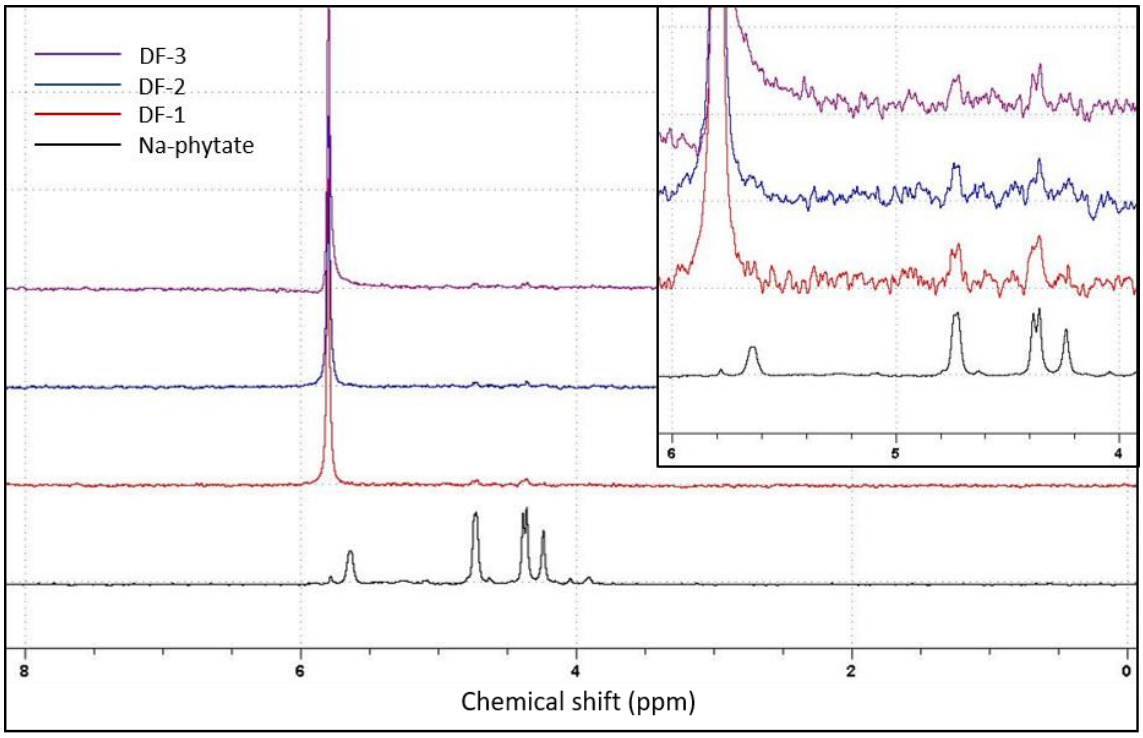

Figure A.3: Solution ^{31}P NMR spectra of 0.25M NaOH + 0.05M EDTA extracts of Digester Feed (DF; n=3). Spectrum is presented between 8 – 0 ppm. **Inset:** Close-up of the orthophosphate monoester region with phytate peaks. Na-phytate (Black) is included for reference. Orthophosphate was measured by integration of the single phosphate peak (~5.8 ppm), and Phytate was measured by integration of the second phytate peak (~4.75 – 4.7 ppm) with comparison to an internal standard of 4mM methylene diphosphonate (MDP; not shown). 100mg of extract was dissolved in 1mL of a mix containing 9 volumes 1M NaOH + 0.1M EDTA, and 1 volume 4mM MDP in D_2O, and 200µL of suspension was diluted to 1mL.

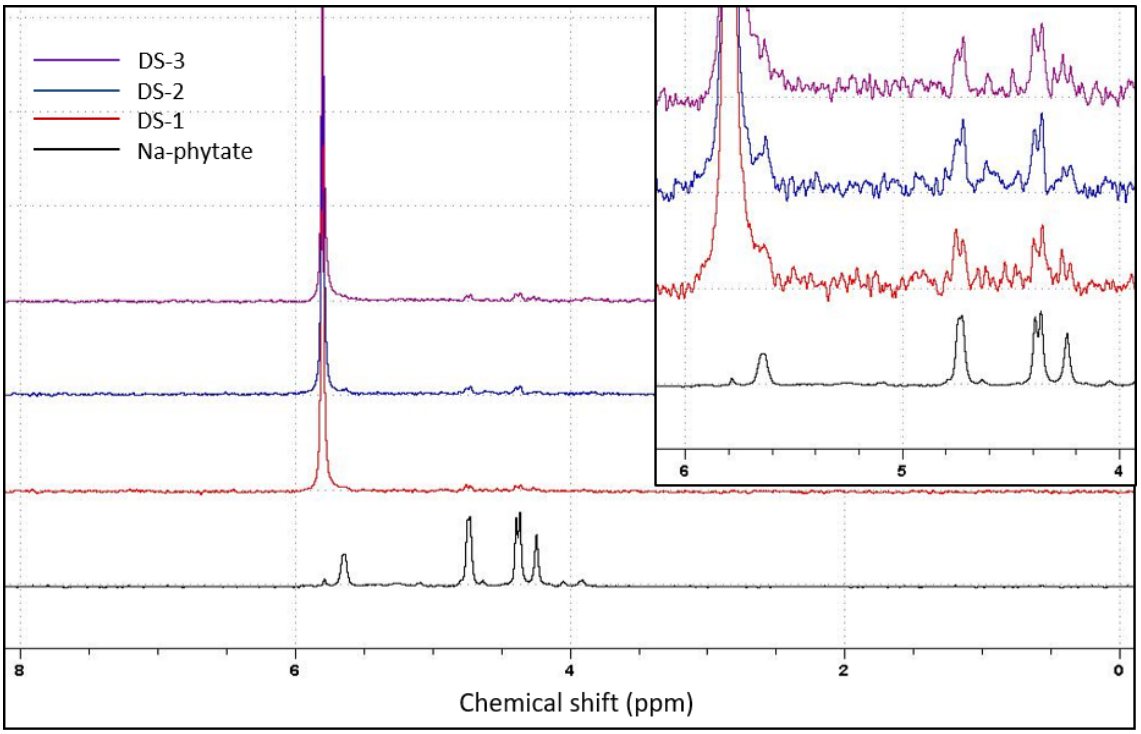

Figure A.4: Solution ^{31}P NMR spectra of 0.25M NaOH + 0.05M EDTA extracts of Digested Sludge (DS; n=3). Spectrum is presented between 8 – 0 ppm. **Inset:** Close-up of the orthophosphate monoester region with phytate peaks. Na-phytate (Black) is included for reference. Orthophosphate was measured by integration of the single phosphate peak (~5.8 ppm), and Phytate was measured by integration of the second phytate peak (~4.75 – 4.7 ppm) with comparison to an internal standard of 4mM methylene diphosphonate (MDP; not shown). 100mg of extract was dissolved in 1mL of a mix containing 9 volumes 1M NaOH + 0.1M EDTA, and 1 volume 4mM MDP in D_2O, and 200µL of suspension was diluted to 1mL.

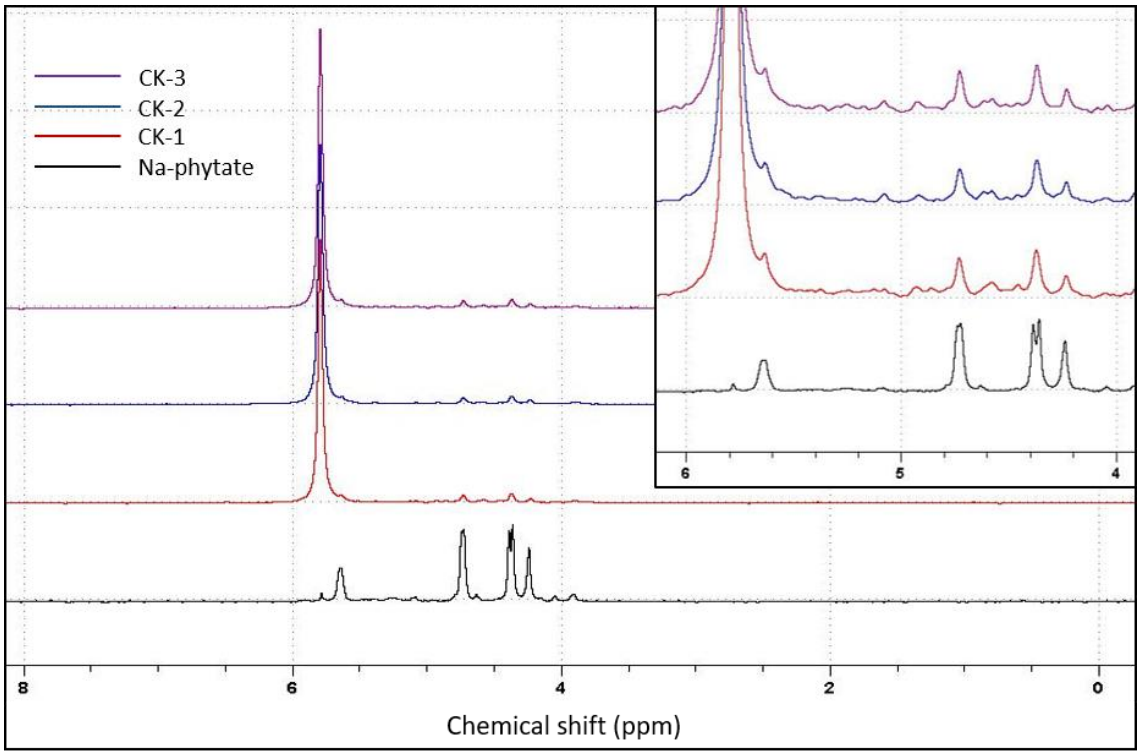

Figure A.5: Solution ^{31}P NMR spectra of 0.25M NaOH + 0.05M EDTA extracts of cake (CK; n=3). Spectrum is presented between 8 – 0 ppm. **Inset:** Close-up of the orthophosphate monoester region with phytate peaks. Na-phytate (Black) is included for reference. Orthophosphate was measured by integration of the single phosphate peak (~5.8 ppm), and Phytate was measured by integration of the second phytate peak (~4.75 – 4.7 ppm) with comparison to an internal standard of 4mM methylene diphosphonate (MDP; not shown). 100mg of extract was dissolved in 1mL of a mix containing 9 volumes 1M NaOH + 0.1M EDTA, and 1 volume 4mM MDP in D_2O, and 200µL of suspension was diluted to 1mL. Signal:Noise ratio is vastly improved in these spectra due to an upgrade NMR apparatus from a mag1 console to AvII console.

Appendix B

Solution ^{31}P NMR Spectra of Soil Extracts

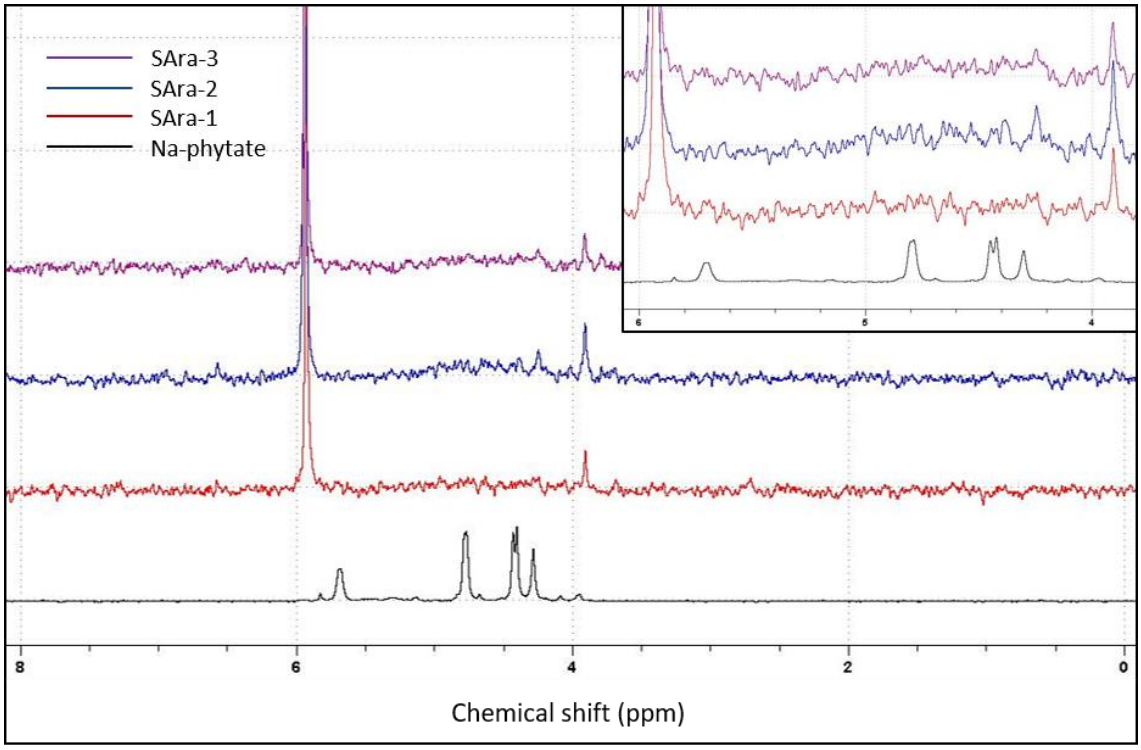

Figure B.1: Solution ^{31}P NMR spectra of 0.25M NaOH + 0.05M EDTA extracts of Spen Arable Soil (SAra; n=3). Spectrum is presented between 8 – 0 ppm. **Inset:** Close-up of the orthophosphate monoester region with phytate peaks. Na-phytate (Black) is included for reference. Orthophosphate was measured by integration of the single phosphate peak (~5.9 ppm), and Phytate was measured by integration of the first phytate peak (~5.7 ppm) with comparison to an internal standard of 4mM methylene diphosphonate (MDP; not shown). 100mg of extract was dissolved in 1mL of a mix containing 9 volumes 1M NaOH + 0.1M EDTA, and 1 volume 4mM MDP in D_2O.

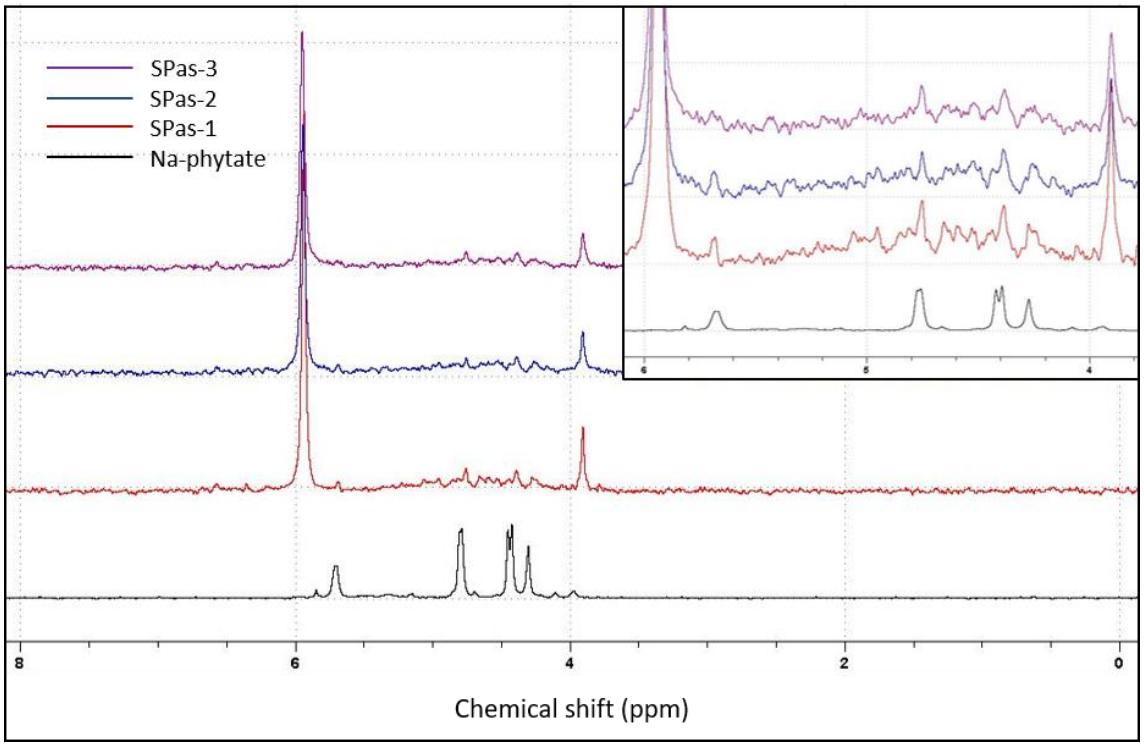

Figure B.2: Solution ^{31}P NMR spectra of 0.25M NaOH + 0.05M EDTA extracts of Spen Pasture Soil (SPas; n=3). Spectrum is presented between 8 – 0 ppm. **Inset:** Close-up of the orthophosphate monoester region with phytate peaks. Na-phytate (Black) is included for reference. Orthophosphate was measured by integration of the single phosphate peak (~5.9 ppm), and Phytate was measured by integration of the first phytate peak (~5.7 ppm) with comparison to an internal standard of 4mM methylene diphosphonate (MDP; not shown). 100mg of extract was dissolved in 1mL of a mix containing 9 volumes 1M NaOH + 0.1M EDTA, and 1 volume 4mM MDP in D_2O.

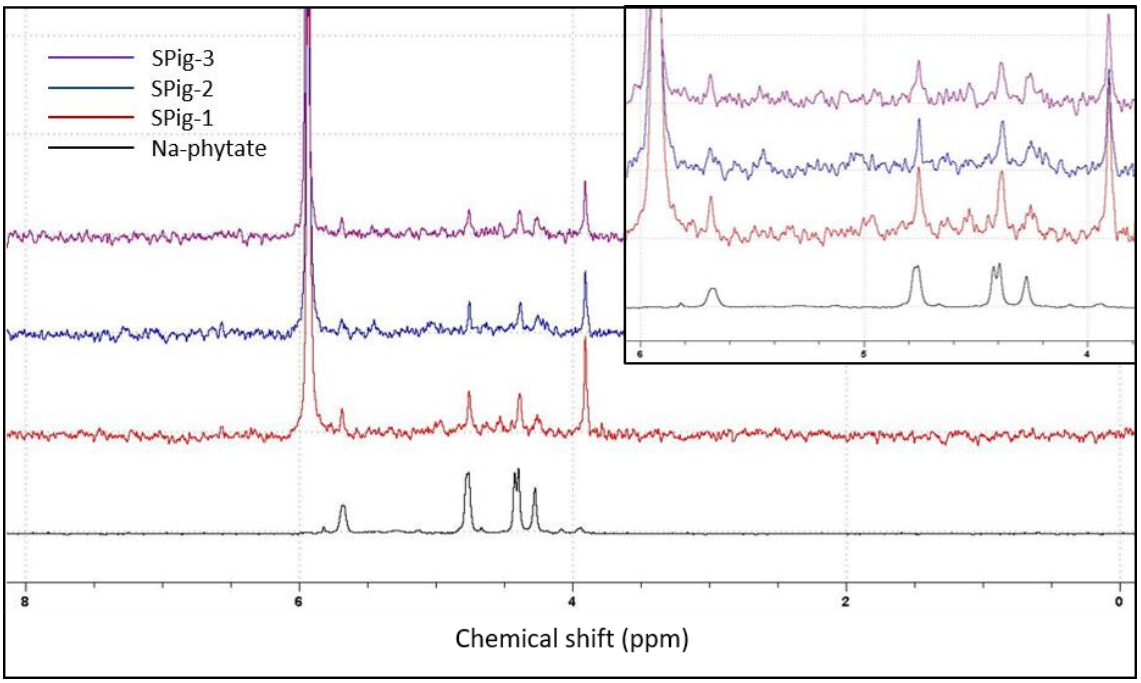

Figure B.3: Solution ^{31}P NMR spectra of 0.25M NaOH + 0.05M EDTA extracts of Spen Pig Pen Soil (SPig; n=3). Spectrum is presented between 8 – 0 ppm. **Inset:** Close-up of the orthophosphate monoester region with phytate peaks. Na-phytate (Black) is included for reference. Orthophosphate was measured by integration of the single phosphate peak (~5.9 ppm), and Phytate was measured by integration of the first phytate peak (~5.7 ppm) with comparison to an internal standard of 4mM methylene diphosphonate (MDP; not shown). 100mg of extract was dissolved in 1mL of a mix containing 9 volumes 1M NaOH + 0.1M EDTA, and 1 volume 4mM MDP in D_2O.

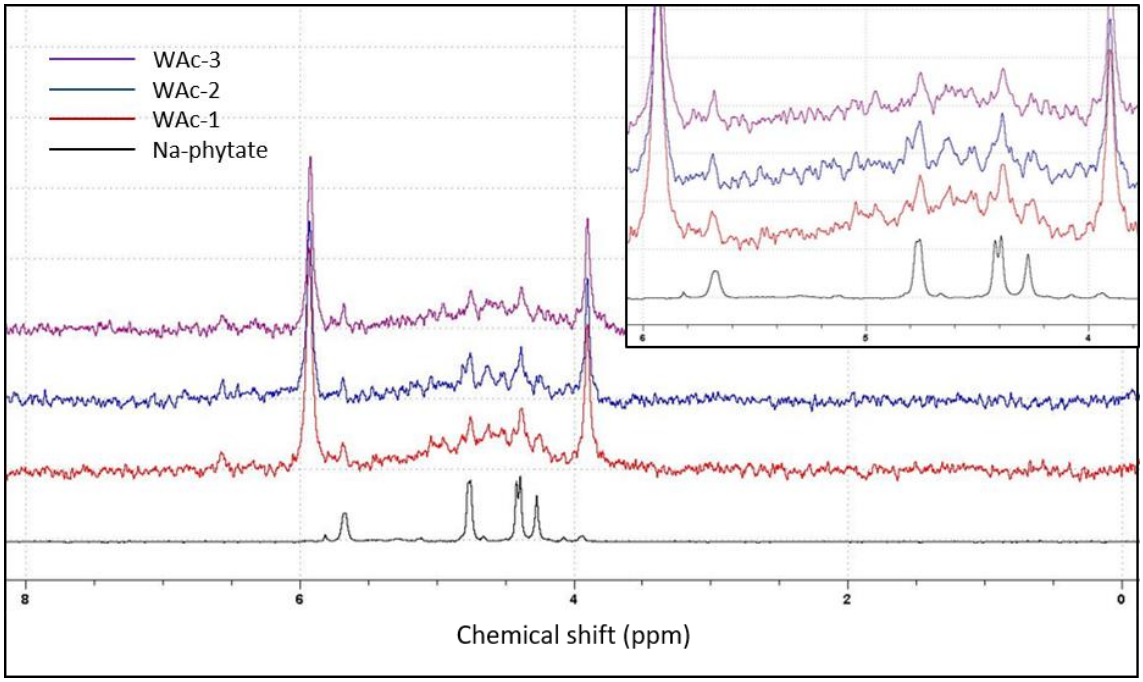

Figure B.4: Solution ^{31}P NMR spectra of 0.25M NaOH + 0.05M EDTA extracts of Wardlow Acid Soil (WAc; n=3). Spectrum is presented between 8 – 0 ppm. **Inset:** Close-up of the orthophosphate monoester region with phytate peaks. Na-phytate (Black) is included for reference. Orthophosphate was measured by integration of the single phosphate peak (~5.9 ppm), and Phytate was measured by integration of the first phytate peak (~5.7 ppm) with comparison to an internal standard of 4mM methylene diphosphonate (MDP; not shown). 100mg of extract was dissolved in 1mL of a mix containing 9 volumes 1M NaOH + 0.1M EDTA, and 1 volume 4mM MDP in D_2O.

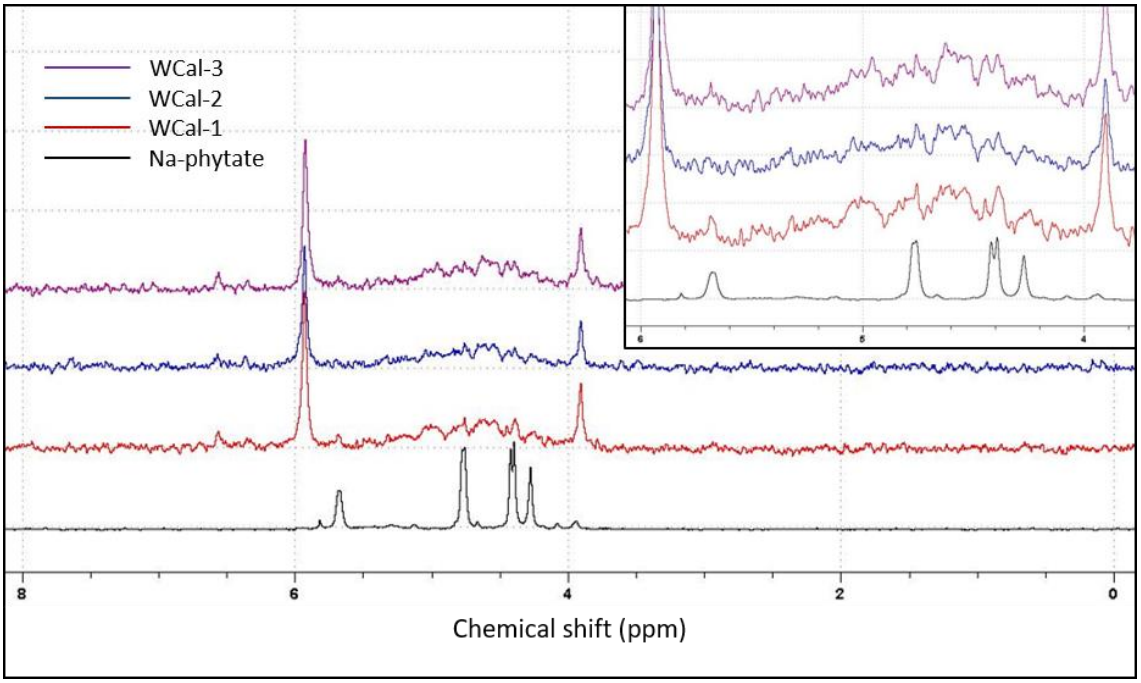

Figure B.5: Solution ^{31}P NMR spectra of 0.25M NaOH + 0.05M EDTA extracts of Wardlow Calcareous Soil (WCal; n=3). Spectrum is presented between 8 – 0 ppm. **Inset:** Close-up of the orthophosphate monoester region with phytate peaks. Na-phytate (Black) is included for reference. Orthophosphate was measured by integration of the single phosphate peak (~5.9 ppm), and Phytate was measured by integration of the first phytate peak (~5.7 ppm) with comparison to an internal standard of 4mM methylene diphosphonate (MDP; not shown). 100mg of extract was dissolved in 1mL of a mix containing 9 volumes 1M NaOH + 0.1M EDTA, and 1 volume 4mM MDP in D_2O.

Appendix C

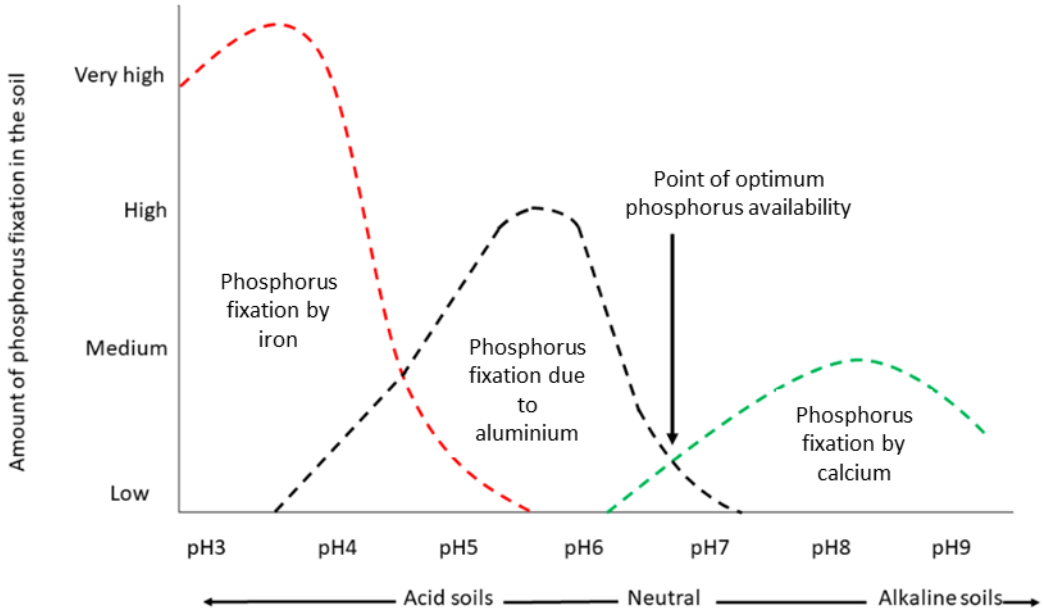

Figure C: A generalised qualitative schematic of the availability of soil P between pH 3 and pH 9. Figure adapted from Penn & Camberato, (2019)